ResearchOnline@JCU

JAMES COOK UNIVERSITY AUSTRALIA

This file is part of the following work:

Chandler, Josie F. (2025) ***Changes in biology and behaviour of crown-of-thorns starfish (Acanthaster cf. solaris) with increasing densities and decreasing food availability.*** **PhD Thesis, James Cook University.**

Access to this file is available from:

https://doi.org/10.25903/7ywf%2Dm254

Copyright © 2025 Josie F. Chandler

The author has certified to JCU that they have made a reasonable effort to gain permission and acknowledge the owners of any third party copyright material included in this document. If you believe that this is not the case, please email researchonline@jcu.edu.au

Changes in biology and behaviour of crown-of-thorns starfish (*Acanthaster* cf. *solaris*) with increasing densities and decreasing food availability

Submitted by

Josie F. Chandler

For the degree of Doctor of Philosophy (PhD)

February 2025





College of Science and Engineering &
ARC Centre of Excellence for Coral Reef Studies,
James Cook University,
Townsville, Queensland, Australia

Acknowledgements

Foremost, I would like to thank my primary advisor, Professor Morgan Pratchett, for his expertise, unwavering support, and invaluable guidance. I am deeply grateful for the incredible opportunities and learning experiences you have provided me over the past few years. I am also thankful for the guidance of my advisors, Dr. Peter Doll and Professor Andrew Hoey. Peter, thank you for stepping up as a new supervisor, offering exceptional feedback, and helping me navigate the complexities of the academic world, as well as being an outstanding fieldwork companion. Andy, thank you for your mentorship and for orchestrating unforgettable experiences during the three Coral Sea Research trips, these expeditions have broadened my skills and enriched my academic journey, I am extremely grateful. I also extend my sincere thanks to Professor Will Figueira at the University of Sydney for imparting his photogrammetry expertise and generously offering his time and resources, which have made this project possible. I would also like to thank Dr. Ciemon Caballes for sharing his expert knowledge and providing guidance through this journey.

I also wish to acknowledge the large group of people who have contributed their time and energy to this project, this work would not have been possible without the assistance of many collaborators, colleagues, and friends to all of whom I am extremely grateful. Firstly, thank you to Deborah Burn who contributed tremendous amounts of her time and expertise to this project, I am extremely grateful for your contributions and friendship during the past few years. Thank you to everyone who has contributed to the hundreds of hours of fieldwork during this PhD: Sarah Kwong, Bethan Lang, Kai Pacey, Sam McCormack and Abby Johandes. It's been a pleasure to experience the ups and downs of fieldwork with such an amazing group of people, thank you for making the long hours of data entry and starfish dissections so enjoyable.

Further thanks go to Agustina Piccaluga for patiently teaching me photogrammetry processes; to Alexia Dubuc for assistance with statistical analysis and to Nikolaos Andreakis and Leo Nankervis who contributed their time and resources during the laboratory components of my PhD. I am also grateful to Dr. Anne Hoggett and Dr. Lyle Vail for logistical support at Lizard Island Research Station, to Captain Rob Benn and the JCU Coral Sea team for making the trips so enjoyable, despite (often) challenging conditions. I extend my gratitude to all the other wonderful people at the institutions, funding bodies and research vessels or stations that supported me.

Funding for this project was provided by the Ian Potter Foundation 50th Anniversary Commemorative Grants Scheme through the Australian Museum's Lizard Island Research Station, the COTS Control Innovation Program and the ARC Centre of Excellence for Coral Reef Studies. I extend

my sincere thanks to everyone associated with these organisations who recognised the value of this research and awarded funds accordingly.

I would also like to acknowledge the Traditional Owners of the Great Barrier Reef area- particularly the Wulgurukaba and Bindal people, and the Dingaal Aboriginal people, the Traditional Owners of Lizard Island (Jiigurru)—for their enduring connection to their land and sea country.

Finally, I am forever grateful for the love and support of my friends and family. To my parents, Kate and Jon Chandler, thank you for instilling in me a love for the natural world, curiosity and adventure, you have made it possible for me to follow my dreams. To my sister Beth Chandler, thank you for paving an adventurous path for me to follow and showing me the importance of doing good for the world, and to my Granny Carole Bates, thank you for your unwavering support and encouragement throughout this journey. Lastly, to Tom, your constant love and support has made this possible; thank you for coming across the world with me, pep talking me when I needed it and cheering for me from start to finish, thank you for believing in me wholeheartedly.

Statement of the Contribution of Others

This thesis was conducted under the supervision of Prof. Morgan Pratchett[1], Dr. Peter Doll[1] and Prof. Andrew Hoey[1]. Specific contributions by supervisors and other collaborators are outlined below.

Chapter	Contributor	Nature of Assistance
Chapter 2	Morgan Pratchett[1]	conceptual / data collection / editorial assistance
	Peter Doll[1]	conceptual / data collection / editorial assistance
	Deborah Burn[1]	data collection / editorial assistance
	Kai Pacey[1]	data collection / GPS data processing
	Ciemon Caballes[2]	conceptual / data collection
	Sarah Lok Ting Kwong[1]	data collection
	Bethan Lang[1]	data collection
Chapter 3	Morgan Pratchett[1]	conceptual / editorial assistance
	Peter Doll[1]	conceptual / editorial assistance
	Will Figueira[3]	conceptual / data collection
	Deborah Burn[1]	data collection
	Agustina Piccaluga	data analysis
	Abby Johandes[1]	data collection
Chapter 4	Morgan Pratchett[1]	conceptual / data collection / editorial assistance
	Peter Doll[1]	conceptual / data collection / editorial assistance
	Will Figueira[3]	conceptual / data collection / editorial assistance
	Deborah Burn[1]	data collection / editorial assistance
	Agustina Piccaluga[3]	data analysis
	Abby Johandes[1]	data collection / editorial assistance
Chapter 5	Morgan Pratchett[1]	conceptual / data collection / editorial assistance
	Peter Doll[1]	conceptual / data collection / editorial assistance
	Ciemon Caballes[2]	conceptual / data collection
	Deborah Burn[1]	conceptual / data collection
	Will Figueira	conceptual
	Kai Pacey[1]	data collection
	Sarah Lok Ting Kwong[1]	data collection
	Bethan Lang[1]	data collection
	Alexia Dubuc[1]	data analysis
Chapter 6	Morgan Pratchett[1]	conceptual / data collection / editorial assistance
	Peter Doll[1]	conceptual / data collection / sample processing / editorial assistance
	Ciemon Caballes[2]	conceptual
	Deborah Burn[1]	data collection / sample processing
	Kai Pacey[1]	data collection / sample processing
	Bethan Lang[1]	data collection / sample processing
	Nikolaos Andreakis[1]	laboratory assistance / sample processing

[1] College of Science and Engineering, James Cook University, Townsville, QLD, 4811, Australia

[2] Marine Laboratory, University of Guam, Mangilao, Guam, 96923, USA

[3] School of Life and Environmental Sciences, University of Sydney, Sydney, NSW, 2006, Australia

Abstract

The primary threat to coral reefs globally is environmental changes, and especially climate-induced coral bleaching. In the Indo-Pacific, environmental change is compounding upon a range of local stressors, foremost of which is outbreaks of coral-eating crown-of-thorns starfish (CoTS; *Acanthaster* spp.), causing widespread coral depletion and reef degradation. The cumulative effects of climate-induced coral bleaching and recurrent CoTS outbreaks is particularly apparent on Australia's Great Barrier Reef (GBR). In contrast to climate-related stressors to coral reefs, CoTS outbreaks may be amenable to mitigation through localized management, however, effective management requires an understanding of the processes driving population dynamics, particularly the triggers that shift populations from latent populations to large-scale outbreaks. The aim of this thesis was therefore, to improve our understanding of the population dynamics of CoTS, to better predict, detect and manage outbreaks of CoTS. This thesis adopts a multifaceted approach to investigating the intrinsic and extrinsic factors that drive CoTS population dynamics, focusing on (i) the processes contributing to population increases and declining food availability and (ii) the mechanisms influencing population breakdown. Additionally, it provides valuable resources and insights to enhance current and future management strategies for CoTS outbreaks.

A review of CoTS behaviour and biology in **Chapter 1** demonstrated distinct differences between low-density and outbreaking population phases. At low densities, CoTS populations are characterized by widely dispersed, large-bodied individuals with low movement and feeding rates, and an initial phase of rapid growth that slows upon reaching sexual maturity. Conversely, populations recorded during outbreaks typically exhibit much smaller modal sizes, with heavy investment into gonad development at an earlier stage, feed indiscriminately and voraciously during the day, and may travel considerable distances. This disparity in population states prompts enquiry into whether such shifts in population traits drive outbreak conditions or are a consequence of them. An understanding of the processes which are triggering these transitions and/or contributing to population increases are important for resolving the initiation of outbreaks. A major challenge in identifying the key drivers of

Population dynamics of CoTS: drivers and impacts

CoTS outbreaks has been the inability to survey populations at low to intermediate densities during the initiation of population outbreaks. Survey limitations have constrained research and monitoring during this critical time and thus delayed proactive management response until populations are already well-established and difficult to contain.

Existing survey methods used to establish the incidence of CoTS outbreaks (e.g., manta tows) are poorly suited to detecting subtle changes in CoTS densities during the initiation and build-up of population outbreaks, as they prioritise broad spatial coverage over fine-scale accuracy. This limitation has hindered our ability to gain detailed insight into the early processes driving outbreak development. Introducing a novel survey method, Scooter-Assisted Large Area Diver-based (SALAD) surveys, **Chapter 2** revealed rapidly increasing densities of CoTS at Lizard Island, in the northern Great Barrier Reef, from 2019 to 2022. Inferred densities of adult CoTS (which account for distinct sets of observed feeding scars where starfish were not detected) increased from 4.90 ha^{-1} (± 0.85 SE) in 2019 to 17.71 ha^{-1} (± 2.3 SE) in 2022. A wide range of size classes were recorded suggesting that recruitment over several years is contributing to increasing densities, a critical insight into the process of population build-up. This study demonstrated the utility of SALAD surveys not only for the early detection of the fifth CoTS outbreak wave on the GBR, but also facilitating research on the critical transition from low densities to population outbreaks.

This thesis identified feeding behavior and prey availability as key drivers of CoTS population dynamics. High-resolution photogrammetry **(Chapter 3)** provided refined estimates of daily feeding, updating historic values that relied on simplistic colony diameter measurements of feeding scars. These previous estimates did not incorporate the three-dimensional complexity of corals or variations in daily feeding rates between individuals and coral prey types. Intensive tracking of eight CoTS over 13 days yielded 90 high-resolution feeding observations, revealing significant variation in feeding activity across successive days. Notably, CoTS do not feed consistently every 24 hours but may remain inactive for 2–3 consecutive days. The mean daily feeding rate at this location was 1.35 colonies per

individual per day (± 0.18 SE), equivalent to 198.4 cm^2 d^{-1} (± 23.86 SE) planar area or 998.83 cm^2 d^{-1} (± 128.69 SE) total 3D surface area. However, substantial variation was observed among and within individuals. 3D modelling of individual feeding scars allowed coral morphology and genus to be accounted for, refining our understanding of species-specific consumption rates and highlighting the role of individual feeding behavior in shaping both reef structure and the trajectory of CoTS population growth. From an areal perspective, *Acropora* corals comprised over 80% of the total (3D) surface area consumed, or 94% when all Acroporidae species were pooled. This intense reliance on *Acropora* suggests that local coral cover and composition may play a crucial role in shaping CoTS outbreaks. Given the increasing vulnerability of *Acropora* corals to multiple disturbances, this dependency may limit CoTS persistence in areas with insufficient coral cover.

While **Chapter 3** provided high-resolution data from a single location, it did not address broader questions about how feeding behaviour varies across different outbreak stages and environmental conditions, an essential consideration for modelling CoTS impact on reef ecosystems. **Chapter 5** explored the intrinsic and extrinsic factors influencing individual feeding rates of CoTS to better understand the processes that may be amplifying their ecological impact. To investigate the key drivers of daily feeding rates, this study employed a large-scale survey approach, analysing feeding data from over 565 individual CoTS on the GBR. Given the need to conduct rapid assessments within a short survey period, methods were developed to efficiently estimate daily feeding rates from field measurements of feeding scars.

Chapter 4 developed this method, enabling comprehensive data on coral morphology (planar area, 3D surface area) to be gathered from simple linear measurements of colony diameter, via conversion metrics. Photogrammetry techniques were used to quantify surface area and model relationships between linear length and a) planar area and b) 3D surface area, for 15 coral morphotaxa groups. The conversion metrics established had high explanatory power, with Bayesian models showing strong non-linear (power) relationships between colony maximum diameter and both total 3D surface area and projected 2D surface area for 13 out of 15 morphotaxa. This demonstrated the

applicability of using rapid field measurements of colony maximum diameter to effectively predict total 3D surface area and projected 2D surface area for a diverse range of different corals. The utility of the relationships established in this chapter extend beyond the large-scale feeding study (**Chapter 5**), from small-scale studies of ecological processes to ecosystem modelling. An additional output of this study was demonstrating substantial variation of surface area to coral diameter ratios between taxa which may be a key factor underpinning feeding preferences. Relationships modelled in this chapter show that an *Acropora* colony with a maximum diameter of 35cm is likely to have a total 3D surface area that is five times larger than a *Montipora* colony with the same colony maximum diameter (*Montipora*: 910cm^2; *Acropora – other:* 4,300cm^2). This data highlights the significant energetic benefits to CoTS of feeding on highly complex corals, compared to morphologically simple corals, and may explain the intense reliance on *Acropora* corals in driving feeding behaviour and movement of CoTS. Local availability of complex corals, particularly *Acropora*, may be contributing to spatiotemporal heterogeneity in the incidence and severity of population outbreaks.

Methodological advancements developed in **Chapter 2** (SALAD surveys) and **Chapter 4** (conversion metrics) enabled investigation into patterns of CoTS feeding drivers**,** via large-scale surveys (**Chapter 5**). This study identified that CoTS body size and local coral cover are key predictors of individual feeding rates. Notably, large CoTS (>40 cm) at high coral cover sites consumed over ten times more coral than small individuals (15–25 cm), with mean daily consumption of 221.99 cm² day^{-1} vs. 18.86 cm² day^{-1} (planar area), respectively. This finding underscores the importance of incorporating context-specific feeding rates into models assessing the impact of CoTS. The large sample size in this study enabled the development of predicted feeding values, categorized by CoTS size class and coral cover class. This output is intended to improve the accuracy of CoTS feeding estimates in ecosystem models and inform management decisions while the underlying causes of population outbreaks continue to be investigated.

Moreover, the results of **Chapter 5** suggest CoTS in high coral cover environments exhibit high feeding efficiency paired with reduced movement distances and time spent searching for prey. In

contrast, individuals in low coral cover environments experience greater foraging effort and reduced energetic intake (tissue area consumed), which likely has significant energetic consequences, potentially limiting outbreak persistence. This hypothesis was tested in **Chapter 6**, where CoTS populations in high-density, coral-depleted environments were monitored. Physiological analyses revealed that individuals in these conditions exhibited depleted nutritional reserves, as indicated by lower Pyloric Caeca Indices and lipid reserves, suggesting that long-term population sustainability may be restricted in coral-depleted environments. Despite reductions in nutritional condition, reproductive investment remained stable, indicating that CoTS may prioritize reproduction even under resource-limited conditions, potentially prolonging outbreaks.

Overall, this thesis advances our understanding of the key processes driving CoTS population build-up and collapse, highlighting the critical role of prey-resource interactions in shaping outbreak dynamics. The development of the SALAD survey method represents a major advancement in early outbreak detection, enabling intervention at a stage when population control is most effective. Empirical findings from monitoring the early stages of outbreak build-up challenge longstanding outbreak hypotheses, shifting the focus toward sustained low-level recruitment as a key driver of population build-up. Additionally, refined estimates of CoTS feeding rates and physiological responses to food limitation highlight the need to update ecological impact models and management thresholds. This thesis provides critical advancements in outbreak prediction, detection and management of outbreaks, supporting more effective reef conservation strategies in an era of accelerating climate pressures.

Table of Contents

Acknowledgements ..... **I**

Statement of the Contribution of Others ..... **III**

Abstract ..... **IV**

Table of Contents ..... **IX**

List of Tables ..... **XII**

List of Figures ..... **XIII**

Chapter 1: General Introduction **1**

1.1 Outbreaks of *Acanthaster* spp. **1**

1.2 Densities **7**

1.2.1 Variation in CoTS densities *8*

1.2.2 Fundamental thresholds *9*

1.3 Variation in CoTS Biology with Population State **11**

1.3.1 Size and growth *12*

1.3.2 Longevity *16*

1.3.3 Fecundity and reproductive condition *18*

1.3.4 Spawning *20*

1.3.5 Spawning aggregations *21*

1.3.6 Population replenishment *22*

1.3.7 Sex ratios *25*

1.4 Variation in CoTS Behaviour with Population State **25**

1.4.1 Feeding selectivity *25*

1.4.2 Feeding rates *28*

1.4.3 Diel behaviour *30*

1.4.4 Movement *31*

1.4.5 Feeding aggregations *32*

1.5 Summary and thesis outline **34**

Chapter 2: Increasing densities of Pacific crown-of-thorns starfish (*Acanthaster* cf. *solaris*) at Lizard Island, northern Great Barrier Reef, resolved using a novel survey method **40**

2.1 Introduction **40**

2.2 Methods **43**

2.2.1 Study site *43*

2.2.2 SALAD survey methods *45*

2.2.3 Statistical analyses *48*

2.3 Results **49**

2.3.1 Inter-annual variation in CoTS density *49*

2.3.2 Size structure *51*

2.4 Discussion 52

Chapter 3: Daily variation in the feeding activity of Pacific crown-of-thorns starfish (*Acanthaster* cf. *solaris*) 58

3.1 Introduction 58

3.2 Methods 61

3.2.1 Diet composition 64
3.2.2 Scar ageing 65
3.2.3 3D modelling feeding scars 67
3.2.4 Statistical analysis 68

3.3 Results 69

3.3.1 Daily activity 69
3.3.2 Feeding rates 70
3.3.3 Diet composition 74
3.3.4 Ageing of feeding scars 75

3.4 Discussion 76

Chapter 4: Predicting 3D and 2D surface area of corals from simple field measurements 81

4.1 Introduction 81

4.2 Methods 85

4.2.1 Data collection 85
4.2.2 Model reconstruction and data extraction 87
4.2.3 Statistical models 88

4.3 Results 90

4.4 Discussion 97

Chapter 5: Spatiotemporal variation in feeding behaviour of Pacific crown-of-thorns starfish (*Acanthaster* cf. *solaris*), including highly resolved daily feeding rates 102

5.1 Introduction 102

5.2 Methods 104

5.2.1 Field surveys 104
5.2.2 Converting field measurements to 2D/3D surface area 107
5.2.3 Data analysis 107

5.3 Results 109

5.3.1 Sampling effort 109
5.3.2 Daily Feeding rates 110

5.4 Discussion 118

Chapter 6: Variation in reproductive and nutritional condition of CoTS with population density and food availability 124

6.1 Introduction 124

6.2 Methods 128
6.2.1 Field collections 128
6.2.2 Pyloric Caeca biochemical analysis: 129
6.2.3 Gonadosomatic Index and Gonad morphometrics: 131
6.2.4 Statistical analysis 131
6.3 Results 133
6.3.1 Regional variation in nutritional condition 134
6.3.2 Regional variation in reproductive condition 134
6.3.3 Variation in nutritional condition along environmental gradients 135
6.4 Discussion 140
Chapter 7: General Discussion 144
7.1 Key processes in population build-up of crown-of-thorns starfish 144
7.2 Key processes in population breakdown of crown-of-thorns starfish 148
7.3 Management Implications 150
7.4 Future Direction in Research 152
References 154
Appendix 1 - Supplementary information for Chapter 1 178
Appendix 2 - Supplementary information for Chapter 4 183
Appendix 2a: 3D Photogrammetry Processes 183
Appendix 2b: Model output and credible intervals 184
Appendix 2c: Bayesian model equation parameters 200
Appendix 2d: Representative images of coral morphotaxa 202
Appendix 3 - Supplementary information for Chapter 5 209
Appendix 4 - Supplementary information for Chapter 6 221

List of Tables

Table 2.1 Summary of Scooter-Assisted Large Area Diver-based (SALAD) surveys conducted at Lizard Island during 2019-2022, with survey distance and survey area per survey year 49

Table 4.1 Model equations and Bayesian R^2 for predicting colony Projected 2D Surface Area (PSA) and Total 3D surface area (TSA) from field measurements of colony maximum diameter (D) for 15 coral morphotaxa. Additional information on model equation parameters (incl. 95% HDIs and SD for parameters α + β) are presented in Supplementary material (Appendix 2c, Table S17 & S18). 95

Table 5.1 Summary of sampling effort at each region with mean environmental conditions from each region as well as the range of values recorded. Data on environmental conditions were collected via SALAD surveys 110

Table 5.2 Predicted values of daily feeding rate from GLMM modelled data. Modelled feeding rates are provided for different size categories of CoTS (rows) and coral cover categories (columns). Daily feeding rate is presented as **(a) No. of colonies** consumed per day, **b) Planar (2D) area** of coral consumed per day (cm^2) and **c) total (3D) surface area** consumed per day (cm^2) 118

Table 6.1 Summary of sampling effort (adult females only) at each region with mean environmental conditions from each region as well as the range of values recorded. Data on environmental conditions were collected via SALAD surveys 133

List of Figures

Figure 1.1 Density estimates of Acanthaster cf. solaris, taken from 50 peer reviewed publications of primary data. Publication dates range from 1969-2022. Where multiple density estimates are stated within the paper, all are included.....7

Figure 2.1 'SALAD surveys' conducted at Lizard Island. **(a)** Lizard Island's location in the Northern Great Barrier Reef, also shown is the putative 'Initiation Box' (dashed box), **(b)** Lizard Island area with survey locations marked in red, **(c)** SALAD survey conducted with a Seascooter, **(d)** Methodology: searches are conducted at two depths simultaneously, with GPS units towed along the surface in floating housings.....45

Figure 2.2 Inter-annual variation in CoTS densities at Lizard Island from 2019 to 2022. **(a)** recorded density estimates based on starfish counts, **(b)** inferred density estimates (accounting for additional, distinct sets of feeding scars where starfish were not detected). Each grey point represents a density estimate for an individual SALAD survey. Boxes and whiskers display 25-75th and 5-95th percentile ranges, respectively. Diamonds and thick lines indicate mean and median values, respectively. 50

Figure 2.3 Inter-annual variation in size frequency distribution of adult CoTS recorded at Lizard Island between 2019 and 2022. Dashed line indicates the mean CoTS diameter (mm) for each survey year 52

Figure 3.1 Maps of study location and sites. **(a)** Lizard Island's location in the northern Great Barrier Reef, Australia **(b)** Lizard Island with survey locations Granite Bluff, Turtle Beach and Casuarina marked in green, **(c)** the locations of CoTS 1-3 tracked at Casuarina, **(d)** the locations of CoTS 4-8 at Turtle Beach & Granite Bluff. Queensland Imagery online aerial photograph library. Accessed May 18, 2024. https://qimagery.information.qld.gov.au/.....62

Figure 3.2 Process of using CIE LAB scale to quantify when CoTS surpass colour intensity (chroma) in line with B2 on a CoralWatch card. **(a)** Adobe Lightroom colour picker presents LAB values for B2 on the CoralWatch card, **(b)** CIE LAB scale with white at the centre and chroma threshold of A= ±6 and B = ±16 marked in orange, in line with CoralWatch card LAB values, **(c)** Adobe Lightroom colour picker presents LAB values of one fresh scar with chroma values below threshold limits (A<6, B<16; see white cross), **(d)** Adobe Lightroom colour picker presents LAB values of one old scar with chroma threshold exceeded (B >16; see red cross), so this scar has surpassed the ageing threshold. 66

Figure 3.3 Daily activity patterns of 8 individual starfish over the survey period (9-13 days). Green points represent the 3D surface areal extent (cm2) of coral consumed during each 24-hour period, grey points represent 24-hour periods when no coral was consumed. Days when no feeding

observations were conducted (due to diving limitations) are marked as crossed circles. Dashed lines represent the average number of colonies consumed over the survey period. Pie charts represent the proportion of 24-hour periods spent feeding (green). 70

Figure 3.4 Daily feeding rates of 8 individual starfish recorded over 9-13 consecutive days, presented as **(a) number of colonies** consumed per day, **(b) planar projected area** of coral consumed per day (cm^2), **(c) total (3D) surface area** of coral consumed per day (cm^2). Each boxplot represents feeding for a single starfish across multiple days of intensive sampling. Large black diamonds and thick horizontal lines represent mean and median values, respectively, box limits the interquartile range, whiskers the 1.5x interquartile range, and small grey diamonds the daily consumption data. Maximum body diameter of each individual CoTS is also presented in panel a. 72

Figure 3.5 Successive feeding bouts documented on a single large colony of tabular Acropora by a single CoTS. Quantification of scar area presents scar length, planar area and total surface area of successive scars 73

Figure 3.6 Total (cumulative) feeding from 9 consecutive days of feeding by 8 individual starfish. Bars represent summed feeding and colours depict proportional feeding on different coral morphotaxa. Total feeding is presented as **(a)** Total number of coral colonies consumed and **(b)** Total 3D surface area of coral consumed (cm^2) 75

Figure 3.7 Ageing process of feeding scars observed. **(a)** Visual progression of a feeding scar (genus Pocillopora) photographed over 14 days in this study. Discolouration beyond the B2 colour threshold on a CoralWatch card occurred between days 6 and 7 for this feeding scar. **(b)** Boxplot showing the number of days (since consumption) at which the B2 colour threshold was surpassed for 9 tracked scars. Boxplot line shows median time, box limits the interquartile range, whisker the 1.5x interquartile range, and filled diamond the mean. Each small point represents an individual scar for which the ageing period was quantified. The shapes and colours of each point indicate the coral taxon and sampling site of the scars.....75

Figure 4.1 (a) Field measurements of colony maximum diameter (cm) **(b)** projected 2D surface area (cm^2) and **(c)** total 3D surface area (cm^2) of the same coral colony. Images taken from Agisoft Metashape v 1.7.6 software during model reconstruction 88

Figure 4.2 Comparison of colony maximum diameter measurements taken from the field (x-axis) with colony maximum diameter derived from model reconstructions using Agisoft Metashape computer software (y-axis) (R^2=0.97, n=159).....90

Figure 4.3 Modelled power relationship between field measurements of colony maximum diameter (cm) and projected (2D) surface area (cm^2) for 15 coral morphotaxa. Black lines represent median posterior distribution and bands represent 99%, 95%, 80% and 50% highest density intervals (HDIs) derived from posterior distribution. Model equations with parameters α + β are presented along with Bayesian R^2 value for each morphotaxon.....92

Figure 4.4 Modelled power relationship between field measurements of colony maximum diameter (cm) and total (3D) surface area (cm2) for 15 coral morphotaxa. Black lines represent median posterior distribution and bands represent 99%, 95%, 80% and 50% highest density intervals (HDIs) derived from posterior distribution. Model equations with parameters α + β are presented along with Bayesian R^2 value for each morphotaxon. 94

Figure 4.5 Median lines of posterior distributions for modelled power relationships between colony maximum diameter and total (3D) surface area for 15 coral morphotaxa.....96

Figure 5.1 Map of the northern Great Barrier Reef, showing five distinct regions (Cape Grenville, Princess Charlotte Bay, Lizard, Cairns and Townsville) where sampling was undertaken in 2023-2024. SALAD surveys were used to collect feeding data across this wide latitudinal gradient.....105

Figure 5.2 Predicted values of daily feeding rate for each body size class of CoTS presented as black diamonds with 95% confidence intervals for **(a) no. colonies** consumed per day, **(b) planar area** of coral consumed per day (cm^2 day^{-1}) and **(c) total (3D) surface area** of coral of coral consumed per day (cm^2 day^{-1}). True data for daily feeding rates recorded for each starfish are also presented as individual points. Boxes and whiskers display 25-75th and 5-95th percentile ranges of true data respectively, thick lines indicate median values.....114

Figure 5.3 Relationship between Total coral cover (%) and Daily feeding rate of CoTS. Daily feeding rate is presented as **(a) 3D surface area (cm^2)** of coral consumed per day by each CoTS, and **(b) number of colonies** consumed per day by each CoTS. Each point represents feeding by one individual starfish. The black line represents the linear regression fit to the data points 115

Figure 5.4 Predicted values of daily feeding rate from GLMM modelled data with fixed effects CoTS body size and coral cover presented. Daily feeding rates are presented as **(a) no. colonies** consumed per day, **(b) planar area** of coral consumed per day (cm^2 day^{-1}) and **(c) 3D surface area** of coral consumed per day (cm^2 day^{-1}). Dark coloured points with error bars represent the predicted value and 95% confidence intervals, faded points represent true daily feeding rate data for individual starfish 117

Figure 6.1 Map of the northern Great Barrier Reef, showing five distinct regions (Cape Grenville, Princess Charlotte Bay, Lizard, Cairns and Townsville) where sampling was undertaken in November 2022. SALAD surveys were used to collect feeding data across this wide latitudinal gradient 128

Figure 6.2 (a) The location of pyloric caeca (pc) and gonads (g) in the dissected arm of A .cf. solaris; **(b)** female starfish after dissection, photographed with full pyloric caeca visible; **(c)** female starfish after dissection and removal of pyloric caeca, photographed.....129

Figure 6.3 Variation in Pyloric Caeca Index (PCI) among Reefs and Regions. Boxes and whiskers display 25–75th and 5–95th percentile ranges, respectively. Large black diamonds represent regional means of PCI. Observed values of PCI for individual starfish are displayed as points.....134

Figure 6.4 Variation in Gonadosomatic Index (GSI) among Reefs and Regions. Boxes and whiskers display 25–75th and 5–95th percentile ranges, respectively. Large black diamonds represent Regional means of GSI. Observed values of GSI for individual starfish are displayed as points 135

Figure 6.5 Relationship between (a) Acropora cover (b) CoTS density and the Pyloric Caeca Index (PCI). Black lines represent the posterior median estimates of PCI as modelled using a Bayesian Generalized Linear Mixed Model (BGLMM). The grey ribbon represents 95% Highest Posterior Density (HPD) intervals as credible intervals. Observed values of PCI are displayed as points 137

Figure 6.6 Relationship between a) Population density, b) Acropora cover (%) and c) Total coral cover on Gonadosomatic Index (GSI; gonad wet weight to total body wet weight ratio). Black lines represent the posterior median estimates of GSI as modelled using a Bayesian Generalized Linear Mixed Model (BGLMM). The grey ribbon represents 95% Highest Posterior Density (HPD) interval as credible intervals. Observed values of GSI are displayed as points.....139

Chapter 1: General Introduction

1.1 Outbreaks of *Acanthaster* spp.

Coral reefs in the Anthropocene are characterized by increasing disturbances and pressures, resulting in widespread and sustained degradation (Hughes et al. 2017; Bellwood et al. 2019; Perry and Alvarez-Filip 2019; Williams et al. 2019). Contemporary pressures to coral reefs are multifaceted and increasing in frequency, intensity and extent mostly due to pervasive and escalating effects of anthropogenic climate change (Hughes et al. 2017; Bellwood et al. 2019). These climate-driven disturbances compound upon and exacerbate perennial disturbances and pressures, including periodic outbreaks of crown-of-thorns starfish (CoTS; *Acanthaster* spp.) causing extensive coral loss, shifts in coral assemblages, and corresponding degradation of reef habitats (Bellwood et al. 2019).

CoTS are a corallivorous starfish which predominantly occur in widely dispersed, low density populations (<1-5 CoTS.ha^{-1}, Chesher 1969a; Pratchett and Cumming 2019a) where they are highly cryptic and nocturnal (Babcock et al. 2016b; Pratchett et al. 2021c). However, their extraordinary reproductive characteristics (Babcock et al. 2016; Pratchett et al. 2021c) make them susceptible to extreme population fluctuations, periodically leading to rapid and pronounced increases in population densities (Moran 1986; Uthicke et al. 2009; Pratchett et al. 2014). The causes and contributors to population increases and population outbreaks of CoTS are not fully understood but have been the focus of substantial research (e.g., Bradbury and Antonelli 1990; Babcock et al. 2016a). During outbreaks, CoTS are capable of collectively consuming vast amounts of coral, especially hard (Order Scleractinia) corals that form the foundation for coral reefs ecosystems (Chesher 1969b; Moran et al. 1992; Kayal et al. 2012). Outbreaks of CoTS have been responsible for severe coral loss in multiple regions (Foo et al. 2024; Uthicke et al. 2024a). In the central GBR, CoTS outbreaks in the 1960's and 1980's reduced coral cover to < 1 % (Chesher, 1969; Done, 1985; Colgan, 1987). More recently major outbreaks of CoTS reduced coral cover from 40% to <5% around Moorea, French Polynesia (Kayal et al. 2012).

Population dynamics of CoTS: drivers and impacts

The incidence and severity of CoTS outbreaks, and corresponding effects on coral reefs, appears to vary geographically (Pratchett et al. 2017b; Uthicke et al. 2024b), possibly reflecting interspecific differences in demography. It is now recognised that there are at least four distinct species of crown-of-thorns starfish with large non-overlapping geographic ranges (*Acanthaster benziei* in the Red Sea, *Acanthaster mauritiensis* and *A. planci* in the Indian Ocean, *Acanthaster* cf. *solaris* in the western Pacific, and *Acanthaster* cf. *ellisii* in the eastern Pacific) (Uthicke et al., 2024b, Haszprunar et al., 2017). The highest incidence and severity of CoTS outbreaks has tended to occur on Australia's GBR (Babcock et al., 2020) and in southern Japan (Yasuda, 2018), within the geographic range of *Acanthaster* cf. *solaris* (Pratchett et al. 2017). This may suggest that this species has demographic traits that further increase the likelihood of population outbreaks (Uthicke et al. 2024b), though the incidence and initiation of outbreaks is often attributed to specific environmental factors that may predominate in certain regions (e.g., Wooldridge and Brodie 2015) There are three primary hypotheses put forward to explain the initiation of CoTS outbreaks; i) the Predator Removal hypothesis (Endean, 1969) which proposes that overfishing of predators released CoTS from normal predatory regulation, facilitating increased size and abundance of adult CoTS, ii) the Terrestrial Runoff hypothesis (Fabricius et al. 2010), which proposes that excess nutrients from land-runoff provided larval CoTS relief from normal nutritional constraints, allowing for increased rates of larval development and survival, and iii) the Natural Causes hypothesis, which proposes that population fluctuations are natural, brought about by inherent biological traits and predator-prey dynamics. Distinguishing which anthropogenic and/or environmental factor(s) are responsible for the onset of rapidly increasing population densities is critical for the most effective management and suppression of population outbreaks. Effective interventions are contingent upon a full understanding of the mechanisms responsible for population initiation and any factors which may be exacerbating population growth.

For the Predator Removal Hypothesis, predatory-release was initially ascribed to intensive depletion of Giant Triton (*Charonia tritonis*) on Australia's Great Barrier Reef (GBR) preceding

seemingly unprecedented population outbreaks of CoTS in the 1960s (e.g., Endean, 1969). More recently, evidence that the incidence and severity of population outbreaks of CoTS has been greatest in areas subject to sustained fishing pressure (Dulvy et al. 2004; Sweatman 2008; Westcott et al. 2020; Kroon et al. 2021), suggests that normally high biomass of fishery target species (e.g., coral trout; *Plectropomus* spp.) may help to suppress population outbreaks of CoTS (Kroon et al. 2021). This work has been corroborated by evidence that risk of predation and quantity of key predators (Spangled emperor, *Lethrinus nebulosus*) was substantially highest at 'no-take' fishing zones on the GBR compared to areas open to fishing (Doll 2024). If predators have a major influence on the population dynamics of CoTS, the spatial distribution of population outbreaks (at least initial population build-up) may be related to local fisheries management and/ or the extent of fishing (Sweatman 2008; Kroon et al. 2021). Whilst it is apparent that predation pressure is capable of influencing CoTS populations to some degree, it is unlikely to be the sole contributor to population outbreaks, especially given that the cyclical nature of observed outbreaks on the GBR cannot be readily explained by sustained depletion of potentially important predators (Pratchett et al. 2017b).

The Terrestrial Runoff Hypothesis relates population outbreaks of CoTS to prey availability during larval development, with some variations of the hypothesis drawing correlations with anthropogenic activities (Birkeland 1982). The Terrestrial Runoff Hypothesis posits that larval CoTS are generally food limited and have very low survivorship during most years and under "normal" conditions (Lucas 1982). Elevated nutrients, and thereby increased availability of plankton prey, may however, occur periodically due to terrestrial runoff and mass input of nutrients due heavy rainfall after a period of extended drought (Birkeland 1982; Wooldridge 2009), with compounding effects if agricultural fertiliser is prevalent in those regions. However, alternative versions of the larval nutrition hypothesis link outbreaks to natural availability of plankton prey on oceanic reefs (Houk et al. 2007; Miller et al. 2015). Regardless of the source of nutrients, increases in food availability and the presumed increases in the nutritional quality of CoTS larvae are then expected to translate to greatly increased survival and developmental success (Lucas 1982; Fabricius et al. 2010). On the GBR,

increased concentrations and availability of nutrients in coastal waters following heavy rainfall events are evident (Devlin and Brodie 2005), however population outbreaks of CoTS do not consistently occur in the aftermath of these events (Pratchett et al. 2014). Moreover, population outbreaks do not exclusively occur on reefs in the immediate proximity of major inputs of land-based nutrients. Locations which are isolated from significant nutrient run-off have experienced population outbreaks (e.g., Roche et al. 2015; Babcock et al. 2016a), and it is unresolved whether low nutrient conditions would sufficiently constrain larval survival to prevent the initiation of population outbreaks (Olson 1987; Wolfe et al. 2017). The recruitment pulse that this hypothesis posits would occur following nutrient-mediated release from starvation and would present as a mass influx of CoTS recruitment in a single season. Investigation into whether this is the pattern of initial population build-up will aid in resolving the influence of this hypothesis.

The Natural Causes hypothesis (Dana et al. 1972; Vine 1973; Beach et al. 1975) suggests that population fluctuations are a natural part of CoTS population dynamics, driven by inherent biological and ecological factors such as episodic reproductive success, favourable larval dispersal conditions, or natural variability in predator-prey relationships (Dana et al. 1972; Vine 1973). Given the immense reproductive capacity of CoTS, very moderate changes in rates of fertilisation or larval survival over successive cohorts have the capacity to initiate population outbreaks (Wilmes et al. 2018). The exact cause of the higher-than-normal recruitment year may be a result of natural vagaries in intrinsic or extrinsic processes (e.g., the enhanced fertilisation success of a naturally aggregated population, or by hydrodynamic larval retention), however it is not thought to be directly linked to anthropogenic activities (Dight et al. 1990; Hock et al. 2014; Wooldridge and Brodie 2015). This hypothesis is strongly tied to the predator-prey dynamic between CoTS and coral which results in oscillations of outbreaks, with coral prey as the limiting factor.

The precise cause(s) of CoTS outbreaks remains equivocal, with no single hypothesis gaining universal support. It is possible that these three major hypotheses are not mutually exclusive, but

Population dynamics of CoTS: drivers and impacts

CoTS outbreaks occur due to the confluence of several different factors (Babcock et al. 2016a). Whilst the unique life-history traits of CoTS appear to naturally predispose them to population fluctuations, anthropogenic factors (e.g., fertilisers, overfishing) may be exacerbating the incidence and severity of population outbreaks. Further, climate-driven changes to the environment which are occurring concurrently, alter the capacity of ecosystems to withstand and respond to population outbreaks, meaning the impacts of each CoTS outbreak are different to the last.

Regardless of what initiates population outbreaks, the consequences of greatly elevated densities of large adult CoTS can be far-reaching. When CoTS reach high densities and spawn, vast quantities of larvae are transported by downstream currents which can result in successive spread of outbreaks over several years (Dight et al. 1990). This phenomenon has been termed 'secondary outbreaks' (Endean 1974; Pratchett 2005; Fabricius et al. 2010) and has been observed on the Great Barrier Reef for each of the major outbreaks which have been documented (Kenchington 1977; Reichelt et al. 1990a; Vanhatalo et al. 2017). Understanding and managing the processes that contribute to primary outbreaks, would have capacity to limit the catastrophic implications of secondary outbreaks. If management could understand and pre-empt the most catalysing changes that lead to exponential population increases, then early interventions could be employed to prevent or contain initial outbreaks, making any management strategy much more tractable.

Despite the ecological importance of early detection, logistical limitations to sampling populations in their low density (pre-outbreak) state have so far hindered our ability to capture these early changes (e.g., Dumas et al., 2022; Pratchett, 2005). Conventional methods for sampling CoTS, such as manta tows and scuba searches, are designed for assessing the large-scale incidence of established population outbreaks. These methodologies are not suitable for sampling CoTS in low densities, which are typically highly cryptic and widely dispersed (Fernandes et al. 1990; Pratchett et al. 2017b). Employing suitable methods to conduct recurrent surveys of an outbreak community over several years could provide unprecedented data on outbreak evolution. Whilst the 'outbreak phase'

is temporally brief and anomalous, rather than the predominant condition, most research on CoTS is initiated and undertaken only after population outbreaks are already established (e.g., Dumas et al., 2022; Pratchett, 2005). Accordingly, there are few studies that have captured the changes that occur before versus during population outbreaks, which leaves considerable gaps in our knowledge of mechanistic underpinning of population build-up, and prevents our ability to intervene early.

There are observed and anecdotal reports of differences in demographics, behaviour and biology of *Acanthaster* at high (e.g., >15 CoTS.ha^{-1}) and very low (e.g., <1 CoTS.ha^{-1}), however the extent of these differences and the transition between population phases remains largely unstudied, for reasons explained above. Comparing quantitative and qualitative data on the biology and behaviour of CoTS to population densities may establish whether there are fundamental shifts in demographics that explain the population increases and decreases. More critically, understanding the processes involved in the initiation of population outbreaks may help to resolve the extent to which anthropogenic pressures (e.g., over-fishing and eutrophication) or natural processes cause or contribute to these phenomena (Babcock et al. 2020).

This chapter outlines what is already known about CoTS behaviour and biology during their low-density state, their high-density state, when it can be definitively distinguished, and their aftermath state, to identify where knowledge gaps lie and begin to understand the transition between outbreak states.

1.2 Densities

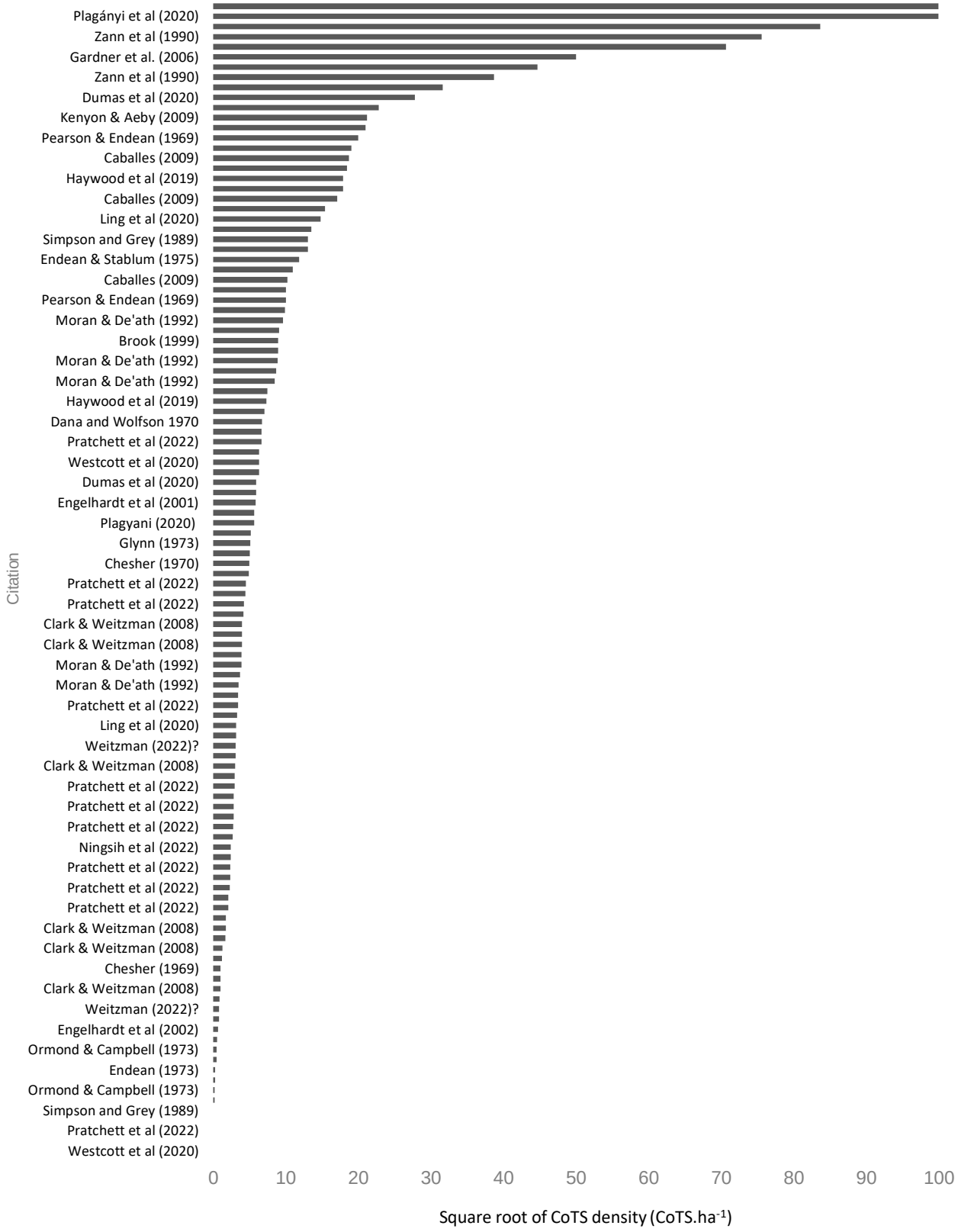


Figure 1.1 *Density estimates of Acanthaster cf. solaris, taken from 50 peer reviewed publications of primary data. Publication dates range from 1969-2022. Where multiple density estimates are stated within the paper, all are included*

1.2.1 *Variation in CoTS densities*

Estimated densities of CoTS vary from 0 CoTS.ha^{-1} (Westcott et al. 2020) to >1,000 CoTS.ha^{-1} (e.g. Kayal et al. 2012b). Previous studies have tended to emphasize a presumed dichotomy between 'non-outbreaking' and 'outbreaking' populations (Moran and De'ath 1992a; Pratchett et al. 2017b), but reported densities reveal a broad continuum of CoTS densities (Figure 1.1). There is evidence too, that the density at which a population is considered ecologically sustainable can vary (Moran and De'ath 1992a). For example, it has been shown that a reef in Japan could sustain high densities of CoTS (>20 CoTS.ha^{-1}) for decades without collapse (Nakamura et al. 2014), whilst on the GBR in 2013/2014, populations were seen to increase rapidly, peak, before rapidly declining with a peak density of only 15 CoTS.ha^{-1} (0.24 CoTS per 2min tow)(Engelhardt 2018). The peak density is likely to be linked to multiple extrinsic factors such as coral cover, coral composition, topography and disease (Engelhardt, 2018; Pratchett et al., 2017), and this could explain why CoTS densities can show considerable variation even locally, among different habitats of the same reef (Pratchett, 2005), making the definition of an outbreak using density alone challenging.

Although, like many organisms, it is possible that CoTS populations are never truly stable (Wallner 1987), outbreaks do not necessarily occur at all reefs. Indeed, the 'non-outbreaking' state is the prevailing state for most CoTS populations, though there is a lack of baseline data on densities of CoTS at reefs that do not experience outbreaks, or during the period between outbreaks. Reports of natural levels vary from 0.05 CoTS.ha^{-1}(Ormond et al. 1973) to <140 CoTS.ha^{-1} (Endean and Stablum 1973). Data on juvenile densities both before and during outbreaks is also lacking, as well as larval densities and settlement rates (Pratchett et al. 2021).

While CoTS densities provide the most relevant measure to compare the extent and severity of outbreaks (Moran 1986), there are considerable challenges to effectively quantifying local CoTS densities (Pratchett et al. 2014), especially at low to moderate densities. Gaining accurate data on densities of CoTS outside of outbreaks would not only improve our understanding of outbreak

population dynamics, but could also be vital for developing early warning systems, where the first signs of changes away from baseline densities could trigger an early intervention. Further work is needed to quantify with certainty the densities of adults, juveniles and larvae whilst non-outbreaking, incipient and in the aftermath of an outbreak.

1.2.2 *Fundamental thresholds*

While it is likely that CoTS populations are inherently unstable, whereby moderate changes in environmental conditions or other extrinsic process can lead to marked changes in local densities, it is commonplace in the literature for CoTS populations to be classified as either 'non-outbreaking' or 'outbreaking' according to their population phase at that time. Qualitative and quantitative definitions of an outbreak date back to the 1960s (Chesher 1969b; Pearson and Endean 1969) and were linked to our understanding of a 'typical' outbreak, with less consideration for the continuum over which populations could exist. The basis for defining an outbreak has been inconsistent over the past 50 years, possibly reflecting variability in population dynamics and corresponding ecological effects of CoTS outbreaks. Chesher (1969) first highlighted the ambiguous and inconsistent nature of definitions and 45 years later Pratchett et al. (2014) reported that ill-defined definitions continue to be problematic.

The concept of an outbreak, being *unsustainable* densities of CoTS, was first alluded to in a qualitative definition by Potts (1981) and more recently expressed by Sweatman and Cappo (2018) "*outbreak densities of starfish consume coral faster than the corals recover and grow*" (pg. 3). These definitions which only consider reductions in local coral cover are thought to be oversimplistic however, as selective feeding by CoTS can still drastically impact a reef and its functioning, without necessarily suppressing local coral cover (Keesing et al. 2019). Moran et al. (1992) calculated what they believed to be 'sustainable limits' for CoTS populations during surveys of 334 reefs on the GBR, by observing that substantial coral mortality was only instigated by populations that exceeded 15 CoTS.ha^{-1}, equivalent to >0.22 per 2-min manta tow (Moran et al. 1992). They proposed 15 CoTS.ha^{-1}

as the operational threshold for outbreaks on the Great Barrier Reef. This quantitative definition has been widely accepted and referenced ever since.

With sustained declines in coral cover at many locations in the Indo Pacific (Bruno and Selig 2007; Mellin et al. 2019) fixed thresholds of CoTS densities to indicate the occurrence of a population outbreak (e.g., >15 CoTS.ha^{-1}; Moran and De'ath 1992) may be outdated (Pratchett et al., 2014). For example, Plagányi et al. (2020) demonstrated that CoTS densities as low as 4 CoTS.ha^{-1} can cause net coral loss, depending on local coral cover and composition. A variation of this sustainable density was proposed by (Keesing and Lucas 1992) who calculated the threshold by taking into account not only CoTS densities but also their feeding rates and the growth/turnover of corals. Their study estimated a similar threshold of 1,000 CoTS.km^{-2}, or 10-15 CoTS.ha^{-1} on reefs with 20% coral cover.

The definitions used to classify outbreaks have changed as our knowledge of CoTS has developed and our motivation for assigning outbreak status has changed. For example, the aforementioned ecological thresholds, which primarily focus on net coral loss, are not useful for management purposes where early prevention of CoTS outbreaks is the goal. More conservative definitions focus on the potential for population growth (and hence future damage) of a population, by considering the reproductive potential at different densities. This approach classifies a critical outbreak density as one where reproductive success can occur (Rogers et al. 2017; Westcott et al. 2020). Rogers et al. (2017b) proposed a density threshold (<3 CoTS.ha^{-1}) below which reproductive success would be disrupted due to an Allee effect. Similarly, Babcock et al. (2020) suggested a reproductive threshold, but importantly considered the non-linear relationship between CoTS abundance and larval production, whereby larval production increases rapidly at certain densities as a result of relieving the Allee effect (Babcock et al. 2020). They suggested the level to be 7-9 adult (2 years+) CoTS.ha^{-1}, above which population outbreaks could develop. The effect of CoTS size and feeding history on fecundity, which is significant (Caballes et al. 2016), was also considered in their model.

Fundamentally, both managers and researchers will benefit from consistent and rigorously established density thresholds to distinguish reefs subject to CoTS outbreaks. It is important that relevant density thresholds consider the specific ecological processes that will further influence the ecological effects of CoTS (including size of individuals, patterns of aggregation, feeding rates, coral cover and composition), which may require dynamic thresholds. Thresholds which account for feeding rates, for example, which are known to vary according to individual body size and prey availability (Keesing and Lucas 1992; Caballes et al. 2016), will be valuable for modelling more realistic estimates of CoTS feeding compared to estimates which scale feeding impact directly with CoTS densities, irrespective of conditions. The most commonly adopted method currently used to distinguish outbreaks on the GBR is based on manta tow surveys (Babcock et al. 2020; Emslie et al. 2020); Westcott et al. 2020) where >1 CoTS per 2-minute manta tow (equivalent to 2,000 m^2) is used to signify an active outbreak. Whilst this is an efficient method for collecting low-resolution density data over large scales, influential aspects of CoTS impact such as CoTS body size (Keesing & Lucas, 1992) are not incorporated.

1.3 Variation in CoTS Biology with Population State

Cheney (1974) was one of the first to recognize that there are fundamental differences in biology and behaviour of CoTS with varying density and food resources. He commented that CoTS in Guam existed in two 'distinct behavioural modes', stating that low-density populations at Piti were dispersed, nocturnal, and hidden, with variable gonad size and state, whilst another high-density population at Catalina Point was found to be aggregated, with uniform gonad size and state, and feeding during the day (Cheney, 1974). His early observations of the two extreme states of CoTS population and behaviour has had little research focus since, however it is relatively well-known that the disparity in population states exists. Building on Cheney's fundamental findings this chapter compiles further information on the differences between the distinct behavioral modes. By doing so, we can understand how and why populations change between the two states, and critically, whether there are shifts in behaviour and/or biology which can explain the population growth.

Population dynamics of CoTS: drivers and impacts

In this section, current knowledge of the biology of CoTS is outlined, in terms of their growth, size and mortality, during their low-density versus high-density states. Herein, non-outbreaking populations will refer to persistent low densities, usually <5 CoTS.ha^{-1}, where CoTS are widely dispersed and have negligible effect on the local abundance of coral prey. Conversely, 'outbreaking' will refer to periodic and temporary increases in local densities, usually 10s to 1000s CoTS.ha^{-1}and visibly abundant on a reef. As it will be important to distinguish between low density populations that preceded versus follow population outbreaks, I will use 'pre-outbreak' and 'post-outbreak' when referring to non-outbreaking populations.

1.3.1 *Size and growth*

Aside from differences in densities, one of the most well documented and noticeable differences between outbreaking versus non-outbreaking populations is the disparity in their body size (Cheney 1974; Moore 1990; MacNeil et al. 2017). During outbreaks, CoTS populations tend to have considerably smaller modal sizes than those found in non-outbreak populations (Kettle, 1990; MacNeil et al., 2017; Pratchett, 2005). Lawrence & Lane (1982) went as far as suggesting an inverse relationship between average body size and density. This theory was supported by a study which involved recurrent sampling of the GBR where starfish found on the well-established outbreak sites of Lizard Island, Emily Reef and Spitfire Reef, were found to have substantially smaller median sizes (~300mm) than those found at reefs with low densities of starfish, such as Centipede and Davies Reefs (~400mm) (MacNeil et al. 2017). The smaller average body sizes found at these outbreaking reefs correspond to records from established outbreaks recorded on the GBR in the 1990s (Engelhardt et al., 1999; Pratchett, 2005). Other inter-reef comparisons from other Pacific locations have also noted this trend (MacNeil et al., 2017; Pratchett et al., 2017; Zann et al., 1990). MacNeil et al. (2017) stated that the maximum diameter of CoTS is usually constrained to <400mm during population outbreaks on the GBR, with a recorded median diameter of 349mm during sampling of outbreaking populations undertaken between 2013-2014 (MacNeil et al. 2017). Similarly, Pratchett et al. (2014) reported the vast majority of starfish during surveys of an outbreak on the GBR were

<450mm. Post outbreak, maximum sizes were recorded to increase from 480mm in 1996, to 620mm in June 1998.

For pre-outbreaking, low-density populations, CoTS have been recorded with much higher mean sizes of 420-510mm (Souter 2007) with extensive reports of individuals as large as 750mm (Stump 1994, Pratchett et al., 2014). The majority of the very large specimens were found on the GBR (Pratchett et al., 2014; Stump, 1994). There is also data on CoTS from *post-outbreak* populations, although data is relatively limited. In contrast to pre-outbreak low density populations, these aftermath populations are dominated by very small individuals (Engelhardt et al. 2001). Pratchett (2005) documented the rapid decrease in mean size of starfish in the aftermath of an outbreak on the GBR and recorded modal sizes drop from 350-400mm during the outbreak, to 250-300mm in the aftermath, with multiple starfish present <150mm. Another study from the central GBR (Mackay reefs) in 1999, found collapsed populations of adult CoTS in the aftermath of an outbreak, resulting in a juvenile-dominant remnant population with max sizes <150mm, and many between 20-40mm (Engelhardt et al. 2001).

The differences in mean body size between populations may be reflective of constrained growth rates and/or limited longevity during population outbreaks (MacNeil et al., 2017). However, the extent to which growth is affected by food quality and quantity, as opposed to being determined by age, is controversial (Deaker et al. 2020). It has been difficult to make assessments of age and growth of CoTS, firstly, due to the logistical difficulties of reliably ageing CoTS (Kettle & Lucas, 1987; Pratchett et al., 2014; MacNeil et al., 2017; Kwong et al., 2021) and secondly due to the number of variables that can play a part in an individual's growth, such as food, temperature, reproduction, wave exposure and competition (Kenchington, 1977; Lucas, 1984; Ormond et al., 1973). These variables make it difficult to know the precise cause of growth disparities within and between populations.

Population dynamics of CoTS: drivers and impacts

Growth rates and growth phases of CoTS have been studied in laboratory settings, and distinct growth phases have been identified during the life span of a starfish, following a von Bertalanffy growth function (Lucas 1984). This growth pattern sees initial rapid growth up until sexual maturation, after which growth slows considerably, presumably due to increasing energy investment in reproduction (Pratchett et al. 2014). These age-specific growth rates, which Lucas (1984) found to be 'remarkably consistent' in the laboratory, could be influenced by the multitude of extrinsic factors in the field. However, Yamaguchi (1973) and Zann et al. (1987) documented growth patterns in the field which were consistent with laboratory observations.

In environments where food is not limited (such as pre-outbreaking populations), CoTS maximum size is only constrained by the higher metabolic requirements that come with increasing size (Keesing 1990). At high densities however, where intraspecific competition for food can be severely limiting, growth rates have been shown to be finite and directly linked to extrinsic factors. The effect of food limitation on growth rates in larval, juvenile and adult life-phases of CoTS has been demonstrated during multiple lab studies (Yamaguchi 1974; Lawrence and Lane 1982; Lucas 1984), and found that starved individuals may not only slow their growth but can actually reduce in size (Chesher 1969b). In addition to quantity, food type has also shown to affect growth rates (Caballes et al. 2016) and maximum size of individuals (Ormond et al. 1973) where CoTS have shown 20-fold differences in maximum size after receiving a sub-optimal diet (Lucas 1984). Field observations by MacNeil et al. (2017) support these laboratory studies, where CoTS in a food-constrained outbreaking population were found to grow more slowly and reach a smaller ultimate size, than CoTS at low densities.

The food available during a CoTS' juvenile phase is likely to be particularly influential on its ultimate size and growth rates, as this is the period when CoTS transition to coral prey and grow rapidly, likely in an attempt to outgrow predators (Keesing 1990). It has been suggested that without sufficient prey available during this stage, such as during an outbreak or post-outbreak, then juvenile

CoTS have the ability to achieve growth stasis and remain as a 'hidden army' in the reef infrastructure until coral conditions are more favourable (Deaker et al. 2020).

It is evident that initial growth and ultimate size is somewhat driven by food availability (Deaker et al. 2019), which could explain the differential mean size of pre-outbreak, outbreak and post-outbreak populations, as a result of access to sufficient nutrition. However high density 'outbreaking' populations are not *always* limited by food, in fact severe food limitation happens late in the outbreak cycle (e.g., Pratchett, 2010), directly before the population crashes. It could be that other environmental pressures related to high-density populations are affecting growth, such as competition for space, reduced predation pressure or differential resource partitioning by outbreaking individuals (Kayal et al., 2012). A comparison of the three population states - pre-, mid- and post-outbreak could help to unravel the role of density vs food availability in size and growth.

Another potential explanation for the smaller ultimate sizes in outbreaking populations could be the different life-history approach adopted by CoTS at high densities. It has been shown that CoTS in outbreaking populations increasingly partition energy into reproductive output rather than somatic growth, meaning they can achieve reproductive maturity at smaller sizes than they would in normal populations (Yamaguchi 1973). Studies have shown that CoTS can reach sexual maturity at sizes as small as 130mm and in an outbreak in Guam, starfish as small as 50mm and 70mm were found with developing gonads (Yamaguchi 1973; Cheney 1974). This adaptation may be a result of prioritising reproduction overgrowth, given the limited energy resources available and the likelihood of earlier mortality in these populations, or it could be that there is no longer a demand to grow large, given the reduced need for predator avoidance or for extreme fecundity in these high-density environments.

Although there is sufficient data on maximum ultimate sizes of CoTS in all three population states, data on growth rates of populations in the field is lacking (Pratchett et al. 2021). The knowledge gap is due to the inherent difficulties of measuring growth in CoTS, as tagging has proven challenging and

growth bands on spines were found to be unreliable (Stump 1994; MacNeil et al. 2017; Kwong et al. 2021). Capturing differential growth rates would allow us to have a better understanding of population recruitment and longevity of individuals, as well as validating the 'hidden army' hypothesis (Deaker et al. 2020).

1.3.2 *Longevity*

Longevity of adult CoTS is much higher in non-outbreaking populations, where individuals attain very large sizes and live up to 12 years (Chesher 1969b) or longer (>14 years; Pratchett et al., 2017). The cause of mortality in these populations is largely unknown, but likely to be as a result of predation or senescence and would follow a determinant Holling Type-III response (Moore 1990). Conversely, there appears to be major constraints on longevity during outbreaks (Pratchett 2005). The cause of death in outbreaking populations is equivocal, especially as high-density populations are often reported to display precipitous declines in abundance (Endean 1969; Pratchett 2005). Potential causes of mass mortality are thought to be starvation and/or disease (Mills 2012), which may be exacerbated by the significant energetic investment in reproduction, especially for female CoTS. Conversely declines in abundance may be attributable to mass migration rather than mass mortality (Endean 1969). Data on mortality rates and causes of mortality in both environments are severely lacking.

Whilst predation rates in the early life stages of CoTS populations are extremely high and influential on their recruitment (Cowan et al. 2020), predation risk appears to decline significantly with increasing size (Caballes et al. 2022). The most likely cause of mortality for CoTS in low density populations with abundant resources is senescence. Despite increased feeding capacity at larger sizes, and with access to high quality prey, the metabolic demands of their biomass and extremely large gonads eventually outweigh their capacity to feed. The energy deficit results in their growth slowing and death follows (Lucas 1984; Kettle and Lucas 1987).

Starvation of CoTS could be expected, as severe outbreaks inevitably lead to depletion of coral prey, and especially highly preferred prey species (Caballes et al. 2016). Although this may be the case for some populations (Endean, 1969), it cannot explain the rapid population declines that occur when coral cover remains intact. For example, Pratchett (2010) reported rapid declines in starfish populations at Lizard Island marking the end of an outbreak, whilst the mean coral cover across all locations was 23%; similar declines were documented by Zann et al. (1987) in Fiji. Moreover, Pratchett (2010) demonstrated simultaneous declines in abundance across multiple size classes, suggesting limited role of senescence. In these situations, there must be another mechanism causing the precipitous declines in CoTS densities.

Another possibility is the rapid transmission of disease through populations, particularly at high densities, brought about as opportunistic pathogens take advantage of the compromised health and condition of CoTS with limited quantity and/or quality of dietary resources and heightened competition (Caballes et al., 2016; Keesing, 1990; Lucas, 1984; Pratchett et al., 2017; Zann et al., 1990). Mills (2012) found that CoTS in high densities invested more energy into immune defense than individuals in a low-density population, suggesting an adaptation preparing them for the higher likelihood of infection that occurs in higher density environments. Similar mass mortalities through disease are well known to occur in other echinoderm species (Birkeland 1989).

Another explanation for early mortality, which may similarly result through compromised energetic condition, is the mass die-off of females after spawning. Some studies have recognized that the sex ratios of populations in the final stages of an outbreak, were severely skewed. For example, in an outbreak at Lizard Island, sampled after the peak densities were already declining, only 2 out of 78 mature starfish were female (Pratchett, 2010), and the same pattern was found for an outbreak in Guam (Caballes et al. 2016). It is thought that these male-skewed populations may result due to the lower survival rates of females who invested considerably more energy into reproduction than their

male counterparts (Stump 1994). Without potential to successfully reproduce, the population would collapse.

Some studies have suggested that longevity of CoTS is compromised due to increased reproductive investment in outbreaking populations (Kettle 1990). Understanding mortality rates and the prevailing cause of mortality in CoTS populations, particularly outbreaking populations, could have important implications for predicting population growth and managing outbreaks effectively.

1.3.3 *Fecundity and reproductive condition*

CoTS are primarily dioecious, sexually reproducing starfish (Yamaguchi 1973). However, recent studies have reported rare cases of cryptic hermaphroditism in some populations (e.g., Guerra et al. 2020; Hart et al. 2021), suggesting occasional deviations from this general reproductive mode. Their phenomenal fecundity is undoubtedly contributing to the initiation and progression of outbreaks (Uthicke et al. 2019), and so it is critical to understand their reproductive dynamics. Investigating differences in reproductive biology and behaviour between the low density and high-density populations will provide an insight into how the reproductive strategies shift over the course of an outbreak and what effects that will have on future progeny.

Given the larger maximum sizes of CoTS recorded in non-outbreaking populations, it is very likely that the reproductive potential of individual CoTS (i.e. fecundity) in low densities is much higher than during outbreaks, however this has never been explicitly investigated. Conand (1984) first described the positive relationship between size and fecundity, while recent studies (Babcock et al., 2016; Pratchett et al., 2021) demonstrated that fecundity increases exponentially with increasing size (diameter) of both male and female CoTS. It has been shown that as CoTS increase in size, their somatic growth slows, and they commit proportionally more energy into gonad development as reproduction is progressively prioritised (Birkeland and Lucas 1990; Caballes and Pratchett 2014; Rogers et al. 2017).

As discussed in the previous section on size, food availability will have a major influence of growth and ultimate size for CoTS. For the same reasons as discussed above, CoTS may be constrained in their growth due to limited resources and consequently have lower reproductive potential as a result of size-based fecundity (Babcock et al. 1994). This idea is supported by a recent study which found that female CoTS with abundant food access, increased in both weight and gonad mass, compared to starved individuals (Caballes et al. 2016), whilst other studies have also recognized a relationship between food availability and reproductive potential (Kettle 1990; Pratchett et al. 2014). Caballes et al. (2016) found that it was not only food abundance that was affecting the reproductive condition of CoTS, but also the prey composition. Where preferred prey items (*Acropora*) were available, the size, quality and quantity of oocytes produced by females were superior to CoTS with access to non-preferred prey (*Porites rus*). Larger and more rounded eggs are known to benefit fertilisation and provide higher nutritional content to progeny during their vulnerable early life stages (Deaker and Byrne 2022).

Whilst CoTS in high densities are markedly smaller, which suggests their gonad potential would be less, there is evidence that these populations partition energy towards gamete production earlier, instead of somatic growth (Cheney, 1974), which standard size-based fecundity models would not account for. This means CoTS in high-density populations could have well-developed gonads from much smaller sizes than the normal population. For example, Yamaguchi (1974) induced spawning in CoTS as small as 150mm in Guam, demonstrating that growth can be slowed but gonads can still be developed at these smaller sizes.

As food quantity and quality will undoubtedly vary between outbreaking and non-outbreaking populations, these findings have implications for the reproductive potential of both. Studying when reproductive condition becomes compromised, and whether this is a linear decline with increasing densities or whether a reproductive threshold is reached, would have important implications for outbreak progression/decline and population modelling.

1.3.4 *Spawning*

Spawning behavior is an important feature of fertilisation success; however, it is relatively understudied in the field, due to the difficulty in predicting and capturing the temporally brief event. To date only Babcock & Mundy (1992) and (Gladstone 1992) have recorded observations of mass spawning events in the field. It is generally assumed that spawning is timed to coincide with optimal conditions for larval survival (Caballes & Pratchett, 2017), and influenced by temperature (Yasuda et al. 2010) and photoperiod (Lucas, 1973). On the GBR, the spawning season also coincides with high nutrient input, enhanced phytoplankton levels & lowered salinity from heavy rainfall, all variables which could promote larval survival (Houk et al. 2007; Caballes and Pratchett 2017). It is predicted that the specific timing of spawning differs between discrete populations (Caballes et al., 2017), and is likely initiated by localized environmental cues

In comparison to other marine invertebrates, CoTS demonstrate exceptionally high fertilisation rates over large distances, for example (Babcock et al. 1994) recorded > 20% fertilisation when female CoTS were 64 metres downstream of males. The superior fertilization success is likely due to the extremely large volumes of gametes that are released during spawning (Babcock et al. 2016b) and also the enhanced competence of sperm over long distance and in low concentrations compared to other marine invertebrates (Benzie et al. 1994). Although gametes of CoTS are able to remain competent and travel long distances, it is the synchrony of spawning that is fundamental for successful fertilisation (Beach et al. 1975), especially for CoTS in low densities. In the absence of conspecifics to synchronously spawn with, CoTS were found more likely to reabsorb their gametes than wastefully shed them, as they are energetically expensive to produce (Babcock et al. 2016b). Fertilisation rates have been measured as high as 99% in the field where spawning synchrony was high (Babcock et al. 1994). The exact trigger of spawning is unknown, but biological cues from spawning conspecifics can act as spawning ‘synchronisers’ (Caballes and Pratchett 2017). Beach et al.

(1975) proved the effect of this by inoculating tanks with gonad pheromones and inducing gamete shedding in CoTS.

The majority of (limited) research on spawning behaviour of CoTS focuses on spatial and temporal features of spawning behaviour (Gladstone 1992; Caballes and Pratchett 2017; Caballes et al. 2021). As such, there have so far been no explicit comparisons of spawning behaviour between low- and high-density populations or with varying food availability. It could be useful to know whether any differences in spawning behaviour or aggregation occur.

1.3.5 *Spawning aggregations*

In addition to spawning in synchrony, population aggregations will increase fertilisation success, especially among low-density populations, by relieving the Allee effect (Lundquist and Botsford 2004). Despite a number of papers describing the role of aggregation on reproduction in other low-density free-spawning marine invertebrates (Levitan and Young 1995; Claereboudt 1999; Mercier and Hamel 2009), there are relatively few papers on its influence for CoTS aside from Babcock et al. (1994) and Rogers et al. (2017). In particular, there is limited evidence to suggest that CoTS do actively aggregate ahead of spawning. Importantly, CoTS may be aggregating for other reasons (as discussed in 'Feeding aggregations' below) which has the capacity to inadvertently increase the fertilization success achieved by low density populations. The formation of low-density aggregations should be explored further due it its potential significant in facilitating of outbreaks.

At low densities and considerable dispersion across a reef, reproductive capacity of CoTS is greatly limited by the distance between individuals (Endean and Cameron 1990). However, it has been modelled that when CoTS in low densities aggregate, the Allee threshold is surpassed, and fertilisation success may be greatly increased (Courchamp et al. 2008; Rogers et al. 2017). Rogers et al. (2017) modelled simulations of various densities and aggregation levels and found that whilst aggregative behaviour greatly increased fertilisation success at low densities (<10 CoTS.ha^{-1}), the benefit of aggregations declined as population density increased (>15 CoTS.ha^{-1}) and aggregating

actually became *detrimental* to reproduction, as high levels of polyspermic fertilisation were found to occur. The models presented in this study were supported by field observations and found that for densities below 3 CoTS.ha^{-1}, aggregation was actually imperative to relieve the Allee effect (Rogers et al. 2017). Interestingly, near- 'optimal' levels of aggregation have been observed in the wild for both high-density populations (Babcock et al. 1994) and low-density spawning populations (Rogers et al. 2017).

The spawning behaviours of CoTS (synchronised spawning, aggregation) have evolved for successful fertilisation over highly dispersed, low-density populations. However, these traits may actually have a detrimental effect on fertilisation success once populations reach high densities, as sperm concentrations are too dense for monospermic fertilisation. More work is needed to ground truth concepts about spawning aggregation and fertilisation in both low density and high-density populations, as it appears that proximity of spawning starfish may be more important than adult densities in determining reproductive success (Pratchett et al., 2017), which has implications for highly aggregated low-density starfish populations. Understanding this area of reproductive dynamics could hold critical answers about outbreak initiation.

1.3.6 *Population replenishment*

Overall rates of population replenishment, encompassing the full succession of processes that influence reproduction, fertilisation, larval development, dispersal, settlement and post-settlement ontogenetic transitions, are fundamental for population growth and initiating population outbreaks (Deaker et al., 2020; Pratchett et al., 2021). There is, however, very limited research on factors affecting population replenishment in the field, especially for low density (pre-outbreaking and post-outbreaking) populations (Keesing and Halford 1992). Fertilisation rates of CoTS are particularly dependent on the distribution and density of CoTS, whereby viable fertilisations may be constrained under widely dispersed, low density population states, but also under high density aggregated population states as a result of polyspermy (Rogers et al. 2017). Unsuccessful fertilisation

in either of these scenarios could significantly constrain reproductive output and population recruitment. Beyond successful fertilisation, the key factors involved in recruitment to the adult population are larval abundance, larval provisioning, settlement and post-settlement competition and survival (Levitan & Sewell, 1998).

For the planktonic larval stages, survivorship is largely governed by the energetic stores that were provided to the larvae during early development, which is shown to be directly related to maternal nutrition (Caballes et al. 2016). Larvae produced during periods of high coral availability have been found to have enhanced survival, particularly in periods of low phytoplankton, compared to larvae produced when maternal nutrition was poor (Caballes et al. 2016). The maternal nutrition of CoTS is likely to be strongly tied to population density and also stage of the outbreak, so larvae survival will also likely be linked to this. When conditions are such that huge quantities of larvae are produced (i.e. during peak adult densities), it does not always translate to high rates of settlement, as this is a significant bottleneck in their early life-history (Lucas 1973), largely due to predation.

Once larvae have survived the planktonic phase, they are evolved to preferentially settle in habitats that would promote their survival and limit their chances of predation (Keesing and Halford 1992; Doll et al. 2021). Larvae select habitats that have proximity to crustose coralline algae (CCA), which is their preferred prey during their early juvenile stages (Deaker and Byrne 2022). Additionally, it has been shown that larvae are attracted to cues of conspecific adults when settling, speculated to be because of the reduced predation risk from coral polyps brought about by feeding adults (Chesher 1969b). Brachiolaria larvae have shown preference for settling on clean coral skeletons (Ormond et al. 1973). After initial metamorphosis, food availability (CCA) is rarely limiting, but their survival is likely moderated by predation (Lucas 1973). Mobile predators (fish & invertebrates) are thought to be responsible for the highest rates of predation (Keesing et al. 2018), and size is a key factor of mortality (Caballes et al. 2022), however little more is known. Zann et al. (1987) followed a

population of small juveniles (18-130mm) in the field and documented mortality as high as 99.3%, however this was attributed to disease.

At around 4-12 months, juvenile CoTS transition to coral feeding juveniles (Yamaguchi 1974), and their growth speeds up considerably as a result of the ontogenetic shift (Lucas, 1984; Wilmes et al., 2020). Although the cue for larvae to settle near feeding conspecifics may be beneficial for the earliest life stages, and for low density populations of CoTS, in high density outbreak populations this may mean that juvenile CoTS don't have access to coral prey once they make this transition as local prey has already been depleted. There is some controversy around the topic, but it has been reported that juveniles have the ability to delay the dietary shift if the availability of coral is not sufficient to support them, this is known as the 'hidden army' hypothesis (Deaker et al. 2020). If the transition does not take place, the normal age:growth trend is considerably altered as the growth is slowed or even stopped completely. It could be possible therefore, that in the aftermath of outbreaks, where corals are depleted to a degree that adult CoTS will not be able to exist, high numbers of juveniles can wait in the rubble until coral is sufficiently replenished. This phenotypic growth plasticity may allow CoTS to persist in times of low coral cover which would influence the population replenishment during an outbreak, however, remaining small does make them more vulnerable to predation. This hidden army hypothesis could explain the high densities of juveniles which have often been found in the coral rubble after the crash of a high-density adult population (Engelhardt et al., 2001; Pratchett, 2005).

Improved understanding of larval settlement, juvenile mortality and juvenile growth stasis will inform our understanding of population replenishment and also renewed outbreak formation; these are critically lacking aspects of CoTS demography. New sampling techniques that enable improved detection and quantification of juveniles (Wilmes et al. 2020) and larvae (Uthicke et al. 2018; Doyle and Uthicke 2021) have recently been developed which will hopefully fill these knowledge gaps. More resolved genetic methods will be highly valuable for ascertaining the source

of larvae arriving into building populations, this development will be key for proving or disproving major theories of outbreak initiation.

1.3.7 *Sex ratios*

The ratio of males to females in a population has the potential to greatly constrain reproductive potential (Stump 1994). Most notably, the predominance of males in the immediate aftermath of population outbreaks (Stump, 1994) may constrain subsequent reproduction and replenishment. Although there are studies which have recorded sex ratios in the field (Nishihira and Yamazato 1974; Stump 1994; Caballes 2017), the body of research is not strong enough to currently assess when and why sex rations become skewed, and if they do, whether it results from density or other factors. Stump (1994) suggested that females may be more likely to die in the aftermath of outbreaks when food is limited, due to their disproportionate energetic investment in reproduction, thereby leading to increasing male bias. Rogers et al. (2017b) modelled different scenarios of biased sex ratios and demonstrated how a female skewed population would have the potential to result in a population explosion. For male biased populations, it was shown that lower reproductive success would be exacerbated by the impact of polyspermy, where the fertilisation of an egg by more than one sperm results in an unviable larva. A better understanding of the dynamics of sex ratios over the course of an outbreak would greatly aid our knowledge of outbreak dynamics and possibly explain rapid increases and declines in population numbers (Rogers et al. 2017).

1.4 Variation in CoTS Behaviour with Population State

CoTS have been found to exhibit plastic behaviour, which is likely influenced by their environment (Moran 1986; Keesing et al. 2019; Ling et al. 2020). Most notably, there have been reported shifts in the feeding behaviour of CoTS, coinciding with increasing densities and the onset of population outbreaks (Moran, 1984). However, it is not clear whether these changes relate to density *per se* or are inherent responses to changes in food availability.

1.4.1 *Feeding selectivity*

Population dynamics of CoTS: drivers and impacts

CoTS feeding behaviour is the primary driver of their impact during outbreaks. Consequently, it has been extensively studied and is relatively well understood across both outbreaking and non-outbreaking populations (Collins, 1975; Keesing, 1990; Ormond et al., 1976; Pearson & Endean, 1969; Pratchett, 2007). It is known that in low densities CoTS do not cause significant coral depletion (Glynn 1974), but conversely may play a valuable role in maintaining or enhancing biodiversity (Porter 1972; Colgan 1987) by selectively consuming 'weedy' fast growing corals and allowing space for a more diverse range of slow-growing corals to settle and grow. This ecological function has been brought about by evolution of strong prey preferences, slow feeding rates and unique body form that allows efficient feeding on branching and tabular corals. At high densities however, these behaviours are no longer beneficial to the environment, and conversely the strong selective feeding can cause rapid and pronounced loss of some taxa (Kayal et al. 2012), negatively effecting the community structure and physical structure of the reef, impacting the ecosystem as a whole.

Since the 1960s it has been known that CoTS in low densities show strong preferences for corals from the Acropororidae and Pocilloporidae families, whilst *Porites*, *Favites* and *Goniastrea* are non-preferred (Pearson and Endean 1969; Collins 1975; Ormond et al. 1976; Keesing 1990; Ling et al. 2020). De'ath and Moran (1998) conducted field studies on the GBR and found that *Acropora* was favoured 14:1 over *Porites*, and additionally there was a preference for tabular growth forms over all other forms. Preference for particular size classes has also been shown (Kenyon and Aeby 2009), but interestingly, preferences in growth form and size were found to vary between coral species. Although the exact feeding preferences a CoTS population exhibits do not tend to alter between seasons or within a region, there is evidence that preferences can be different with different geographic locations (Pratchett, 2001). The exact reason for these feeding preferences is not entirely clear, but it is thought that corals which enable the most efficient feeding are likely to be preferred (Moran 1986, Foo et al 2024, Keesing 2019). A laboratory study found that the order of sequential feeding of available corals, was correlated with their relative feeding efficiencies (Keesing 2021) .

Whilst Acroporidae and Pocilloporidae corals are selected for and consumed disproportionately to their availability, it has been shown that CoTS will consume a very wide range of different coral prey, especially when prey is limited (Moran 1986; Keesing 1990). This is most likely a result of reduced access to preferred prey, rather than a shift in prey preferences. In environments where coral cover is severely reduced (<10%) CoTS have been found to consume non-preferred taxa at much higher rates, and the non-preferred prey were consumed according to their local availability (Keesing et al. 2019). Breakdown of prey selectivity is a behaviour which can be explained by the Optimal Foraging Theory (MacArthur and Pianka 1966; Hughes 1980) whereby animals attempt to maximise energy input per unit of effort. In situations where preferred prey are scarce or absent, the starfish attempts to meet minimum metabolic needs without expending effort foraging, and so consumes a broader range of prey items in relative proportion to their abundance. This is typical of observations during severe outbreaks or after bleaching events. For example, (Keesing 1990) found that faviids which were normally avoided in the presence of acroporids, were consumed at much higher proportions when coral cover was <10%. Although CoTS are primarily corallivores (Jangoux and Lawrence 1982), there have even been reports of adult CoTS consuming non-scleractinian prey, such as Alcyonacea, zoanthids and coralline algae, in increasing abundance when overall coral cover was low (Glynn 1987; Keesing 1990).

Where preferred taxa are not locally available, CoTS have to choose between foraging large distances in search of preferred prey (Ling et al. 2020) or consuming non-preferred taxa; this trade-off is not well understood and both behaviours have been observed. The compromise of feeding on locally available, non-preferred prey may save energy expenditure, however these sub-optimal prey items may have commensal defences, low nutritional value, or inefficient growth forms and requires higher feeding frequency, which may similarly negatively impact the health of the individuals (Caballes et al. 2016). CoTS were found to be more susceptible to disease (Pratchett, 2007) when they were feeding in areas where resources were reduced, which is likely as a result of their nutritionally compromised condition. Preferential consumption of preferred corals clearly benefits

CoTS, such that CoTS have been shown to grow faster and larger (Lucas 1984; Wilmes et al. 2020) and produce higher quality larvae (Caballes 2009) on these diets, thus the benefits of feeding on preferred prey may be so much greater that foraging great distances is overall beneficial.

1.4.2 *Feeding rates*

Understanding individual rates of coral consumption is critical for assessing the ecological impact of CoTS. Further, understanding variation in feeding rates with respect to environmental conditions is vital for realistic predictions of CoTS impact under different scenarios. Despite their importance, data on feeding rates of CoTS in low density and high-density populations remain limited (Keesing & Lucas 1992; Foo et al. 2024). A recent review by Foo et al. (2024) reported that feeding rates for CoTS on the GBR average 227 ± 108 cm^2 day^{-1}, however inconsistencies in data collection methods reviewed were highlighted. Other reported measurements of feeding rate include 378 cm^2 day^{-1} (Chesher 1969a); 116-187 cm^2 day^{-1} (Pearson and Endean 1969), 150 cm^2 day^{-1} (Glynn 1974); 350 cm^2 day^{-1} (Larkum 1988) and the area of a starfish's disk per day (Laxton 1974).

Early estimates of daily feeding rates (1960s – 1990s, Chesher 1969a; Glynn 1974; Larkum 1988) relied upon broad-scale coral cover depletion measurements, providing gross estimates with coarse accuracy and limited insight into individual-level feeding rates. The few studies that did assess individual consumption involved caged starfish (Pearson and Endean 1969) or laboratory experiments (Yamaguchi, 1974), limiting their ecological relevance. The first field-based assessment of individual CoTS feeding rates under natural conditions was conducted by Keesing & Lucas (1992) which involved monitoring tagged individuals over 2–5 days and estimating feeding rates based on maximum feeding scar diameters. Their findings highlighted significant influences of body size and season, with large adults (>40 cm) consuming 161 cm^2 day^{-1} in winter and 357–478 cm^2 day^{-1} in summer, while smaller individuals (20–39 cm) consumed 66 cm^2 day^{-1} in winter and 155–234 cm^2 day^{-1} in summer. The number of coral colonies consumed per day was also found to be lower in winter (0.2 colonies /day) than in summer (0.9–1.0 colonies/day), with an overall mean of 0.8

colonies/day. Seasonal variations were attributed to poikilothermic responses to temperature changes or energy demands for gametogenesis and gonad growth (Lucas 1973).

As discussed in the Fundamental Threshold section (1.2.2), the feeding rates presented by Keesing and Lucas (1992) remain foundational and were used to define "sustainable" limits of CoTS densities on GBR reefs. Whilst sustainable densities were obtained by relating individual feeding rates to the average annual turnover in well-established coral assemblages, these rates assume that *per capita* feeding rates are constant with respect to density, without incorporation of potential influences from individual-level variables (i.e. body size) or other environmental conditions (prey composition).

Few studies have compared feeding rates at different population densities. Understanding how feeding rates change between low- and high-density populations is key to predicting coral loss as outbreaks develop. It could be expected that intraspecific competition during high density events may impact the urgency of feeding (Keesing 1990), as it does in other echinoderm species which have been shown to increase grazing rates and preferences in the presence of high densities of conspecifics (Wright et al. 2005). If CoTS feeding rates vary with density, this may accelerate coral loss and resource depletion which should be an important consideration in CoTS management. Foo et al. (2024) present one of the few assessments of feeding rate in accordance with density status; their review compared feeding rates between studies with known population densities to determine whether there was a strong trend, it was determined that population density was not having a strong influence on daily feeding rate.

Whilst the effect of density has not been thoroughly explored, there is a small body of work that investigates the influence of prey availability on feeding rates, which has ramifications for different outbreak conditions. Pratchett et al. (2014) found that CoTS consumed less coral when preferred prey was abundant, whereas Millican et al. (2024) identified that coral consumption was almost three times higher (733.8 cm^2 day^{-1} vs 259.8 cm^2 day^{-1}) at locations where preferred prey

(*Acropora*) were in higher abundance. Keesing and Lucas (1992) also found that starfish fed at greater levels in areas of high coral cover, but this was only significant for large starfish (>40cm) feeding at night. Understanding how feeding rates change with prey availability will be important for refining feeding rate estimates and improving predictions of CoTS impacts as coral community compositions shift. Caballes et al. (2016) conducted one of the few species-specific feeding studies, though it was in a laboratory setting. Further research is needed to determine whether feeding rates differ between coral taxa.

Feeding estimates presented in the literature primarily use planar area measurements, which align with two-dimensional coral cover assessments but overlook the three-dimensional structure of corals. Incorporating three-dimensional surface area of corals into feeding estimates would provide a more comprehensive understanding of CoTS feeding physiology and the reliance of CoTS on different coral taxa. More field-based data on CoTS feeding rates is warranted, especially using techniques which can provide accurate assessments of feeding scars and provide data from a 3D surface areal perspective. In particular, understanding of how feeding rates vary in relation to prey availability, coral composition, and density dependence, are needed to determine how feeding rates vary across environmental gradients, which will improve predictions of CoTS outbreaks and their consequences for coral reef ecosystems.

1.4.3 *Diel behaviour*

There is some evidence that CoTS change their diel habits according to size and CoTS density, however this area of research is limited due to the small number of studies which have been conducted at night (Keesing 1990; Burn et al. 2020; Pratchett et al. 2020). The majority of literature states that CoTS are nocturnal (Chesher 1969a; Pearson and Endean 1969; Moran 1986; Burn et al. 2020; Ling et al. 2020) and feed mostly at night, however there are also reports of CoTS feeding diurnally and also continuously (Chesher 1969b), especially at high densities. Keesing (1990) noted that diel behaviour was influenced strongly by the size of individuals whereby small starfish (<20cm)

almost always fed nocturnally and remained cryptic during the day, whilst large starfish (>40cm) were primarily diurnal feeders but were seen feeding both day and night, and were rarely cryptic. Zann et al. (1990) observed similar behaviour by CoTS in Fiji and noted that intermediate sized starfish varied in their behaviour. The nocturnal feeding preference of CoTS is unlikely to be related to the accessibility of prey, as it is in other nocturnal feeding animals, but may represent the threat of diurnally active predators such as large predatory fishes (Ling et al 2020, Cowan et al 2017). The pattern of increased daytime feeding at larger sizes, is likely to be related to the relieved need for predator avoidance at larger sizes.

If size was the primary predictor of daytime feeding, then outbreaking populations with their smaller ultimate size would be expected to feed nocturnally. However, there is further data to suggest that it is not only size which affects diel feeding behaviour, but also starfish density. Chesher (1969a), Cheney (1974) and Pearson & Endean (1969) found that CoTS in low densities were largely nocturnal and cryptic during daytime hours, however changed their behaviour once densities built up and showed no light avoidance once in high density populations. This behaviour adaptation may be as a result of limited predation threat through 'safety in numbers', lack of available refuge space or more likely due to high intraspecific competition for live coral (and reducing prey availability), which results in the continuous need to feed. Conversely though, both Ormond et al. (1973) and Kenchington & Morton (1976) suggested that cryptic behaviour was unrelated to density.

1.4.4 *Movement*

The movement behaviour of CoTS is undoubtedly linked to their feeding ecology but may also be linked to reproductive aggregation. CoTS have been found to show clear differences in their daily displacement between low density and high-density populations (Souter 2007; Ling et al. 2020). Keesing and Lucas (1992) proposed that movement behaviour was directly related to percent live coral cover, whereby diel behaviour and distance travelled could be predicted by availability of preferred prey. This has also been supported by Barham et al. (1973), Souter (2007), Keesing and

Lucas (1992) and Ling et al. (2020a) who found that for CoTS in low densities with adequate food supply, distance travelled per day was low (mean 1m.day^{-1}), whilst in areas of severely depleted coral cover it was considerably further (mean 10m.day^{-1}).

Ling et al. (2020) proposed two distinct movement behaviour modes for CoTS which were determined by the availability of coral: 1) termed 'homing' behaviour was the short daily displacement to nearby preferred prey colonies (usually *Acropora*) and directed movement back to familiar refuge spots, this was only possible in areas with abundant preferred prey, and 2) was termed 'roaming' behaviour which was the outward movement from refuge spots but without returning, usually in response to limited preferred prey. Whilst homing behaviour usually resulted in negligible daily movement of less than one metre per day, the behavioural switch to roaming forays as a result of prey-searching, involved movement over much larger distances found to be up to 19m per day (Ling et al. 2020). The percentage of available *Acropora* was found to be the strongest predictor of daily displacement, when factors such as location, depth, starfish size and *Acropora* cover were considered.

1.4.5 *Feeding aggregations*

The active movement of CoTS in search of optimal prey is hypothesized to explain the formation of feeding aggregations (Dana et al. 1972; Vine 1973; Caballes 2009; Ling et al. 2020). Although factors such as local recruitment, reproductive behaviour, temperature or storm-generated wave exposure may play some role in determining aggregations (Wilson 1972). There is a growing body of evidence to suggest that aggregations of starfish are a result of movement in response to prey limitation (Ormond et al. 1973; Caballes 2009; Haywood et al. 2019; Ling et al. 2020). Ling et al. (2020)'s hypothesis that CoTS roam extensively as they forage for preferable feeding environments could explain the formation of localized aggregations and the patchy distribution of CoTS on a reef. Aggregations may be formed as roaming CoTS are attracted to distinct areas where coral cover remains high, and then revert to localized homing behaviour. Haywood et al. (2019) described

aggregated populations of CoTS on restricted areas of high coral cover in Northwest Australia after bleaching events, reporting no CoTS on adjacent low coral areas. Similar trends have been recorded in the West Pacific (Dana et al. 1972), Fiji (Weber & Woodhead 1970), and in Western Australia (Keesing et al. 2019). Reichelt et al. (1990) also demonstrated that aggregative behaviour would occur using a model simulation of a food limited environment.

The exact mechanism of aggregation, whereby CoTS may travel large distances in search of suitable prey, is thought to be brought about by chemoattraction of either conspecifics, or by the prey itself. Ormond et al. (1973) and Vine (1973) suggested that it was the feeding of conspecifics that attracted starfish to the site rather than the coral itself, which was demonstrated through a field study which saw CoTS moving together after feeding by other conspecifics commenced. However, Caballes (2009) hypothesized that CoTS respond to chemical signals of the coral prey itself suggesting that the chemical signals are first detected over large distances which initially attracts CoTS to an area of suitable prey, and then at smaller spatial scales CoTS use chemoreception to discriminate between preferred colonies based on palatability and other preference criteria. In laboratory experiments, Caballes (2009) showed that CoTS were attracted to crude extracts of preferred prey such as *Acropora* and *Pocillopora*, but were not attracted to extracts of non-preferred prey like *Porites* or *Diploastrea*.

Caballes (2009) demonstrated that the act of extraoral feeding by CoTS resulted in tissue damage and enzymatic cleavage and it was this chemical reaction, which was attracting other starfish, producing stronger attractant signals than the corals give out alone. This strong attraction to chemical compounds released during feeding, could explain why CoTS also show preference for corals where other CoTS are currently feeding, or for corals with recent partial mortality, giving preference to these colonies over intact ones (Ormond et al. 1973; Ling et al. 2020). This behaviour has been shown to result in mini aggregations where multiple CoTS are often found feeding on large

table corals or on groups of preferred species (Ormond et al. 1973). These studies support the idea that it is the chemoattractant effect of the coral itself, rather than the conspecifics (Collins 1975).

For movement and reef scale distribution, it seems that food availability is a stronger determinant of behaviour than density. It is therefore possible, and likely, that aggregation could occur where CoTS in low densities are driven closer together through food limitation. In recent years, chronic and/or sudden reductions in live coral cover have been documented as a result of climate induced events (Fabricius et al., 2008; Pratchett et al., 2013). The preferred prey of CoTS (i.e. acroporid corals) are among the most vulnerable corals to ocean warming and marine heatwaves, and as a result, the availability of this prey has been confined at many reefs, especially on the GBR (Dietzel et al. 2020; Pratchett et al. 2021b). Both Keesing et al. (2019) and Haywood et al. (2019) have recorded CoTS in low densities aggregating around isolated patches of coral after geographically different bleaching events. The adaptive behaviour which leads to the aggregation of low-density CoTS on patches of healthy reef may play an important role in enhanced fertilisation success, as large and highly fecund CoTS which would normally be dispersed find themselves at 'optimal' aggregation levels (Rogers et al. 2017). An increased understanding of the mechanisms that lead to aggregations and the implications of low-density populations aggregating should be explored for their role in outbreak initiation (Rogers et al. 2017; Ling et al. 2020).

1.5 Summary and thesis outline

Chapter 1 revealed striking differences in the biology and behaviour of CoTS between low-density and high-density population states (Appendix 1, Table S1). While the outbreaking population state of CoTS is well-studied, significant knowledge gaps exist regarding key characteristics of CoTS during their low-density phases. This discrepancy likely stems from differences in research effort and funding, which have predominantly focused on CoTS during their conspicuous and highly destructive outbreak phase. Additionally, the cryptic nature and low detectability of CoTS at low densities

present practical challenges for data collection, further contributing to difficulties in resolving these knowledge gaps.

Contrasting population modalities have been identified, however it is the transition between population phases which is a key focus of this thesis. Understanding the processes that cause or contribute to the initiation of population outbreaks may help to resolve the underlying cause(s) of these phenomena. Current survey methods for sampling CoTS populations have not been designed to identify population build-up but rather are focused upon documenting the distribution and intensity of outbreaks which are already established, over large spatial scales. Consequently, there is very limited research and data on the important (and relatively finite) early transition period when CoTS densities first increase, ultimately leading to population outbreaks. Surveying this critical transition period is fundamental for our understanding of the process(es) which are causing dynamic changes between population states and identifying the root cause of population outbreaks. Overcoming logistical barriers will enable baseline data on low density populations to be captured for the first time and facilitate tracking of CoTS populations during critical transitions.

An essential, but often overlooked aspect of CoTS population dynamics, is the process of population decline following peak outbreak densities. **Chapter 1** highlighted the lack of field data on the mechanism(s) driving these precipitous declines. While prey depletion at extreme densities is expected to compromise individual fitness, direct evidence of this remains undocumented. Understanding the resilience of CoTS populations existing in high-density, low-prey conditions, including their physiological and reproductive condition, will be crucial for predicting outbreak longevity and improving population models.

This thesis seeks to address key knowledge gaps related to population dynamics of CoTS, specifically the processes involved in the initiation and breakdown of population outbreaks. Insights gained will allow prevailing outbreak theories to be challenged and will contribute to determining whether population build-ups are primarily driven by anthropogenic activities and/or natural

fluctuations. Identification of the primary driver(s) of outbreak initiation is critical for effective management decisions and mitigation of widespread impacts, especially given the challenges of controlling populations which have already spawned. Until the root cause of population outbreaks is determined, strategic direction of CoTS culling provides the best opportunity to suppress CoTS impact. Ecological thresholds, which guide strategic culling efforts, offer a potential management tool, however their effectiveness depends on a more nuanced understanding of CoTS population dynamics.

Within this thesis, I aimed to fill key knowledge gaps highlighted above related to our understanding of CoTS outbreaks. I took a multifaceted approach to identifying the processes involved in the initiation and breakdown of population outbreaks, with the goal of improving our ability to predict and prevent population outbreaks and thereby suppress their ecological impacts on coral reefs in the Anthropocene. Specifically, the overarching goal of the research was to *advance our understanding of the intrinsic and extrinsic processes that are affecting i) initial increases in population densities that are the inevitable forebearer of population outbreaks and ii) population declines in the aftermath of peak densities*, to provide a holistic understanding of major drivers of population dynamics. This would facilitate improved prediction, prevention, and in the interim, management, of CoTS outbreaks. I aimed to achieve this through five distinct data chapters:

Chapter 2 (Chandler et al. 2023) presents a novel survey method, necessary to resolve changes in the abundance of CoTS before and during the initiation of population outbreaks. This chapter aimed to overcome logistical barriers that have historically limited the detection of CoTS outside peak densities. The design constraints of traditional survey methods (i.e., manta tows) mean that their capacity for detecting highly cryptic CoTS in low-density populations is limited. Within this chapter, an innovative survey protocol is developed with the aim of resolving specific changes in absolute densities, in order to survey during early-stage population build-up for the first time. By applying this novel approach at Lizard Island (northern GBR) over four consecutive years in the lead

up to an anticipated outbreak (Babcock et al. 2020), I aimed to capture early shifts in CoTS behaviour and biology during the initiation of renewed population outbreaks. Capturing data during this critical transition would represent a major breakthrough in our early detection and intervention capabilities compared to conventional methods, and also provide critical data for testing outbreak initiation theories.

Building on this, **Chapters 3, 4** (Chandler et al. 2024)**,** and **5** investigate how shifts in CoTS behaviour and biology contribute to population growth of CoTS that lead to outbreaks, and corresponding effects on coral cover and composition. Feeding behaviour is a key determinant of CoTS impact, and these chapters explore whether environmental or individual-level factors may be exacerbating feeding rates (and hence coral loss) during outbreaks, and whether these drivers can be accounted for during modelling exercises of coral loss and management decisions. To improve our knowledge of the processes involved with CoTS ecological impact during an outbreak, it is crucial to: (1) obtain higher resolution daily feeding estimates using advanced technologies (**Chapter 3**) and (2) identify key drivers of feeding rate variation (**Chapter 5**).

Chapter 3 lays the foundation of our feeding chapters by collecting fine-scale data on CoTS feeding. Baseline data on *per capita* daily feeding rates is necessary to update outdated feeding rates (Keesing and Lucas 1992) which used simplistic measurements of daily feeding (colony diameter measurements) and do not account for three-dimensional complexity of corals or variation in daily feeding rates in relation to coral prey. To gain high-resolution data on individual feeding rates, I conducted an intensive field tracking study of eight individual CoTS, capturing every coral consumed using underwater photogrammetry techniques. This approach allowed coral morphology and genus to be accounted for, refining our understanding of species-specific consumption rates and highlighting the role that individual feeding plays in shaping both the environment and the trajectory of CoTS population growth. While this study provided high-resolution data at a single location, it did

not address broader questions about how feeding behaviour varies across different outbreak stages and environmental conditions.

To address this gap, **Chapter 4** develops conversion metrics that enable large-scale CoTS feeding data to be standardized into meaningful surface area metrics. This methodological advancement was a necessary precursor to **Chapter 5**, where these standardized feeding metrics are applied to investigate the intrinsic and extrinsic factors driving daily feeding rates across a large-scale study.

Following on, **Chapter 5** investigates the key drivers of daily feeding rate, to understand which factors, such as population density and/or prey availability, are compounding upon CoTS ecological impact by eliciting changes in feeding behaviour. This large-scale study of 565 individual starfish, spans a continuum of environmental conditions to enable space for time comparisons of CoTS feeding. This chapter integrates methodologies established in **Chapters 2**, **3** and **4**. By using our novel sampling methodology (SALAD surveys), methods of ageing feeding scars, and converting to multi-dimensional feeding data, this chapter provides new insights into the role of food availability in shaping CoTS behaviour - an important consideration for (future) food-limited environments.

While earlier chapters focus on outbreak initiation and progression, **Chapter 6** shifts focus to the later stages of outbreaks, investigating whether behavioural and physiological changes allow CoTS to persist in increasingly constrained outbreak environments, or whether they lead to compromised physiological condition, which might ultimately lead to population collapse. This chapter examines how outbreak conditions affect reproductive and nutritional status of CoTS - factors that influence both outbreak longevity and spread. Understanding the mechanisms which ultimately lead to outbreak breakdown are necessary for a full understanding of outbreak dynamics.

Overall, these chapters highlight the intrinsic and extrinsic drivers of CoTS population increase and population breakdown, advancing our ability to predict and mitigate population outbreaks, ultimately improving conservation efforts for coral reef ecosystems.

Chapter 2: Increasing densities of Pacific crown-of-thorns starfish (*Acanthaster* cf. *solaris*) at Lizard Island, northern Great Barrier Reef, resolved using a novel survey method[1]

2.1 Introduction

Population outbreaks of crown-of-thorns starfish (CoTS, *Acanthaster* spp.) are one of the foremost causes of coral mortality throughout Indo-Pacific coral reefs (Chesher 1969b; Osborne et al. 2011a; Trapon et al. 2011; Baird et al. 2013; Saponari et al. 2015), contributing to widespread declines in coral cover and diversity (Moran 1986; Kayal et al. 2012; Lane 2012; Tkachenko and Hoang 2022). The initiation of population outbreaks (often referred to as 'primary outbreaks'; *sensu* Moran (1986), Endean (1974) is increasingly attributed to progressive build-up of CoTS densities due to successive recruitment events and cumulative increases in their local reproductive output (e.g., Pratchett (2005), Wooldridge & Brodie (2015). The underlying mechanism(s) that cause or facilitate population outbreaks are largely unresolved (Babcock et al. 2016a; Pratchett et al. 2021a), though there are persistent theories ascribing some role for anthropogenic activities. More specifically, over-fishing of key predatory species, such as giant triton *Charonia tritonis* (Endean 1969) and predatory fishes (Ormond et al. 1990; Sweatman 1996; Mendonca et al. 2010) may release CoTS from predator-mediated population regulation, and thereby facilitate increased rates of recruitment and adult population growth (*Predator Removal Hypothesis;* (Endean 1969). This hypothesis has been corroborated by evidence of increased incidence and severity of population outbreaks in areas subject to sustained fishing pressure (Dulvy et al. 2004; Sweatman 2008; Kroon et al. 2021). Alternatively, the *Terrestrial Runoff Hypothesis* (Birkeland 1982) proposes that pulses of increased nutrients (and hence

[1] This chapter was published as Chandler, J.F., Burn, D., Caballes, C.F., Doll, P.C., Kwong, S.L.T., Lang, B.J., Pacey, I.P. and Pratchett, M.S. (2023) Increasing densities of Pacific crown-of-thorns starfish (*Acanthaster* cf. *solaris*) at Lizard Island, northern Great Barrier Reef, resolved using a novel survey method. *Scientific Reports* 13:19306

larval food availability) caused by heavy rainfall on high islands may have released planktotrophic CoTS larvae from food limitation, elevating their developmental success and survival rates and therefore exacerbating population growth (Birkeland 1982; Brodie et al. 2005; Fabricius et al. 2010). However, it is still unknown whether low nutrient conditions would sufficiently constrain larval survival to prevent the initiation of population outbreaks (Olson 1987; Wolfe et al. 2017).

Debate surrounding the putative cause(s) of population outbreaks remains ongoing, with no single hypothesis gaining unequivocal support (Babcock et al. 2016). It is also possible that spatiotemporal variation in CoTS abundance is attributable to inherent life-history traits of CoTS (e.g., extreme fecundity; (Uthicke et al. 2009; Hock et al. 2014; Pratchett et al. 2021c). Local hydrodynamic patterns have been proposed as a potential mechanism for larval retention, leading to higher-than-normal recruitment success at specific reef locations (Black et al. 1995; Hock et al. 2014) and could explain why some reefs or regions are more predisposed to self-seeding (Miller 2000; Fabricius et al. 2010). Regardless of the proximate cause(s) of population outbreaks, 'primary outbreaks' build up over time and give rise to extremely large quantities of planktonic larvae which are thought to spread to nearby and downstream reefs, resulting in subsequent population outbreaks termed 'secondary outbreaks' (*sensu* Endean 1974). Effective management is conditional upon improved understanding of the causes(s) of population outbreaks, particularly pertaining to the potential role of anthropogenic drivers.

Early detection (if not prevention) of increasing starfish densities represents the best opportunity to prevent the initiation and spread of population outbreaks and mitigate their destructive impact on coral assemblages (Pratchett et al. 2017b; Babcock et al 2020). However, our ability to detect the onset of population outbreaks has been severely constrained by difficulties in surveying CoTS outside of peak adult densities (Fernandes et al. 1990; Pratchett et al. 2017b). This is partly due to the attention-deficit cycle of CoTS research and funding that closely mirrors the cycles of CoTS population outbreaks (Hoey et al. 2016), though there are also substantial logistical constraints to effectively

monitoring CoTS, especially low-density populations. Current surveillance is largely reliant on manta tows (Emslie et al. 2020; Westcott et al. 2020), which provide only very coarse estimates of CoTS densities (Fernandes et al. 1990; MacNeil et al. 2016). Manta tows are rapid, broad-scale surveys whereby snorkelers are towed behind a moving boat, typically covering ~2,000 m² (0.2ha) in 2 minutes. Such methods have utility in establishing where population outbreaks presently exist, once they are well established, and have been vital in directly informing the Crown-of-thorns Starfish Control Program on Australia's Great Barrier Reef (GBR) (Westcott et al. 2021). However, they lack the sensitivity to detect subtle changes in adult CoTS density, particularly during the early build-up phase. This limitation arises from the rapid survey speed and the reliance on CoTS being fully exposed and visible from the surface, which is relatively rare during non-outbreaking conditions, due to the species' cryptic behaviour and tendency to shelter within the reef matrix during the day.

Our inability to detect changes in starfish densities during the early stages of CoTS population outbreaks has prevented us from establishing precisely when localised and system-wide population outbreaks begin, thereby hindering our understanding of their root cause(s). Population outbreaks have historically been recognised once sufficiently high densities of adult CoTS have surpassed a notional abundance or density threshold (i.e., 0.22 CoTS per manta tow or 15 CoTS.ha^{-1} *sensu* Moran & De'ath (1992b); 10 CoTS.ha^{-1} *sensu* Keesing and Lucas (1992) defined for management and research purposes. Under this definition, however, the purported timing of initiation relies on the detection of a population outbreak, which likely occurs years after densities first started building, thereby masking the potential root cause(s) of initial population growth. For the earliest possible detection of population outbreaks, it is thus not only absolute CoTS densities which are noteworthy, but equally the first signs and rate of population growth. Because current surveillance approaches do not have the capacity to detect these subtle changes, developing a survey method which overcomes the logistical difficulties of surveying highly cryptic, low-density CoTS would enable monitoring of population dynamics at a much higher resolution and resolve these inherent issues pertaining to the detection of population build-up.

Since the 1960s there have been four distinct waves of CoTS population outbreaks documented on the GBR (Pearson and Endean 1969; Reichelt et al. 1990a; Pratchett 2005; Babcock et al 2020), with their initiation and spread seeming to follow a relatively consistent spatiotemporal pattern. With each of these cycles, successive, elevated annual recruitment has been proposed to first occur within a finite area in the Northern GBR (14° S to 17° S) (Kenchington 1977; Miller 2000; Pratchett 2005; Vanhatalo et al. 2017), which has consequently been termed the 'Initiation Box' (Pratchett et al. 2014; MacNeil et al. 2017; Vanhatalo et al. 2017). Based on the periodicity (14-17 years) of past cycles, it is expected that a new wave of population outbreaks will commence in the northern GBR between 2025-2027 (Babcock et al 2020). The purpose of this study was to undertake CoTS population monitoring of a key geographic area within the 'Initiation Box' (Lizard Island) at a higher resolution than has previously been possible. This fine-scale surveillance using a novel survey method would attempt to detect the first signs of CoTS population build-up, which would mark a key development in our early detection capability. Moreover, population size structure data collected during surveys offers important insights into historic recruitment and population dynamics in this key location, which may consequently corroborate or contradict putative hypotheses for the initiation of CoTS population outbreaks.

2.2 Methods

2.2.1 *Study site*

This study was conducted on reefs around Lizard Island (14°40'S, 145°27'E) in the northern GBR, Australia (Figure 2.1a, b). Lizard Island's location in the northern extent of the purported 'Initiation Box' (Figure 2.1a) has made it a key site for investigating the initiation and southward spread of CoTS population outbreaks. Since monitoring of GBR reefs for CoTS began in 1966 (Moran 1986), Lizard Island has reported elevated densities of CoTS that surpass indicative thresholds of a population outbreak on three occasions (Moran 1986; Miller 2000; Pratchett 2005). Although there is no empirical data on the earliest stages of population build-up during each of these cycles, it is presumed that the populations increased slowly and progressively to start with, followed by a pattern of rapid and dramatic population growth and eventually a precipitous decline (Stump 1996; De'ath and Moran

1998; Pratchett 2005). On each occasion, pronounced increases in population size at Lizard Island and surrounding reefs have directly preceded the southward spread of 'secondary outbreaks' (Dight et al. 1990; Moran et al. 1992), and this area has consequently been hypothesised to be a 'seed area' for region-wide population outbreaks (Reichelt et al. 1990a; Pratchett 2005). Understanding the specific dynamics of CoTS populations at Lizard Island could hold critical answers to how and why population outbreaks begin (Pratchett et al. 2014).

In this present study, a total of 13 survey sites were selected around Lizard Island, predominantly on the leeward side of the island (Fig. 1b), owing to weather constraints. The surveyed region extends from North Reef in the north, to Palfrey and South Islands in the south (Fig. 1b). Each of these sites were extensively surveyed in four consecutive years from 2019 to 2022.

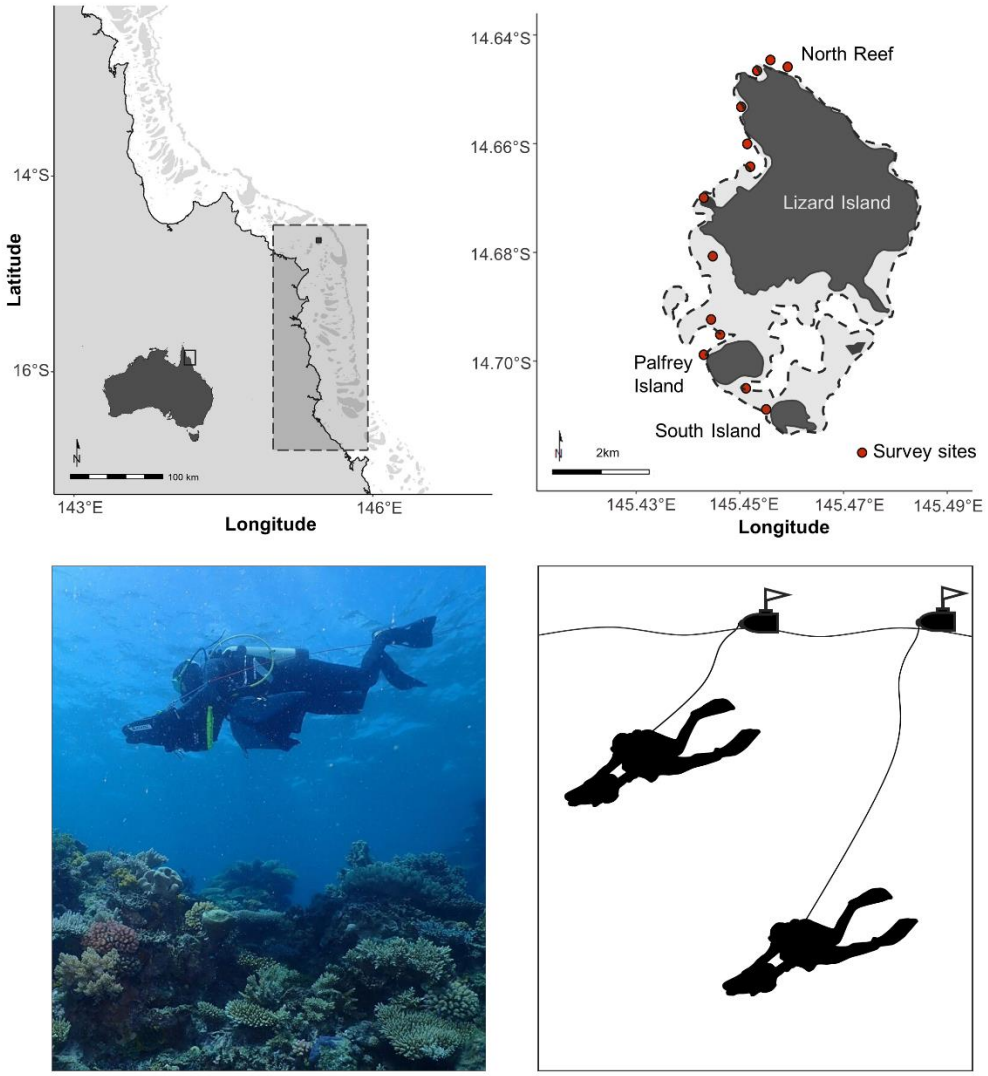


Figure 2.1 *'SALAD surveys' conducted at Lizard Island.* ***(a)*** *Lizard Island's location in the Northern Great Barrier Reef, also shown is the putative 'Initiation Box' (dashed box),* ***(b)*** *Lizard Island area with survey locations marked in red,* ***(c)*** *SALAD survey conducted with a Seascooter,* ***(d)*** *Methodology: searches are conducted at two depths simultaneously, with GPS units towed along the surface in floating housings.*

2.2.2 *SALAD survey methods*

To effectively survey CoTS at very low densities, when individuals are known to be widely dispersed (Chesher 1969b) and generally cryptic during daylight hours (Cheney 1974; Burn et al. 2020; Ling et al. 2020), a novel survey method was developed, namely Scooter-Assisted Large Area Diver-based (SALAD) surveys (Figure 2.1c, d). To account for the low densities of CoTS, it was necessary to survey large spatial areas, while also allowing for intensive searching for CoTS concealed within the reef matrix. Therefore, this novel survey method involved *in situ* CoTS surveys using Yamaha (500Li)

Seascooters (Figure 2.1c, d), which enabled greatly increased areal extent of individual surveys, while ensuring divers had full autonomy to vary the speed of travel during SALAD surveys, depending on habitat complexity and the presence of feeding scars, and could stop as necessary to search for CoTS. During SALAD surveys divers were able to survey up to 1.1 hectares (11,000 m^2) of reef area per dive.

SALAD surveys were undertaken by pairs of SCUBA divers, where each diver searched a distinct depth range or habitat, to the extent that was possible given the reef topography and water visibility. Each diver surveyed 2.5 m either side of their median plane, for a total of a 5-m wide survey area. Survey pairs therefore remained > 5m apart to avoid pseudo replication of observations (i.e., re-surveying the same area). Survey pairs were divided into two roles, specifically one diver (shallow) would survey along the reef crest (2-4 m), whilst the other diver (deep) would survey along reef slope (5-9m); adjusting as necessary to remain within sight of each other.

In order to determine the total distance surveyed (and thereby determine overall area searched) during each SALAD survey, a surface-float housing a GPS unit (Garmin eTrex 10) was tethered to each diver (see Figure. 2.1d). The GPS unit recorded the start and end points of each survey track, and continuously recorded the GPS location at 60 second intervals. Recorded GPS track data was converted to CSV format and tracks were then scrubbed in statistical software R (R Core Team 2021) using speed, distance, and time parameters to identify and remove any track segments where divers were not engaged in conducting surveys (e.g., moving to or from site in boat). Distance was then calculated for each cleaned track using the 'distHaversine' function of the R package 'geosphere' (Hijmans 2022). The resulting survey-specific search area per diver was specified to be 5m wide (i.e., 2.5 m either side) along the central line of the survey path, which was assumed to represent the diver's median plane.

Given COTS are generally cryptic, especially at small size and during daylight hours (Cheney 1974; Burn et al. 2020), the initial detection of individuals is generally based on the appearance of conspicuous feeding scars, rather than direct detection of the starfish (Miller et al. 2009; MacNeil et

al. 2016). As such, discounting individuals which are not readily visible during daytime searches is thought to considerably underestimate CoTS abundances (Fernandes et al. 1990; MacNeil et al. 2016). Importantly, the SALAD method allows rigorous assessment of coral colonies to distinguish CoTS feeding scars from other common stressors (e.g., coral disease or predation by *Drupella* spp.). When feeding scars are clearly discernible and easily attributed to individual starfish (which is only possible at low to moderate densities), local densities of CoTS may be inferred based on the number of distinct clusters of feeding scars. Because this study hoped to capture the subtle, early changes in population densities, distinct sets of feeding scars (where no starfish was detected) were recorded in addition to CoTS counts, this was thought to represent a more accurate indicator of adult CoTS abundance on a reef where detectability is low. A feeding cluster was identified as either a trail of progressive feeding scars or a distinct patch where multiple fresh scars were present within close proximity, separated from another cluster by an expanse of reef without any feeding scars. Estimates of CoTS abundance that take account of feeding scars are referred to herein as 'inferred' densities (as opposed to 'recorded'), being the number of recorded CoTS detected summed with the number of distinct sets of CoTS feeding scars not assigned to a recorded starfish (i.e., CoTS + Scars). If there was uncertainty about whether a set of scars was related to an identified starfish or a cryptic starfish, then only the actual starfish was counted. For each starfish located, the body size (i.e., maximum diameter) was recorded by measuring the longest width of the starfish using a slate ruler or measuring tape. Although the size of starfish is known to be influenced by extrinsic factors such as diet and competition (Yamaguchi 1974; Lawrence and Lane 1982; Lucas 1984), this size-frequency distribution data provides a coarse indication of age structure and historic recruitment to the population (*sensu* Stump 1996), Pratchett (2005) and hence population dynamics. Based on taxon-specific size at age relationships (Pratchett et al. 2014), any <150 mm diameter CoTS likely represents recent recruitment cohorts (≤ 2 years), while observations of a wide range of size classes denote multiple recruitment events over a prolonged period. Size data were grouped into size classes with 50mm bin ranges and subsequently used to produce size frequency distributions for each survey year.

2.2.3 *Statistical analyses*

To investigate temporal and spatial variation in CoTS densities at Lizard Island, a generalized linear mixed effects model (GLMM) was used to model the effects of year (2019-2022) and zone (reef crest and slope). Site was included as a random effect with random intercepts to account for spatial variability in CoTS densities. CoTS densities were modelled against a Poisson distribution with a log link function, whilst transect length was added as an offset to account for the differing areal extent of each survey. Tukey's pairwise comparisons were calculated using estimated marginal means to test for significant differences in CoTS abundances among years. 95% confidence intervals (CI) were generated for these pairwise comparisons, whereby statistically significant differences are determined where CIs do not overlap 1. Surveys were conducted in June-August and October-December, however, data were pooled by year to test for inter-annual variation as there was found to be no influence of sampling period on inferred CoTS densities (ANOVA, $F_{1, 127} = 1.433$, $p = 0.233$). Statistical analyses are presented for two alternative estimates of CoTS density; one for recorded CoTS densities and one for inferred CoTS densities. To investigate temporal variation in the body size of CoTS, a second GLMM modelled the effect of year on the diameter of CoTS, including site as a random effect. The size data were modelled against a Gaussian distribution and a glmmTMB ANOVA (Wald II) was computed to test for significant variation in mean CoTS diameter among years.

All statistical analyses were performed in the R statistical and graphical environment (R Core Team 2021), with models built using the *glmmTMB* package (Brooks et al. 2017). For each model, goodness of fit was assessed, and combinations of fixed and random effects were tested and retained only if they improved the fit of the model, based on the Akaike Information Criterion (AIC). Each model was validated, including checks of simulated residuals and dispersion, using the *DHARMa* package (Hartig 2018). The *emmeans* package (Lenth et al. 2018) was used for pairwise comparisons of estimated marginal means. Boxplots and size-frequency distribution plots were computed using the *ggplot2* package in R (Wickham 2016).

Table 1.1 *Summary of Scooter-Assisted Large Area Diver-based (SALAD) surveys conducted at Lizard Island during 2019-2022, with survey distance and survey area per survey year*

Year	No. of surveys (n)	Cumulative distance of survey paths (m)	Combined survey area (Ha)	Recorded no. of CoTS	Inferred no. of CoTS (CoTS + sets of scars)
2019	36	40,744	19.72	34	91
2020	38	42,332	21.17	26	77
2021	22	33,096	16.54	52	111
2022	34	19,999	10.00	85	161
Total	**130**	**136,171**	**67.43**	**197**	**440**

2.3 Results

2.3.1 *Inter-annual variation in CoTS density*

A total of 130 SALAD surveys were conducted at Lizard Island between 2019 and 2022, encompassing a total survey area of 67.4 hectares and detecting a total of 197 adult CoTS (Table 1). Over the four years, recorded densities of CoTS ranged from 0 to 35.9 CoTS.ha^{-1} among individual SALAD surveys, while inferred densities (including distinct sets of feeding scars) ranged from 0 to 46.8 CoTS.ha^{-1}. In 2019 and 2020, the densities of starfish remained relatively low (Figure 2.2a, b), with mean recorded CoTS densities of 1.82 ha^{-1} (± 0.48 SE) in 2019 and 1.18 ha^{-1} (± 0.31 SE) in 2020 (Figure 2.2a), and inferred densities of 4.90 ha^{-1} (± 0.85 SE) in 2019 and 3.53 ha^{-1} (± 0.72 SE) in 2020 (Figure 2.2b).

In 2021, mean recorded densities (3.14 CoTS.ha^{-1} ± 0.58 SE) and inferred densities of CoTS (6.29 CoTS.ha^{-1} ± 0.91 SE) were found to be significantly higher than in 2020 (recorded CI: 1.47 - 4.32; inferred

CI: 1.26 - 2.51). Subsequently, surveys conducted in 2022 found further significant and considerable increases in mean CoTS densities compared to 2021 for both recorded density estimates (CI: 2.37 - 6.76) and inferred density estimates (CI: 4.36 – 5.47). In 2022, the mean recorded density of CoTS was 9.41 individuals ha^{-1} (± 1.66 SE), while the mean inferred density of CoTS (17.71 CoTS.ha^{-1} ± 2.30 SE) exceeded the critical density threshold of 15 CoTS.ha^{-1}. At the survey level, CoTS densities above this density threshold were detected during 7 and 16 surveys in 2022 for recorded and inferred densities, respectively. Notably, mean densities in 2022 were substantially higher than in 2019 (recorded CI 3.62 – 11.78; inferred CI 2.35 – 4.74) and 2020 (recorded CI 5.67 – 17.95; inferred CI 2.88 – 5.53). Recorded and inferred density estimates present a similar trend of increasing densities from 2020 to 2022, whereby mean inferred density estimates were consistently higher in each of these years (Figure 2.2a, b).

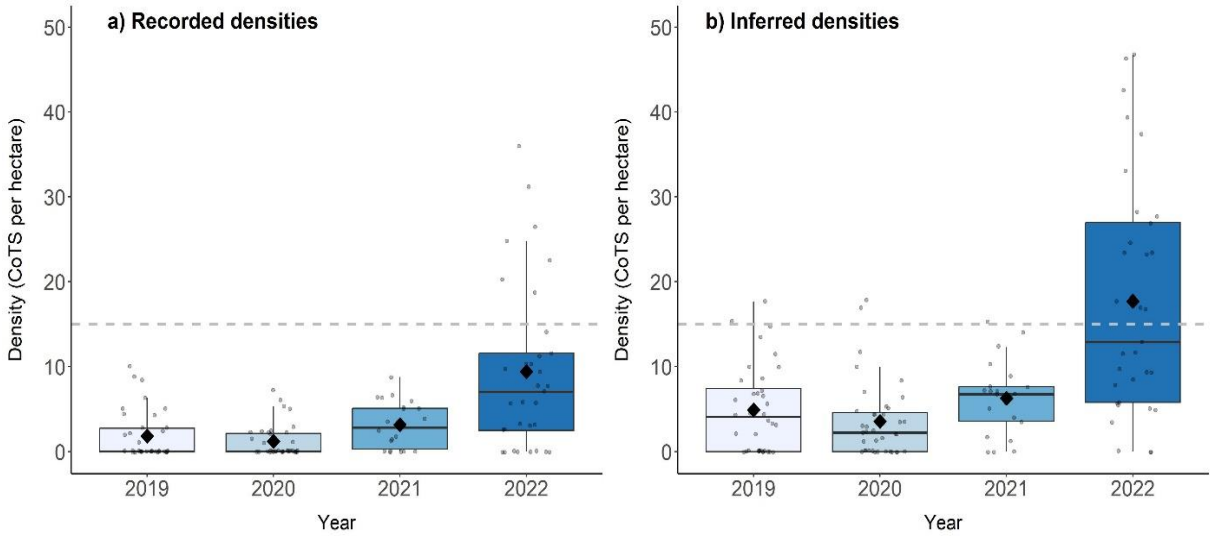


Figure 2.2 *Inter-annual variation in CoTS densities at Lizard Island from 2019 to 2022.* ***(a)*** *recorded density estimates based on starfish counts,* ***(b)*** *inferred density estimates (accounting for additional, distinct sets of feeding scars where starfish were not detected). Each grey point represents a density estimate for an individual SALAD survey. Boxes and whiskers display 25-75th and 5-95th percentile ranges, respectively. Diamonds and thick lines indicate mean and median values, respectively. Horizontal dashed line represents the critical density threshold of 15 CoTS.ha^{-1} indicative of an outbreaking population (Moran and De'ath 1992b).*

There was no significant effect of zone (depth) on recorded CoTS densities during any of the years (CI 0.79- 1.46). Overall, the fixed effects in the model (year and zone) were found to explain 44%

of variability observed in recorded (marginal R^2 = 0.439) and inferred CoTS densities (R^2m = 0.427), with the model explaining 70% of variation (conditional R^2 = 0.701) for recorded density estimates and 75% for inferred density estimates (R^2c = 0.753).

2.3.2 *Size structure*

The diameter of COTS recorded during SALAD surveys ranged from 100 – 600 mm, with a broad range of sizes recorded in every year (Figure 2.3). The size data GLMM reported no significant variation in mean CoTS diameter among survey years (glmmTMB ANOVA, X^2 [3, n = 194] = 2.826, p = 0.419) and very few small starfish (<150 mm diameter) were recorded (total of 3 individuals). The size-frequency distribution remained relatively consistent among years; however, slightly higher proportions of CoTS were present in the large size classes in 2021 and 2022, with some individuals between 550 to 600 mm in diameter. There was a temporal shift towards larger size classes, whereby the modal size class in 2020 was 300 - 350 mm, compared to 400 - 450 mm in years 2021 and 2022 (Figure 2.3).

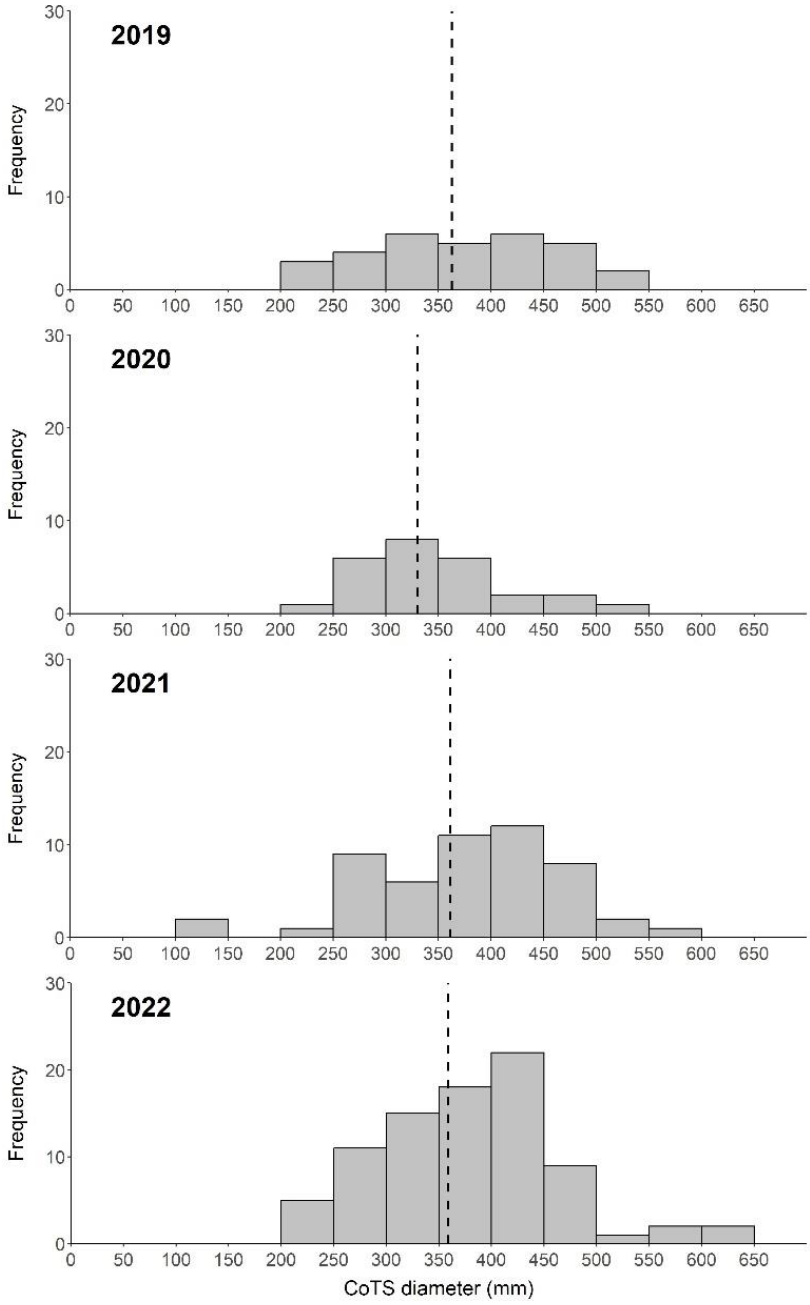


Figure 2.3 *Inter-annual variation in size frequency distribution of adult CoTS recorded at Lizard Island between 2019 and 2022. Dashed line indicates the mean CoTS diameter (mm) for each survey year*

2.4 Discussion

Increasing densities recorded during this study signal the onset of a renewed CoTS population outbreak at Lizard Island in the northern GBR, representing the 5th documented outbreak since the 1960s. Based on the historic periodicity of previous cycles, a renewed population outbreak was not predicted to start until 2025-2027 (Babcock et al. 2020). However, the detection (and reported

initiation) of all previous CoTS population outbreaks has been based solely upon the detection of absolute densities of adult CoTS above the nominal density threshold of 15 CoTS.ha^{-1} (Moran 1986; Moran et al. 1992; Pratchett 2005). Such conspicuously high densities represent fully established population outbreaks which have been identified considerably later than the initial conception and first apparent density changes would have occurred. However, there has previously been no method capable of detecting the early density changes that signify the actual onset of a population outbreak, hindering both our understanding of outbreak driver(s) and early intervention efforts. To resolve this long-lasting conundrum and overcome the inherent limitations of previous methods to effectively resolve low density CoTS, this study used the novel SALAD survey method, which integrates thorough CoTS searches within large area surveys. These innovative surveys reveal substantial and significant increases in CoTS densities at Lizard Island over the past few years, and inferred densities surpassed the established density threshold that signifies population outbreaks in 2022. The documented increase in local densities over this multi-year period presents a strong indication that the anticipated renewed population outbreak has in fact already started at this key location within the 'Initiation Box' and marks an important development in our capability to detect and suppress CoTS population outbreaks before they take hold.

Whilst the SALAD surveys recorded significant and considerable increases in CoTS densities between 2020 and 2022, other monitoring programs operating in the region, which used manta tows to collect data, have detected no such temporal variation during the same years at Lizard Island (Australian Institute of Marine Science 2023). This disparity demonstrates the value of the new SALAD survey method for reliable density estimates and, importantly, for early detection purposes. The SALAD survey method is enabling us to detect the first signs of increasing CoTS densities years before other conventional monitoring techniques. Our findings suggest that the onset of the four reported population outbreaks on the GBR would have similarly been detectable years before their initiation was officially recorded, had this method been accessible at the time. The newfound capacity to monitor low-density CoTS populations has also enabled baseline density data to be collected for the

first time. These data will be invaluable for improving our understanding of population dynamics and allow for future comparisons of baseline data between populations of different regions and even between different *Acanthaster* species. Most importantly, this monitoring method will allow us to detect future deviations from baseline densities, which has considerable potential as an early warning system for swift and effective management intervention.

To infer more accurate estimates of population density, this study recorded distinct sets of CoTS feeding scars, as previously implemented in the monitoring of CoTS populations (Miller et al. 2009; Kayal et al. 2012). CoTS are extremely cryptic during daytime surveys (Burn et al. 2020), particularly at low population density, which can result in substantial density underestimation, even in the case of extensive areal searches to locate the starfish (e.g., SALAD survey method). In areas with low to intermediate CoTS densities, where the starfish are generally widely dispersed (Chesher 1969b), distinct sets of feeding scars can be readily attributed to a single CoTS feeding in isolation. In most such cases, the inclusion of feeding scars in density estimates will simply reduce density underestimation and provide a more accurate measure of abundance than reliance on locating the highly cryptic starfish themselves. With detectability or 'sightability' highlighted as a key constraint to accurate survey data for CoTS (Fernandes et al. 1990; MacNeil et al. 2016), this inclusion of scars represents the most robust method of estimating CoTS densities by essentially buffering for any potential spatial or temporal heterogeneity in detectability which may be related to CoTS density, body size, reef complexity, season or time of day. There are, however, inherent limitations associated with this approach, particularly in areas with elevated densities, where feeding patches may overlap and sets of scars become more difficult to discern. Feeding scars may also be misassigned to CoTS which have moved on or are feeding over a large area rather than within a distinct patch (Keesing and Lucas 1992). On the other hand, the rigorous assessment of potential feeding scars during SALAD surveys ensures the correct differentiation from other potential stressors, such as coral disease or predation by *Drupella* spp. (Beeden et al. 2008), which contrasts another critical limitation of other survey methods to obtain accurate abundance at low CoTS densities (e.g., manta tow, remotely operated or autonomous

underwater vehicles). On balance, the inclusion of feeding scars in the monitoring of CoTS populations is still more likely to underestimate than overestimate true densities. As many previous studies have not included feeding scars in published abundance estimates, the new insights gained from this data should be interpreted accordingly, especially in the context of the established threshold that signifies population outbreaks.

Whilst abundance data has proven critical for capturing the initial shift from latent to proliferating population, size frequency data collected during this study provides additional insight into how this population build-up may have occurred. Inherent limitations to detecting <100mm CoTS hinder precise insights into recruitment patterns; however, our size frequency data allows for a coarse age and recruitment cohort allocation of individuals (Stump 1996; Pratchett 2005). Size structure data from Lizard Island revealed that this population represents various size classes (100 - 600 mm), with no single dominant size class (i.e., recruitment cohort). This suggests that recruitment to this population has occurred over an extended, multi-year period (e.g., Pratchett (Pratchett 2005), rather than through a single mass recruitment pulse (e.g., Zann *et al*. 1987). This insight into historic recruitment processes can act to establish what putative drivers may have played a role in the initiation of this population outbreak. For example, our results do not support the idea that an episodic event (e.g., a flood) caused increased recruitment (Terrestrial Runoff Theory), since there is no dominant peak in recruitment documented in this study, but rather a range of different size classes including recent recruitment.On the contrary, our findings suggests that a prolonged accumulation of individuals was/is increasingly adding progeny to the population pool and thereby causing the population size increase. It remains unknown what processes are driving this continually elevated recruitment, although high rates of larval retention due to weak and bidirectional currents in this area may be a contributing factor (Scandol and James 1992; Black et al. 1995; Hock et al. 2014; Miller et al. 2015). Thus, an improved understanding of the larval supply and recruitment dynamics that precede adult population build-up may provide broadly applicable insights into the precise cause(s) of population outbreaks.

Population dynamics of CoTS: drivers and impacts

The data on size structure documented in this study also provide an important insight into the reproductive capacity of the building population, as fecundity of CoTS is strongly size-dependent, whereby reproductive capacity increases exponentially with diameter, particularly in females (Pratchett et al. 2021a). Based on the large average size of the population recorded in 2022, which includes high proportions of large-bodied individuals in the 400-600mm size classes, we can extrapolate that at least half of the female population will be producing upwards of 20 million oocytes per individual, per spawning season (Pratchett et al. 2021a). As a result, a substantial number of competent larvae arising from this population will likely settle and recruit into CoTS populations at Lizard Island and well-connected northern GBR reefs every upcoming summer (Hock et al. 2014; Doll et al. 2021, 2023). While such significant larval supply inherently contributes to the spatial spread of this population outbreak, it could also result in a positive feedback loop at Lizard Island, whereby high rates of self-recruitment further reinforce, if not accelerate, localised population growth (Uthicke et al. 2009). These insights on size frequency and reproductive potential have important application for the prioritisation and allocation of population control efforts, because the targeted control of a building population made up of larger individuals (such as Lizard Island), may prove more efficient and effective in slowing the progression of population outbreaks than targeting a higher density population which is made up of smaller individuals.

In conclusion, this study has provided strong evidence that the anticipated renewed population outbreak of CoTS (e.g., Babcock et al. 2020) has already commenced in the northern GBR. The novel monitoring approach developed to reveal this proliferation of CoTS provides an important opportunity for early intervention, and will enable improved understanding of the patterns and processes involved in initiation of population outbreaks (Pratchett et al. 2014; Pratchett and Cumming 2019). Considering the spatiotemporal dynamics and severe impact of previous population outbreaks (Babcock et al. 2020), suppression of population growth at key locations such as Lizard Island may contribute to slowing the spread of widespread outbreaks. Further in-depth monitoring of CoTS populations in the

northern GBR and other regions may provide important insights into the irruptive population dynamics of CoTS, and where, when and why CoTS population outbreaks initiate.

Chapter 3: Daily variation in the feeding activity of Pacific crown-of-thorns starfish (*Acanthaster* cf. *solaris*)

3.1 Introduction

Climate change, especially severe marine heatwaves and corresponding mass coral bleaching is the foremost threat to coral reefs in the Anthropocene (Hughes et al. 2017). However, coral depletion driven by the feeding activity of outbreaking populations of crown-of-thorns starfish (CoTS, *Acanthaster* spp.) remains a major contributor to coral loss throughout the Indo Pacific (Tkachenko and Hoang 2022; Seveso et al. 2024). On Australia's Great Barrier Reef (GBR) CoTS have been responsible for widespread coral loss (Mellin et al. 2019; Castro-Sanguino et al. 2023; Matthews et al. 2024) resulting from four chronic outbreaks occurring since 1960s, with the fifth major outbreak recently commenced (Chandler et al. 2023) [**Chapter 2**]). With limited options for reef managers to affect necessary changes in international policies to moderate escalating effects of climate change, effective management of the population outbreaks of CoTS represents the foremost opportunity to redress widespread and sustained coral loss, and thereby maximise opportunities for natural adaptation among coral population and communities to changing environmental conditions.

The ecological impacts of CoTS are fundamentally dependent on their feeding behaviour, not only in terms of the overall extent of coral loss that occurs during major outbreaks (e.g., Kayal et al. 2012b), but also shifts in the structure of coral assemblages due to highly selective feeding (e.g., Li et al. 2023). In general, CoTS have strong feeding preferences for corals from the Acropororidae and Pocilloporidae families, whilst Poritidae and Merulinidae corals are non-preferred (Keesing 2021; Collins 1975; Keesing 1990; Ling et al. 2020; Ormond et al. 1976; Pearson & Endean 1969). The evolution of these strong prey preferences are thought to be determined by a multitude of factors, which enable variously affect the differential nutritional benefit (Keesing 2021).

Despite extensive data on CoTS prey preferences, empirical data on individual feeding rates and the factors driving variation within and between individuals remain limited. Most existing

estimates of CoTS feeding rates come from studies conducted between the 1960s and 1990s, which provide only coarse approximations from single linear measurements of feeding scars and prey corals (e.g., maximum diameter), rather than accounting for the full extent of coral consumption. Reported feeding rates vary widely, with estimates ranging from 116–187 cm^2 day^{-1} (Pearson and Endean 1969) to 66–478 cm^2 day^{-1} (Keesing and Lucas 1992), with additional values of 150 cm^2 day^{-1} (Glynn 1974), 160–320 cm^2 day^{-1} (Endean and Stablum 1973), and 350 cm^2 day^{-1} (Larkum 1988). In many cases, feeding rates were derived from linear measurements converted to two-dimensional (2D) projected areas, which do not capture the structural complexity of corals. More recent studies (e.g., Millican et al. 2024) have used software such as ImageJ to estimate projected planar areas with greater resolution. However, these methods still do not account for the three-dimensional (3D) structure of corals, including height and complexity, which may influence feeding estimates. Only Caballes et al. (2016) has taken measurements of the 3D areal extent of coral consumed by CoTS, which was conducted during a laboratory experiment.

Feeding rates presented by Keesing and Lucas (1992) (66-478cm^2day^{-1} planar area) have been used to establish sustainable thresholds of CoTS populations, which informed decision-making on the Great Barrier Reef (GBR). Given the importance of these daily feeding rates, and improved capacity to estimate feeding rates by directly measuring the areal extent of feeding scars, as well as accounting for differences in tissue surface area of corals, it is prudent to revisit and verify estimated daily feeding rates of CoTS. Furthermore, it has also been proposed that feeding behaviour may vary between sites of variable coral composition (Keesing and Lucas 1992; Caballes et al. 2016; Millican et al. 2024), which would imply that ecological modelling projections should vary according to environmental conditions. Improved understanding of species-specific and mixed diet feeding rates are necessary to provide updated values of daily feeding that account for local prey availability and coral composition.

Feeding rates of CoTS are generally expressed as the average area of coral that is consumed per individual starfish per day (e.g., Keesing and Lucas 1992; Millican et al. 2024) with limited account of variation in feeding activity and rates over successive days, or between individual starfish. Whilst these average feeding rates are useful for assessing potential coral loss with increasing densities of CoTS, they overlook potentially important information on individualistic differences in feeding behaviour. For example, it is not known whether CoTS exhibit characteristic grazing habits, whereby the amount of coral consumed is relatively consistent from day to day and limited by the local abundance and distribution of prey corals. Conversely, CoTS may exhibit a 'feast and famine' feeding strategy (*sensu* De Cuyper et al. 2015), whereby periods of intensive feeding activity may be followed by periods of inactivity. Establishing the predominant feeding habitats may provide insights into the extent to which CoTS are food limited and maximise feeding activity to meet energetic demands. This difference will be important to understand how populations might fare in future scenarios when food availability is likely to become more limited (Dietzel et al. 2020; Pratchett et al. 2021b), and metabolic demands may increase with temperature (Lang et al. 2021).

One of the foremost factors that is known to influence the specific feeding activity and rates of CoTS, is the availability of different coral prey (Ling et al. 2020; Millican et al. 2024). Higher feeding rates have been recorded for *Acropora* corals in the laboratory (Caballes et al. 2016) and in habitats that are *Acropora*-dominated (Millican et al. 2024), with much more limited feeding rates recorded on *Porites* (Caballes et al. 2016). These differential feeding rates strongly reflect known differences in prey preferences. However, prey preferences cannot be explained by apparent differences in tissue composition and nutritional value (e.g., Keesing and Lucas 1992; Caballes et al. 2016), and may therefore, reflect differences in feeding efficiency (Keesing 2021). More specifically, the amount of nutrients extracted during individual feeding bouts, whereby CoTS evert their stomach and simultaneously digest coral tissues in direct contact with their stomach folds (Brauer et al. 1970), would vary with size and complexity of different corals (Kenyon and Aeby 2009), and thereby the overall tissue surface area.

Most studies of CoTS feeding do not account for variation in the three-dimensional (3D) structure of corals, which has a major bearing on the overall tissue surface area of different prey corals (Zawada et al. 2019). This may be justified because CoTS feeding studies are generally centred around understanding the ecological impacts, and 2D horizontal planar estimates of daily feeding rates are much more relevant in estimating overall coral loss. However, failure to account for the extensive morphological variation among corals, may obscure key determinants of differential feeding rates and preferences. Effectively accounting for the 3D structure of prey corals and overall tissue surface area will provide much relevant information of CoTS feeding rates (Keesing and Lucas 1992), notwithstanding logistical challenges to effectively account for the 3D structure of highly complex corals. However, the development and increasing application of underwater close-range photogrammetry (Remmers et al. 2024), have afforded new opportunities to measure the tissue surface area of highly complex corals.

This study used close range photogrammetry to provide highly resolved estimates of daily feeding rates of individual CoTS. The high-resolution data collected will contribute to updating and refining our knowledge of daily feeding rates as well offering insight into the reliance of CoTS on different coral genera and providing a deeper understanding of the daily energetic intake of CoTS on mixed-species diets. Daily sampling of individual CoTS will also provide unprecedented insights into the temporal consistency of feeding activity, to allow for improved understanding of feeding strategies and constraints.

3.2 Methods

This study was conducted at Lizard Island (14°40’S, 145°27’E) in the northern GBR, Australia (Figure 3.1a, b), during November - December 2023. Ten adult starfish (30-60cm) were selected with at least 50 metres separating individual starfish. Given that CoTS are known to exhibit generally small home ranges when food resources are readily available (Ling et al. 2020), it was anticipated that CoTS at these high coral cover sites would not overlap during the course of the study. However, feeding

areas for two of the initial starfish in the study overlapped with feeding areas of other (non-focal) individuals, and so monitoring of these two starfish were discontinued and only the results for the eight starfish feeding in isolation are presented (see Figure 3.1c-d).

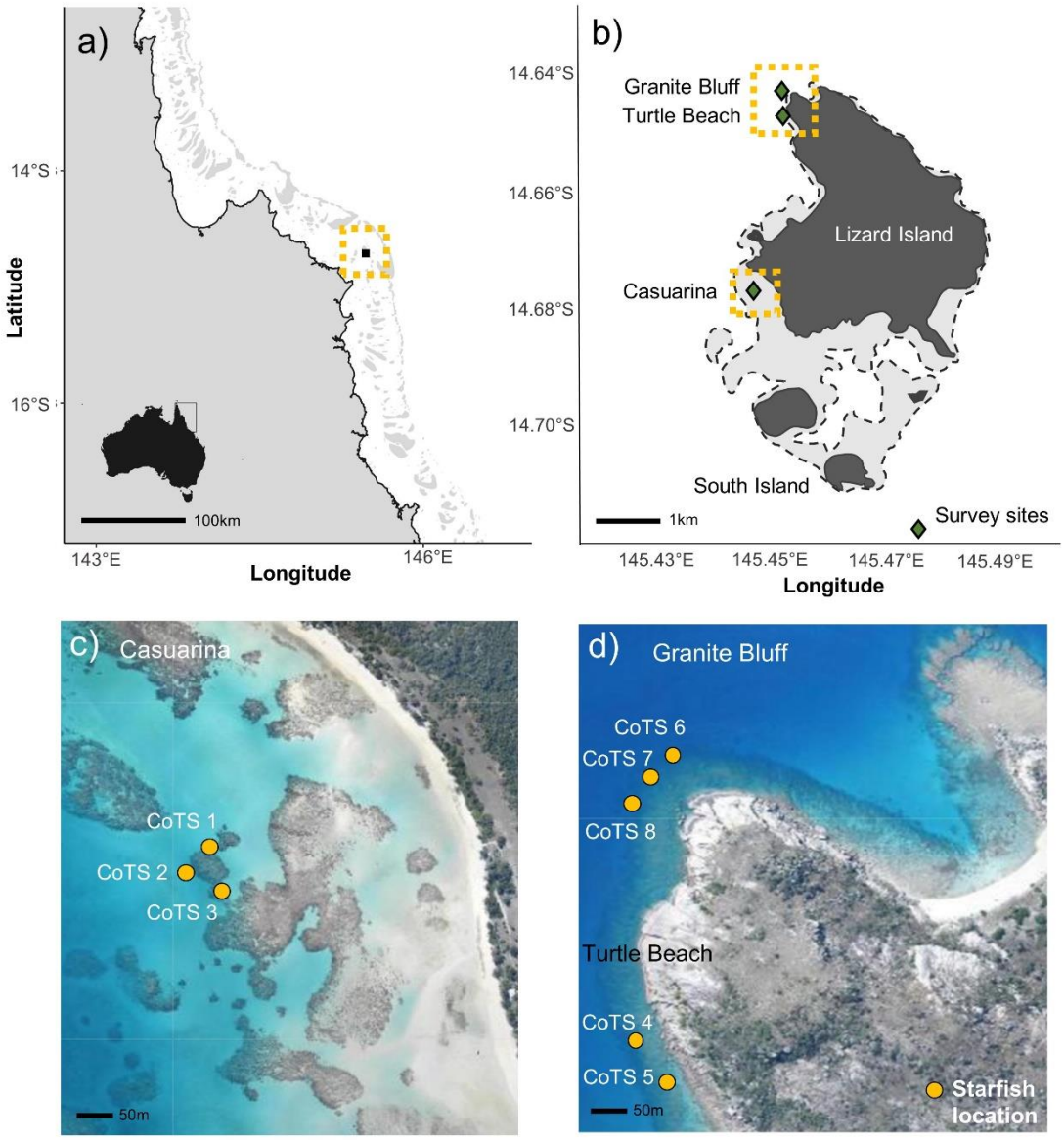


Figure 3.1 *Maps of study location and sites.* ***(a)*** *Lizard Island's location in the northern Great Barrier Reef, Australia* ***(b)*** *Lizard Island with survey locations Granite Bluff, Turtle Beach and Casuarina marked in green,* ***(c)*** *the locations of CoTS 1-3 tracked at Casuarina,* ***(d)*** *the locations of CoTS 4-8 at Turtle Beach & Granite Bluff. Queensland Imagery online aerial photograph library. Accessed May 18, 2024. https://qimagery.information.qld.gov.au/*

The focal CoTS were tracked between 9-13 days, to quantify the extent of live coral consumption during successive 24-hour periods. For results where cumulative feeding is compared among individuals, only 9 days of data are compared for all CoTS. Due to diving limitations, there were 2 days during the 13-day survey period where no diving took place and consequently no observations were conducted on these days (25/11 and 30/11). For these periods (24-26/11 and 29/11-1/12) the quantity of coral consumed over 48 hours has been split into two equal values, to provide more realistic values of daily feeding. For figures presenting daily activity over the survey period (Figure 3.3) the days of no diving are marked on the figure, however caution should be taken when interpreting feeding values on the following days (26/11 and 1/12), as these feeding values were from a 48-hour period, it is not distinguishable whether these quantities were consumed during one feeding bout, or over two consecutive nights.

On Day 0, a thorough search of the localized reef area was conducted and all feeding scars that were present in the vicinity to each of the focal starfish were marked with blank cattle tags. The location of the starfish was also marked with a tag ('Day 0') and recorded on a drawn map. For all successive days of the study each tracked starfish was revisited every 24 hours and any new scars that were present were counted, identified to genus, measured (maximum diameter), 3D modelled and marked with numbered tags. The new location of the starfish was also marked with 'Day X' tags as well as being recorded on the drawn map. No starfish went missing for more than one 24-hour period during the surveillance period. Due to the intensive nature of this tracking study, there was no cause for physically tagging the individual starfish because movements within each 24-hour period were small and easy to track. Focal CoTS were easily identified based on known size of individuals and proximity to previous day's position.

Daily consumption of coral was calculated for each starfish by summing together all fresh feeding scars consumed in the 24-hour period. Three metrics of daily feeding were derived: (1) the total number of colonies fed on per day, calculated from raw observation data; (2) the total planar

(2D) area of consumed coral per day; and (3) the total 3D surface area of consumed coral per day, derived from photogrammetry analysis (see '3D modelling feeding scars'). The 'total number of colonies per day' reflects the number of distinct coral colonies that a starfish fed on, regardless of whether the entire colony was consumed or only partially. As such, this metric provides a behavioural indicator of feeding frequency or prey-switching, rather than areal intake. The planar and 3D surface area metrics more accurately capture the extent of coral tissue area consumed and are better suited to estimating energetic intake and coral loss. Mean daily feeding estimates were calculated for each CoTS by averaging daily coral consumption over the surveillance period.

All CoTS tracked in this study were measured to the nearest centimetre to record maximum body diameter. At the conclusion of the study, individuals were dissected and weighed to determine (a) sex and (b) Gonadosomatic Index (GSI), used as a proxy for reproductive investment. GSI was calculated as the gonad wet weight divided by the total body wet weight, multiplied by 100. These data were captured to identify whether these intrinsic factors may be significantly influencing individual feeding rates.

3.2.1 *Diet composition*

The prey coral for each feeding scar in the study was identified to genus level *in situ*. However, for comparison of CoTS diets, corals were grouped by morphotaxa. Taxa were selected based on their relative abundance in the environment and some taxa, namely *Acropora, Montipora* and *Porites,* were refined further into morphotaxa groups to demonstrate the most common growth forms observed i.e., *Montipora* – encrusting, *Porites* – massive, *Acropora* – table, *Acropora* – other, *Acropora* – staghorn. The resulting 11 morphotaxa groups were: *Acropora* – other, *Acropora* – table, *Acropora* – staghorn, *Astreopora, Galaxea, Goniastrea, Lobophyllia, Montipora* – encrusting, *Porites* – massive, *Pocillopora and Stylophora.* Three further groups 'Other – branching', 'Other – massive' and 'Other – encrusting' were included to encompass all other possible corals, where 'branching' was defined as colonies with numerous branches, usually including secondary branches which are smaller

offshoots growing from the primary branches, 'Massive' was defined as colonies with hemispherical growth and 'Encrusting' was defined as colonies with low relief that followed the contour of the reef.

3.2.2 *Scar ageing*

Recurrent sampling of corals within the feeding areas of individual CoTS provided a unique opportunity to rigorously assess successive changes in the appearance of feeding scars in the days immediately following known consumption, which is important for calibrating feeding rates based on one-off sampling (Chandler et al. 2023 [**Chapter 2**]). On multiple occasions CoTS were observed returning to the same large coral colony to feed on consecutive nights (i.e., Figure 3.5), which allowed for easy observations of scar ageing and also quantification of scar size for known individuals.

Changes in colour intensity of corals that were known to be consumed by CoTS on a particular day were therefore, monitored daily for up to 14 days, to quantify the process of scar ageing. The time (in days) taken for CoTS feeding scars to turn from 'fresh' to the point where scars are overgrown with turf algae is relatively unknown but important for understanding recent feeding activity of CoTS during SALAD surveys (Chandler et al. 2023, [**Chapter 2**]**, Chapter 5**]). To capture this ageing process, fresh feeding scars known to be <24 hours old were photographed alongside a CoralWatch card every day for the duration of the study. Photographs of feeding scars were taken from a distance of 30 cm using an Olympus TG-6 camera without flash, with the white balance adjusted separately for each depth.

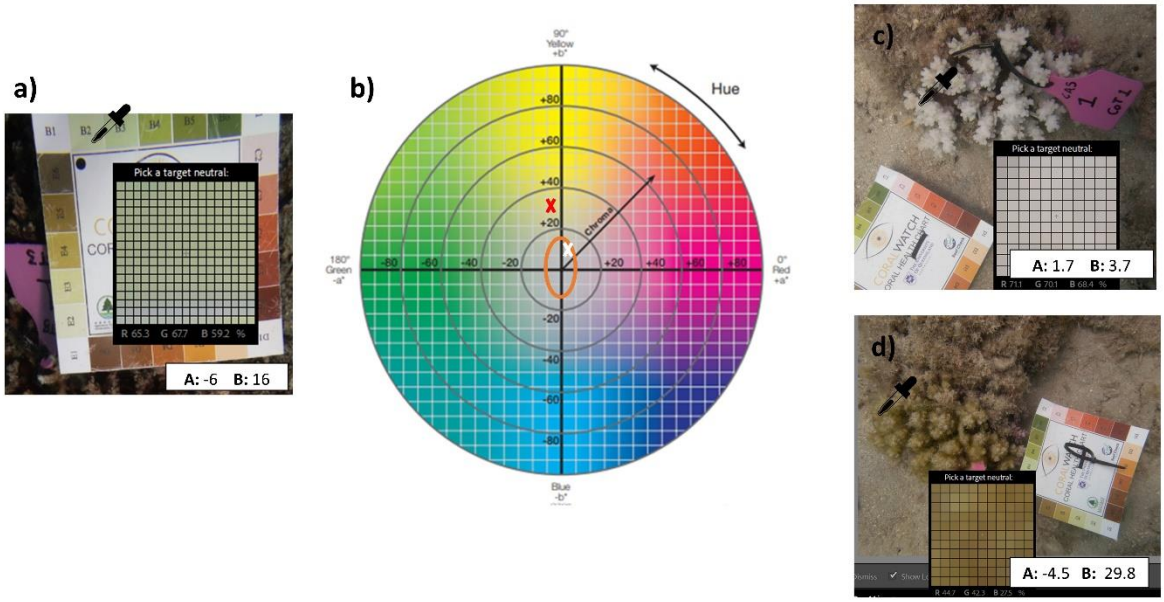


Figure 3.2 *Process of using CIE LAB scale to quantify when CoTS surpass colour intensity (chroma) in line with B2 on a CoralWatch card.* ***(a)*** *Adobe Lightroom colour picker presents LAB values for B2 on the CoralWatch card,* ***(b)*** *CIE LAB scale with white at the centre and chroma threshold of A= ±6 and B = ±16 marked in orange, in line with CoralWatch card LAB values,* ***(c)*** *Adobe Lightroom colour picker presents LAB values of one fresh scar with chroma values below threshold limits (A<6, B<16; see white cross),* ***(d)*** *Adobe Lightroom colour picker presents LAB values of one old scar with chroma threshold exceeded (B >16; see red cross), so this scar has surpassed the ageing threshold.*

The time taken for fresh scars to progress beyond the colour of a category B2 on a CoralWatch card was quantified, as this colour threshold has previously been used as the point of exclusion for recording feeding scars during SALAD surveys (Chandler et al. 2023, [**Chapter 2**]). For quantitative determination of the time taken for feeding scars to surpass the colour threshold of a B2, a CIELAB colour space was used to quantify when the lightness and chroma (colour intensity) of the scar exceeded that of the Coral Watch category B2, quantifying in this way would reduce observer bias. Adobe Lightroom colour dropper feature was used to detect the LAB colour of the scar, where L= lightness, A=red/green and B= yellow/blue. LAB values of the scar were compared directly to the known LAB values of the Coral Watch card. Given that white on a CIELAB colour chart has values of A=0 and B=0 , and the 'B2' category of the Colour Watch card has values of A= -6 and B = 16, any scar colour that exceeds the Colour Watch card's chroma values on the LAB colour scale

(i.e., when A= < -7 or B= > 16) can be considered darker than the Coral Watch card and officially surpasses the ageing threshold. This process was carried out on the nine series of ageing photos for each scar and an ageing factor was determined for each series, see Table 2.2. The ageing factor was averaged over the nine separate scars to quantify mean ageing factor.

3.2.3 *3D modelling feeding scars*

Gopro Hero 11 Black cameras were used to collect close-range imagery of individual colonies for 3D modelling. Structure from motion techniques (SfM) described by Ferrari et al. (2017) were followed, however 4K video footage (30fps) was used instead of timelapse imagery due to faster in-water data collection capability, allowing for more replicates per morphotaxa. Additionally, custom-built scaling objects (Agisoft Metashape coded targets, 12bit, inverted, 20% of full size, target centres 60 mm apart) were incorporated into the scene. Image acquisition involved filming the colony from all angles, moving in arcs from top to bottom. Videos were filmed in natural lighting. Agisoft Metashape v 1.7.6 software was used for processing of videos and model building. Jpeg frames were extracted from the 4k videos as every 4th frame. Image sets ranged from 150 to 1400 images, depending on length of video (averaged ~1 minute) which was related to coral size and complexity.

Three dimensional models were reconstructed from image sets using Agisoft Metashape software (parameters outlined in Supplementary material, Appendix 2a, Table S1). Any extraneous mesh material that was not part of the colony was removed using Agisoft Metashape selection tools. Models were scaled using at least two sets of independent scale bars (60 mm in length) from the coded target objects described above. Resulting models had an average mesh resolution (distance between vertices) of 1.86 mm and average ground sample distance of 0.18 mm/pixel. Models were cropped as a) the entire coral colony and b) the scar only. Colony 3D area was extracted using the Mesh-Area tool in Agisoft Metashape. In order to extract 2D area, the model must first be projected onto a 2D plane in a manner similar to what would be done by somebody taking a top-down picture of the coral in the field for this same purpose. Thus, the models were visually orientated in the

software to replicate a top-down field of view, where the z-axis was aligned perpendicular to this view plane. Once this was done, the 2D area of the colony and the scar was estimated using the Export Report tool within the software with projection set to the X-Y plane.

3.2.4 *Statistical analysis*

To investigate which factors were driving variation in daily feeding rate, a generalized linear mixed effects model (GLMM) was used to model the effects of CoTS ID, body size and Gonadosomatic Index (GSI) on the planar area of coral consumed per day. GSI was calculated using the formula (gonad wet weight/total body wet weight x 100). CoTS ID was initially included as a fixed effect in the model to test for potential differences in daily feeding rate between individual CoTS, however this approach resulted in rank deficiency and model convergence issues, indicating that the model could not reliably estimate separate coefficients for each individual. To address this issue, CoTS ID was treated as a random effect instead and so Gonadosomatic Index ('GSI') and 'body size' were included as fixed effects and 'Site' and 'CoTS ID' were included as random effects with random intercepts. The daily feeding rate data was modelled against a Gaussian distribution with an identity link function. The response variable was log-transformed to address non-normality prior to model fitting.

All statistical analyses were performed in the R statistical and graphical environment, with models built using the *glmmTMB* package (Brooks et al. 2017). For each model, goodness of fit was assessed, and combinations of fixed and random effects were tested and retained only if they improved the fit of the model, based on the Akaike Information Criterion (AIC). Each model was validated, including checks of simulated residuals and dispersion, using the *DHARMa* package (Wickham 2016). Boxplots and stacked barplots were computed using the *ggplot2* package in R (Hartig 2018).

3.3 Results

3.3.1 *Daily activity*

All CoTS exhibited days with no feeding during the survey period, and across all CoTS there was an average of 65% of nights with feeding activity and 35% of nights with no feeding (Figure 3.3). On occasions where no feeding was observed over a 24-hour period it was recorded that CoTS were located in the same location as the day before and so it has been inferred that no movement took place; no CoTS remained inactive for more than 3 consecutive days. Days of feeding versus days of inactivity were often consecutive, with periods usually lasting 2-4 days. Overall, there were no strong patterns of feeding and resting that were consistent among individuals or directly linked to surface area consumption.

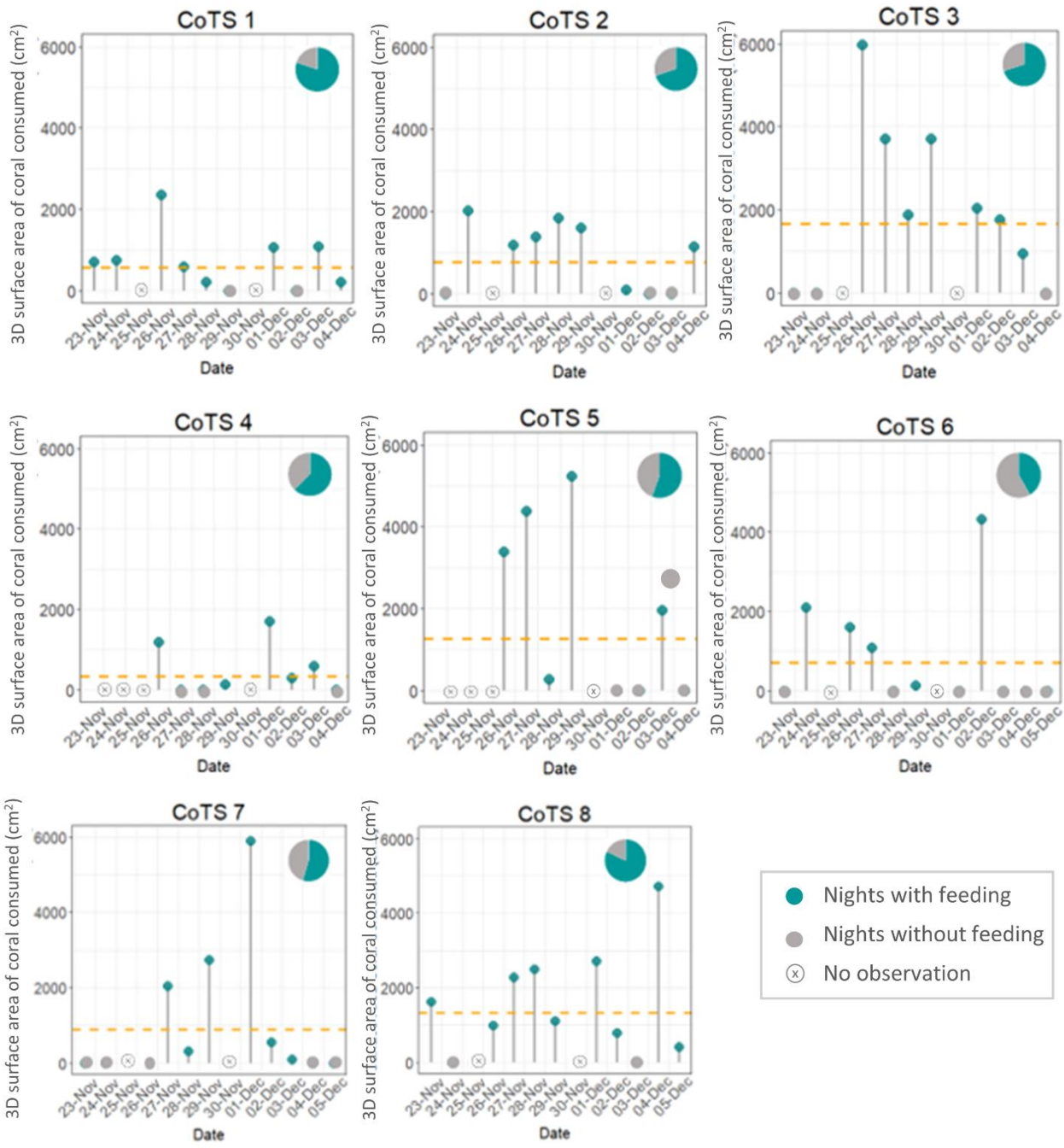


Figure 3.3 *Daily activity patterns of 8 individual starfish over the survey period (9-13 days). Green points represent the 3D surface areal extent (cm2) of coral consumed during each 24-hour period, grey points represent 24-hour periods when no coral was consumed. Days when no feeding observations were conducted (due to diving limitations) are marked as crossed circles. Dashed lines represent the average area of coral consumed over the survey period. Pie charts represent the proportion of 24-hour periods spent feeding (green).*

3.3.2 *Feeding rates*

The mean daily feeding rates for individual CoTS was 1.35 coral colonies (± SE 0.18) per day or 198.4cm^2 d^{-1} (± 23.86 SE) planar area per day or 998.83 cm^2 day^{-1} (SE 128.69) total 3D surface area per day. The aforementioned mean feeding rates account for the multiple days during the survey period where no feeding was recorded, which is an important consideration. For example, the mean number of colonies consumed on occasions when CoTS were foraging was 2.3 colonies per 24-hour period, which is considerably higher.

Daily areal consumption values were highly variable between days and among starfish (Figure 3.4), ranging from 0 to 9 colonies a day, 0cm^2 day^{-1} to 1,261.0cm^2 day^{-1} (planar area), and 0cm^2 day^{-1} to 5,242.8cm^2 day^{-1} (3D surface area). Despite marked variation in feeding activity among days and between starfish, values averaged over the whole survey period for each starfish were relatively consistent (Figure 3.4), especially for planar area of coral consumed with 5 out of 8 CoTS having individual mean feeding rates between 115-200cm^2 day^{-1} (Figure 3.4).

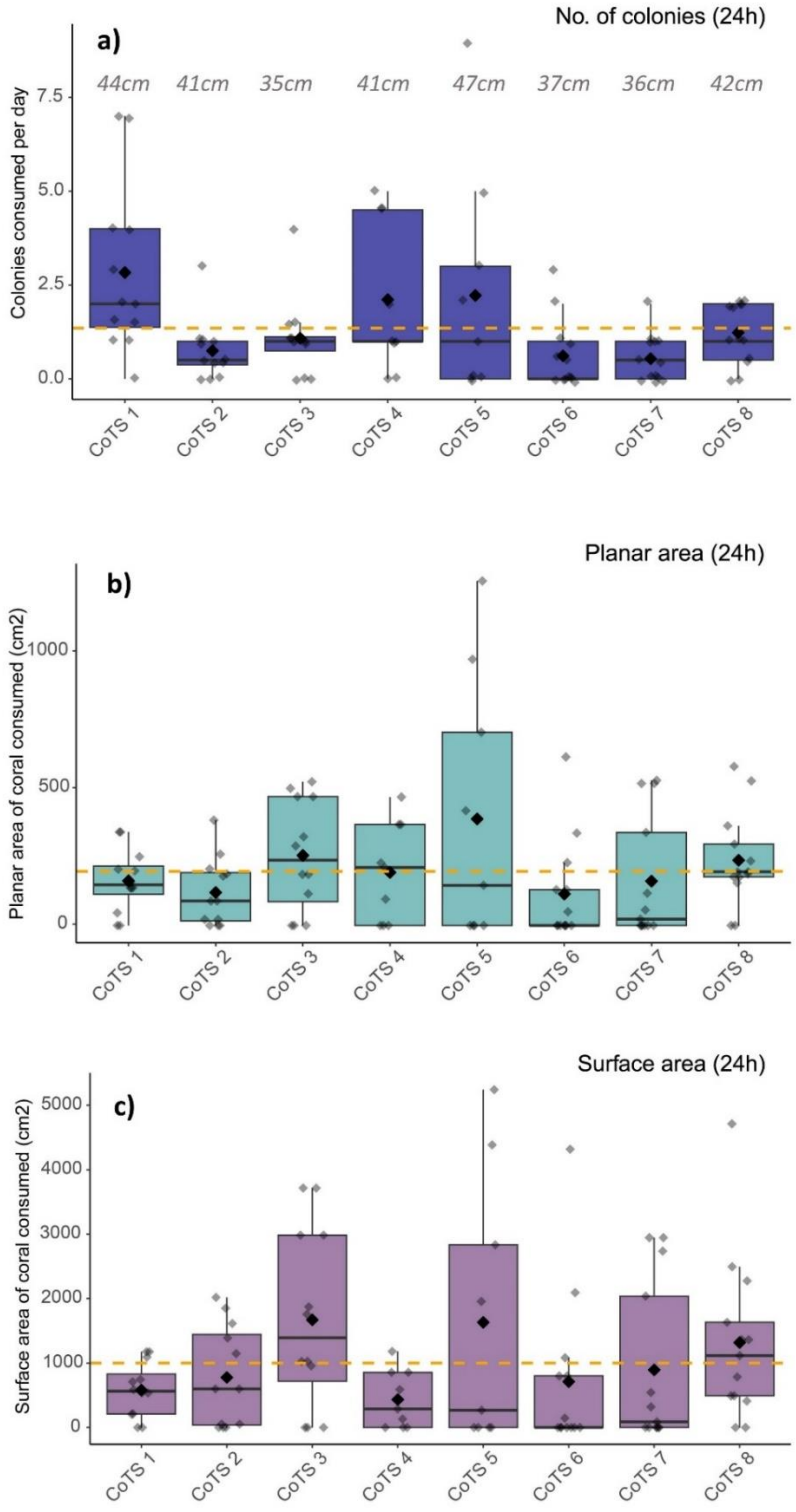


Figure 3.4 *Daily feeding rates of 8 individual starfish recorded over 9-13 consecutive days, presented as* ***(a) number of colonies*** *consumed per day,* ***(b) planar projected area*** *of coral consumed per day (cm^2),* ***(c) total (3D) surface area*** *of coral consumed per day (cm^2). Each boxplot represents feeding for a single starfish across multiple days of intensive sampling. Large black diamonds and thick horizontal lines represent mean and median values, respectively, box limits the interquartile range, whiskers the 1.5x interquartile range, and small*

grey diamonds the daily consumption data. Maximum body diameter of each individual CoTS is also presented in panel a.

When daily surface area consumption was summed over the 9-day survey period for each starfish (effectively representing cumulative tissue consumption), total surface area consumption was highly variable among individuals, ranging from 3,897.4 cm^2 (CoTS 4) to 20,036.9 cm^2 (CoTS 3; Figure 3.6b).

There were no significant differences in daily feeding rates among individual CoTS in this study, for any metric of daily feeding rate. Initially, a model with CoTS ID as a random effect was fitted but showed no significant improvement in model fit (AIC=159.01). The model without CoTS ID as a random effect had a lower AICc (157.01) and therefore was selected as the final model, this demonstrated that there was no significant effect of CoTS ID on daily feeding rate. There was also no significant effect of body size (p=0.497) or GSI (p=0.753) on the daily feeding rate of CoTS (planar area). It was not possible to investigate the role of sex on feeding rate because 7 out of 8 CoTS were female (dissection was conducted after the study's conclusion).



Figure 3.5 *Successive feeding bouts documented on a single large colony of tabular Acropora by a single CoTS. Quantification of scar area presents scar length, planar area and total surface area of successive scars*

In addition to quantifying feeding rates, this study also captured patterns of feeding on corals in terms of visitation on successive days. Consumption of very large prey corals often occurred

through successive feeding bouts often over multiple days (Figure 3.5). Feeding was observed to progress laterally across coral colony surface, which allowed for direct comparisons of scar size of an individual with known diameter on a consistent coral morphology.

3.3.3 *Diet composition*

A total of 17 different coral genera were consumed during this study, which were assigned to 15 morphotaxa groups. '*Acropora* – Other' colonies were consumed in excess of all other colonies for six out of eight CoTS (Figure 3.6a), with a maximum of 12 *Acropora* colonies consumed by one CoTS during the 9 days (CoTS 5) and a minimum number of four *Acropora* colonies (CoTS 4 and CoTS 6). '*Acropora* – Other' accounted for 51% of all coral colonies consumed during the study. The second most favoured coral taxon was *Montipora*, accounting for 18% of all coral colonies consumed, followed by *Pocillopora* (5%) and *Astreopora* (5%). These values represent distinct colonies that were fed on, although in many cases only partially.

The relative contributions of different taxa to CoTS' diet differ depending on how feeding rates are compared. When relative consumption of coral taxa is explored from a 3D surface areal perspective (Figure 3.6b), '*Acropora* – other' accounts for 82% of all feeding, *Montipora* only accounts for 9%, followed by *Pocillopora* (3%) and '*Acropora* – table' (2%). The proportion of '*Acropora* – other' surface area consumed by each individual CoTS ranged from 41.6% of the diet (CoTS 4) to 99.4% (CoTS 3), with '*Acropora* – other' contributing to >80% of total coral area intake for 5 out of 8 CoTS. Acroporidae corals (which encompasses *Acropora, Montipora* and *Astreopora* corals from this study) accounted for 94% of the coral intake in this study (3D surface area, all CoTS pooled).

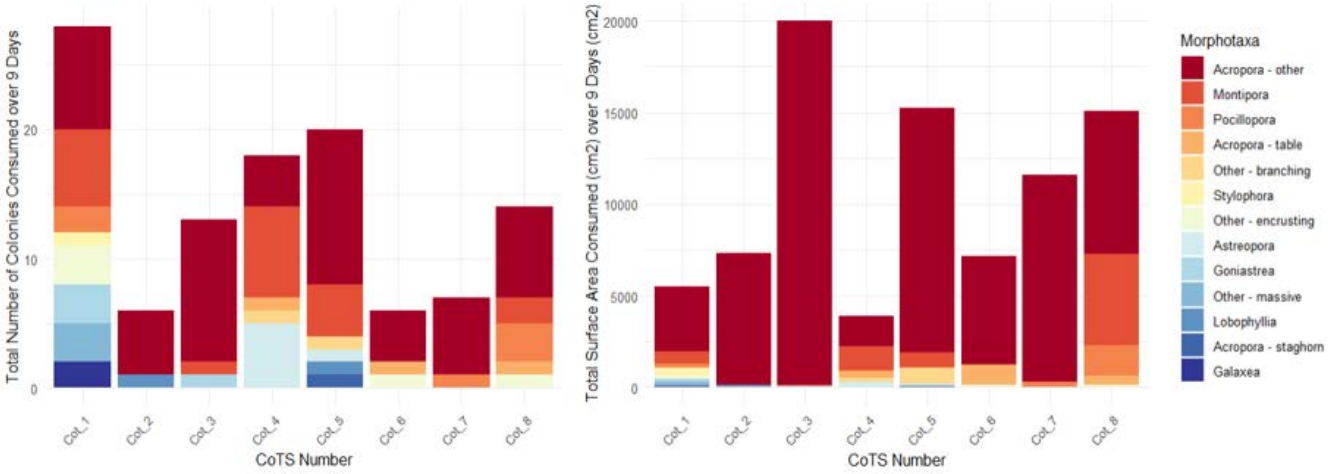


Figure 3.6 *Total (cumulative) feeding from 9 consecutive days of feeding by 8 individual starfish. Bars represent summed feeding and colours depict proportional feeding on different coral morphotaxa. Total feeding is presented as* ***(a)*** *Total number of coral colonies consumed and* ***(b)*** *Total 3D surface area of coral consumed (cm²)*

3.3.4 *Ageing of feeding scars*

Scars took between 3-7 days to surpass the chroma values associated with a Level 2 on the CoralWatch card. The time taken for feeding scars to discolour in winter was estimated to be slightly longer, presumably due to the slower growth of turf algae.

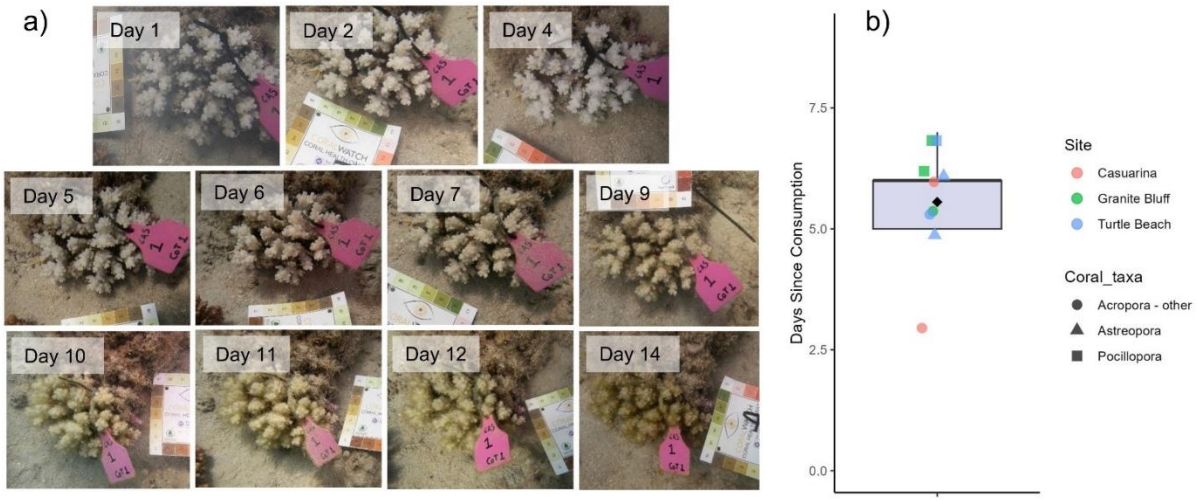


Figure 3.7 *Ageing process of feeding scars observed.* ***(a)*** *Visual progression of a feeding scar (genus Pocillopora) photographed over 14 days in this study. Discolouration beyond the B2 colour threshold on a CoralWatch card occurred between days 6 and 7 for this feeding scar.* ***(b)*** *Boxplot showing the number of days (since consumption) at which the B2 colour threshold was surpassed for 9 tracked scars. Boxplot line shows median*

time, box limits the interquartile range, whisker the 1.5x interquartile range, and filled diamond the mean. Each small point represents an individual scar for which the ageing period was quantified. The shapes and colours of each point indicate the coral taxon and sampling site of the scars.

3.4 Discussion

Intensive research into the daily feeding rates of adult CoTS revealed that feeding activity varies greatly among successive days, whereby most CoTS exhibited consecutive days without any apparent feeding activity interspersed with days of very intensive feeding. In fact, feeding activity was only recorded on 65% of the nights within the observation period, with no individual starfish feeding on every night of the study period. This suggests that on any given day only 65% of CoTS in a population might actually feed, which has consequences for their ecological impacts but also for detectability of CoTS based on occurrence of recent feeding scars. Whilst consecutive days of inactivity were common, no CoTS remained inactive for longer than 3 consecutive days which suggests that this may be the limit for fasting for individuals in this size range. Interestingly, no obvious patterns in motivation for rest were found, either as a time-based motivation, or related to the number colonies or areal consumption of coral, inferring that periods of inactivity did not appear to be directly motivated by satiation. For example, after a large feeding bout on day 4 of the study (471cm^2 planar area), CoTS 3 continued to feed at high rates for the following three consecutive nights, whereas CoTS 6 consumed a small quantity (50.2cm^2) and was inactive for the following 2 nights. No consistent feeding strategy was observed among individuals, but rather, there appeared to be individual differences in feeding approach where some individuals consumed multiple small corals of different genera frequently (CoTS 1) whereas other individuals consumed fewer, larger colonies with obvious preference for a single taxon (*Acropora*) and longer periods of inactivity (CoTS 5, CoTS 7). This variability in behaviour suggests that rest periods and foraging behaviour are perhaps motivated by other factors than satiation. It may be that CoTS feed opportunistically based on local availability of different prey corals, until factors (i.e. predation risk, temperature or chemical cues) deter feeding.

This study revealed considerable variation in areal extent of coral consumed, over consecutive days and also among individuals. Daily feeding bouts were recorded as high as 9 colonies or 1,261cm^2 day^{-1} (planar area) for a single starfish in a 24-hour period. These values demonstrate the ability of individual CoTS to consume vast amounts of coral during 24-hour periods, but such large feeding bouts were not sustained. Average daily feeding rates are much lower (198.39cm^2 day^{-1} ± 23.86 SE), mainly because they incorporate multiple days of no feeding, which is the most appropriate metric for establishing net coral loss. Our mean daily feeding rate calculated for all CoTS in this study closely corresponds with the feeding rate (231 cm^2 day^{-1} ± 122 SE) reported by Foo et al. (2024) for CoTS (*Acanthaster* cf. *solaris*) within the central and western Pacific.

The highly resolved feeding rates presented in this paper were enabled by the use of underwater photogrammetry to provide detailed estimates of the areal extent of individual feeding scars, accounting for the complex 3D structure of some prey corals. Daily feeding rates are presented in three distinct formats; the number of colonies consumed per day, the projected planar (2D) area of coral consumed per day, and the overall (3D) surface area of coral consumed per day. These different metrics offer different perspectives on CoTS feeding; the number of colonies consumed provides insights into feeding activity and movement, the planar area estimates provide indication of the cumulative ecological impacts of CoTS feeding, whilst overall surface area serves as a proxy for approximate tissue area consumed providing improved understanding of potential differences in feeding efficiency between complex versus simple corals. This unique perspective on daily feeding provides insight into the physiological trade-offs of feeding choices.

When cumulative feeding over the entire survey period was compared between CoTS, considerable differences between individuals were identified (Figure 3.6). It could be reasonably assumed that CoTS of the same species, subject to similar environmental conditions and living in comparable habitats, would exhibit very similar feeding activity and rates. However, pronounced differences among individual CoTS were found, especially when comparing the overall 3D surface

area of coral consumed (Figure 3.6b), which may likely affect energetic intake. These apparent differences could not be explained based on differences in body size (cf. Yamaguchi 1974; Birkeland and Lucas 1990; Keesing and Lucas 1992) though there were limited differences in the body size (35-47cm) of focal individuals. Moreover, post-hoc dissection of focal individuals determined that 7 out of 8 CoTS were female, which all had very similar investment into gonad production (GSI), so this was also unlikely to be influencing consumption rates. It is possible that individual differences are manifest due to obvious heterogeneity in temporal patterns of feeding, such that longer term studies would be needed to ascertain potential differences in overall energetic intake, which would affect individual condition and fitness.

Diet composition was found to strongly influence daily feeding rate and cumulative feeding, which is likely due to the taxa-specific differences in morphological complexity that inherently influence the areal extent of coral tissue consumed. By accounting for differences in the overall (3D) surface area consumed, this study revealed important taxonomic differences in the rates of 2D versus 3D feeding. In this study *Acropora* corals were fed on in excess to all other taxa, and contributed disproportionately to total tissue area consumed by all CoTS pooled (82% of all tissue area). This dominance could be a result of the local environment where *Acropora* corals were abundant, but is also likely as a result of the highly complex growth form of this genus, offering a large areal extent of surface area for every colony consumed. *Acropora* colonies have been shown to have surface area coverage that is over five times as large as encrusting corals of the same colony diameter (**Chapter 4**), which may explain why this genus accounted for the majority of tissue area consumed, despite numerous colonies of other taxa being consumed which are morphologically less complex (*Montipora, Astreopora,* etc). It is apparent that colonies such as *Acropora* which have highly complex growth forms are providing a high energetic return for every colony consumed. Of course, tissue thickness, tissue accessibility, energetic content and digestibility also contribute to overall energetic return of these colonies (Keesing 2021) in addition to areal extent of tissue, though there is evidence that *Acropora* does have high energetic content and protein content, compared to

other corals (Keesing 2021). These insights reinforce the notion that *Acropora* is an efficient feeding choice for CoTS, and helps to explain the feeding preferences for this genus which have been well-documented in the literature (e.g., Pratchett 2007; Ling et al. 2020). Given that Acroporidae corals as a whole accounted for 94% of total surface area consumed by all CoTS pooled, this raises concerns about how CoTS will fare in future scenarios where these corals are forecast to diminish (Pratchett et al. 2021).

Daily tracking of the feeding activity of CoTS during this study has provided a unique opportunity to also track the progression of scar ageing over 13 days. The period of time taken for fresh scars to reach the colour hue of 'aged' (overgrown with turf algae, comparable to colour chart B2) was determined to be 5-6 days in the summer (Figure 3.7), which complimented the work of Cummings (2002) that reported coral injuries at this latitude in the summer to become discoloured in 3-5 days. This knowledge of scar ageing will enable daily feeding rates to be calculated from large-scale surveys, with the assumption that recorded 'fresh' scars will have been consumed within this known time period.

Conclusion

This chapter resolved that feeding activity of CoTS varies greatly among successive days. Most notably, it revealed that CoTS do not consistently feed in consecutive 24-hour periods, but may remain inactive and do not feed for periods of 2-3 days. This has obvious implications for establishing their ecological impact, but also affects detectability, as CoTS are often well hidden during extensive periods between feeding bouts. Highly resolved mean daily feeding rates presented herein were found to fit within the range of previous feeding studies, albeit at the smaller end of the continuum which is likely because of the multiple days of no feeding which were captured within the 2-week monitoring period. These rates of feeding, which appropriately include periods of inactivity, will be useful for updating ecological models of CoTS impact to reef assemblages. Further investigation into the role that different intrinsic and extrinsic factors are having in driving variation in CoTS feeding

rate will be useful for effectively predicting the ecological effects of CoTS in different regions and environmental settings. It is likely that starfish feeding behaviour is determined by a complex interaction of factors (including body size, prey availability and composition), and understanding these drivers is important for understanding and predicting their ecological effects in coral reef ecosystems.

Chapter 4: Predicting 3D and 2D surface area of corals from simple field measurements[2]

4.1 Introduction

Scleractinian corals form the framework of tropical coral reefs, providing structure for essential habitats, including for critical early life stages of both ecologically and economically important species (Luckhurst and Luckhurst 1978; Almany 2004; Graham 2014). Additionally, coral reefs provide valuable ecosystem goods and services to tropical and subtropical nations; their structures forming natural barriers to oceanic wave energy, buffering shorelines from erosion and flooding (Moberg and Folke 1999; Reguero et al. 2021) as well as providing protein and income for coastal communities (Cruz-Trinidad et al. 2014; Eddy et al. 2021). As the most widely used indicator of reef health, coral cover has been estimated using a variety of methodologies which are largely based on measuring the relative abundance (and size) of benthic substrate types (Leujak and Ormond 2007). The two-dimensional (2D) surface area of coral, or the area of occupancy, is commonly estimated based on simple field measurements (e.g., point-intercept or line-intercept methods (Hill and Wilkinson 2004). Notably, the ubiquity of 2D (planar) representations of benthic communities facilitates standardization and comparison between and within different reef monitoring programs (House et al. 2018).

While 2D approaches continue to be useful for fast estimates and comparisons of benthic cover and composition (Ferrari et al. 2017; Urbina-Barreto et al. 2021a), they are lacking in a third dimension which provides insight into the structural complexity of corals and reefs. Given that the

[2] This chapter was published as Chandler, J.F., Figueira, W.F., Burn, D., Doll, P.C., Johandes, A., Piccaluga, A. and Pratchett, M.S. (2024) Predicting 3D and 2D surface area of corals from simple field measurements. *Scientific Reports* 14(1):20549.

morphological complexity of corals is a key determinant of habitat facilitation for reef organisms (Luckhurst and Luckhurst 1978; Almany 2004; Graham 2014), the inclusion of three-dimensional (3D) structure in reef health assessments incorporates an aspect of ecosystem health which is overlooked by using planar estimates of coral cover alone. Quantifying the structural complexity of coral reefs is increasingly recognized as an important aspect of ecosystem monitoring, as topographic complexity is not only a key driver of biodiversity and productivity of reef ecosystems (Komyakova et al. 2013; Newman et al. 2015; Torres-Pulliza et al. 2020; Fisher 2023), but also has consequences for calcification rates, wave attenuation potential and other reef functions. The dual process of coral growth and skeletal erosion drive changes in habitat structure over time which is important for understanding evolving reef function (Ferrari et al. 2017; Urbina-Barreto et al. 2021a). As such, surveys that fail to incorporate 3D aspects of coral reefs into data collection are overlooking important ecological parameters.

The 3D complexity of individual coral colonies is a necessary component to describe the surface area of live tissue and understand biological processes such as metabolism, photosynthesis, reproductive potential, and nutrient uptake (Dahl 1973; Alcala and Vogt 1997; Holmes 2008). Moreover, precise quantification of live tissue and other 3D characteristics of individual colonies facilitates assessment and modelling of key demographic processes, including the growth and reproduction of coral colonies (Meiling et al. 2020; Lange et al. 2022). Surface area is, therefore, a valuable metric for both the monitoring and modelling of these colony-level processes.

Researchers have been attempting to estimate surface area of individual coral colonies since as early as the 1950s (Odum and Odum 1955). Accurately capturing the fine-scale complexity of the coral structures, however, has proven difficult. Early methods used geometric approximations based on shapes comparable to coral morphologies (Odum and Odum 1955). This work was followed by surface indices (SI) or ‘scaling factors’ which converted field measurements of colony diameter and planar area to 3D surface area, using theoretical approximations (Dahl 1973; Holmes 2008). The

conversions were based on crude geometric representations of shapes such as hemispheres, discs, and branched cylinders to approximate 'massive', 'plate-like', and 'branched' coral morphologies, respectively. The resulting surface area estimates invariably underestimate true surface area (Alcala and Vogt 1997; Laforsch et al. 2008), especially for complex growth forms. Despite these limitations, the SI concept demonstrated the potential for applying pre-determined mathematical relationships to measured parameters for surface area estimates. Additional techniques attempting to quantify 3D surface area of corals have included wrapping colonies in aluminium foil and subsequently measuring the area of material required to cover the surface of the coral (Marsh 1970), dipping corals in either paraffin wax (Stimson and Kinzie 1991), dye (Hoegh-Guldberg 1988) or latex (Meyer and Schultz 1985), then removing the liquid coating and measuring the volume of the liquid, and more recently the use of CT scans and X-rays (Laforsch et al. 2008). Whilst some of these methods (i.e., wax dipping) were found to produce relatively accurate and repeatable estimations of surface area (Naumann et al. 2009), most methods were underestimating the complex corallite architecture of the corals and consequently underestimating the actual coral tissue surface area. Another drawback of these methods was that they required the collection and destruction of the colony.

In recent years, the revolution of modern aquatic photogrammetry techniques (Drap 2012; Figueira et al. 2015) has enabled *in situ* assessments of coral surface area to be calculated through a non-destructive and highly resolved method. In comparison to traditional methods of measuring coral surface area, photogrammetry has been proven to produce data with higher precision and lower error (Urbina-Barreto et al. 2021b; Lechene et al. 2024), alongside enabling extraction of additional metrics such as volume and shelter capacity (Ferrari et al. 2022). The drawback, however, is that the process of photogrammetry is time consuming and requires specialist software and training (Bythell et al. 2001; Urbina-Barreto et al. 2021a), as well as some reliance on favourable environmental conditions (e.g., currents, swell, visibility). Recent advances in photogrammetry have enabled mapping of relatively large spatial scales (hundreds of square metres; Remmers et al. 2024) with high accuracy and precision, which can provide information on habitat structural complexity and

demographic rates, including at an individual colony level (Figueira et al. 2015; Urbina-Barreto et al. 2021b; Remmers et al. 2024). However, the time and processing power required to render and analyse these data-heavy models can be restrictive, especially if timely data generation is required (Rossi et al. 2020; Urbina-Barreto et al. 2021b; Remmers et al. 2024). Conversely, lower resolution measurements, such as the diameter of coral colonies, are fast and easy to obtain, and they can be collected either via *in situ* tape measurements or alternatively obtained from photographs, even from historical datasets.

The objective of this paper was to take advantage of opportunities afforded by photogrammetry to quantify total 3D surface area and projected 2D surface area of different coral morphotaxa, and to test how these parameters relate to explore opportunities to rapidly estimate total 3D surface area and projected 2D surface area of different coral morphotaxa, based on simple field-based measurements (colony maximum diameter). Whilst this is not the first study to describe the relationship between coral diameter and 3D surface area of corals (Bythell et al. 2001; Courtney et al. 2007; Holmes 2008; House et al. 2018; Aston et al. 2022) , previous studies have only converted a small number of broad-level coral morphologies. For example, House *et al.* (2018) established predictive relationships between 2D and 3D surface area, specific to three broad morphotypes ('branching', 'encrusting' and 'massive') based on a total of 22 specimens, however these broad groupings do not adequately capture the morphological heterogeneity of coral species in the Indo-Pacific. More recently, Aston et al. (2022) established predictive relationships between planar area and a whole suite of 3D structural metrics in addition to surface area (volume, spatial refuge, shelter size factor, etc.), for seven morphotaxa of corals on the GBR ("Branching *Pocillopora*", "Digitate *Acropora*", "Corymbose *Acropora*", "Tabular *Acropora*", "Massive", "Branching *Isopora*" and "Branching *Porites*"), built from the photogrammetry of 69 specimens. The morphotaxa presented in the study were more refined than the morphotype groupings used by House et al. (2018), but do not encompass the full range of morphologies present in the region, meaning some coral forms (e.g., staghorn *Acropora*, encrusting corals) cannot be modelled using these published relationships.

Here, taxon-specific conversion metrics are provided, with morphotaxa categories encompassing all common scleractinian corals on Australia's Great Barrier Reef (GBR). Equation parameters are presented for 12 specific morphotaxa and three 'Other' categories, enabling surface area metrics to be extracted by any researcher with measurements of colony diameter from field surveys or photographs. This information can be used by researchers and managers to provide a more rigorous representation of available coral as community habitat and tissue biomass, and for estimating biological and physical processes of corals. It also presents an opportunity to assess fine-scale changes in colony growth and recovery (Holmes 2008) at a reef level.

4.2 Methods

4.2.1 *Data collection*

To construct relationships between simple linear measurements of colony maximum diameter and colony surface area (both projected 2D surface area and total 3D surface area), predictive models for various morphotaxa were built. Measurements of colony maximum diameter were collected in the field and surface area metrics were extracted in the lab using 3D photogrammetry software.

Field sampling for this study was conducted at Lizard Island (14°40'S, 145°27'E) in the northern Great Barrier Reef, Australia, in November and December 2023. Corals were selected from five sites (between 2-10m depth); namely North Point, Granite Bluff, Turtle Beach and Casuarina Beach and Big Vicki's on the North-West and West of the Island.

10 coral genera (*Acropora, Astreopora, Fungia, Goniastrea, Lobophyllia, Montipora*, *Pocillopora, Porites*, *Seriatopora and Stylophora*) were pre-selected due to their dominance on coral reefs around Lizard Island, collectively accounting for 84.45% of hard coral cover based on Point intercept Transect (PIT) surveys at these sites, as per methodology outlined by Hill & Wilkinson (2004). Due to the morphological heterogeneity of *Acropora* spp. this genus was further split into the

three common morphotaxa '*Acropora* – table', '*Acropora* – staghorn' and '*Acropora* – Other', and for the genera *Montipora* and *Porites* the dominant growth forms were specified as '*Montipora* – encrusting' and '*Porites* – massive'. To establish relationships for corals which were not encompassed by these 12 morphotaxa groups, corals from less common genera were haphazardly chosen and later grouped together to form three 'Other' morphotaxa: 'Other – branching', 'Other – encrusting' and 'Other – massive'. Here, 'massive' was defined as colonies with a hemispherical structure, 'encrusting' was defined as colonies with low relief that grow against the substrate and 'branching' was defined as colonies that have numerous branches, usually including secondary branches which are smaller offshoots growing from the primary branches.

The resulting 15 morphotaxa modelled in this study were: *Acropora* – other (n = 13 colonies), *Acropora* – staghorn (n = 14), *Acropora* – table (n = 13), *Astreopora* (n = 9)*, Fungiidae* (n = 6)*, Goniastrea* (n = 11)*, Lobophyllia* (n = 10)*, Montipora* encrusting (n = 11), *Pocillopora* (n = 13)*, Porites* – massive (n = 9), *Seriatopora* (n = 9)*, Stylophora* (n = 10)*, Other – branching* (n = 6)*, Other – encrusting* (n = 13), and *Other - massive* (n = 12). Replicates for each morphotaxon were determined based on the structural complexity and morphological variation within each morphotaxon. For morphotaxa with open and complex growth forms (i.e., *Acropora* – staghorn), a disproportionately higher number of replicates were used, to account for predicted uncertainty in model fit. In contrast, for morphotaxa with relatively consistent morphology (i.e., *Fungia*), fewer replicates were required because surface area was expected to scale quite consistently with size. Where possible, replicate colonies were selected over an even spread of size classes from small to large. In total, models were built for 159 colonies across the 15 morphotaxa.

For each of the 15 morphotaxa, relationships were established between a) colony maximum diameter and projected 2D surface area and b) colony maximum diameter and total 3D surface area. To establish relationships, the replicate colonies from each morphotaxon covered a wide and representative range of colony sizes. For each coral colony, *in situ* measurements of colony maximum

diameter were taken using a tape measure based on the longest length, with only living tissue included in the measurements. Where necessary, multiple measurements were taken to determine colony maximum diameter. For all morphologies, colonies were measured from a planar perspective rather than wrapping around the colony contour. Field measurements of colony maximum diameter ranged from 3cm to 150cm. After measurements were taken, each colony was imaged for 3D modelling (see 'Model reconstruction and data extraction').

4.2.2 *Model reconstruction and data extraction*

GoPro Hero 11 Black cameras were used to collect close-range imagery of individual colonies for 3D modelling. Structure from motion techniques (SfM) were followed, as described by Ferrari *et al.,*(2017). However, instead of timelapse imagery, 4K video footage (30fps) was used for faster in-water data collection, enabling more replicates per morphotaxon. Additionally, custom-built scaling objects (Agisoft Metashape coded targets, 12bit, inverted, 20% of full size, target centres 60 mm apart) were incorporated into the scene. Image acquisition involved filming the colony from all angles, moving in a sweeping motion to form arcs from top to bottom. Agisoft Metashape v 1.7.6 software was used for processing of videos and model building. Jpeg frames were extracted from the 4k videos every 4th frame. Videos varied in length according to the size and complexity of corals being filmed, where larger and/or more complex corals required more thorough and lengthy videos to capture full extent of colony surface area. Accordingly, image sets used to build 3D models varied in size. Mean video length was 1 minute, while image sets ranged from 150 to 1400 images.

Three dimensional models were reconstructed from image sets using Agisoft Metashape software (parameters outlined in Supplementary material, Appendix 2a, Table S1). Models were scaled using at least two sets of independent scale bars (60 mm in length) from the coded target objects described above. Resulting models had an average mesh resolution (distance between vertices) of 1.86 mm and average ground sample distance of 0.178 mm/pixel. Any extraneous mesh material that was not part of the colony was removed using Agisoft Metashape selection tools.

Colony 3D surface area was extracted using the Mesh-Area tool in Agisoft Metashape. In order to extract 2D surface area, the model was first projected onto a 2D plane, in the same aspect as a top-down image taken of the colony *in situ*. To do this, the models were visually oriented in the software to replicate a top-down field of view, where the z-axis was aligned perpendicular to this view plane (e.g., Figure 4.1a-c). Once this was done, the 2D area of the colony was estimated using the Export Report tool within the software with projection set to the X-Y plane.

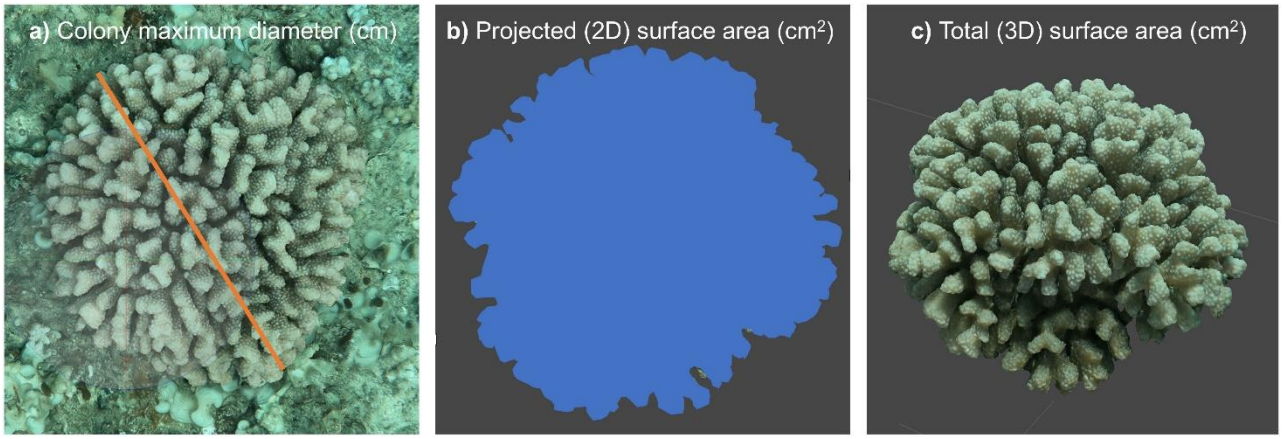


Figure 4.1 (a) *Field measurements of colony maximum diameter (cm)* ***(b)*** *projected 2D surface area (cm²) and* ***(c)*** *total 3D surface area (cm²) of the same coral colony. Images taken from Agisoft Metashape v 1.7.6 software during model reconstruction*

4.2.3 *Statistical models*

The relationships between colony maximum diameter and surface area metrics were explored for each morphotaxon using Bayesian generalized linear modelling (GLM) with a gaussian distribution. An approximate power-law relationship between coral maximum diameter and surface area was assumed based on underlying geometric properties of corals as well as evidence in the literature for allometric power-scaling relationships of corals (Dornelas et al. 2017; Urbina-Barreto et al. 2021a; Aston et al. 2022). Logarithmic transformations were performed for both variables to meet model assumptions and the power-law of these relationships allowed for a linear regression model to subsequently be fitted. Specifically, log-transformed linear length data (field measurement of colony maximum diameter, cm) was modelled against log-transformed projected 2D surface area

(cm^2) or against log-transformed total 3D surface area (cm^2). Weakly informative priors were selected based on visual exploration of the data following transformation. Bayesian posteriors were generated via a No-U-Turn Sampler (NUTS), run with three Markov Chain Monte Carlo (MCMC) chains, each for 15,000 iterations (excluding the first 5,000 warm-up samples) with a thinning rate of 12. All chains were found to be well-mixed and converged (all Rhat <1.01) on a stable posterior and were validated using the 'DHARMa' package (Hartig 2018) residuals and posterior probability checks. Data were back-transformed to the original scale after modelling for ease of parameter interpretation. To visualise the regression models, the posterior distribution for each morphotaxon was summarized with median lines using the 'posterior_predict' function.

To demonstrate the range over which the posterior distribution credibly lies, for interpretation of model uncertainty, bands of probability have been incorporated into the key figures (Figure 4.3 & 4.4) representing different Highest Density Intervals (HDIs 0.99, 0.95, 0.8, 0.5). HDIs represent the range within which a specified proportion of the posterior distribution falls; i.e. 0.95 HDI band encompasses 95% of the posterior distribution. Narrower HDIs denote more precise model estimates. Highest Density Intervals were calculated and visualized using the 'tidybayes' package.

Tables were produced to present model predictions over a range of field measurements for each morphotaxon, as an easily interpretable presentation of modelled data. Each predicted value (estimated marginal means, 'emmeans') was presented together with the range of credible values (as 95% HPDs) for that estimate. These tables are presented in Supplementary material (Appendix 2b, Tables S2-16) and were designed to be used by practitioners for interpreting the range of uncertainty around their model estimates for given sizes/morphotaxon. Emmeans were calculated using the 'emmeans' package (Lenth et al. 2018). All statistical models were performed in R version 4.3.1 (R Core Team 2021) via the 'brms' package (Bürkner 2017).

4.3 Results

To assess the utility of rapid field measurements of colony maximum diameter, it was first necessary to establish the capacity to consistently and accurately measure colony diameter in the field. To validate this approach, field measurements of colony length were compared to estimates of colony maximum diameter extracted from 3D models, with results indicating a very high correlation (Figure 4.2, $R^2 = 0.97$).

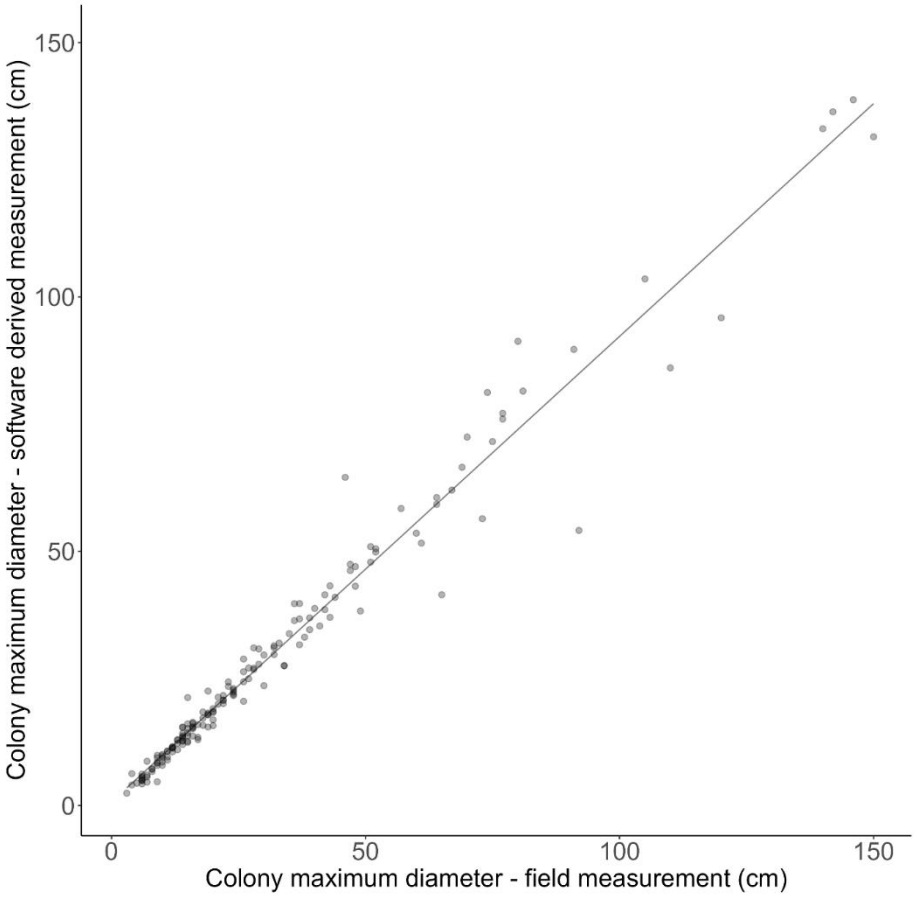


Figure 4.2 *Comparison of colony maximum diameter measurements taken from the field (x-axis) with colony maximum diameter derived from model reconstructions using Agisoft Metashape computer software (y-axis) (R^2=0.97, n=159).*

Strong non-linear (power) positive relationships (Bayesian R^2 values >0.9; Table 4.1) between rapid field measurements of colony maximum diameter and projected 2D surface area were observed for 13 of the 15 morphotaxa. These include *Acropora* – other (R^2=0.99), *Acropora* – table (R^2=0.95),

Astreopora (R^2=0.94)*, Fungia* (R^2=0.99)*, Lobophyllia* (R^2=0.97)*, Montipora* – encrusting (R^2=0.95)*, Pocillopora* (R^2=0.94)*, Porites* – massive (R^2=91), *Seriatopora* (R^2=0.97)*, Stylophora* (R^2=0.96)*,* Other – branching (R^2=0.94), Other – encrusting (R^2=0.96) and Other – massive (R^2=0.96)(Figure 4.3). While to a lesser extent, a positive relationship was also identified for *Acropora* – staghorn (R^2=0.84) *and Goniastrea* (R^2=0.89) (Figure 4.3, Table 4.1).

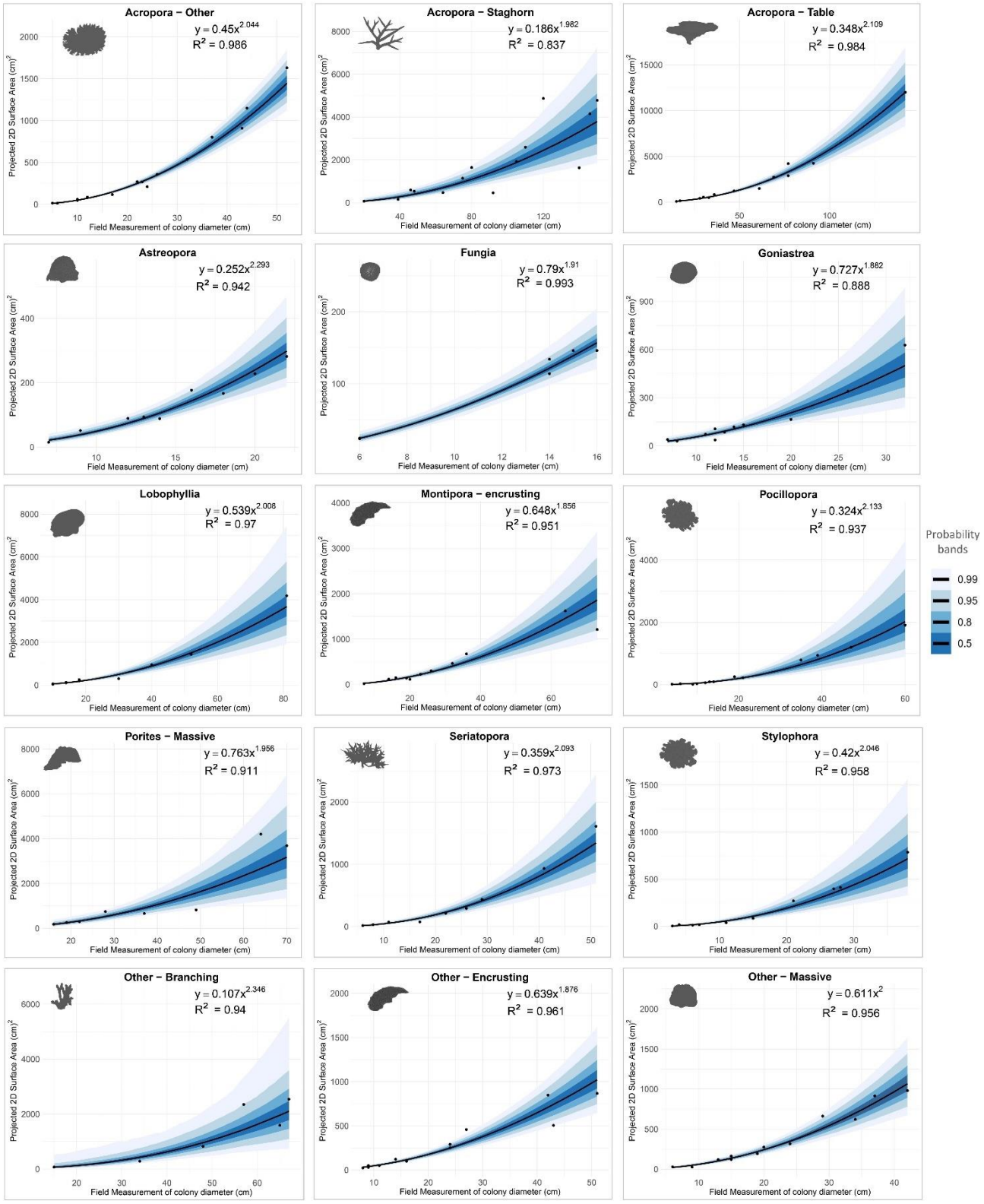


Figure 4.3 *Modelled power relationship between field measurements of colony maximum diameter (cm) and projected (2D) surface area (cm^2) for 15 coral morphotaxa. Black lines represent median posterior distribution*

and bands represent 99%, 95%, 80% and 50% highest density intervals (HDIs) derived from posterior distribution. Model equations with parameters α + β are presented along with Bayesian R^2 value for each morphotaxon.

Strong non-linear (power) positive relationships (Bayesian R^2 values >0.9; Table 4.1) between colony maximum diameter and total 3D surface area were observed for 11 of the 15 morphotaxa. These include *Acropora* – other (R^2=0.95)*, Acropora* – table (R^2=0.95)*, Fungia* (R^2=0.96)*, Lobophyllia* (R^2=0.96)*, Montipora* – encrusting (R^2=0.92)*, Pocillopora* (R^2=0.95)*, Seriatopora* (R^2=0.97)*, Stylophora* (R^2=0.96)*,* Other – branching (R^2=0.96), Other – encrusting (R^2=0.93) and Other – massive (R^2=0.91)(Figure 4.4). While to a lesser extent, a positive relationship was also identified for *Acropora* – staghorn (R^2=0.81) and *Astreopora* (R^2=0.82) and weaker relationships were identified for *Goniastrea* (R^2=0.77) *and Porites* – massive (R^2=0.75) (Figure 4.4, Table 4.1).

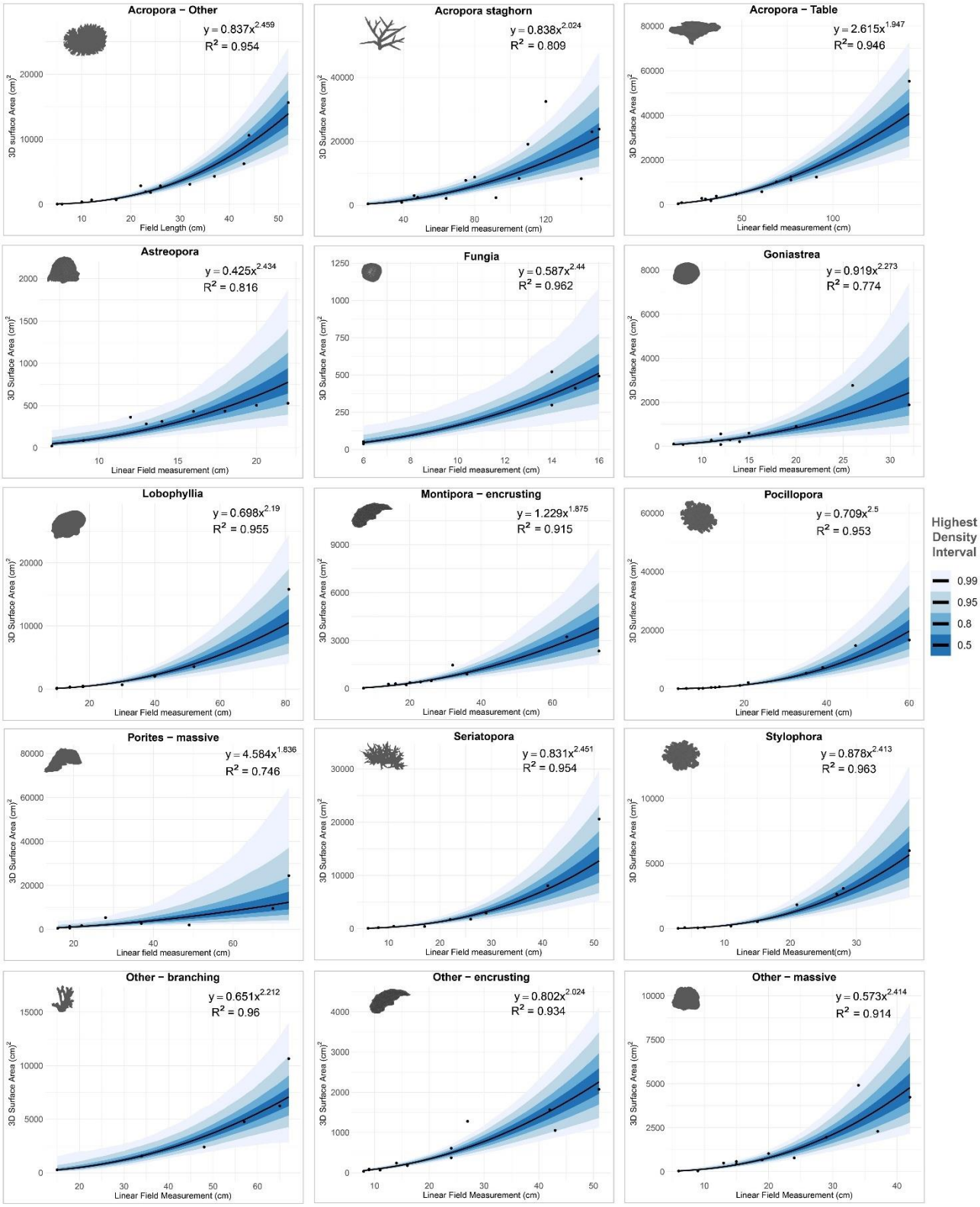


Figure 4.4 *Modelled power relationship between field measurements of colony maximum diameter (cm) and total (3D) surface area (cm2) for 15 coral morphotaxa. Black lines represent median posterior distribution and*

bands represent 99%, 95%, 80% and 50% highest density intervals (HDIs) derived from posterior distribution. Model equations with parameters α + β are presented along with Bayesian R^2 value for each morphotaxon.

Table 4.1 *Model equations and Bayesian R^2 for predicting colony Projected 2D Surface Area (PSA) and Total 3D surface area (TSA) from field measurements of colony maximum diameter (D) for 15 coral morphotaxa. Additional information on model equation parameters (incl. 95% HDIs and SD for parameters α + β) are presented in Supplementary material (Appendix 2c, Table S17 & S18).*

Coral morphotaxon	Projected 2D Surface Area (PSA)		Total 3D Surface Area (TSA)	
	Model equation	R^2	Model equation	R^2
Acropora - other	$PSA = 0.448D^{2.046}$	0.99	$TSA = 0.837D^{2.459}$	0.95
Acropora - staghorn	$PSA = 0.186D^{1.981}$	0.84	$TSA = 0.838D^{2.024}$	0.81
Acropora - table	$PSA = 0.346D^{2.111}$	0.98	$TSA = 2.615D^{1.947}$	0.95
Astreopora	$PSA = 0.252D^{2.293}$	0.94	$TSA = 0.425D^{2.434}$	0.82
Fungia	$PSA = 0.790D^{1.910}$	0.99	$TSA = 0.587D^{2.440}$	0.96
Goniastrea	$PSA = 0.727D^{1.882}$	0.89	$TSA = 0.919D^{2.273}$	0.77
Lobophyllia	$PSA = 0.539D^{2.008}$	0.97	$TSA = 0.698D^{2.190}$	0.96
Montipora - encrusting	$PSA = 0.667D^{1.848}$	0.95	$TSA = 1.229D^{1.875}$	0.92
Pocillopora	$PSA = 0.324D^{2.133}$	0.94	$TSA = 0.709D^{2.50}$	0.95
Porites - massive	$PSA = 0.763D^{1.956}$	0.91	$TSA = 4.58D^{1.836}$	0.75
Seriatopora	$PSA = 0.359D^{2.093}$	0.97	$TSA = 0.831D^{2.451}$	0.97
Stylophora	$PSA = 0.420D^{2.46}$	0.96	$TSA = 0.878D^{2.413}$	0.96
Other - branching	$PSA = 0.107D^{2.346}$	0.94	$TSA = 0.651D^{2.212}$	0.96
Other - encrusting	$PSA = 0.639D^{1.876}$	0.96	$TSA = 0.802D^{2.024}$	0.93
Other - massive	$PSA = 0.611D^{2.00}$	0.96	$TSA = 0.573D^{2.414}$	0.91

Models differed in their scaling relationships (Figure 4.5), though there were similarities found between certain groups of morphotaxa. Tightly branching morphotaxa (*Acropora* – Other, *Pocillopora*, *Seriatopora* and *Stylophora*; see blue hues in Figure 4.5) all follow very similar power relationships; however, this relationship is considerably different to the trajectory shared by encrusting corals (*Montipora* and Other-encrusting, see green hues in Figure 4.5) and massive corals (see pink/purple hues in Figure 4.5). These data provide insight into differences in the 3D surface area to colony maximum diameter ratios among morphotaxa.

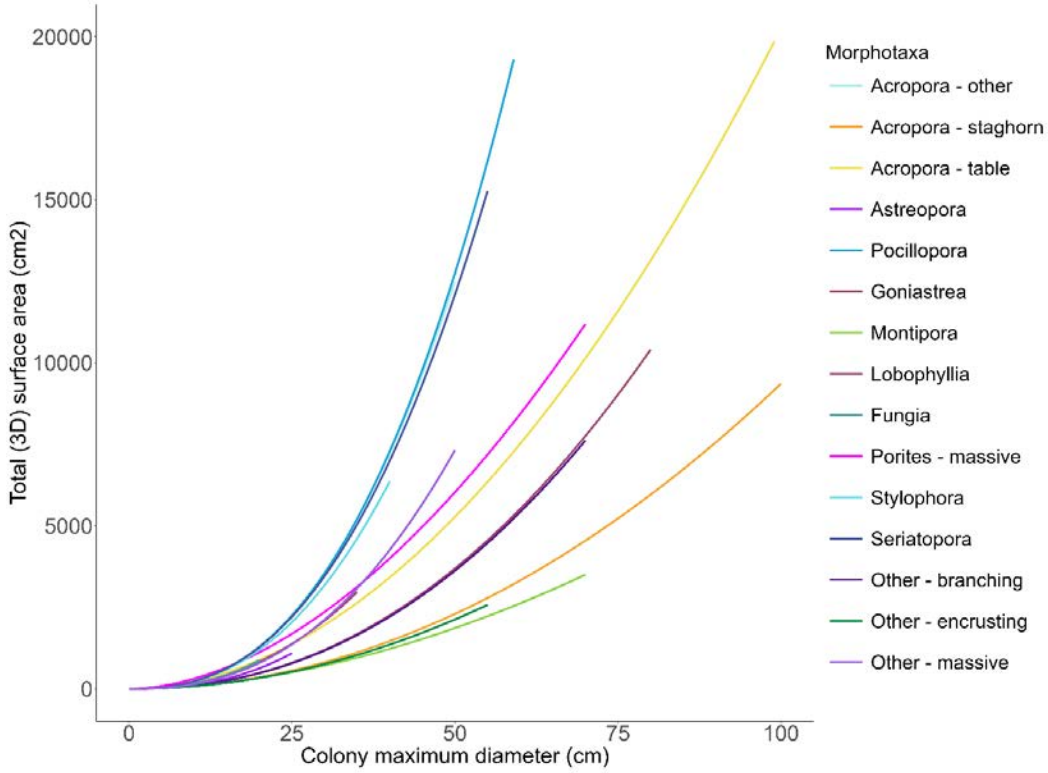


Figure 4.5 *Median lines of posterior distributions for modelled power relationships between colony maximum diameter and total (3D) surface area for 15 coral morphotaxa*

An inherent consideration of this work is the uncertainty associated with model-derived estimates. To clearly present this to users bands of probability have been incorporated into the key figures (HDIs 0.99, 0.95, 0.8, 0.5) (Figure 4.3 & 4.4) to demonstrate the range over which the posterior distribution credibly lies. Tables of predicted values (Emmeans) have also been produced for each morphotaxon and the associated HDIs of each estimate (Supplementary material, Appendix 2b, Tables S2-S16). Figure 4.3 & 4.4 show variability in HDI band width between morphotaxa, representing variation in model certainty. Trends of increasing HDI width at larger colony sizes were evident for most morphotaxa, especially for those with very large colony maximum diameters such as staghorn *Acropora*. Caution should therefore be taken when interpreting results for staghorn *Acropora* colonies at the larger end of the size continuum, or avoided if precise estimates are

required. Variation in model certainty is likely related to the extent of morphological plasticity within each morphotaxa which is why disproportionately higher numbers of replicates were sampled for morphotaxa containing complex and variable growth forms. Tables of predicted values (Emmeans) for each morphotaxon and the associated HDIs of estimates are presented in Supplementary material, Appendix 2b, Tables S2-S16, which enable the interpretation of uncertainty levels associated with different colony sizes.

4.4 Discussion

Long-standing logistical constraints to accurately quantifying surface area of corals have hindered our understanding of their ecological function (e.g., McWilliam *et al*. 2020). Here, it is shown that rapid field measurements of colony maximum diameter can be used to effectively predict total 3D surface area and projected 2D surface area for a diverse range of different corals, providing meaningful ecological metrics for various applications. By modelling detailed non-linear relationships between colony size and surface area for 15 different coral morphotaxa, previously established conversion metrics are built upon (Courtney et al. 2007; House et al. 2018; Aston et al. 2022) and a valuable resource for reef monitoring programs is created. Previous studies have demonstrated the feasibility of converting measurements of colony maximum diameter to metrics of 3D and 2D surface area (Courtney et al. 2007; Holmes 2008; House et al. 2018; Aston et al. 2022), however the scope of these published conversions have been restrictive, with the most wide-ranging study (Aston et al. 2022) producing relationships for seven morphotaxa groups which does not encompass all growth forms in the Indo-Pacific. The variation in scaling relationships that was recorded between morphotaxa in this study (Figure 4.5) demonstrates the importance of taxa-level data for obtaining the best possible model parameters.

The modelled power-relationships I established between colony maximum diameter and 3D surface area indicated very strong relationships ($R^2 > 0.90$) for 11 out 15 of the morphotaxa. The four morphotaxa that exhibited lower model- fit values ($R^2 = 0.75$-0.89) were staghorn *Acropora*,

Astreopora, *Goniastrea* and massive *Porites*, and the use of these four predictive models for obtaining surface area values should be approached with some caution. Surprisingly, *Astreopora*, *Goniastrea* and massive *Porites* have simple growth forms but were found to produce only moderately strong relationships, largely owing to irregular height to width ratios due to their susceptibility to partial mortality (Burn et al. 2022; Jones et al. 2023), obscuring the relationship between field measurement of planar diameter and surface area (see example images of massive *Porites* in Supplementary material, Appendix 2d). For staghorn *Acropora*, confidence in posterior draws was found to be strong at smaller sizes but weakens considerably at larger colony sizes (>80cm), likely due to the variability in branch density and hence surface area at larger colony sizes (see example images of staghorn *Acropora* in Supplementary material, Appendix 2d). Thus, the use of these conversion metrics for very large colony sizes of staghorn *Acropora* should be avoided. For all other morphotaxa, surface area scaled well with size, and the conversion metrics can be used with relative confidence. In order for users to interpret model precision and confidence over the range of morphotaxa and colony sizes that they are working with, I have included tables presenting model uncertainty (Supplementary material, Appendix 2b, tables S2-S16). An additional consideration of this study is that the morphological plasticity of conspecific corals that occur in accordance with environmental exposure (i.e., hydrodynamics, sedimentation; Doszpot et al. 2019; Million et al. 2022) and depth (Anthony et al. 2005; Hoogenboom et al. 2008), may affect the representativeness of the corals I imaged which were selected from just one location. As the corals selected represent the dominant growth forms within each morphotaxon (see Supplementary Material, Appendix 2d), the presented relationships should sufficiently encompass corals from most other locations. However, practitioners working in different regions to this study should exercise caution when working with these conversion metrics. Additional model equations for morphotaxa not captured here and/or colonies from other tropical Indo-Pacific regions can be produced by replicating our methodology.

The relationships presented here have utility for a wide range of applications from small-scale studies of ecological processes to ecosystem modelling. At a colony level, applications could include

the extrapolation of any processes which are standardized to biotic surface area such as symbiont density, chlorophyll concentration, and metabolic processes (Hoegh-Guldberg 1988; Fisher et al. 2007; Holmes 2008; Veal et al. 2010). Scaling up colony level processes to a reef scale via complementary field surveys or with remote sensing imagery would also be possible (Andréfouët and Payri 2001; Holmes 2008). Given that the surface area of corals is a known descriptor of tissue biomass, it can be a proxy for potential nutrient intake of coral predators (Keesing 1990). Refining our knowledge about the total tissue area availability (and total protein) for a given colony can provide insight into the underlying explanations for feeding preferences by key coral predators. For crown-of-thorns starfish (*Acanthaster* spp.), for which feeding preferences are well studied (Ormond et al. 1976; Keesing and Lucas 1992; De'ath and Moran 1998; Keesing 2021), there remains uncertainty around the basis of feeding choices where nutritional value and availability alone cannot explain preferences (Johansson et al. 2016; Keesing 2021). This work has demonstrated the substantial variation of surface area to coral diameter ratios between taxa which may be a key factor underpinning the apparent feeding preferences. For example, our relationships show that a *Pocillopora* colony with a maximum diameter of 40cm is likely to have a total 3D surface area more than six times as large as the total 3D surface area of *Montipora* with the same colony maximum diameter (*Montipora*: 1150cm^2; *Pocillopora*: 7,234cm^2). Crown-of-thorns starfish feed by everting their stomach over coral structures and dissolving the majority of the tissue area (Keesing 1990), and so a high tissue area reward for limited effort of feeding and foraging may explain feeding choices, especially when feeding *efficiency* is thought to be the key determinant of preferences.

Surface area metrics can also provide modelers and managers with valuable parameters related to reef growth, for example for modelling calcification rates of corals; a vital parameter in the calculation of carbonate budget models. With the increasing use of carbonate budgets as a method for evaluating reef status and trends in ecosystem function over time (Lange et al. 2020), methods that enable accurate and efficient surface area measurements of coral colonies, provide a useful contribution to reef-scale calcification modelling (Perry et al. 2012; Lange et al. 2020; Husband et al.

2022). An important development in the efficiency and scale of this work has been the development of Coral Colony Rugosity Indices (CCRI) by Husband et al. (2022) which enable calcification rates to be calculated from planar measurements of corals. These CCRI conversion metrics facilitate the conversion of datasets, including carbonate modelling of historic data. As a further development of this work, our study presents an alternative method for converting measurements of colony maximum diameter, derived from field data or images, to morphotaxon-specific surface area values. As such, a future application of this work could be combining the surface area values of corals (obtained using our conversion metrics) with species-specific calcification rates as an alternative approach for gaining high resolution estimates of coral carbonate production.

This work also has applications for studying temporal and spatial trends in coral growth rates. In coral growth studies, quantification of the 3D structure of individual colonies provides a more rigorous representation of total growth compared to linear colony measurements or planar projected areas (Holmes et al. 2008). Studies of coral growth, in particular those that monitor outplanted corals from restoration activities, can often span large areas and include thousands of colonies (Maya et al. 2016; Foo and Asner 2019). This paper presents an opportunity to conduct rapid field measurements of outplanted colonies and gain estimates of colony growth over time, especially as coral restoration and recovery research has gained major interest in recent years after impacts of cumulative disturbances (Pratchett et al. 2021b; Bozec et al. 2022; Mudge and Bruno 2023).

Moreover, this study has application for assessing additional aspects of coral demography, such as competition, fecundity, and partial mortality of corals. The surface area occupied by different coral species can be monitored to assess the dynamic interplay of coral growth and competition on a reef in 2D and 3D space, which is important for understanding coral community dynamics and their response to disturbance (Cresswell et al. 2020). In particular, monitoring space occupancy of corals after major disturbance events can further our understanding of recovery trajectories and inform

ecological models. Surface area metrics can also provide insight into reproductive potential of corals, as coral morphology and size can be used as a proxy for reproductive potential of individuals (Álvarez-Noriega et al. 2016). Using this approach to estimate surface area therefore provides a valuable tool for studying key processes that drive reef resilience and recovery.

Conclusion

Coral colony surface area is an important ecological parameter and serves as a fundamental determinant of physical and biological processes as well as ecosystem services. As such, there is a demand for obtaining highly resolved estimates of coral surface area. This method presents a process for rapidly gaining highly resolved morphotaxon-specific surface area estimates from easily obtained measurements of coral colony maximum diameter. Large datasets of colony diameter measurements can be converted to surface area metrics using the model equations provided. Coral colony measurements can be collected in the field using tape measures or alternatively extracted from photographs (including historic image sets), enabling researchers to gather valuable surface area metrics without complex equipment or software. This approach cannot replicate the precision and accuracy of conducting photogrammetry on every colony, however, the benefit of scaling up to large datasets makes this trade-off worthwhile and this approach highly valuable. Key applications of this approach include the 1) extrapolation of processes standardized to biotic surface area (e.g., photosynthesis, calcification), 2) assessment of tissue biomass for ecological studies (e.g., coral predator ecology), 3) upscaling from colony-scale to reef carbonate production, 4) quantification of coral growth (e.g., for reef restoration monitoring), and 5) assessment of coral demographics and space competition.

Chapter 5: Spatiotemporal variation in feeding behaviour of Pacific crown-of-thorns starfish (*Acanthaster* cf. *solaris*), including highly resolved daily feeding rates

5.1 Introduction

Crown-of-thorns starfish (CoTS, *Acanthaster* spp.) are highly effective and efficient coral feeders (Birkeland 1989), capable of consuming and thereby killing large quantities of reef-building hard corals (order Scleractinia). At low densities of CoTS, the net ecological effect of their feeding is negligible, especially in areas with higher cover of fast-growing corals (Glynn 1974, Pratchett et al. 2009). However, during periods of very high population densities, and particularly during population outbreaks (Chesher 1969a; Kayal et al. 2012), the cumulative effects of their feeding can be substantial and cause severe and widespread coral depletion (Birkeland and Lucas 1990; Pratchett et al. 2009; Tkachenko and Hoang 2022). The occurrence and ecological impacts of population outbreaks tend to vary regionally, possibly reflecting interspecific differences in the biology and behaviour of CoTS (Pratchett et al. 2017b; Foo et al. 2024), of which there are at least five species with generally distinct geographic ranges (Uthicke et al. 2024b).

Population outbreaks of the western Pacific CoTS (*Acanthaster* cf. *solaris*) are one of the foremost contributors to coral loss in the western Pacific (Bruno and Selig 2007; Mellin et al. 2019; Pratchett et al. 2021b), compounding upon other increasing disturbances, such as mass coral bleaching (Bellwood et al. 2019; Virgen-Urcelay and Donner 2023). Acroporid corals, in particular, are sustaining major losses, as both the preferred prey of CoTS (Pratchett 2007), and one of the most susceptible taxa to climate-induced mass coral bleaching (e.g., Loya et al. 2001) and severe tropical storms (Madin and Connolly 2006; Keesing et al. 2019). Whilst these fast-growing corals have traits that allow for rapid recovery following disturbance events (Emslie et al. 2024), the confluence of major population outbreaks of CoTS and mass coral bleaching has led to localised extirpation of *Acropora* corals in some areas (Foo et al. 2024), with potential to limiting reef recovery. Effective

CoTS management is therefore crucial for minimising ongoing coral loss and thereby enhancing reef resilience in the face of escalating environmental change.

CoTS have evolved extremely efficient feeding mechanisms to predate on hard corals, everting their stomachs to simultaneously digest large areas of coral tissue (Brauer et al. 1970; Birkeland and Lucas 1990). The size of the stomach when everted covers a planar area roughly equivalent to the size of the oral disc (Birkeland and Lucas 1990), though it can effectively cover highly complex surfaces, such that the overall tissue surface area consumed increases with the three-dimensional complexity of corals (**Chapter 3**). Despite the important ecological effects that result from CoTS feeding, few studies have directly quantified the daily feeding rates of CoTS. Initial estimates of feeding rates (378 cm^2 day^{-1} Chesher, 1969a; 150 cm^2 day^{-1}, Glynn, 1973) were based upon broad-level assessments of cumulative coral loss, which were then standardized by the local densities of adult CoTS. Keesing and Lucas (1992) conducted daily feeding assessments for individual tagged CoTS by identifying the conspicuous feeding scars, which are particularly visible in the first few days after feeding events (Chandler et al. 2024 **[Chapter 4]**). They measured the linear dimensions of all feeding scars, providing data on both the number and size of corals consumed. This was then reported as the two-dimensional planar area of coral killed (Keesing and Lucas, 1992). This data enabled rates of coral loss caused by CoTS feeding to be assessed in relation to available coral cover.

There has been limited research on CoTS feeding since Keesing and Lucas (1992), up until 2024 (Millican et al. 2024, **Chapter 3**). **Chapter 3** built upon foundational knowledge of feeding rate data by providing new insights into daily variation in the feeding behaviour of CoTS over successive days. The study reported mean daily feeding rates of 198.4cm^2 d^{-1} (± 23.86 SE) and highlighted significant variation between individuals and between days, whereby most individuals exhibited multiple days of no feeding. Whilst this was an important contribution to our knowledge of CoTS feeding potential and strategies, this intensive tracking study was necessarily limited to a small number of CoTS (n=8) and conducted at one location (Lizard Island, northern GBR). Feeding rates of CoTS are, however,

likely to be influenced by intrinsic (e.g., metabolic demands of starfish) and extrinsic (e.g., quantity and quality of food available) factors (Wright et al. 2005), and expected to vary over a continuum of biological and environmental conditions (Keesing and Lucas, 1992).

Keesing and Lucas (1992) showed that feeding rates of CoTS varied among individuals depending on body size and season. However, feeding rates will also be dependent upon the local distribution, abundance and composition of coral prey. Gaining data on how feeding rates vary under different conditions is central to understanding the rate of coral loss imposed by CoTS populations. This is critical for predicting the cumulative effects of CoTS in different spatial and temporal scenarios, something which is imperative for effective management of the reef.

The objective of this chapter was to assess large-scale variation in daily feeding rates of *A. cf. solaris* and determine whether feeding rates vary spatially, seasonally and/or as a result of other factors at an individual or environmental level, including investigating whether there were density-dependent differences in feeding rate. This chapter builds upon data gained in **Chapter 3** as well as leveraging methods developed in **Chapter 4** to investigate feeding over a large scale from both a 2D and 3D perspective. In addition to investigating drivers of daily feeding rate through this sample design, this data will also allow us to understand the feeding tradeoffs of CoTS in different coral cover and population density regimes, and what this means for their energetic intake, which may ultimately lead to a better understanding of population breakdown.

5.2 Methods

5.2.1 *Field surveys*

To collect feeding rate data across a large spatial scale, Scooter-Assisted Large Area Diver-based (SALAD) Surveys were conducted (Chandler et al. 2023 **[Chapter 2]**) across five distinct regions of the central, northern and far northern GBR (Townsville, Cairns, Lizard, Princess Charlotte Bay and Cape Grenville; Figure 5.1) between March 2023 and March 2024. This large-scale sampling allowed

for the assessment of CoTS feeding behaviour across a gradient of environmental conditions, with marked difference in coral cover, coral composition and CoTS densities (Table 5.1). Data collected in May - October was classed as 'Winter' (water temperature 24-26^{o}C), data collected from November - April was classed as 'Summer' (Water temperature 27-31^{o}C).

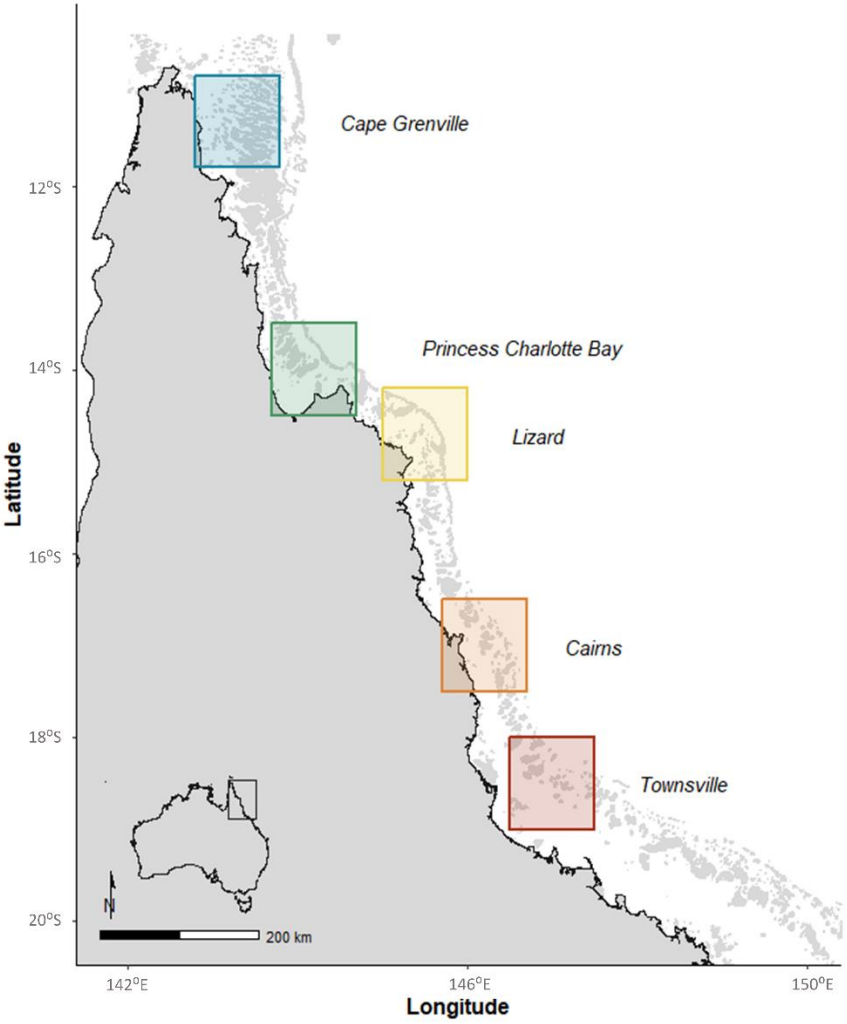


Figure 5.1 *Map of the central and northern Great Barrier Reef, showing five distinct regions (Cape Grenville, Princess Charlotte Bay, Lizard, Cairns and Townsville) where sampling was undertaken in 2023-2024. SALAD surveys were used to collect feeding data across this wide latitudinal gradient*

During SALAD surveys at 3-5 reefs within each region, the detection of conspicuous clusters of feeding scars triggered a thorough search of the local environment for location of the associated

starfish. Detailed searches were conducted to rule out feeding by more than one individual and/or mortality by factors other than CoTS predation (i.e. disease, *Drupella* spp.). For each CoTS located, the maximum diameter of the starfish was measured and the distinct cluster of fresh scars in proximity to the individual was recorded. Feeding data was only collected when feeding scars could be confidently attributed to a single starfish feeding in isolation, making it challenging to collect feeding data in areas with very high densities of starfish. Only 'fresh' feeding scars were recorded, which were defined as any colonies which showed signs of recent consumption (tissue sloughing and mucous coverage) or were presenting bare, white skeleton which was not overgrown with turf algae. To limit subjectivity by observers, this algal growth was defined as having a colouration which did not exceed a category B2 rating on a Coral Watch Coral Health card (see **Chapter 3**). Daily monitoring of feeding scars that resulted from known feeding activity (e.g., **Chapter 3**) revealed that feeding scars stay white (lighter than a B2) for roughly 5 days in summer months (water temp >27ºC) and 7 days in winter months (water temp <26ºC), these seasonal time frames were termed 'ageing factors'. Any feeding scars which were characterised as being 'fresh', according to this threshold, were assumed to have been consumed within these time periods (ageing factors). All scars consumed by an individual starfish were pooled together and the total consumption by an individual was converted to a daily feeding rate by dividing the cumulative feeding by the ageing factor for the respective season. The number of colonies consumed per day was also calculated as an alternative metric of daily feeding rate, reflecting the number of distinct coral colonies that a starfish fed on, regardless of whether the entire colony was consumed or only partially, as an indication of feeding frequency and prey-switching, rather than areal intake.

For relevant feeding scars, the prey coral was identified to genus and the maximum diameter of feeding scar and coral colony was measured (nearest cm). Following methods described below, each colony diameter measurement was converted to a surface area value for the relevant coral, and then daily feeding rates were calculated accordingly.

In addition to collecting feeding data for individual starfish, SALAD surveys also recorded CoTS densities for each site which could be investigated as a possible driver of feeding behaviour. Similarly, coral cover and composition were recorded at the start and end of each SALAD survey using 50 m Point Intercept Transects (PIT). The PIT data for total coral cover for each survey site was classified into coral cover categories (0-15%, 15-30%, 30-50%, >50%) and *Acropora* categories (<10%, 10-30%, >30%). Similarly, CoTS were classified into body size categories (<15cm, 15-25cm, 25-40cm, >40cm). These are the same CoTS size categories used by the GBR CoTS culling teams when collecting size structure data, so that our results can easily be applied to population data that is being collected on known populations. As there were not many replicates in the <15cm size category these individuals were not included in the feeding model.

5.2.2 *Converting field measurements to 2D/3D surface area*

In this study I saw value in presenting daily feeding rates in three different forms (coral colonies consumed, planar (2D) area of coral consumed (cm^2) and total (3D) surface area of coral consumed (cm^2) as they offer different perspectives on daily feeding (**Chapter 3**). In order to estimate the 2D and 3D surface area of feeding scars, we used empirically derived calibrations for each of 15 distinct taxa (Chandler et al 2024 [**Chapter 4**]) to convert measurements of the maximum diameter of the scar (cm), into projected (2D) planar area of scar (cm^2), and total (3D) surface area of scar. There are inherent constraints in using calibration curves to estimate the 2D and 3D areas of individual feeding scars, recognising that there was unexplained variation in the empirical relationships between coral diameter versus 2D and 3D area (Chandler et al 2024 [**Chapter 4**]). I did not account for this variance and acknowledge that the relationships themselves might vary regionally. However, it was not feasible to use photogrammetry to estimate 2D and 3D areas for all feeding scars considered in this study (n > 2,600 feeding scars), thus this was a tradeoff necessary to obtain extensive data across a large spatial gradient.

5.2.3 *Data analysis*

Although the study employed a regional sampling design, broad-scale regional comparisons were not the focus. Instead, feeding rates were analysed in relation to the environmental gradients that exist across the latitudinal range.

Generalized linear mixed effects models (GLMM) were fitted to investigate the major environmental and biological drivers of feeding rate. Separate GLMMs were fitted for the three metrics of daily feeding rate: 1) Total (3D) surface area, 2) Planar (2D) projected area and 3) Number of colonies. All feeding rate data was log-transformed to meet normality assumptions and back transformed for analysis. Data was modelled against a gaussian distribution with an identity link function. Analyses were based on the daily feeding rates for each individual CoTS (n = 565), whereby relevant size information of all feeding scars was combined and then divided by a season-specific 'ageing factor'.

Given the range of possible predictors, Boosted Regression Trees (BRT) and Random Forests (RF) were run for variable selection. The full set of variables considered were CoTS body size, population density, total coral cover (%), *Acropora* cover, season, month, water temperature, latitude, region and reef.

BRT analysis indicated that CoTS body size, population density and *Acropora* cover had the strongest relative influence. Similarly, RF analysis also identified CoTS body size, population density and *Acropora* cover as the variables which contributed the most to model's predictive accuracy. For model selection, the variables selected during the BRT selection process were included, as well as total coral cover category and season, as these factors would intuitively be expected to influence feeding rate. Since our primary interest was in these ecological variables, including region would have introduced confounding effects (collinearity), making it difficult to disentangle the true influence of each variable, thus region was not included in the model. For continuous predictors (CoTS body size, population density, total coral cover, *Acropora* cover), data were categorized into discrete bins to facilitate the generation of model-derived feeding estimates, which would be a key

output of this study for ecological modelling. Variable selection process for each of the three models is set out in the Supplementary Material (Appendix 3, Table S1, S6, S11).

Relevant combinations of fixed and random effects were tested and retained only if they improved the fit of the model, based on the Akaike Information Criterion (AICc). The model that was selected (lowest AIC score) included: CoTS body size category, Total coral cover category and population density category (with no interactions), with Site as a random effect with random intercepts. Neither Season nor *Acropora* cover improved model fit (AIC score) and were therefore excluded, however it is noteworthy that *Acropora* cover resulted in a model with only a marginally lower AIC score. Total coral cover and *Acropora* cover data in this study were strongly positively correlated ($R^2 = 0.77$, $F = 1914$, $df = 1, 548$, $p < 0.001$).

Tukey's pairwise comparisons were calculated using estimated marginal means to test for significant differences in feeding rates between groups. 95% confidence intervals (CI) were generated for these pairwise comparisons whereby statistically significant differences are determined where CIs do not overlap 1.

5.3 Results

5.3.1 *Sampling effort*

This study estimated daily feeding rates for 565 individual starfish from 208 SALAD surveys conducted across 24 reefs in 5 regions, based on field measurements of over 2600 feeding scars. Feeding data was collected over a continuum of environmental conditions: Total coral cover ranged from 5.66% (Lynchs Reef, Townsville) to 90.34% (Eagle Reef, Lizard) (with *Acropora* in the range from 0% to 75.11%), Population density ranged from 1.69 CoTS.ha^{-1} (Corbett Reef, Princess Charlotte Bay) to 73.68 CoTS.ha^{-1} (Banfield Reef, Townsville), Temperature ranged from 24^{o}C (John Brewer Reef, Townsville in July) to 31^{o}C (Lizard Reef, Lizard in February). Average environmental conditions of each Region are outlined in Table 5.1, although it is important to note that conditions varied

considerably within each region. Notably, there were reefs with high coral cover and low CoTS densities (e.g. Hopkinson Reef, Townsville) as well as reefs with high coral cover and high CoTS densities (e.g. Eagle Reef Lizard), allowing for meaningful ecological comparisons of the relevant influence of coral cover vs population densities. Although the study employed a regional sampling design, feeding rates were analysed in relation to the continuous environmental variables that exist across the range of reefs sampled.

Table 5.1 *Summary of sampling effort at each region with conditions from each region as well as the range of values also recorded. Data on coral cover and population densities were collected via SALAD surveys*

Region	N (starfish)	Total coral cover (%)		*Acropora* cover (%)		Mean Population density (CoTS.ha^{-1})	
		Mean	Range	Mean	Range	Mean	Range
Cape Grenville	**75**	**27.40**	10.73 – 45.00	**9.79**	0.00 – 33.00	**17.94**	1.92 – 37.5
Princess Charlotte Bay	**36**	**36.53**	18.01 – 52.14	**17.65**	2.72 – 44.41	**17.25**	1.70 – 33.74
Lizard	**284**	**46.04**	12.71 – 90.34	**28.75**	6.17 – 75.75	**27.88**	2.89 – 61.11
Cairns	**8**	**21.88**	13.18 – 38.92	**4.18**	2.16 – 5.78	**6.38**	5.096 – 8.96
Townsville	**162**	**27.07**	5.65 – 48.88	**19.90**	0.00 – 44.00	**30.80**	2.96 – 73.68

5.3.2 *Daily Feeding rates*

Variable selection processes were conducted separately for each of the three measures of feeding rate (colonies consumed·day^{-1}, planar area consumed·day^{-1}, and 3D surface area·day^{-1}), however, the same set of predictors were retained in each case. Exploratory analysis using Boosted Regression Trees (BRT) indicated that season, month, and latitude had minimal influence on daily feeding rates and were therefore excluded from the final models. Body size, total coral cover, and population density were included as fixed effects, and each presented as categorical variables (see Table 5.2), while site was included as a random effect to account for site-level variation. *Acropora* cover, region, and reef were excluded due to collinearity with other predictors.

Across all measures of feeding rate (colonies consumed·day^{-1}, planar area consumed·day^{-1}, and 3D surface area·day^{-1}), CoTS body size was a significant predictor of daily feeding rate ($p<0.001$). Feeding rates increased significantly with body size category, with larger CoTS consuming more colonies and greater overall area of coral tissue (Figure 5.2). Predicted values for each size class from the GLMM are presented below.

The relationship between coral cover and daily feeding rate varied depending on the response variable used. When expressed as planar area consumed·day^{-1} or 3D surface area·day^{-1}, feeding rates were positively correlated with coral cover (Figure 5.3). In contrast, when measured as colonies consumed·day^{-1}, no significant trend was observed (Figure 5.3). The results of the individual GLMMs are detailed below.

i. Colony-level estimates of feeding rate

The mean daily feeding rate recorded across all starfish was 0.81 (± 0.02 SE) colonies a day, the daily feeding rate varied considerably among CoTS, from 0.14 colonies a day to 3.6 colonies a day.

The GLMM modelled data with colony-level feeding rate as the response variable explained only 16.09% of the variation in feeding rates ($R^2 = 0.16$), with 13.28% attributed to fixed effects alone. This was considerably lower than the other two GLMMs. The model showed that there was a significant positive effect of the categorical predictor CoTS body size ($p<0.001$). Pairwise contrasts found significant differences between all body size classes ($p<0.05$), except between the two smallest size categories '15-25cm' and '<15cm' ($p=0.31$; Appendix 3, Table S5, S10, S15). Estimated marginal means of daily feeding rate increased for each body size class (Figure 5.2; Appendix 3, Tables S4, S9, S14). Coral cover was not found to have a significant effect on daily feeding rate (number of colonies), for any combinations of coral cover categories ($p > 0.05$). Similarly, population density did also not have a significant effect on daily feeding rate ($p>0.05$).

ii. Planar (2D) area estimates of feeding rate

The mean daily feeding rate recorded across all starfish was 164.04cm^2 day^{-1}± 8.30 SE planar area, daily feeding rates varied considerably among CoTS, from 1.58 cm^2 day^{-1} to 2,135.29 cm^2 day^{-1}.

The GLMM modelled data with *Planar Area Feeding Rate* as the response variable, explained 43.8% of the variation in feeding rates (R^2 = 0.438)**,** with 35.76% attributed to fixed effects alone. The model showed that there was a significant positive effect of CoTS body size ($p<0.001$), with significant differences between all body size classes ($p<0.001$; Appendix 3, Tables S5, S10, S15). Estimated marginal means of daily feeding rate increased for each body size class (Figure 5.2; Appendix 3, Tables S4, S9, S14).

Coral cover category had a significant positive effect on planar daily feeding rate ($p <0.05$), however post-hoc analysis revealed that significant differences were only observed between the highest coral cover category (>50%) and all other categories (>50%/0-15%, p=0.02; >50%/15-30%, p=0.02; >50%/30-50%, p=0.01). Population density did not have a significant effect on daily feeding rate ($p>0.05$).

iii. 3D surface are estimates of feeding rate

The mean daily feeding rate recorded across all starfish was 900.46 cm^2 day^{-1} ± 42.93 SE total (3D) surface area and varied considerably among CoTS, from 8.00 cm^2 day^{-1} to 7,420.72 cm^2 day^{-1}.

The GLMM modelled data with *3D Surface Area Feeding Rate* as the response variable explained 43.52% of the variation in feeding rates (R^2=0.435), with 34.01% attributed to fixed effects alone. The model showed that there was a significant positive effect of CoTS body size category ($p<0.001$), with significant differences between all body size classes ($p<0.001$; Appendix 3, Tables S5, S10, S15). Estimated marginal means of daily feeding rate increased for each body size class (Figure 5.2; Appendix 3, Tables S4, S9, S15).

Coral cover category had a significant positive effect ($p<0.05$) on 3D daily feeding rate, however post-hoc analysis revealed that significant differences were only observed between the highest coral cover category (>50%) and categories 0-15% ($p=0.03$) and category 30-50% ($p=0.035$), there was no significant difference between highest coral cover category and category 15-30% ($p=0.12$). Population density did not have a significant effect on daily feeding rate ($p>0.05$).

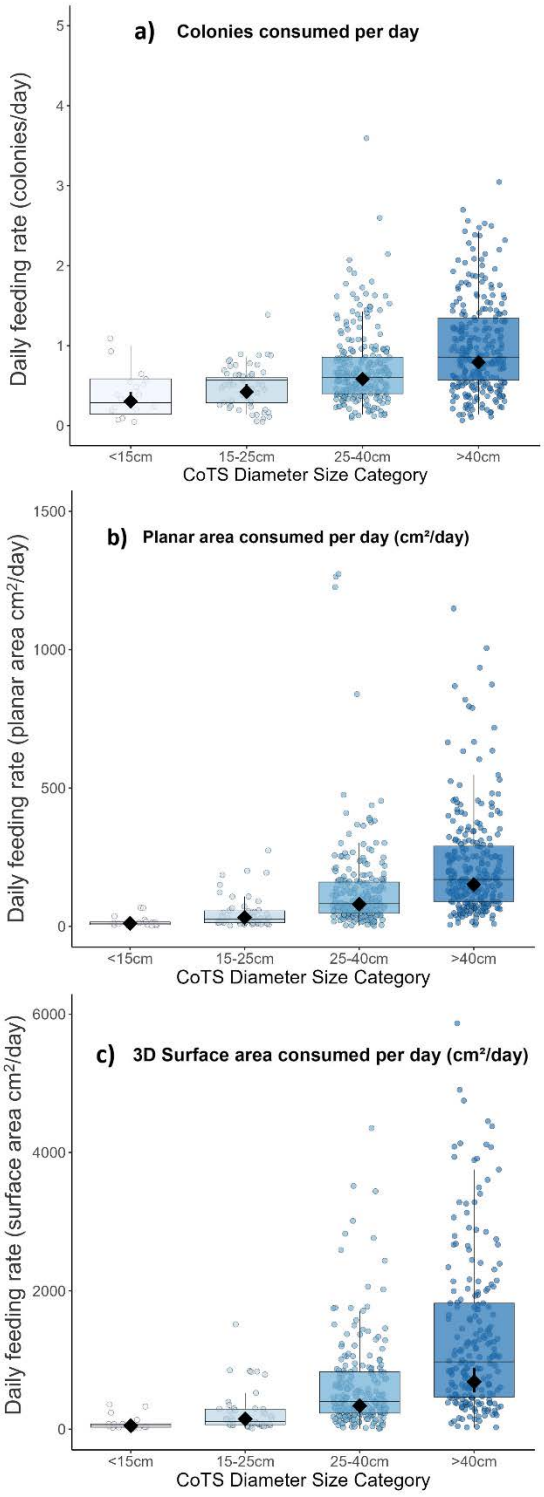


Figure 5.2 *Predicted values of daily feeding rate for each body size class of CoTS presented as black diamonds with 95% confidence intervals for* ***(a) no. colonies*** *consumed per day,* ***(b) planar area*** *of coral consumed per day (cm^2 day^{-1}) and* ***(c) total (3D) surface area*** *of coral of coral consumed per day (cm^2 day^{-1}). Observed daily feeding rate data recorded for each starfish are also presented as individual points. Boxes and whiskers display 25-75th and 5-95th percentile ranges of true data respectively, thick lines indicate median values*

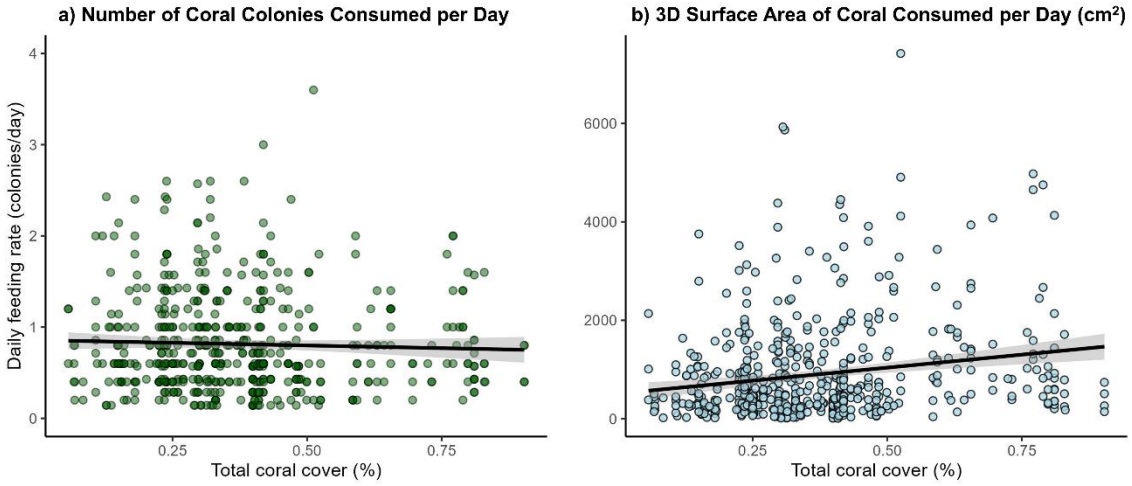


Figure 5.3 *Relationship between Total coral cover (%) and Daily feeding rate of CoTS. Daily feeding rate is presented as* ***(a) number of colonies*** *consumed per day by each CoTS, and* ***(b) 3D surface area (cm²)*** *of coral consumed per day by each CoTS. Each point represents feeding by one individual starfish. The black line represents the linear regression fit to the data points*

Estimated marginal means of daily feeding rate were generated for combinations of each CoTS size class and coral cover category (Figure 5.4). These predicted values are presented in Table 5.2a-c, and will be a key output of this study. Predicted values for each size class with coral cover held constant are presented in Supplementary Material (Appendix 3, Table S4a, S9a, S14a). Predicted values for each coral cover category with CoTS size class held constant are also presented in Supplementary material (Appendix 3, Table S4b, S9b, S14b).

Modelled means of daily feeding rate were found to increase considerably at high coral cover sites (>50% coral cover) for both areal estimates of feeding (planar area, 3D surface area, Figure 5.4b, 5.4c). This increase at higher coral cover sites was true for all size classes of CoTS, but the difference was most pronounced for CoTS >40cm (Figure 5.4). Modelled means were markedly lower for the lowest coral cover category (0-15%) for both areal estimates of feeding (planar area, 3D surface area), the middle two coral cover categories, 15-30% and 30-50%, had relatively consistent levels of daily feeding across all size categories and metrics (colonies, planar and 3D surface area). Whilst

predicted values of surface area are considerably greater at higher coral cover categories, and considerably lower at low coral cover categories, the number of colonies consumed remained consistent across all coral cover classes, only increasing with body size (Figure 5.4).

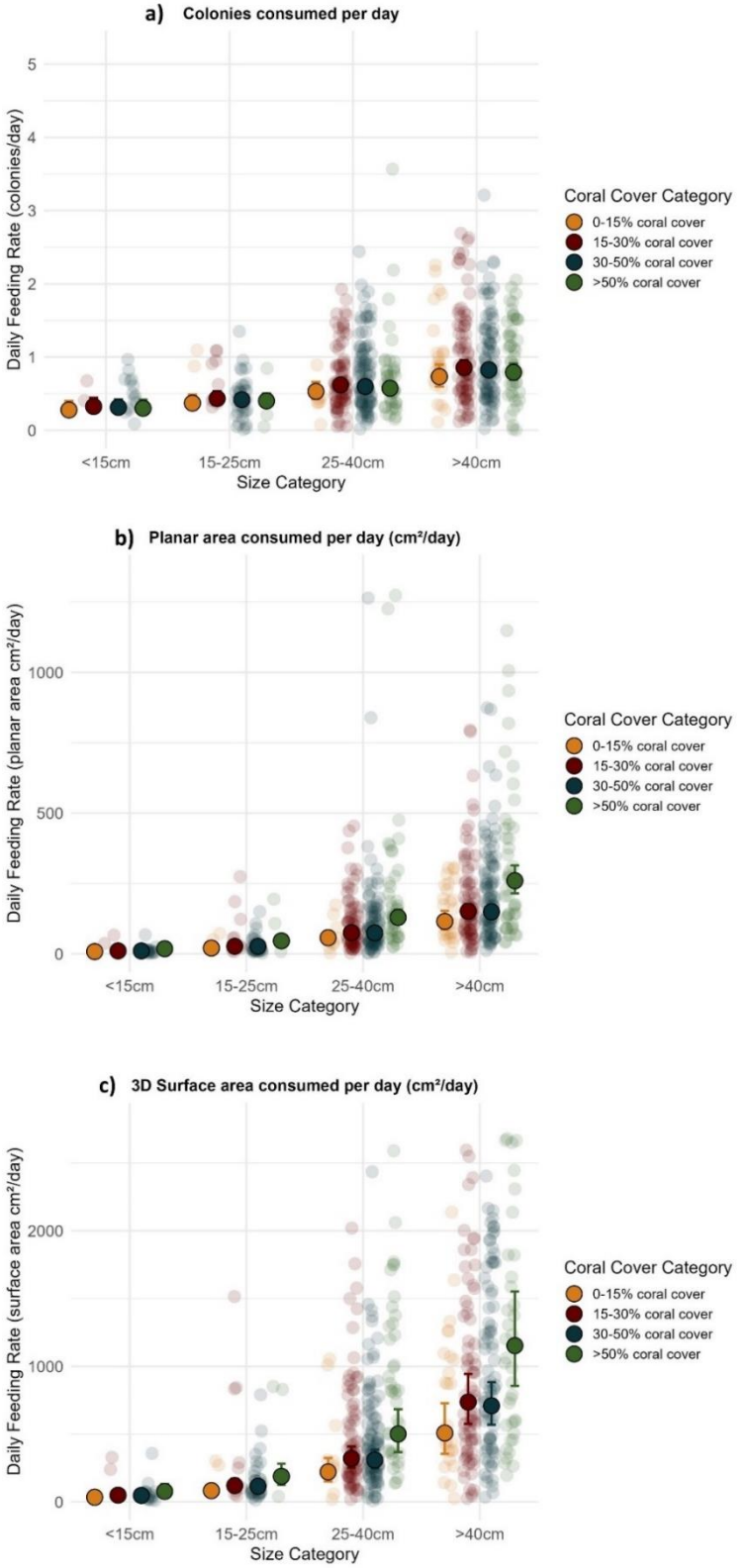


Figure 5.4 *Predicted values of daily feeding rate from GLMM modelled data with fixed effects CoTS body size and coral cover presented. Daily feeding rates are presented as* ***(a) number of colonies*** *consumed per day,* ***(b) planar area*** *of coral consumed per day (cm^2 day^{-1}) and* ***(c) 3D surface area*** *of coral consumed per day (cm^2 day^{-1}). Dark coloured points with error bars represent the predicted value and 95% confidence intervals, faded points represent true daily feeding rate data for individual starfish*

Table 5.2 *Predicted values of daily feeding rate from GLMM modelled data. Modelled feeding rates are provided for different size categories of CoTS (rows) and coral cover categories (columns). Daily feeding rate is presented as* ***(a) Number of colonies*** *consumed per day,* ***b) Planar (2D) area*** *of coral consumed per day (cm^2) and* ***c) total (3D) surface area*** *consumed per day (cm^2)*

1a	0-15% Coral cover			15-30% Coral cover			30-50% Coral cover			>50% Coral cover		
Size category	Prediction	Lower CI	Upper CI	Prediction	Lower CI	Upper CI	Prediction	Lower CI	Upper CI	Prediction	Lower CI	Upper CI
15-25cm	0.38	0.28	0.52	0.41	0.32	0.53	0.40	0.33	0.50	0.38	0.29	0.50
25-40cm	0.53	0.41	0.68	0.57	0.49	0.68	0.56	0.48	0.65	0.53	0.43	0.64
>40cm	0.75	0.59	0.94	0.81	0.68	0.97	0.79	0.68	0.92	0.75	0.62	0.90

1b	0-15% Coral cover			15-30% Coral cover			30-50% Coral cover			>50% Coral cover		
Size category	Prediction	Lower CI	Upper CI	Prediction	Lower CI	Upper CI	Prediction	Lower CI	Upper CI	Prediction	Lower CI	Upper CI
15-25cm	18.86	12.45	28.59	23.25	16.49	32.76	22.61	16.67	30.66	36.73	25.14	53.67
25-40cm	52.17	37.06	73.44	64.29	50.80	81.38	62.53	50.91	76.80	101.59	76.97	134.09
>40cm	114.00	82.58	157.38	140.49	110.37	178.83	136.64	111.26	167.81	221.99	169.95	289.97

1c	0-15% Coral cover			15-30% Coral cover			30-50% Coral cover			>50% Coral cover		
Size category	Prediction	Lower CI	Upper CI	Prediction	Lower CI	Upper CI	Prediction	Lower CI	Upper CI	Prediction	Lower CI	Upper CI
15-25cm	84.60	54.61	131.04	121.16	84.43	173.87	114.89	83.37	158.34	191.40	128.42	285.27
25-40cm	231.56	161.59	331.85	331.65	258.81	424.98	314.50	253.32	390.46	523.92	391.23	701.61
>40cm	536.98	382.45	753.95	769.07	596.60	991.39	729.30	587.47	905.36	1214.92	917.20	1609.28

5.4 Discussion

Cumulative feeding by elevated densities of large CoTS causes extensive coral loss and contributes to coral reef degradation (e.g., Kayal et al. 2012b). Accurately predicting individual feeding rates of CoTS is critical for modelling ecological impacts of population outbreaks, particularly when scaled up to estimate total coral loss. This study highlights the importance of incorporating not only CoTS size but also local coral cover into feeding models, as both were found to significantly influence daily feeding rates (see also Plagányi et al. 2020b). I found considerable variation in individual feeding rates among starfish, with significant effects of both body size and prey availability on daily feeding rate. Notably, large CoTS (>40 cm) at high coral cover sites consumed over ten times more coral than small individuals (15–25 cm) at low coral cover sites (planar area: 221.99 cm² day^{-1} vs. 18.86 cm² day^{-1}). These results demonstrate the value of incorporating context-specific feeding rates into models assessing the impacts of CoTS on reefs.

Season, latitude and population density were all considered as potential predictors of spatiotemporal variation in daily feeding rate, but no significant influence was detected. For all CoTS surveyed, a mean daily feeding rate of 164.04cm^2 (± 8.30 SE) planar area (cm^2) per day, with a range from 1.58 cm^2 a day to 2,135 cm^2 a day was recorded, which is within the range of prior estimates of planar feeding for this region (i.e. 198.4 cm² day^{-1} ± 23.86 SE, **Chapter 3**; 194-445 cm² day^{-1}, Souter, 2007; 155-234 cm² day^{-1}, Keesing and Lucas, 1992; 116-187 cm² day^{-1}, Pearson and Endean, 1969). The relatively low feeding rates in this study (*cf*. Foo et al. 2024) likely reflect the inclusion of non-feeding days in the dataset (**Chapter 3**). Crucially, this study has demonstrated the limitations of using a population-wide feeding rate, as both environmental factors (e.g. coral cover) and individual traits (e.g. body size) were found to strongly influence feeding rates. The large variation among individual CoTS recorded within our dataset demonstrates the range of factors at play, some of which cannot account for (e.g. nutritional history, metabolic demands) and further, several factors are likely acting synergistically to affect the feeding behaviour of individuals.

Body size was found to be the strongest predictor of daily feeding rate for CoTS, both in terms of total (3D) surface area, planar (2D) area and number of colonies consumed. This finding is supported by other studies recording large individuals to consume more coral in comparison to small individuals (Keesing 1990; Keesing and Lucas 1992), which is attributable to both the increased feeding potential afforded by larger body sizes as well mass-specific increases in metabolic and energetic demands of larger individuals (Yamaguchi 1974; Lang et al. 2021; Deaker and Byrne 2022). Not only do large individuals have large stomachs and are capable of consuming a greater area of coral in a single feeding bout, but are less constrained in when they feed due to reduced predation risk (Cowan et al. 2017; Ling et al. 2020).

Total coral cover had a significant positive effect on feeding rates, with particular influence at high coral cover sites (>50%). However, this trend was only apparent for planar area and overall tissue surface area consumption, with no evidence that the number of colonies consumed per day

increased in high coral cover environments. So, whilst CoTS consume more coral tissue area in high cover sites, they do not increase the number of distinct colonies that are consumed, suggesting that it is the increased size of corals that affords greater feeding rates. Most high coral cover sites on the GBR are dominated by complex branching corals such as *Acropora*, and indeed in this study 78% of variation in total coral cover was explained by *Acropora* cover. Complex branching corals, including *Acropora* and *Pocillopora* have higher tissue surface area, compared to other corals of similar dimensions (Chandler et al. 2024 [**Chapter 4**]), which greatly increases the overall tissue surface area of coral consumed with each feeding bout. This increased feeding efficiency when feeding on *Acropora* corals is further enhanced by reductions in the distance moved and time spent in search of prey. Ling et al. (2020) showed that when local abundance of *Acropora* spp. is high (>30%), CoTS exhibit high site fidelity and conspicuous homing behaviour, but when *Acropora* cover is low, CoTS tend to roam and move large distances in search of prey. This aligns with our findings and raises questions about the energetic constraints faced by CoTS in these food-limited environments, which we know are expending more energy (searching effort) and receiving lower energetic intake (low surface area of corals) compared to CoTS in high cover environments. Living in these constrained environments is likely to have consequences for individual condition and fitness (e.g., Caballes et al. 2016) and starvation has been proposed as a key factor in the collapse of high-density populations, however this hypothesis has never been verified from the field. Assessing the physiological condition of CoTS in prey-depleted environments will be crucial for understanding outbreak longevity and predicting population dynamics under future scenarios where coral cover declines and structurally complex corals become rare (Pratchett 2010; Dietzel et al. 2020). If *Acropora*-dominated environments are essential for sustaining high CoTS densities, it is possible that widespread coral loss could impose natural constraints on future outbreaks.

Previous studies have suggested that feeding rates fluctuate seasonally (Keesing and Lucas 1992, Foo et al. 2024), potentially due to temperature-mediated metabolic demand (Lang et al. 2021) and seasonal gametogenesis (Lucas 1973; Keesing and Lucas 1992). However, I did not find a

significant effect of season or water temperature on feeding rates (see also Souter 2007). The design of our study, which spanned 8° of latitude, allowed us to investigate the effect of temperature in isolation from gametogenesis stage by surveying across a gradient of water temperature during the same 2-week periods. There was no evidence that feeding rate was linked to water temperature, though the temperature range was relatively narrow (2-3 °C) and there was also likely to be a multitude of other environmental factors contributing to variability over this latitudinal gradient. When data from a single site (Lizard Island) were compared between winter (25–26°C) and summer (27–28°C), feeding rates were notably higher in summer, particularly during the spawning period. However, this trend was not statistically significant. Resolving the effects of temperature on feeding rates is essential for understanding CoTS' feeding capacity under future climate scenarios. Laboratory studies have shown that CoTS metabolism increases with temperature (Lang et al. 2021), suggesting that feeding demand may intensify with ocean warming. If CoTS do increase their feeding rate with sustained increases in baseline ocean temperatures, then this could present a double threat for corals as they face elevated thermal stress alongside increased CoTS predation rates. With increasingly depleted coral assemblages, elevated metabolic requirements may eventually outstrip energy intake potential which will impair CoTS survival. More work in this area is necessary to produce predicted values of daily feeding under dynamic warming scenarios.

Density-dependent feeding rates have been observed in various echinoderm species, particularly sea urchins (Benedetti-Cecchi et al. 1998; Wright et al. 2005), which can lead to significant ecological shifts. In this study, I tested whether population density, independent of coral cover, influenced daily feeding rates but found no significant effect on the number of colonies consumed, planar area, or 3D surface area consumption rates. This finding aligns with Foo et al. (2024), who similarly reported no relationship between population density, outbreak status, and planar feeding rates for CoTS. One possible explanation is that the population densities observed in this study (0–73.7 CoTS.ha^{-1}, Table 5.1) represent moderate levels compared to severe outbreaks (e.g., >1,000 CoTS.ha^{-1}; Kayal et al. 2012b), which may not be high enough to induce behavioural

changes. Alternatively, effects of increasing population density may scale directly with size and abundance of CoTS (i.e. *per capita* feeding rates are insensitive to density), and individual feeding rates are more sensitive to corresponding changes in the distribution, abundance and composition of prey corals. Although attributing feeding scars to individual CoTS becomes increasingly difficult at high densities, total feeding impact can be approximated by comparing cumulative scar area to the number of starfish present. While this approach lacks individual resolution, it may still reveal general patterns in feeding efficiency or density-driven competition.

Insights gained from this study have demonstrated the value of considering environmental (coral cover and composition) and biological factors (body size) when investigating ecological consequences of CoTS outbreaks. Here, I present predicted values of daily feeding which account for both coral cover and size structure of populations (Table 2), enabling considerable improvements in CoTS impact forecasting. These predicted values have application for assessing ecological impact of populations with a known size structure and coral cover environment, where cumulative effects of CoTS feeding can be modelled with higher accuracy than models that scale directly with CoTS densities. Predicted values of feeding were designed to match current data structures used by CoTS culling teams (size structure data collection) and AIMS LTMP (coral cover assessments) on the GBR. I have presented data on both 2D planar areal extent of daily feeding and 3D surface areal extent of daily feeding because different groups will benefit differently from these findings; planar area as an indication of benthic coral loss and 3D surface area as an indication of daily tissue intake for physiological interpretation and outbreak persistence modelling. With informed management decisions providing the best chance for safeguarding the resilience of the reef, the information arising from this research will be a vital pre-requisite in improving ecological threshold estimates (Babcock et al. 2014).

Conclusion

Effectively predicting and modelling ecological impacts of CoTS outbreaks is contingent upon accurate assessments of daily feeding rates *per capita*. Estimates of daily feeding which inform management decisions must account for the considerable variation in daily feeding that is associated with environmental and biological conditions. This study identified CoTS body size and coral cover as highly influential drivers of daily feeding rate, and a key output of this paper is predicted values of daily feeding under different combinations of these variables for improved ecological modelling capability. Further, this study identified the influential role that local coral coverage is having on feeding behaviour (and likely physiological condition) of CoTS, which may account for cyclical changes in their population dynamics on the GBR and thus be of critical importance in the distribution and initiation/collapse of population outbreaks (Babcock et al. 2020). This highlights the need to quantify coral cover, including *Acropora* cover, across all ongoing monitoring and modelling efforts used to inform CoTS management.

Chapter 6: Variation in reproductive and nutritional condition of CoTS with population density and food availability

6.1 Introduction

At elevated densities, during 'outbreaks', crown-of-thorns starfish (CoTS) often cause significant and widespread coral loss, with far-reaching consequences for coral reef ecosystems (Pratchett et al. 2014). The fundamental cause(s) of outbreaks are not yet resolved (Babcock et al. 2016a), but the capacity for CoTS to exhibit rapid and pronounced increases in population size is unequivocally linked to their exceptional fecundity and reproductive capacity (e.g., Uthicke et al. (2009). Fecundity of CoTS increases exponentially with size, with larger females capable of producing >100 million eggs per year (Pratchett et al. 2021c). Moreover, CoTS are capable of exceptionally high fertilisation rates (>70%) compared to other marine invertebrates (Babcock et al. 1994). These unique reproductive traits are likely to have evolved to enable population persistence in widely dispersed, low-density populations (Babcock et al. 1994; Benzie et al. 1994), but also facilitate population outbreaks. Importantly, moderate changes in rates of fertilisation, larval survival or settlement can lead to marked changes in local densities of CoTS within reef environments (Wilmes et al. 2018).

There have been five distinct episodes of CoTS outbreaks recorded on Australia's Great Barrier Reef (GBR) beginning in approximately 1959-1962 (Pearson and Endean 1969), 1979 (Endean 1982), 1993-1995 (Sweatman et al. 1998; Pratchett 2005), 2010-2013 (Osborne et al. 2011b), and 2022 (Chandler et al. 2023 [**Chapter 2**], Uthicke et al. 2024a). Each episode of outbreaks is seemingly initiated by sustained increases in CoTS densities on the reefs in the northern GBR during successive years of elevated recruitment (Pratchett 2010; Vanhatalo et al. 2017; Chandler et al. 2023 [**Chapter 2**]). Once outbreaks become established, they give rise to vast quantities of planktonic larvae with prolonged competency periods, which propagate subsequent and potentially even more extreme CoTS outbreaks on downstream reefs (e.g., Vanhatalo et al. 2017). Distinct episodes of CoTS

outbreaks may ultimately affect >32% of reefs across the GBR (Matthews et al. 2020), with considerable ecological, cultural and economic repercussions.

Population fluctuations in the local abundance of adult CoTS are ultimately linked to rates of recruitment, which are therefore pivotal in determining the initiation and spread of outbreaks (Pratchett et al. 2021c; Deaker and Byrne 2022), with the difference between strong and weak recruitment events having profound ecological consequences. Factors such as adult fecundity, maternal provisioning and environmental drivers of larval survival and dispersal collectively regulate the extent of recruitment to individual reefs, yet the processes governing these stages remain poorly understood. While several studies have considered the influence of water quality and nutrient availability on larval survival (Wolfe et al. 2017), relatively few have investigated the extent to which food availability and corresponding effects on the nutritional condition of spawning adults may be regulating CoTS reproduction and recruitment rates (see Caballes et al., 2016). Given the exceptional reproductive capacity of CoTS (Babcock et al. 2016b; Pratchett et al. 2021c), understanding intrinsic factors that moderate reproduction and larval development may be critical for explaining spatiotemporal variation in population replenishment, with consequences for the formation and breakdown of outbreaks (Caballes et al. 2016).

Laboratory studies have demonstrated that maternal nutrition significantly influences reproductive output and larval survival of western Pacific CoTS, *Acanthaster* cf. *solaris* (Caballes et al. 2016). Caballes et al. (2016) showed that CoTS which were given access to preferred prey (*Acropora* spp.) had higher physiological condition (based on Pyloric Caeca Index (PCI)) than conspecifics given access to non-preferred prey (*Porites* spp.) or starved, and these differences were further reflected in the quality and quantity of eggs and larvae. Most critically, larvae produced by females that had fed on *Acropora* spp. exhibited very high rates of larval development and survival, independent of access to planktonic prey (Caballes et al. 2016). Despite the important influence of prey availability and nutritional condition of adult CoTS for realizing their exceptional reproductive capacity, few studies

have considered the availability of preferred prey (as distinct from overall coral cover, e.g., Plagányi et al. (2014) in understanding population dynamics.

During severe outbreaks, CoTS are subject to increasing depletion of prey corals, and especially preferred prey species (Pratchett 2010, Osborne et al. 2011). *Acropora* corals, which are the preferred prey of CoTS (Pratchett et al., 2014; Ling et al., 2020, Keesing, 2021) are also highly vulnerable to climate-induced coral bleaching (Loya et al. 2001), and cyclones (Madin and Connolly 2006) resulting in boom-bust dynamics of *Acropora* assemblages with recurrent sequences of disturbance, recovery and reassembly (Morais et al. 2024). *Acropora* corals are favoured by CoTS due to their structural and nutritional characteristics which facilitate highly efficient feeding (**Chapter 4**, Keesing 2021b). However, when *Acropora* corals become scarce, CoTS are forced to travel greater distances in search of optimal prey (Ling et al. 2020) or resort to feeding on non-preferred coral taxa (Pratchett 2010), both of which may constrain energy available for growth and reproduction.

Whilst laboratory studies have examined the impacts of alternate prey on CoTS physiology and demography (George 1996; Caballes et al. 2016; Caballes and Pratchett 2017; Keesing 2021), no studies have examined spatiotemporal variation in the physiological condition or demography of CoTS in relation to population densities or food availability. In other echinoderms (e.g., *Oreaster reticulatus*), high population densities are associated with reduced reproductive investment, depletion of energy reserves and diminished somatic growth, due to intraspecific competition for resources (e.g., Scheibling 1981). Similar density-dependent mechanisms may operate for CoTS populations, especially during extreme outbreaks, but this has never been explored. Furthermore, disentangling the relative role of food availability versus population density on physiological condition will aid in our understanding of the drivers of outbreak persistence and collapse.

CoTS outbreaks often end with an abrupt and dramatic population decline (Chesher 1969a; Pearson and Endean 1969; Pratchett 2010), but the mechanisms that initiate population collapse remain poorly understood. Theories include mass migration of individuals (Endean 1969) or mass

mortality (Pratchett 2005) driven by resource depletion and/or disease (Mills 2012). Evidence from other echinoderm species suggests that extended periods of resource scarcity (and low quality prey) will lead to progressive declines in the energetic reserves stored in the pyloric caeca (Jangoux and van Impe 1977). These nutrient reserves are required for basic functions like metabolism, growth, reproduction and immune response, and so physiological function may become compromised. In the field, high-density populations with limited resources have been found to prioritize gamete production over somatic growth (Yamaguchi 1973; Cheney 1974). Prioritization of reproduction at the expense of other essential processes may result in post-spawning mortality, particularly among females, which invest more heavily in gamete production compared to male counterparts (Stump 1994). Post-spawning mortality of female CoTS would lead to sex-skewed populations, which is a trend which has been observed in the field in some late-stage outbreaks (e.g. Pratchett 2010; Caballes et al. 2016). Mass mortality due to disease has also been proposed as a potential driver of population collapse, as diseases are known to cause widespread mortality in other echinoderm species (Birkeland 1989). Rapid disease spread may be facilitated by a breakdown of immune defences, in nutritionally deprived populations. However, field observations of mass mortality events in CoTS have never been witnessed in the field, likely due to the rapid decomposition of individuals and their cryptic behaviour when they are stressed or diseased (De'ath and Moran 1998).

Understanding the physiological and reproductive changes that occur with variation in prey quality and quantity, such as during severe outbreak conditions, may be fundamental in understanding the persistence, and especially termination of population outbreaks. A more comprehensive understanding of how outbreak progression is impacting individual condition and demography would also give us improved ability to predict and model population dynamics. Accordingly, this study explores spatial variation in the physiological and reproductive condition of CoTS relative to local population densities and food availability. More specifically, this study tests for variation in energetic reserves (lipid and protein stores in the pyloric caeca) and reproductive metrics

(GSI, oocyte size) of individual CoTS sampled at distinct regions in the northern Great Barrier, capitalizing on marked differences in the population status of CoTS and coral assemblages.

6.2 Methods

6.2.1 *Field collections*

This study was conducted during November 2022, with sampling conducted at five distinct regions along the central, northern and far-northern Great Barrier Reef (GBR); Townsville, Cairns, Lizard, Princess Charlotte Bay and Cape Grenville (Figure 6.1).

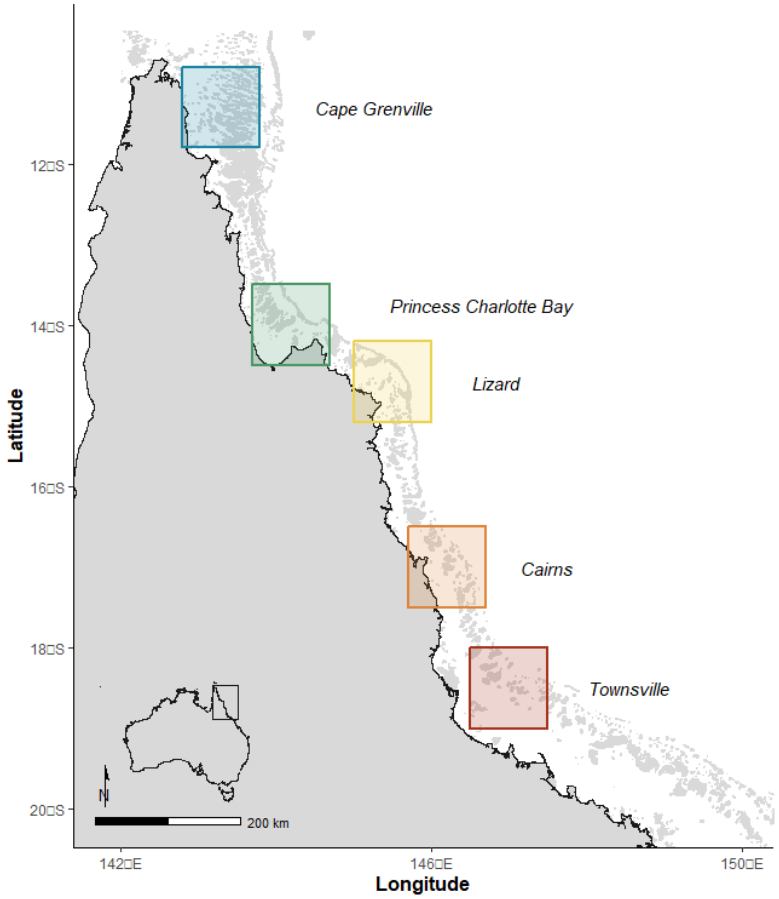


Figure 6.1 *Map of the central and northern Great Barrier Reef, showing five distinct regions (Cape Grenville, Princess Charlotte Bay, Lizard, Cairns and Townsville) where sampling was undertaken in November 2022. SALAD surveys were used to collect feeding data across this wide latitudinal gradient*

Within each region, 3 reefs were surveyed, and three sites were surveyed per reef. Scooter-Assisted Large Area Diver-based (SALAD) surveys were conducted at two depths at each site to

quantify variation in CoTS size and abundance, following (Chandler et al. 2023, [**Chapter 2**]). To quantify coral composition and thereby, food availability, 50m Point Intercept Transects (PIT) were conducted at the start and end of each SALAD survey, recording all corals to genus. This study followed a similar survey design to **Chapter 5**, however data for this chapter was collected on an independent trip.

At each reef, adult starfish were collected and processed *ex situ* to determine individual reproductive and nutritional condition. Starfish were held in fresh seawater until dissection. Individual starfish were photographed, measured, no. of legs counted and weighed (total body wet weight). Sex was identified through incision of the proximal arm region and visual inspection. 5ml gonad samples were collected for all starfish and stored in 10% formalin, samples of pyloric caeca were also collected for all starfish and stored in a liquid nitrogen dewar at -80^{o}C onboard the vessel, pyloric caeca were also photographed against a colour chart for colour reference. For female starfish, full dissections were carried out (Figure 6.2b and 6.2c) and total gonad wet weight and total pyloric caeca wet weight were recorded to calculate Gonadosomatic Index (GSI) and Pyloric Caeca Index (PCI). 88 female starfish (27-43cm) were sampled and processed.

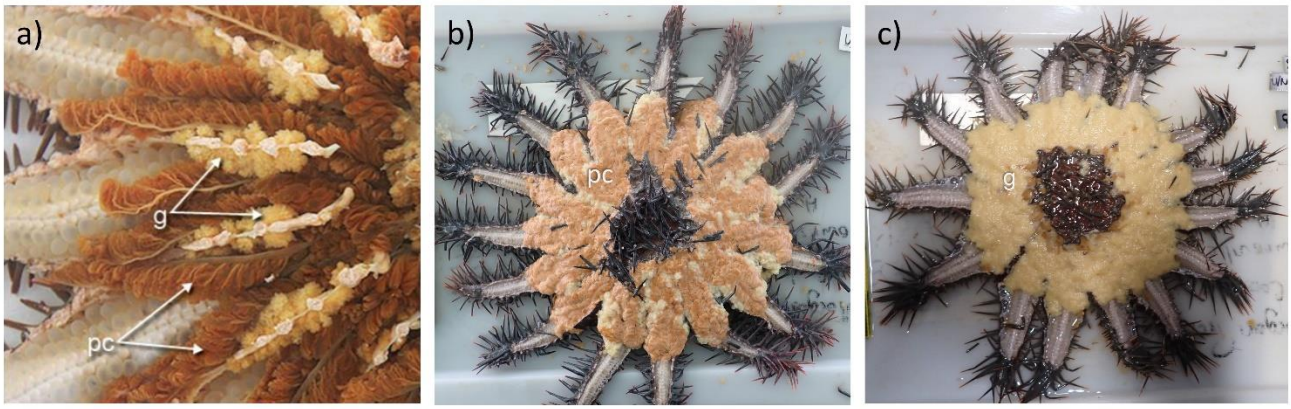


Figure 6.2 (a) *The location of pyloric caeca (pc) and gonads (g) in the dissected arm of A .cf. solaris;* ***(b)*** *female starfish after dissection, photographed with full pyloric caeca visible;* ***(c)*** *female starfish after dissection and removal of pyloric caeca, photographed*

6.2.2 *Pyloric Caeca biochemical analysis:*

The pyloric caeca is a critical energy reserve organ in asteroids, where essential nutrients such as proteins and lipids are stored (Jangoux and van Impe 1977). It serves as a key indicator of overall nutritional condition (Jangoux and van Impe 1977; Joly-Turquin et al. 2013; Caballes et al. 2016). The Pyloric Caeca Index (PCI), defined as the ratio of pyloric caeca wet weight to total body wet weight, is widely used to assess nutritional condition of asteroids (van der Plas and Voogt 1982), including CoTS (Caballes et al. 2016), as it reflects the nutrient reserves of an individual. A high PCI indicates a large, well-developed pyloric caeca, signifying good nutritional condition and energy reserves, while a low PCI suggests a smaller pyloric caecum, indicative of poor condition or potential starvation. PCI offers a holistic measure of the physiological condition of CoTS, reflecting the overall status of its energy and nutrient reserves. For this study I calculated the PCI by weighing the pyloric caeca and expressing this as a proportion of the overall body weight (Pyloric caeca wet weight/ total body wet weight).

Additionally, to provide more highly resolved insight into CoTS condition, the lipid and protein contents of the pyloric caeca were individually quantified. I investigated the proportions of protein and lipid in the pyloric caeca as this can be indicative of CoTS' resilience to stress, growth potential, and reproductive capacity (Oudejans et al. 1979; Raymond et al. 2004; Pastor-de-Ward et al. 2007). For example, high lipid levels typically indicate good nourishment levels of starfish and good energy reserves available for growth and reproduction. Protein levels are more closely associated with the synthesis of structural components, enzymatic functions, and metabolic activity, so protein levels can be indicative of starfish's ability to maintain normal function and immune response.

Biochemical content analysis of the pyloric caeca was conducted in the laboratory to ascertain lipid and protein content. Pyloric caeca samples which had been snap frozen at -80C were dried and homogenized. Total lipid was measured gravimetrically by the method of Bligh and Dyer (1959). Soluble protein was measured by the by the colorimetric modified method (Folin method) of

Lowry et al. (1951) with bovine serum albumin as the standard. Lipid quantification was conducted at the James Cook University aquaculture laboratory (J. Chandler) and protein quantification was conducted externally by researchers at Deakin University.

6.2.3 *Gonadosomatic Index and Gonad morphometrics:*

Two indices were chosen to present reproductive condition: 1) Gonadosomatic Index (GSI)(relative mass of oocytes) and 2) oocyte measurements (quality of oocytes). Gonadosomatic Index (GSI) was calculated for each individual starfish as a metric of overall reproductive potential. GSI is the ratio of gonad wet weight to total body wet weight (gonad wet weight/ total body wet weight), and it provides a measure of the proportional reproductive investment by individuals, taking into consideration CoTS body size (Farmanfarmaian et al. 1958). Other studies of asteroid reproductive condition have used GSI to quantify reproductive potential (Caballes et al. 2016; Pratchett et al. 2021c), including for comparing reproductive output among localities and populations (Parker et al. 2018).

Oocyte measurements were conducted to provide insight into the quality and maturity of oocytes of CoTS under different conditions, following Caballes et al. (2016). Gonad samples were preserved in 10% formalin for post-hoc analysis of morphometrics. Gonads were dehydrated through a graded series of ethanol solutions and then embedded in paraffin wax blocks which were subsequently sectioned. The sections were mounted on glass slides and stained with hemotoxylin and eosin (H&E) to enhance detail. The samples were then examined under a microscope and photographed. ImageJ was used to measure the longest length and area of 20 randomly selected oocytes from each starfish.

6.2.4 *Statistical analysis*

Bayesian generalized linear mixed-effects models (estimated using MCMC sampling with 3 chains of 7000 iterations and a warmup of 1500) were used to test the effect of coral cover and

population density on: 1) Physiological condition (as PCI and and % lipid content) and 2) Reproductive condition (as GSI and also as mean oocyte area); see model formulas in Supplementary Material (Appendix 4, Table S1). Random intercepts for '1|Site' were included to account for the nested structure of the data and to capture unexplained variability at different spatial scales. 'Day of survey' was also included as a random effect to account for the potential influence of gametogenesis progression during the 14 days sampling period. Given that CoTS body size has already been embedded into the response variables (PCI and GSI) to provide a comparable index across individuals of different sizes, it was not included as a random or fixed effect in the model to reduce complexity of the model and obscure other predictors. For oocyte size, the 'relative mean oocyte area' was used as the response variable (oocyte size/body size) to also account for body size. Oocyte size was averaged across 20 replicate oocytes measured for each individual starfish.

The fixed effects included in the study were '*Acropora* cover'/ 'Total coral cover' (separate models), 'Population density' and 'Lipid content'. Lipid content was included as a fixed effect to understand the relationship between lipid content and reproductive condition and also its relationship with overall PCI. Protein content autocorrelated with PCI and so was not included in any models. VIF (Variation Inflation Factor) checks were conducted to test predictors for collinearity, there was found to be weak correlation between *Acropora* cover and CoTS population density, however, there was no significant collinearity, so these predictors were both included. '*Acropora* cover' and 'total coral cover' were log-transformed to improve normality of these predictors, and all predictors were scaled. Priors over parameters were set as normal distributions. DHARMa residuals were used to check model fit.

Interactive models were run to investigate whether the effect of coral cover is dependent on population density, however there was no statistically significant effect of this interaction, and more simple models improved model fit (AIC). The interaction was removed from the model as it was not adding any explanatory power to the model. The models' explanatory power was substantial, R^2

values are presented in the results section. Each model formula is presented in Supplementary Material (Appendix 4, Table S1).

6.3 Results

CoTS were sampled across a gradient of population densities and coral cover, with marked regional differences in CoTS densities, total coral cover and *Acropora* cover (Table 6.1). Most notably, there was capacity to assess independent effects of high CoTS densities versus low cover of preferred prey (*Acropora*). For example, at McSweeney Reef in the Cape Grenville region, CoTS were sampled from a high population density of 23.70 CoTS.ha^{-1} with low total coral cover at 16.25% (with 5.50% *Acropora* cover). In contrast, at Elford Reef in the Cairns region, CoTS were sampled from a low population density of 2.04 CoTS.ha^{-1}, while total coral cover was significantly higher at 49.69% (with 29.50% *Acropora* cover). Comparison of nutritional and reproductive condition between these extremes, as well as along the spectrum of population densities, has allowed for the influence of outbreak conditions to be quantified. To disentangle the effects of population density versus coral cover on CoTS condition, sites were included that exhibited high CoTS densities (>20 CoTS.ha^{-1}) with contrasting coral cover levels, such as McSweeney Reef (very low coral cover, 16.25%) and Eagle Reef (very high coral cover, 70.67%).

Table 6.1 *Summary of sampling effort (adult females only) at each region with mean environmental conditions from each region as well as the range of values recorded. Data on environmental conditions were collected via SALAD surveys*

Region	N (female)	Total coral cover		*Acropora* cover		Mean Population density (CoTS.ha^{-1})		Sex ratio (F:M)
		Mean	Range	Mean	Range	Mean	Range	
Cape Grenville	**37**	**20.81%**	(16.25 – 36.32)	**6.45%**	(4.00 – 16.25)	18.37	0.00 – 26.90	2.06
Princess Charlotte Bay	**13**	**44.88%**	(19.30 – 52.50)	**27.21%**	(5.67 – 40.33)	23.97	0.73 – 37.54	0.65
Lizard	**27**	**43.34%**	(21.73 – 70.67)	**27.36%**	(3.67 – 63.33)	26.01	0.74 – 73.23	1.13
Cairns	**9**	**30.56%**	(18.00 – 49.69)	**9.39%**	(4.50 – 29.50)	2.07	0.78 – 3.24	1.43
Townsville	**10**	**32.29%**	(19.42 – 58.61)	**19.94%**	(11.75 – 38.50)	22.31	2.96 – 27.54	1.22

6.3.1 *Regional variation in nutritional condition*

PCI values varied considerably within regions and among reefs (Figure 6.3), ranging from 0.04 at Reef U/N-049 in the Cape Grenville region, to 0.12 at North Direction Reef in the Lizard region. Despite high variability, some regional trends were observed. Most notably, CoTS from the Cape Grenville region had considerably lower mean PCI values compared to other regions (regional mean for Cape Grenville: 0.68 + SE 0.003, compared to Princess Charlotte Bay: 0.80 + SE 0.003; Lizard: 0.84 + SE 0.003; Cairns: 0.78 + SE 0.062; Townsville: 0.91 + SE 0.005). Reef UN-160 in Cape Grenville was an exception to the low PCI values where a small subset of individuals (n = 3) exhibited considerably higher PCI values. Townsville and Lizard regions had highest mean PCI values. Variation in environmental conditions between regions were observed and are outlined in Table 6.1, however it is important to note that there was considerable variation in environmental conditions within each region.

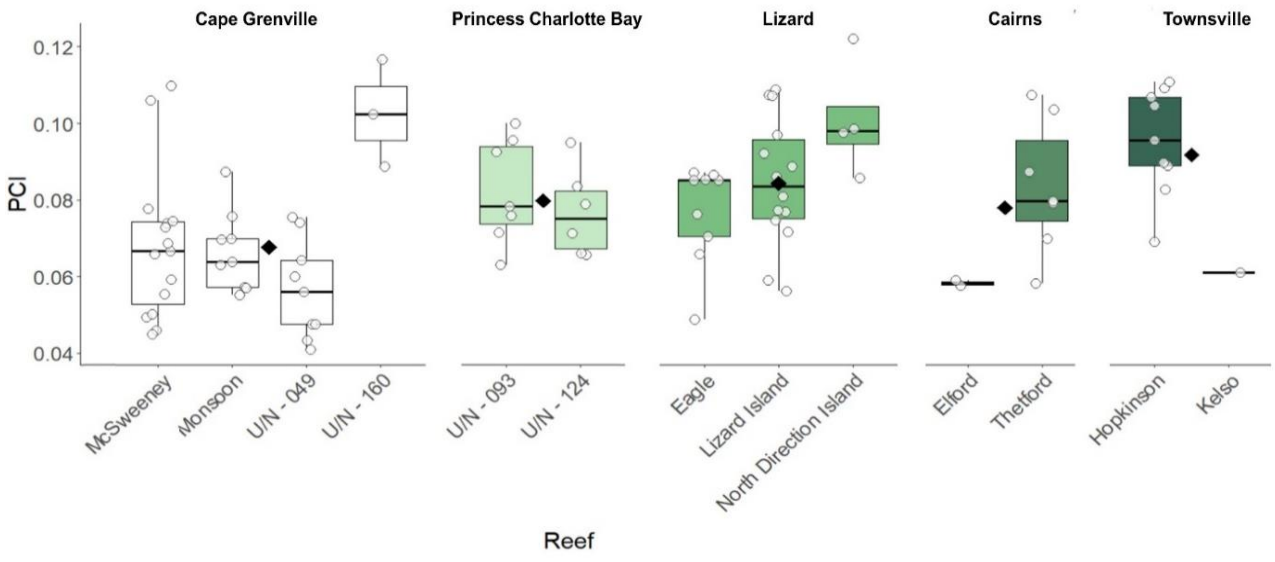


Figure 6.3 *Variation in Pyloric Caeca Index (PCI) among Reefs and Regions. Boxes and whiskers display 25–75th and 5–95th percentile ranges, respectively. Large black diamonds represent regional means of PCI. Observed values of PCI for individual starfish are displayed as points*

6.3.2 ***Regional variation in reproductive condition***

Gonadosomatic Index (GSI) was quantified as a proxy of the reproductive condition of CoTS. GSI values varied considerably within and between regions (Figure 6.4), values ranged from 0.008 at Reef U/N-093 in the Princess Charlotte Bay region, to 0.33 at Lizard Reef in the Lizard region. Despite high variability, some regional trends were observed. Cairns and Princess Charlotte Bay had considerably lower mean GSI values, compared to Cape Grenville and Lizard which were similar in their mean GSI values (Regional mean for Cairns: 0.069 + SE 0.016 and Princess Charlotte Bay 0.067 + SE 0.016 compared to Cape Grenville: 0.146 + SE 0.008; Lizard: 0.153 + SE 0.015; and Townsville: 0.098 + SE 0.016).

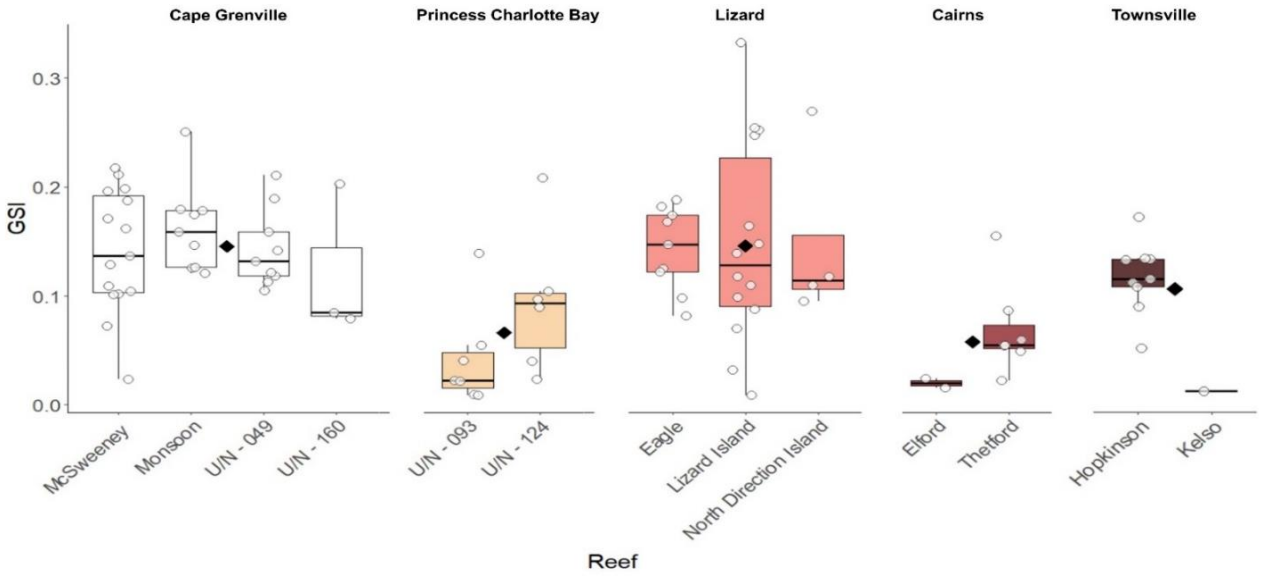


Figure 6.4 *Variation in Gonadosomatic Index (GSI) among Reefs and Regions. Boxes and whiskers display 25–75th and 5–95th percentile ranges, respectively. Large black diamonds represent Regional means of GSI. Observed values of GSI for individual starfish are displayed as points*

6.3.3 *Variation in nutritional condition along environmental gradients*

i. Nutritional condition - PCI

PCI ranged from 0.04 to 0.12 with a mean value of 0.078 (+SE 0.002). As shown above, considerable variation in PCI values was found among starfish, including among individuals at the same site with similar body size

Population dynamics of CoTS: drivers and impacts

GLMMs were conducted to ascertain the relative influence of various (scaled) predictors: Total coral cover, *Acropora* cover (log-transformed), population density on the PCI. Because Total coral cover and Acropora were strongly correlated, two separate models were run that included them both separately, to understand the relative influence of each. The model including *Acropora* demonstrated substantial explanatory power (R^2= 0.38, 95% CI [0.23, 0.49]), with fixed effects alone explaining 23% of the variance (marginal R^2 = 0.23, 95% CI [0.09, 0.39]). The model including *Total coral cover* demonstrated substantial explanatory power (R^2= 0.331, 95% CI [0.194, 0.463]), with fixed effects alone explaining 19% of the variance (marginal R^2 = 0.19, 95% CI [0.058, 0.341]). The model which included *Acropora* cover had highest exploratory power.

The results of the Bayesian generalized linear mixed-effects model which included *Acropora* cover found strong evidence for a positive effect of *Acropora* cover on PCI (Figure 6.5a), with a median effect size of 0.0065 (95% CI [0.0006, 0.0124]) and a 98.3% probability of being positive (Figure 6.5a), meaning higher *Acropora* cover is associated with increased PCI (better nutritional condition). In contrast, population density had a negative association with PCI (Figure 6.5b) (Median = -0.0082, 95% CI [-0.0135, -0.0029]), with a 99.8% probability of a negative effect, meaning lower densities of CoTS were associated with a higher PCI (better nutritional condition).

The magnitude of both effects was small (*Acropora* cover: 0.0065, population density: -0.0082); however, the consistent direction of posterior distributions and narrow credible intervals suggest biologically meaningful trends that reflect an influence of environmental conditions on physiological condition.

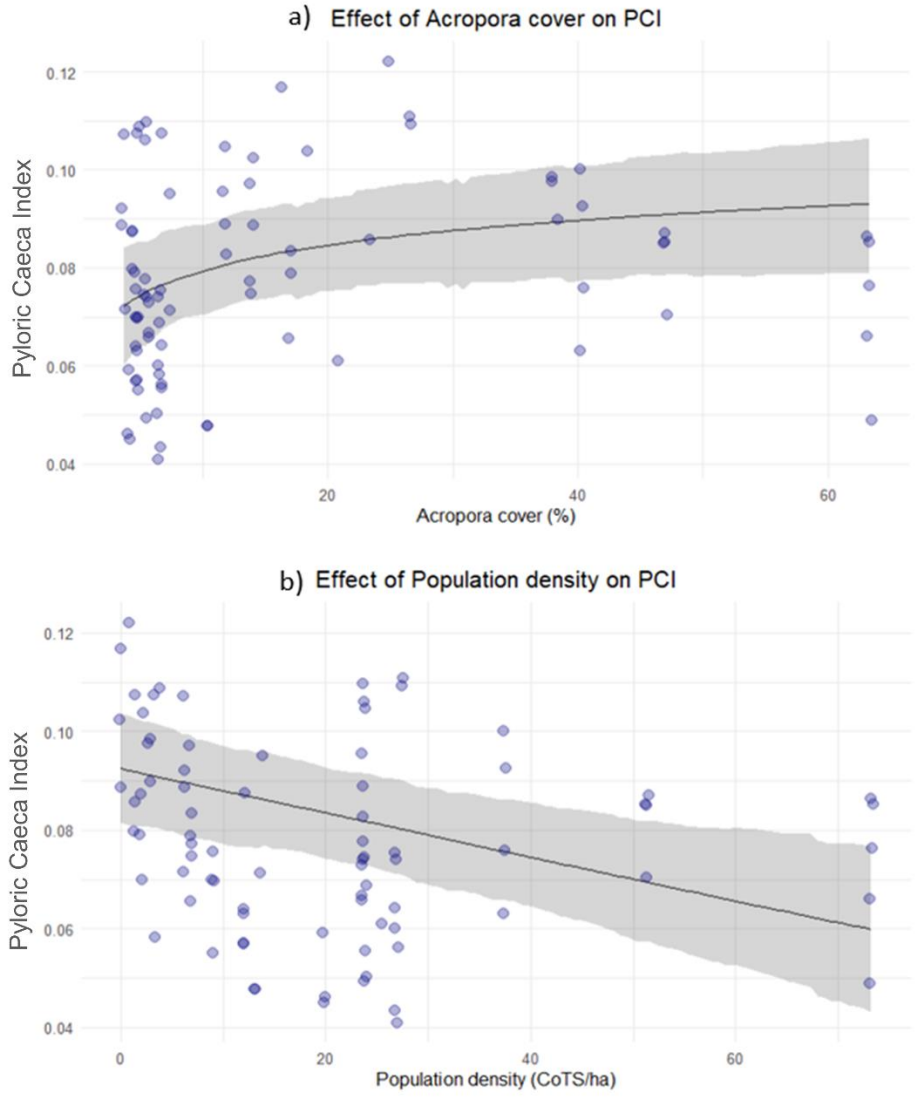


Figure 6.5 *Relationship between (a) Acropora cover (b) CoTS density and the Pyloric Caeca Index (PCI). Black lines represent the posterior median estimates of PCI as modelled using a Bayesian Generalized Linear Mixed Model (BGLMM). The grey ribbon represents 95% Highest Posterior Density (HPD) intervals as credible intervals. Observed values of PCI are displayed as points*

The model which included total coral cover found no evidence for an effect of total coral cover on PCI (Supplementary Material, Appendix 4, Figure S1). The median effect size for total coral cover was 0.0027 (95% CI [-0.0043, 0.0093]). As the credible interval includes zero, the direction of the

effect is imprecise. These results suggest that percentage cover of *Acropora*, is more strongly associated with PCI than total coral cover.

ii. Nutritional condition - Lipid content of pyloric caeca

As a second proxy for nutritional condition, I modelled the lipid content (%) of the pyloric caeca as a function of the predictors outlined above. Lipid content of the pyloric caeca was positively associated with *Acropora* cover, indicating that higher *Acropora* cover corresponds with increased lipid content (better nutritional condition). In contrast, population density had a negative association with lipid content, with a 94.7% probability of a negative effect, although confidence intervals overlapped zero in both cases.

Acropora cover showed a median effect size of 2.54 (95% CI: -0.65, 5.90), while CoTS density had a median effect size of -2.51 (95% CI: -5.61, 0.53). These trends suggest that higher *Acropora* cover and lower population densities (i.e., more favourable conditions) contribute to increased lipid reserves, reflecting improved nutritional condition and lipid reserved.

iii. Reproductive condition - Gonadosomatic Index (GSI)

GSI ranged from 0.008 to 0.33 with a mean value of 0.126 (+ SE 0.007). Overall, there was a lot of variability in GSI between individuals and among sites, especially at low coral cover sites (Figure 6.6). For example, CoTS at a low coral cover site (McSweeney reef; 5.5% *Acropora* cover) had GSI values ranging 0.071 to 0.217 for CoTS of the same body size experiencing the same environmental conditions.

There was no clear evidence of an effect of population density, *Acropora* cover or total coral cover on GSI. Median effect sizes were small for all predictors and their credible intervals included zero indicating uncertainty in the direction of any potential effect (Population density: 95% CI [-0.01, 0.02]; *Acropora* cover: 95% CI [-0.03, 0.009]; and Total coral cover: 95% CI [-0.04, 0.00]).

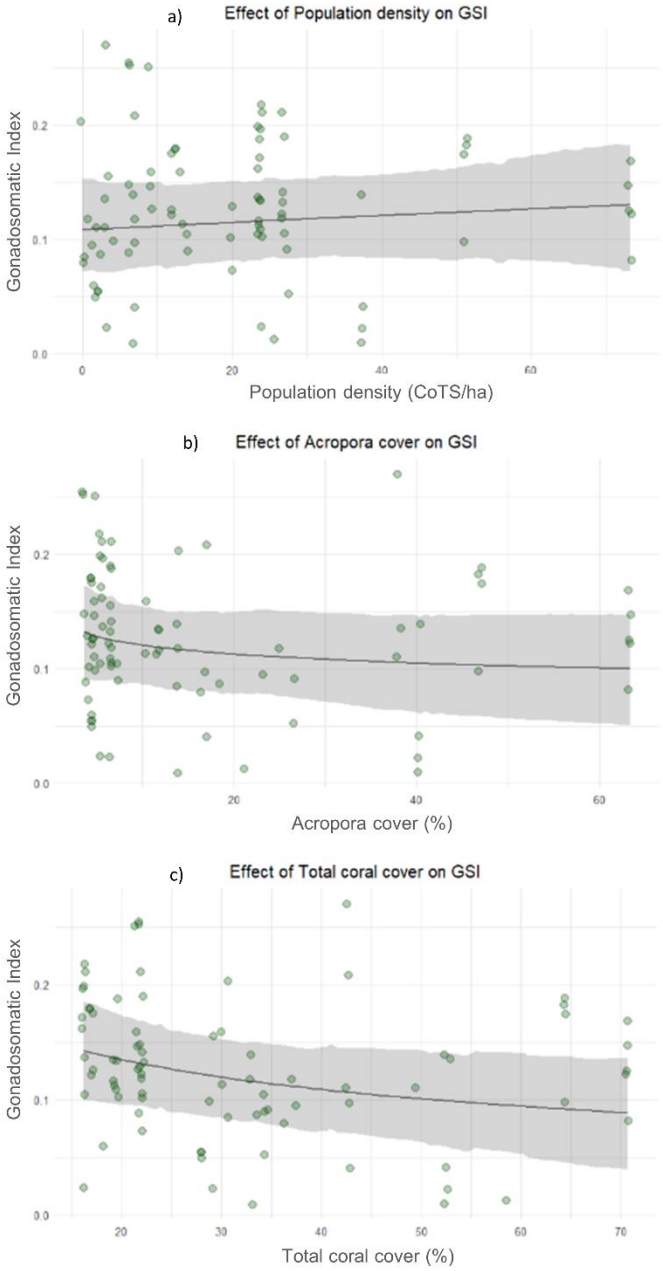


Figure 6.6 *Relationship between a) Population density, b) Acropora cover (%) and c) Total coral cover on Gonadosomatic Index (GSI; gonad wet weight to body wet weight ratio). Black lines represent the posterior median estimates of GSI as modelled using a Bayesian Generalized Linear Mixed Model (BGLMM). The grey ribbon represents 95% Highest Posterior Density (HPD) interval as credible intervals. Observed values of GSI are displayed as points*

iv. Reproductive condition – Oocyte size

BGLMMs were run with Mean Oocyte Area as the response variable as an alternative proxy of reproductive condition. The model indicated no significant effect of either CoTS density (Estimate = -0.0001, 95% CI [-0.001, 0.001]), *Acropora* cover (Estimate = -0.00008, 95% CI [-0.001 to 0.001]) or Total coral cover (Estimate = -0.00008, 95% CI [-0.001 to 0.001]) on oocyte size (Supplementary material, Appendix 4, Figure S2). The posterior estimates for the fixed effects were tightly constrained around zero, with narrow credible intervals, further supporting the conclusion that neither *Acropora* cover nor CoTS density had a measurable impact on oocyte area. The fixed effects explained only 4.6% of variability in oocyte area (Marginal R^2: 0.046; 95% CI [-0.00002, 0.181])

v. Gametogenesis and PCI

I found no relationship between PCI and GSI (Supplementary material, Appendix 4, Figure S3). This was tested to demonstrate that recorded differences in pyloric caeca condition (PCI and lipid/protein stores) are not driven by temporal progression in gametogenesis over the course of the survey trip, but rather linked to environmental conditions. It is known that some asteroids (but not all) present an inverse relationship between GSI and the pyloric caeca index (PCI) as gametogenesis progresses (e.g. Farmanfarmaian et al. 1958; Scheibling 1981).

6.4 Discussion

CoTS outbreaks are by definition unsustainable (e.g., Pratchett et al. 2014), whereby elevated densities of large starfish rapidly deplete coral prey (especially preferred prey species). This, in turn, is expected to contribute to prey limitation, with repercussions for physiological condition and population persistence of the CoTS themselves. This study showed that the individual-level physiological and reproductive impacts to CoTS may be constrained by local prey quality and quantity, and more specifically, the local abundance of *Acropora* spp.

Acropora spp. are among the most preferred prey of corallivores, including CoTS, as evident from the disproportionate consumption of *Acropora* corals, especially when highly abundant

(Tokeshi and Daud 2011; Keesing et al. 2019). The preferential consumption of *Acropora* is attributed to increased nutritional quality and feeding efficiency (**Chapter 3**, **Chapter 4**), resulting in greater energy available for growth and reproduction (Keesing 2021). While this study did not explicitly consider the feeding history of individual CoTS, CoTS in habitats with low (<10%) cover of *Acropora* spp. tended to have lower lipid reserves and lower PCI compared to CoTS in habitats with >10% cover of *Acropora*. Similarly, a negative trend was observed between CoTS density and nutritional condition (PCI) of individual CoTS, potentially reflecting coral depletion in areas of higher Cots abundance. However, these patterns should be interpreted with caution, as they are based on a limited number of sites with high coral cover or high CoTS densities, and considerable variability was observed among individuals within these sites. Regional comparisons, which capture the combined effects of coral cover and population density existing over a natural gradient, identified broad trends among regions but also identified considerable variation within reefs and sites. Most notably, considerably depleted nutritional condition (PCI) was observed for CoTS from Cape Grenville, which is a region of high population densities and low coral coverage, when compared to CoTS from Lizard, which is a site of high population densities but high coral cover (Figure 6.3). These results underscore the pivotal role of *Acropora* corals in maintaining the nutritional condition of CoTS, with potential consequences for individual growth (Keesing 2021) and reproductive capacity (Caballes et al. 2016). It is also possible that some of the regional differences in reproductive and nutritional condition reflect differences in mean body size among regions, as body size is known to influence both PCI and GSI (Caballes et al. 2016).

Despite the influence of *Acropora* cover and population density on the nutritional condition of CoTS, apparent variation in the GSI or oocyte size of CoTS was not explained by variation in prey availability or CoTS densities. Notably, there was very large variation in GSI recorded among CoTS at sites with <5% *Acropora* cover (Figure 6.6). This may signify that there are drivers outside of the predictors I tested for which are having an overwhelming effect on recorded GSI, or it may represent the divergent strategies in energetic allocation for CoTS subject to significant energetic constraint.

These findings suggest that CoTS may allocate disproportionate energy towards reproduction despite resource constraints and limited nutritional reserves. However, prioritising of limited resources for reproductive output at the expense of physiological function, has implications for individual persistence, and may result in post-spawning mortality, especially among females. Interestingly, the sex ratio of CoTS populations has been shown to become increasingly male-biased towards the end of outbreaks (Stump 1994), which is attributed to increased mortality among females that have higher energetic investment into reproduction. I did not find evidence of sex-skewed populations within this study, however, re-monitoring these populations to assess post-spawning mortality and potential shifts in sex ratios would provide valuable insight into the role of post-spawning mortality in driving population collapse. It is possible that reproductive breakdown follows a threshold-driven pattern rather than a gradual decline, with individuals allocating resources to reproduction until physiological limits are reached.

Although reproductive investment of individual CoTS varied greatly, independent of prey availability and CoTS densities, the potential implications for larval viability and survival require further investigation. It has been shown that CoTS' larvae survival, particularly in food-limiting conditions, is tightly tied to maternal nutritional history because this governs the energetic stores provided to larvae during early development (Caballes 2016). Given the evidence of depleted lipid stores in the maternal population, it is possible that offspring may be poorly provisioned which will ultimately affect their recruitment to the adult population. However, the lipid content of oocytes was not directly measured in this study. A better understanding of larval provisioning and survival in food-limited field environments is essential for a full comprehension of the long-term consequences of resource depletion for CoTS population dynamics.

This study used space-for-time comparisons to assess variation in the individual physiological and reproductive condition of CoTS among reefs and regions with varying prey availability and CoTS densities. Although this design enabled us to effectively sample over a continuum of environmental

conditions, it has not encompassed the full extent of extreme conditions under which CoTS may feasibly exist, most critically the population densities observed were in the range 0 – 73 CoTS.ha^{-1} however population outbreaks have been recorded to exceed 1,000 CoTS.ha^{-1} (e.g. Kayal et al. 2012b). Further, only one time point during the outbreak cycle has been sampled which prevents us from tracking condition over time. Recurrent sampling of CoTS populations through time is warranted, and throughout the period from before the initiation of outbreaks to after local population collapses, to better understand the potential role of density-dependence and or prey limitation on individual condition and population dynamics. Understanding the processes driving population outbreaks and collapse is critical for effectively modelling and managing CoTS. Importantly, this study suggests that careful consideration needs to be given to the local abundance of *Acropora* corals, rather than coral cover more generally, to better understand key drivers of population dynamics.

Conclusion

Understanding how extrinsic factors (especially availability of specific prey corals) influence the individual condition and population dynamics of CoTS is important for predicting population dynamics, and in particular, the initiation of outbreaks and subsequent population collapse. Whilst prolonged exposure to low *Acropora* coral cover (and thus non-preferred prey) seemed to be amplifying the progression of physiological breakdown in terms of depleting PCI, it was not (yet) impacting reproductive condition. Whether ongoing investment into reproductive output ultimately comes at the cost of post-spawning mortality and/or poor-quality larvae will be an indication of population resilience. Given that it is the phenomenal reproductive potential of CoTS that enable the large-scale and chronic spread of outbreaks, understanding the threshold of reproductive breakdown is important for understanding outbreak cessation.

Chapter 7: General Discussion

Coral reefs are increasingly threatened in the Anthropocene, as the cumulative effects of perennial disturbances are compounded by anthropogenic pressures, including climate change (Hughes et al. 2017; Bellwood et al. 2019; Perry and Alvarez-Filip 2019; Williams et al. 2019). In the Indo-Pacific, cumulative disturbance events have significantly reduced the scleractinian cover of coral reefs (Hughes et al. 2017) and resulted in shifts in coral composition due to taxonomic differences in susceptibility and resilience (Kubicek et al. 2019; Burn et al. 2023). Whilst some of the foremost threats to coral reefs (e.g., coral bleaching), have been unequivocally linked to anthropogenic climate change (Hoegh-Guldberg 1999; Sully et al. 2019), the causes(s) of other major threats such as crown-of-thorns starfish outbreaks (*Acanthaster spp.;* CoTS) are still equivocal. Even so, managing outbreaks of CoTS to minimize their ecological effects on coral assemblages is even more important given the increasing effects of environmental change. Though effective management (and containment or suppression) of the CoTS outbreaks is contingent upon an understanding of the processes that cause or contribute to initiation of outbreaks.

This thesis gained empirical data on the intrinsic and extrinsic processes that are i) exacerbating population increase (and decreasing food availability) and ii) influencing population breakdown, thereby improving our understanding of the mechanistic underpinning of CoTS population fluctuations. The data gained has allowed a much more holistic understanding of CoTS outbreak dynamics, with applications that span outbreak prediction, prevention, and (in the interim) management, of CoTS outbreaks.

7.1 Key processes in population build-up of crown-of-thorns starfish

One of the major barriers to resolving the root cause of population initiation has been our inability to survey CoTS populations during the critical (and temporally brief) transition from low densities to the apparent onset of population outbreaks, largely due to inherent design constraints of current survey methodologies (i.e. manta tow, see **Chapter 2**). Accordingly, **Chapter 2** developed the

Scooter-assisted Large Area Diver-based (SALAD) survey, a novel method which provides high-resolution surveillance of CoTS populations and an unprecedented opportunity to assess temporal changes in abundance, behaviour and biology of CoTS, including subtle changes when CoTS are at low densities (Chandler et al. 2023 [**Chapter 2**]). By identifying these changes considerably earlier than traditional methods have been capable of, there is new opportunity for early intervention, potentially prior to mass spawning and secondary waves of outbreaks (Babcock et al. 2020). Recurrent sampling using the SALAD survey method at Lizard Island showed that densities of CoTS were relatively constant (at approximately 5 CoTS.ha^{-1}) from 2019 until 2021, but increased thereafter (Figure 2.2). This data confirms the initiation of renewed outbreaks on Australia's GBR, consistent with predictions that outbreaks would reoccur between 2025-2027 (Babcock et al. 2020), based on the period (15-17 years) between the initiation of previous outbreaks. Importantly, the new method allowed data to be collected during the critical transition period, as CoTS populations shifted from a low-density population to a population rapidly approaching the notional threshold of an outbreak (15 CoTS.ha^{-1}; Keesing and Lucas 1992). This advancement represents a significant improvement in early detection capabilities and provides invaluable data for developing an early warning system for CoTS outbreaks.

Beyond early detection, the SALAD method has offered a unique opportunity to better understand the drivers of outbreaks by providing unprecedented demographic data before and during the transition period. Notably, size structure analysis of the population at Lizard Island indicated the presence of multiple cohorts, rather than a single influx of new recruits in a single year. This data challenges the basis of the Terrestrial Runoff Hypothesis, which proposes that outbreaks are initiated by a pulse of highly elevated recruitment following favourable environmental conditions for larval survival, such as those induced by significant terrestrial runoff events or otherwise (Birkeland 1982). On the contrary, moderate increases in CoTS densities since 2021 were recorded which suggests that sustained low-level recruitment, rather than abrupt recruitment pulses, may be responsible for outbreak initiation (see also Pratchett 2005).

Population dynamics of CoTS: drivers and impacts

Our early detection of the fifth documented outbreak on the northern Great Barrier Reef since the 1960s (**Chapter 2**, also Chandler et al. 2023), has confirmed that the pattern of outbreak dynamics at this location is cyclical, as its emergence was predicted to occur (albeit two years later) due to the consistent trends of outbreak build-up and breakdown that have occurred in previous cycles (Pratchett 2005; Babcock et al. 2020). These recurrent outbreaks cannot be readily explained by the Predator Removal Hypothesis (*sensu* Pearson and Endean 1969), whereby it is difficult to ascribe seemingly consistent fluctuations in the abundance of CoTS to overfishing and sustained depletion of putative predators. The data generated in this chapter challenges two of the major hypotheses of outbreak initiation, necessitating a shift in focus toward alternative drivers which facilitate a gradual, but pronounced build-up of CoTS densities. Potential explanations for this trend likely relate to larval production or supply. Identifying the source of the recruits to this population will be of critical importance for resolving the processes at play.

A key pattern that emerged through this thesis has been that *Acropora* corals may be playing an influential role in population build-up, and population persistence. It has become increasingly apparent through data collected in **Chapters 1, 3, 5 & 6** that prey availability, and specifically proportional benthic cover of *Acropora spp.,* is likely to be a key driver of spatiotemporal variation in the demography and behaviour of CoTS. And further, it may in fact explain the occurrence and initiation of population outbreaks. In **Chapter 3** I identified that *Acropora* corals were disproportionately contributing to the diet of CoTS, and whilst strong prey preferences for *Acropora* corals are widely reported (e.g., Pratchett 2007; Ling et al. 2020a; Foo et al. 2024), our data on feeding rates based on overall (3D) tissue surface area provided new insights into the relative feeding efficiency on complex corals. This chapter revealed that *Acropora* corals were contributing to over 80% of the total coral surface area consumed by CoTS during a 13-day field study, however importantly, this high surface area consumption of *Acropora* corals was achieved through the consumption of relatively few individual colonies. The apparent efficiency of feeding on *Acropora* corals highlighted in this chapter was further reinforced in **Chapter 4** where it was determined that

complex branching corals, such as *Acropora*, provide over five times as much surface area (tissue area), compared to an encrusting coral of the same colony diameter. Paired with high recorded values for nutritional condition of *Acropora* (Keesing 1990), these data have provided a basis for why *Acropora* corals may be highly influential in driving physiological and behavioural differences as well as spatiotemporal distribution in CoTS, as it is beneficial for CoTS to seek out these prey types for optimal energetic intake.

Chapter 5 presented data to demonstrate that CoTS in low coral cover environments were consuming the same number of colonies as CoTS in high coral cover environments but receiving considerably less surface area (tissue area) for their efforts (Figures 5.3, 5.4), likely because of the dominance of more structurally complex corals at high coral cover sites. Given the sparseness of suitable prey in low coral cover environments, this data implies that CoTS may be travelling great distances to forage whilst simultaneously receiving low energetic intake in terms of tissue consumption area and non-preferred prey (Keesing 2021). These findings support previous studies (i.e. Ling et al. 2020a) which have proposed that behavioural shifts in foraging behaviour may occur when preferred prey are absent or limited, as CoTS shift to long-range foraging behaviour ('roaming') in search of preferred prey. This behavioural change that is posited to occur has the potential to result in feeding aggregations of CoTS, as it is energetically beneficial for individuals to seek out preferred prey in increasingly patchy and constrained habitats (Caballes 2009; Haywood et al. 2019; Keesing et al. 2019; Ling et al. 2020). The importance of feeding aggregations for low-density populations is considerable because increased proximity of individuals has the potential to cause elevated reproductive output of a population relative to its size, as optimal monospermic fertilisation is achieved by aggregated low-density populations (Rogers et al. 2017). The Natural Causes Hypothesis posits that population outbreaks may be driven by inherent biological traits and ecological factors such as episodic reproductive success or variability in predator-prey relationships (Dana et al. 1972; Vine 1973). It appears possible that prey-driven changes in spatial distribution of

CoTS may explain the occurrence or severity of population outbreaks (Pratchett et al. 2014; Foo et al. 2024).

The data gained in the aforementioned chapters have improved our understanding of outbreak initiation, by challenging some of the major hypotheses of initiation and by identifying the gradual accumulation of CoTS as the mechanism by which populations are building, with possible links to prey availability. Future work is still needed to pinpoint the exact process(es) around Lizard Island that are driving enhanced recruitment success over successive years, and of particular research focus should be investigation into the accumulation of low-density CoTS in response to decreasing *Acropora* cover.

7.2 Key processes in population breakdown of crown-of-thorns starfish

The persistence of CoTS outbreaks is a critical variable for predicting CoTS ecological impacts and overall population dynamics. However, there is limited data on the processes that contribute to rapid population collapses, that often occur at the end of outbreaks. Starvation has been proposed as a potential cause of population collapse, however there is evidence of CoTS population outbreaks dissipating even when local coral cover is still high (Pratchett 2010). To fill this research gap, **Chapter 6** tested the hypothesis that decreasing food availability and increasing population densities were negatively impacting the nutritional and physiological condition of CoTS, to investigate whether starvation is the most likely driver of population collapse. Laboratory studies (e.g. Caballes et al. 2016) have shown that prey limitation significantly impacts CoTS physiological and reproductive condition. If similar effects occur in the field, this would have important implications for population collapse, and help explain cyclical pattern of population outbreaks.

The findings of **Chapter 6** revealed that increasingly constrained outbreak conditions, in terms of increasing densities and decreasing food availability, are indeed detrimental to the physiological condition of CoTS (decreased PCI and lipid stores). However, nutritional condition was found to be

highly variable among individuals from the same reef (Figure 6.3), suggesting that other factors, aside from prey availability and density, are also impacting individual condition. Local availability of *Acropora* cover was found to amplify physiological compromise, with CoTS at sites with very low *Acropora* cover (<10%) presenting reduced nutritional condition (PCI), regardless of population density. These findings corroborate the data gained in **Chapters 3, 4 & 5**, regarding the intense reliance of CoTS on *Acropora* corals for population persistence. The compromised nutritional condition of CoTS in low coral cover environments is likely due to the energy deficit that results from having to search great distances for limited energetic return, as preferred prey become locally depleted **(Chapter 5).**

Whilst this data on nutritional condition suggests that prey limitation can influence CoTS physiological status, the relationship with *Acropora* cover was variable across individuals suggesting that other factors may also play an important role in shaping nutritional condition. It is also possible that CoTS are more tolerant of low food availability than previously assumed, particularly during the early stages of an outbreak, or that they require less coral to maintain baseline physiological processes, a pattern observed in other echinoderms such as sea urchins. Simultaneously, the data on reproductive output yielded unexpected results. Despite evidence of considerable nutritional depletion, the reproductive condition of CoTS at these sites (GSI and oocyte area) remained unaffected. Although this suggests reproductive resilience, we can infer from the data that investment in reproduction has occurred at the expense of overall condition, potentially leading to post-spawning mortality and imminent population collapse. Additionally, while oocyte quantity and quality appeared normal, data on larval provisioning was lacking. It is possible that depleted lipid stores in adult CoTS result in poorly provisioned larvae with reduced survival potential (*sensu* Caballes et al. 2016), preventing recruitment into the adult population. Resolving these factors is essential for a comprehensive understanding of population breakdown and the role of prey limitation in CoTS population dynamics. Given that it is the phenomenal reproductive potential of

CoTS that facilitate the large-scale and chronic spread of outbreaks, understanding the persistence of reproductive output under resource-limited conditions is critical.

This thesis has emphasised the importance of *Acropora* in the occurrence and initiation of population outbreaks, as well as population breakdown. The critical influence of *Acropora* spp. on the behaviour and demographics of CoTS may be important for understanding and predicting the occurrence and spatial distribution of population outbreaks in the future, with coral cover and composition a key determinant of outbreak intensity and duration. In a future warming scenario where reefs are even more depleted and with potentially constrained biodiversity , the progression pattern of outbreaks will likely be affected. Lower peak densities may be supported but CoTS impacts on coral communities may be just as significant and detrimental. The synergistic effects of more intense climate events and continued severe CoTS predation, will undoubtedly affect the recovery potential of reefs.

7.3 Management Implications

This thesis has contributed to improved understanding of the processes involved in marked population fluctuations of CoTS, which is fundamental for establishing effective and lasting management solutions (Pratchett et al. 2014). Until the drivers of population outbreaks are fully understood and effectively managed (if possible), the predominant management strategy will continue to centre around culling CoTS on reefs with apparent and established outbreaks (Matthews et al. 2024). Preemptive culling in areas with low, but increasing densities of CoTS, will be potentially much more effective in minimizing coral loss caused by CoTS, and has the capacity to prevent initiation and spread of outbreaks. SALAD surveys provide unprecedented opportunities to detect the early onset of CoTS outbreaks (Chandler et al. 2023 [**Chapter 2**]), marking a major breakthrough in our ability to mitigate the impact of CoTS on Indo-Pacific reefs.

Chapters 4, 5 & 6 have contributed new data for understanding the specific ecological effects of CoTS, which are relevant for understanding management thresholds. The data provided in this thesis may be useful for updating these thresholds. The estimates of daily feeding presented in **Chapter 3** & **5** were constructed via photogrammetry techniques and so provide highly resolved estimations of consumption rates, at higher accuracy than historic feeding rates which underpin current thresholds. Historic methods which these thresholds are based upon were collected via simple field measurements of CoTS feeding scar diameter over a comparatively short survey period (3-5 days, Keesing and Lucas 1992), the findings of our daily feeding rate study in **Chapter 3** highlight the importance of gaining feeding data over longer survey periods, due to significant variation in feeding between days. Further, the feeding rates established in **Chapter 5** take into consideration the strong influence that environmental factors (i.e. local coral cover) and intrinsic factors (i.e. body size) are having on individual feeding rates, demonstrating that feeding rates may vary by ten-fold, depending on these factors (Figure 5.2). The importance of incorporating these variables into ecological threshold calculations was highlighted and provide modelled feeding rates which can be applied to dynamic situations for most accurate predictions of CoTS impacts and spread during modelling exercises. Further, data gained in **Chapter 6** on patterns of physiological and reproductive compromise improve our ability to predict persistence of CoTS populations which will be beneficial for modelling outbreak longevity. However, more data is needed to understand the point of reproductive breakdown.

Given that the extent of CoTS ecological impact is a function of CoTS densities, feeding capacity and outbreak duration, the data collected and presented within this thesis has improved our ability to predict population dynamics and their associated impact to coral reefs. With effective modelling capabilities, management decisions can be made which appropriately capture population trajectories and trade-offs.

7.4 Future Direction in Research

Some of the prevailing hypotheses related to the initiation of population outbreaks have been challenged by the data presented in this thesis, showing that increasing densities at Lizard Island are due to accumulation of CoTS from multiple cohorts. These revelations have influence over future research avenues, as we attempt to hone in on the exact process(es) which are driving enhanced recruitment success at this important location. Methods which identify the source population of larvae arriving at a building population will be highly valuable for understanding how elevated recruitment is arising, and more resolved genetic methods would be a potential route to this knowledge. Oceanographic modelling of the area may also be useful for resolving whether larval retention and self-recruitment is a possible process causing elevated recruitment. Research into mechanisms that lead to aggregations, and the implications of low-density populations aggregating should also be a research priority.

The findings of this thesis highlight the necessity of considering prey-resource interactions in outbreak models, and especially the availability of *Acropora* spp. Similarly, it appears that coral composition (or the abundance of *Acropora* spp.) has greater utility than estimates of coral cover, in understanding and predicting population dynamics of CoTS. Accordingly, it will be beneficial to consider thresholds of *Acropora* cover which define the point at which CoTS behaviour and biology are shifting. Ling et al. (2020a) has established the coral cover threshold at which foraging behaviour shifts, and further research along these lines would be beneficial for management decisions.

Additionally, future efforts to continue SALAD sampling of this outbreaking population over the entire course of an outbreak would provide invaluable data on outbreak evolution and importantly, when the threshold of outbreak collapse will occur.

Conclusion

This thesis has advanced our understanding of the ecological processes that drive CoTS population fluctuations, providing critical insights into both the build-up and breakdown of outbreaks. This work has challenged prevailing hypotheses of outbreak initiation and revealed the importance of gradual population accumulation, likely influenced by prey availability, particularly *Acropora* coral cover. Whilst it is possible that natural predator-prey oscillations have always occurred through time for CoTS and have gone relatively unnoticed (Vine 1973), changes in environmental and habitat conditions on reefs in the Anthropocene may be exacerbating the occurrence and effects of CoTS outbreaks. Changes in the distribution and abundance of preferred prey, for example, may be leading to aggregations of adult CoTS in small areas of coral refugia, which elevates their reproductive output relative to population size and the risk of future population outbreaks.

These findings not only refine our understanding of CoTS ecology but also have direct implications for management strategies, particularly in the early detection and suppression of outbreaks before they reach destructive thresholds. By incorporating ecological, physiological, and behavioural data into management models, we can improve decision making and speed to intervention, which has considerable ecological and economic repercussions. This work contributes considerable knowledge to the mitigation of CoTS impacts, with important implications for reef conservation in an era of escalating environmental change. Future research should build upon these findings by investigating larval connectivity, behavioural aggregation mechanisms, and the precise thresholds at which prey limitation drives population collapse.

References

Alcala MLR, Vogt H (1997) Approximation of coral reef surfaces using standardized growth forms and video counts. 2:

Almany GR (2004) Differential effects of habitat complexity, predators and competitors on abundance of juvenile and adult coral reef fishes. Oecologia 141:105–113

Álvarez-Noriega M, Baird AH, Dornelas M, Madin JS, Cumbo VR, Connolly SR (2016) Fecundity and the demographic strategies of coral morphologies. Ecology 97:3485–3493

Andréfouët S, Payri C (2001) Scaling-up carbon and carbonate metabolism of coral reefs using in-situ data and remote sensing. Coral Reefs 19:259–269

Anthony KRN, Hoogenboom MO, Connolly SR (2005) Adaptive variation in coral geometry and the optimization of internal colony light climates. Funct Ecol 19:17–26

Aston EA, Duce S, Hoey AS, Ferrari R (2022) A Protocol for Extracting Structural Metrics From 3D Reconstructions of Corals. Front Mar Sci 9:

Australian Institute of Marine Science (2023) Annual summary report of coral reef condition 2022/23. Australian Institute of Marine Science, Townsville. https://www.aims.gov.au/monitoring-great-barrier-reef/gbr-condition-summary-2022-23

Babcock R, Mundy C (1992) Reproductive biology, spawning and field fertilization rates of Acanthatser planci. Mar Freshw Res 43:525

Babcock R, Plagányi É, Bee Morello E, Rochester W, Hoey J, Pratchett M (2014) What are the important thresholds and relationships to inform the management of Crown-of-Thorns Seastar.

Babcock RC, Dambacher JM, Morello EB, Plagányi ÉE, Hayes KR, Sweatman HPA, Pratchett MS (2016a) Assessing different causes of Crown-of-Thorns starfish outbreaks and appropriate responses for management on the great barrier reef. PLoS One 11:

Babcock RC, Milton DA, Pratchett MS (2016b) Relationships between size and reproductive output in the crown-of-thorns starfish. Mar Biol 163:

Babcock RC, Mundy CN, Whitehead D (1994) Sperm diffusion models and in situ confirmation of long-distance fertilization in the free-spawning asteroid Acanthaster planci. Biological Bulletin 186:

Babcock RC, Plagányi ÉE, Condie SA, Westcott DA, Fletcher CS, Bonin MC, Cameron D (2020) Suppressing the next crown-of-thorns outbreak on the Great Barrier Reef. Coral Reefs 39:1233–1244

Baird AH, Pratchett MS, Hoey AS, Herdiana Y, Campbell SJ (2013) Acanthaster planci is a major cause of coral mortality in Indonesia. Coral Reefs 32:803–812

Barham EG, Gowdy EG, Wolfson FH (1973) Acanthaster (Echinodermata, Asteroidea) in the Gulf of California. US Natl Mar Fish Serv Fish Bull

Beach DH, Hanscomb NJ, Ormond RFG (1975) Spawning pheromone in crown-of-thorns starfish. Nature 254:

Beeden R, Willis BL, Raymundo LJ, Page CA, Weil E (2008) Underwater cards for assessing coral health on Indo-Pacific reefs.

Bellwood DR, Pratchett MS, Morrison TH, Gurney GG, Hughes TP, Álvarez-Romero JG, Day JC, Grantham R, Grech A, Hoey AS, Jones GP, Pandolfi JM, Tebbett SB, Techera E, Weeks R, Cumming GS (2019) Coral reef conservation in the Anthropocene: Confronting spatial mismatches and prioritizing functions. Biol Conserv 236:604–615

Benedetti-Cecchi L, Bulleri F, Cinelli F (1998) Density dependent foraging of sea urchins in shallow subtidal reefs on the west coast of Italy (western Mediterranean). Mar Ecol Prog Ser 171:203–211

Benzie JAH, Black KP, Moran PJ, Dixon P (1994) Small-scale dispersion of eggs and sperm of the crown-of-thorns starfish (Acanthaster planci) in a shallow coral reef habitat. Biological Bulletin 186:

Birkeland C (1982) Terrestrial runoff as a cause of outbreaks of Acanthaster planci (Echinodermata: Asteroidea). Mar Biol 69:

Birkeland C (1989) The influence of echinoderms on coral-reef communities. Echinoderm Studies

Birkeland C, Lucas JS (1990) Acanthaster planci: major management problem of coral reefs.

Black K, Moran P, Burrage D, De'ath G (1995) Association of low-frequency currents and crown-of-thorns starfish outbreaks. Mar Ecol Prog Ser 125:185–194

Bligh EG, Dyer WJ (1959) A rapid method of total lipid extraction and purification. Can J Biochem Physiol 37:

Bozec YM, Hock K, Mason RAB, Baird ME, Castro-Sanguino C, Condie SA, Puotinen M, Thompson A, Mumby PJ (2022) Cumulative impacts across Australia's Great Barrier Reef: a mechanistic evaluation. Ecol Monogr 92:

Bradbury RH, Antonelli PL (1990) What Controls Outbreaks? pp 278–290

Brauer RW, Jordan MJ, Barnes DJ (1970) Triggering of the Stomach Eversion Reflex of Acanthaster planci by Coral Extracts. Nature 228:344–346

Brodie J, Fabricius K, De'ath G, Okaji K (2005) Are increased nutrient inputs responsible for more outbreaks of crown-of-thorns starfish? An appraisal of the evidence. 51:266–278

Brooks ME, Kristensen K, Benthem KJ, van, Magnusson A, Berg CW, Nielsen A, Skaug HJ, Mächler M, Bolker BM (2017) glmmTMB Balances Speed and Flexibility Among Packages for Zero-inflated Generalized Linear Mixed Modeling. R J 9:378

Bruno JF, Selig ER (2007) Regional decline of coral cover in the Indo-Pacific: Timing, extent, and subregional comparisons. PLoS One 2:

Bürkner PC (2017) brms: An R package for Bayesian multilevel models using Stan. J Stat Softw 80:

Burn D, Hoey AS, Matthews S, Harrison HB, Pratchett MS (2023) Differential bleaching susceptibility among coral taxa and colony sizes, relative to bleaching severity across Australia's Great Barrier Reef and Coral Sea Marine Parks. Mar Pollut Bull 191:114907

Burn D, Matthews S, Caballes CF, Chandler JF, Pratchett MS (2020) Biogeographical variation in diurnal behaviour of Acanthaster planci versus Acanthaster cf. Solaris. PLoS One 15:

Burn D, Matthews S, Pisapia C, Hoey AS, Pratchett MS (2022) Changes in the incidence of coral injuries during mass bleaching across Australia's Coral Sea Marine Park. Mar Ecol Prog Ser 682:97–109

Bythell J, Pan P, Lee J (2001) Three-dimensional morphometric measurements of reef corals using underwater photogrammetry techniques. Coral Reefs 20:193–199

Caballes CF (2009) The role of chemical signals on the feeding behavior of the crown-of-thorns seastar, Acanthaster planci (Linnaeus, 1758). MSc Thesis.

Caballes CF (2017) Environmental influences on the reproductive biology and early life history of the crown-of-thorns starfish.

Caballes CF, Byrne M, Messmer V, Pratchett MS (2021) Temporal variability in gametogenesis and spawning patterns of crown-of-thorns starfish within the outbreak initiation zone in the northern Great Barrier Reef. Mar Biol 168:

Caballes CF, Messmer V, Raymundo ML, Pratchett MS (2022) Prevalence and severity of sublethal injuries in crown-of-thorns starfish relative to marine reserves in the Great Barrier Reef. Aquat Conserv 32:993–1004

Caballes CF, Pratchett MS (2014) Reproductive biology and early life history of the crown-of-thorns starfish.

Caballes CF, Pratchett MS (2017) Environmental and biological cues for spawning in the crown-of-thorns starfish. PLoS One 12:

Caballes CF, Pratchett MS, Buck ACE (2017) Interactive effects of endogenous and exogenous nutrition on larval development for crown-of-thorns starfish. Diversity (Basel) 9:

Caballes CF, Pratchett MS, Kerr AM, Rivera-Posada JA (2016) The Role of Maternal Nutrition on Oocyte Size and Quality, with Respect to Early Larval Development in The Coral-Eating Starfish, Acanthaster planci. PLoS One 11:e0158007

Castro-Sanguino C, Bozec Y, Condie SA, Fletcher CS, Hock K, Roelfsema C, Westcott DA, Mumby PJ (2023) Control efforts of crown-of-thorns starfish outbreaks to limit future coral decline across the Great Barrier Reef. Ecosphere 14:

Chandler JF, Burn D, Caballes CF, Doll PC, Kwong SLT, Lang BJ, Pacey KI, Pratchett MS (2023) Increasing densities of Pacific crown-of-thorns starfish (Acanthaster cf. solaris) at Lizard Island, northern Great Barrier Reef, resolved using a novel survey method. Sci Rep 13:19306

Chandler JF, Figueira WF, Burn D, Doll PC, Johandes A, Piccaluga A, Pratchett MS (2024) Predicting 3D and 2D surface area of corals from simple field measurements. Sci Rep 14:20549

Cheney DP (1974) Spawning and aggregation of Acanthaster planci in Micronesia.

Chesher RH (1969a) Destruction of Pacific Corals by the Sea Star Acanthaster planci. 165:

Chesher RH (1969b) Acanthaster planci: Impact on Pacific coral reefs. Final report to US Department of Interior

Claereboudt M (1999) Fertilization success in spatially distributed populations of benthic free-spawners: A simulation model. Ecol Modell 121:

Colgan MW (1987) Coral reef recovery on Guam (Micronesia) after catastrophic predation by Acanthaster planci. Ecology 68:

Collins ARS (1975) Biochemical investigation of two responses involved in the feeding behaviour of Acanthaster planci (L.). III. Food preferences. J Exp Mar Biol Ecol 17:

Conand C (1984) Distribution, reproductive cycle and morphometric relationships of Acanthaster planci (Echinodermata: Asteroidea) in New Caledonia, western tropical Pacific. Echinodermata.

Courchamp F, Berec L, Gascoigne J (2008) Mechanisms for Allee effects. Allee Effects in Ecology and Conservation. Oxford University Press, pp 18–61

Courtney LA, Fisher WS, Raimondo S, Oliver LM, Davis WP (2007) Estimating 3-dimensional colony surface area of field corals. J Exp Mar Biol Ecol 351:234–242

Cowan ZL, Ling SD, Caballes CF, Dworjanyn SA, Pratchett MS (2020) Crown-of-thorns starfish larvae are vulnerable to predation even in the presence of alternative prey. Coral Reefs 39:293–303

Cowan ZL, Pratchett M, Messmer V, Ling S (2017) Known predators of crown-of-thorns starfish (Acanthaster spp.) and their role in mitigating, if not preventing, population outbreaks. Diversity (Basel) 9:

Cresswell AK, Thomson DP, Haywood MDE, Renton M (2020) Frequent hydrodynamic disturbances decrease the morphological diversity and structural complexity of 3D simulated coral communities. Coral Reefs 39:1147–1161

Cruz-Trinidad A, Aliño PM, Geronimo RC, Cabral RB (2014) Linking Food Security with Coral Reefs and Fisheries in the Coral Triangle. Coastal Management 42:160–182

De Cuyper A, Clauss M, Hesta M, Janssens GPJ (2015) Feeding strategies in wild carnivores: Progress report of a model approach.

Dahl AL (1973) Surface Area in Ecological Analysis: Quantification of Benthic Coral-Reef Algae. Mar Biol 23:239–249

Dana TF, Newman WA, Fager EW (1972) Acanthaster aggregations: interpreted as primarily responses to natural phenomena. Pac Sci 26:

Deaker DJ, Agüera A, Lin H-A, Lawson C, Budden C, Dworjanyn SA, Mos B, Byrne M (2020) The hidden army: corallivorous crown-of-thorns seastars can spend years as herbivorous juveniles. Biol Lett 16:20190849

Deaker DJ, Byrne M (2022) Crown of thorns starfish life-history traits contribute to outbreaks, a continuing concern for coral reefs. Emerg Top Life Sci 6:

De'ath G, Moran PJ (1998) Factors affecting the behaviour of crown-of-thorns starfish (Acanthaster planci L.) on the Great Barrier Reef: 1: Patterns of activity. J Exp Mar Biol Ecol 220:83–106

Devlin MJ, Brodie J (2005) Terrestrial discharge into the Great Barrier Reef Lagoon: nutrient behavior in coastal waters. Mar Pollut Bull 51:9–22

Dietzel A, Bode M, Connolly SR, Hughes TP (2020) Long-term shifts in the colony size structure of coral populations along the Great Barrier Reef. Proceedings of the Royal Society B: Biological Sciences 287:20201432

Dight IJ, James MK, Bode L (1990) Modelling the larval dispersal of Acanthaster planci. Coral Reefs 9:

Doll PC, Messmer V, Uthicke S, Doyle JR, Caballes CF, Pratchett MS (2021) DNA-Based Detection and Patterns of Larval Settlement of the Corallivorous Crown-of-Thorns Sea Star (Acanthaster sp.). Biological Bulletin 241:

Doll PC, Uthicke S, Caballes CF, Diaz-Pulido G, Abdul Wahab MA, Lang BJ, Jeong SY, Pratchett MS (2023) Settlement cue selectivity by larvae of the destructive crown-of-thorns starfish. Biol Lett 19:

Doll PC, Tebbett SB, Ling SD, Coenradi SL, Burn D, Hoey AS, Emslie MJ, Pratchett MS (2024) Elevated predation on crown-of-thorns-starfish attributable to a single fisheries species. In review (Current Biology)

Dornelas M, Madin JS, Baird AH, Connolly SR (2017) Allometric growth in reef-building corals. Proceedings of the Royal Society B: Biological Sciences 284:

Doszpot NE, McWilliam MJ, Pratchett MS, Hoey AS, Figueira WF (2019) Plasticity in three-dimensional geometry of branching corals along a cross-shelf gradient. Diversity (Basel) 11:

Doyle J, Uthicke S (2021) Sensitive environmental DNA detection via lateral flow assay (dipstick)—A case study on corallivorous crown-of-thorns sea star (Acanthaster cf. solaris) detection. Environmental DNA 3:

Drap P (2012) Underwater Photogrammetry for Archaeology. Special Applications of Photogrammetry. InTech,

Dulvy NK, Freckleton RP, Polunin NVC (2004) Coral reef cascades and the indirect effects of predator removal by exploitation. Ecol Lett 7:

Dumas P, Peignon C, Dumas M, Bourgeois B, Gossuin H, Fiat S (2022) Destructive outbreaks of the corallivorous starfish Acanthaster cf. solaris spare coral assemblages in the shallowest reef flat areas in New Caledonia. ICES Journal of Marine Science 79:2161–2161

Eddy TD, Lam VWY, Reygondeau G, Cisneros-Montemayor AM, Greer K, Palomares MLD, Bruno JF, Ota Y, Cheung WWL (2021) Global decline in capacity of coral reefs to provide ecosystem services. One Earth 4:1278–1285

Emslie MJ, Bray P, Cheal AJ, Johns KA, Osborne K, Sinclair-Taylor T, Thompson CA (2020) Decades of monitoring have informed the stewardship and ecological understanding of Australia's Great Barrier Reef. Biol Conserv 252:108854

Emslie MJ, Logan M, Bray P, Ceccarelli DM, Cheal AJ, Hughes TP, Johns KA, Jonker MJ, Kennedy E V., Kerry JT, Mellin C, Miller IR, Osborne K, Puotinen M, Sinclair-Taylor T, Sweatman H (2024) Increasing disturbance frequency undermines coral reef recovery. Ecol Monogr 94:

Endean R (1969) Report on investigations made into aspects of the current Acanthaster planci (crown-of-thorns) infestations of certain reefs of the Great Barrier Reef. Queensland.

Endean R (1974) Acanthaster planci on the Great Barrier Reef. 563–576

Endean R (1982) Crown-of-thorns starfish on the great barrier reef. Endeavour 6:10–14

Endean R, Cameron A (1990) Acanthaster planci population outbreaks. Ecosystems of the World 25:419–437

Endean R, Stablum W (1973) A study of some aspects of the crown-of-thorns starfish (Acanthaster planci) infestations of reefs of Australia's Great Barrier Reef. Atoll Res Bull 167:

Engelhardt U (2018) Outbreaks of crown-of-thorns starfish on the Great Barrier Reef. Current Status, Emerging Trends and Developing Issues of Concern.

Engelhardt U, Hartcher M, Cruise J, Engelhardt D, Russell M, Taylor N, Thomas G, Wiseman D (1999) Fine-scale surveys of crown-of-thorns starfish (Acanthaster Planci) in the central Great Barrier Reef region.

Engelhardt U, Hartcher M, Taylor N, Cruise J, Engelhardt D, Russell M, Stevens I, Thomas G, Williamson D, Wiseman D (2001) Crown-of-thorns starfish (Acanthaster planci) in the central Great Barrier Reef region. Results of fine-scale surveys conducted in 1999-2000. Technical Report No.32.

Fabricius KE, De'ath G, Puotinen ML, Done T, Cooper TF, Burgess SC (2008) Disturbance gradients on inshore and offshore coral reefs caused by a severe tropical cyclone. Limnol Oceanogr 53:

Fabricius KE, Okaji K, De'ath G (2010) Three lines of evidence to link outbreaks of the crown-of-thorns seastar Acanthaster planci to the release of larval food limitation. Coral Reefs 29:593–605

Farmanfarmaian A, Giese AC, Boolootian RA, Bennett J (1958) Annual reproductive cycles in four species of West Coast starfishes. Journal of Experimental Zoology 138:355–367

Fernandes L, Marsh H, Moran PJ, Sinclair D (1990) Bias in manta tow surveys of Acanthaster planci. Coral Reefs 9:155–160

Ferrari R, Figueira WF, Pratchett MS, Boube T, Adam A, Kobelkowsky-Vidrio T, Doo SS, Atwood TB, Byrne M (2017) 3D photogrammetry quantifies growth and external erosion of individual coral colonies and skeletons. Sci Rep 7:

Ferrari R, Leon JX, Davies AJ, Burns JHR, Sandin SA, Figueira WF, Gonzalez-Rivero M (2022) Advances in 3D Habitat Mapping of Marine Ecosystem Ecology and Conservation. Front Mar Sci 8:

Figueira W, Ferrari R, Weatherby E, Porter A, Hawes S, Byrne M (2015) Accuracy and precision of habitat structural complexity metrics derived from underwater photogrammetry. Remote Sens (Basel) 7:16883–16900

Fisher WS (2023) Relating fish populations to coral colony size and complexity. Ecol Indic 148:

Fisher WS, Davis WP, Quarles RL, Patrick J, Campbell JG, Harris PS, Hemmer BL, Parsons M (2007) Characterizing coral condition using estimates of three-dimensional colony surface area. Environ Monit Assess 125:347–360

Foo SA, Asner GP (2019) Scaling up coral reef restoration using remote sensing technology. Front Mar Sci 6:

Foo SA, Millican HR, Byrne M (2024) Crown-of-thorns seastar (Acanthaster spp.) feeding ecology across species and regions. Science of The Total Environment 930:172691

George SB (1996) Echinoderm egg and larval quality as a function of adult nutritional state. Oceanologica Acta 19:297–308

Gladstone W (1992) Observations of crown-of-thorns starfish spawning. Mar Freshw Res 43:535

Glynn PW (1974) The Impact of Acanthaster on Corals and Coral Reefs in the Eastern Pacific. Environ Conserv 1:295–304

Glynn PW (1987) Some ecological consequences of coral-crustacean guard mutualisms in the Indian and Pacific Oceans. Symbiosis 301–324

Graham NAJ (2014) Habitat complexity: Coral structural loss leads to fisheries declines. Current Biology 24:

Guerra V, Haynes G, Byrne M, Yasuda N, Adachi S, Nakamura M, Nakachi S, & Hart MW (2020). Nonspecific expression of fertilization genes in the crown-of-thorns *Acanthaster* cf. *solaris*: unexpected evidence of hermaphroditism in a coral reef predator. Molecular Ecology, 29(2), 363–379.Hart MW, Guerra VI, Allen JD, & Byrne M (2021). Cloning and selfing affect population genetic variation in simulations of outcrossing, sexual sea stars. Biological Bulletin, 241(3), 286–302. https://doi.org/10.1086/717293

Hartig F (2018) DHARMa: residual diagnostics for hierarchical (multi-level/mixed) regression models.

Haszprunar G, Vogler C, Wörheide G (2017) Persistent gaps of knowledge for naming and distinguishing multiple species of crown-of-thorns-seastar in the Acanthaster planci species complex. Diversity (Basel) 9:

Haywood MDE, Thomson DP, Babcock RC, Pillans RD, Keesing JK, Miller M, Rochester WA, Donovan A, Evans RD, Shedrawi G, Field SN (2019) Crown-of-thorns starfish impede the recovery potential of coral reefs following bleaching. Mar Biol 166:

Hijmans RJ (2022) Geosphere: Spherical Trigonometry.

Hill J, Wilkinson C (2004) Methods for Ecological Monitoring of Coral Reefs.

Hock K, Wolff NH, Condie SA, Anthony KRN, Mumby PJ (2014) Connectivity networks reveal the risks of crown-of-thorns starfish outbreaks on the Great Barrier Reef. Journal of Applied Ecology 51:1188–1196

Hoegh-Guldberg O (1988) A method for determining the surface area of corals. Coral Reefs 7:113–116

Hoegh-Guldberg O (1999) Climate change, coral bleaching and the future of the world's coral reefs. Mar Freshw Res

Hoey J, Campbell ML, Hewitt CL, Gould B, Bird R (2016) Acanthaster planci invasions: Applying biosecurity practices to manage a native boom and bust coral pest in Australia. Management of Biological Invasions 7:213–220

Holmes G (2008) Estimating three-dimensional surface areas on coral reefs. J Exp Mar Biol Ecol 365:67–73

Holmes G, Ortiz J, Kaniewska P, Johnstone R (2008) Using three-dimensional surface area to compare the growth of two Pocilloporid coral species. Mar Biol 155:421–427

Hoogenboom MO, Connolly SR, Anthony KRN (2008) Interactions between morphological and physiological plasticity optimize energy acquisition in corals. Ecology 89:1144–1154

Houk P, Bograd S, Woesik R Van (2007) The Transition Zone Chlorophyll Front can Trigger Acanthaster planci Outbreaks in the Pacific Ocean: Historical Confirmation. J Oceanogr 63:

House JE, Brambilla V, Bidaut LM, Christie AP, Pizarro O, Madin JS, Dornelas M (2018) Moving to 3D: Relationships between coral planar area, surface area and volume. PeerJ 6:

Hughes RN (1980) Optimal foraging theory in the marine context. Annual Review of Marine Biology and Oceanography 18:

Hughes TP, Kerry JT, Álvarez-Noriega M, Álvarez-Romero JG, Anderson KD, Baird AH, Babcock RC, Beger M, Bellwood DR, Berkelmans R, Bridge TC, Butler IR, Byrne M, Cantin NE, Comeau S, Connolly SR, Cumming GS, Dalton SJ, Diaz-Pulido G, Eakin CM, Figueira WF, Gilmour JP, Harrison HB, Heron SF, Hoey AS, Hobbs JPA, Hoogenboom MO, Kennedy E V., Kuo CY, Lough JM, Lowe RJ, Liu G, McCulloch MT, Malcolm HA, McWilliam MJ, Pandolfi JM, Pears RJ, Pratchett MS, Schoepf V, Simpson T, Skirving WJ, Sommer B, Torda G, Wachenfeld DR, Willis BL, Wilson SK (2017) Global warming and recurrent mass bleaching of corals. Nature 543:373–377

Husband E, Perry CT, Lange ID (2022) Estimating rates of coral carbonate production from aerial and archive imagery by applying colony scale conversion metrics. Coral Reefs 41:1199–1209

Jangoux M, van Impe E (1977) The annual pyloric cycle of Asterias rubens L. (echinodermata: Asteroidea). J Exp Mar Biol Ecol 30:165–184

Jangoux M, Lawrence JM (1982) Echinoderm nutrition. Echinoderm nutrition

Johansson CL, Francis DS, Uthicke S (2016) Food preferences of juvenile corallivorous crown-of-thorns (Acanthaster planci) sea stars. Mar Biol 163:1–7

Joly-Turquin G, Dubois P, Leyzour S, Pernet P, De Ridder F, Pintelon R, Guillou M (2013) Contrasting relationships between pyloric caecum and gonad growth in the starfish *Asterias rubens:* combined field and experimental approaches. Journal of the Marine Biological Association of the United Kingdom 93:1073–1086

Jones N, Pratchett M, Milligan R, Gilliam D (2023) High incidence of partial colony mortality constrains realized growth for three coral species in southeast Florida. Mar Ecol Prog Ser 721:59–70

Kayal M, Vercelloni J, Lison de Loma T, Bosserelle P, Chancerelle Y, Geoffroy S, Stievenart C, Michonneau F, Penin L, Planes S, Adjeroud M (2012) Predator crown-of-thorns starfish (Acanthaster planci) outbreak, mass mortality of corals, and cascading effects on reef fish and benthic communities. PLoS One 7:

Keesing JK (1990) Feeding biology of the crown-of-thorns starfish, Acanthaster planci (Linnaeus).

Keesing JK (2021) Optimal Foraging Theory Explains Feeding Preferences in the Western Pacific Crown-of-Thorns Sea Star Acanthaster sp. Biological Bulletin 241:303–329

Keesing JK, Halford AR, Hall KC (2018) Mortality rates of small juvenile crown-of-thorns starfish Acanthaster planci on the Great Barrier Reef: Implications for population size and larval settlement thresholds for outbreaks. Mar Ecol Prog Ser 597:

Keesing JK, Lucas JS (1992) Field measurement of feeding and movement rates of the crown-of-thorns starfish Acanthaster planci (L.). Mar Biol EcoL 156:89–104

Keesing JK, Thomson DP, Haywood MDE, Babcock RC (2019) Two time losers: selective feeding by crown-of-thorns starfish on corals most affected by successive coral-bleaching episodes on western Australian coral reefs. Mar Biol 166:

Kenchington RA (1977) Growth and recruitment of Acanthaster planci (L.) on the Great Barrier Reef. Biol Conserv 11:

Kenchington RA, Morton B (1976) Two surveys of the crown of thorns starfish over a section of the Great Barrier Reef (Australia). Report of the Steering Committee for the crown of thorns survey.

Kenyon JC, Aeby GS (2009) Localized outbreak and feeding preferences of the crown-of-thorns seastar Acanthaster Planci (echinodermata, asteroidea) on reefs off oahu, HAWAII.

Kettle BT (1990) Variations in biometric and physiological parameters of Acanthaster planci (L.) (Echinodermata; Asteroidea) during the course of a high density outbreak.

Kettle BT, Lucas JS (1987) Biometric relationship between organ indices, fecundity, oxygen consumption and body size in *Acanthaster planci* (L.) (Echinodermata; Asteroidea). Bull Mar Sci 41:

Komyakova V, Munday PL, Jones GP (2013) Relative importance of coral cover, habitat complexity and diversity in determining the structure of reef fish communities. PLoS One 8:

Kroon FJ, Barneche DR, Emslie MJ (2021) Fish predators control outbreaks of Crown-of-Thorns Starfish. Nat Commun 12:

Kubicek A, Breckling B, Hoegh-Guldberg O, Reuter H (2019) Climate change drives trait-shifts in coral reef communities. Sci Rep 9:3721

Kwong SLT, Villacorta-Rath C, Doyle J, Uthicke S (2021) Quantifying shedding and degradation rates of environmental DNA (eDNA) from Pacific crown-of-thorns seastar (Acanthaster cf. solaris). Mar Biol 168:

Laforsch C, Christoph E, Glaser C, Naumann M, Wild C, Niggl W (2008) A precise and non-destructive method to calculate the surface area in living scleractinian corals using X-ray computed tomography and 3D modeling. Coral Reefs 27:811–820

Lane DJW (2012) Acanthaster planci impact on coral communities at permanent transect sites on Bruneian reefs, with a regional overview and a critique on outbreak causes. Journal of the Marine Biological Association of the United Kingdom 92:803–809

Lang BJ, Donelson JM, Caballes CF, Doll PC, Pratchett MS (2021) Metabolic Responses of Pacific Crown-of-Thorns Sea Stars (Acanthaster sp.) to Acute Warming. Biol Bull 241:347–358

Lange ID, Molina-Hernández A, Medellín-Maldonado F, Perry CT, Álvarez-Filip L (2022) Structure-from-motion photogrammetry demonstrates variability in coral growth within colonies and across habitats. PLoS One 17:

Lange ID, Perry CT, Alvarez-Filip L (2020) Carbonate budgets as indicators of functional reef “health”: A critical review of data underpinning census-based methods and current knowledge gaps. Ecol Indic 110:

Larkum AWD (1988) High rates of nitrogen fixation on coral skeletons after predation by the crown of thorns starfish Acanthaster planci. Mar Biol 97:503–506

Lawrence JM, Lane JM (1982) The utilization of nutrients by post-metamorphic echinoderms. Echinoderm Nutrition. pp 331–371

Laxton JH (1974) Aspects of the ecology of the coral-eating starfish Acanthaster planci. Biological Journal of the Linnean Society 6:

Lechene MAA, Figueira WF, Murray NJ, Aston EA, Gordon SE, Ferrari R (2024) Evaluating error sources to improve precision in the co-registration of underwater 3D models. Ecol Inform 81:

Lenth R, Singmann H, Buerkner P, Herve M (2018) emmeans: Estimated marginal means, aka least-squares means.

Leujak W, Ormond RFG (2007) Comparative accuracy and efficiency of six coral community survey methods. J Exp Mar Biol Ecol 351:168–187

Levitan D, Sewell M (1998) Fertiization sucess in free-spawning marine invertebrates: review of the evidence and fisheries implications.

Levitan DR, Young CM (1995) Reproductive success in large populations: empirical measures and theoretical predictions of fertilization in the sea biscuit Clypeaster rosaceus. J Exp Mar Biol Ecol 190:

Li Y, Huang X, Yu K, Chen X, Wei F, Chen B, Yao Q, Liao Z, Wang L (2023) Impacts of selective feeding of crown-of-thorns starfish on the coral community in the South China Sea. Mar Freshw Res 74:982–993

Ling SD, Cowan ZL, Boada J, Flukes EB, Pratchett MS (2020) Homing behaviour by destructive crown-of-thorns starfish is triggered by local availability of coral prey. Proceedings of the Royal Society B: Biological Sciences 287:

Lowry OH, Rosebrough NJ, Farr AL, Randall RJ (1951) Protein measurement with the Folin phenol reagent. J Biol Chem 193:

Loya Y, Sakai K, Yamazato K, Nakano Y, Sambali H, van Woesik R (2001) Coral bleaching: the winners and the losers. Ecol Lett 4:122–131

Lucas JS (1973) Reproductive and larval biology of Acanthaster planci (L.) in Great Barrier Reef Waters. Micronesica 9:

Lucas JS (1982) Quantitative studies of feeding and nutrition during larval development of the coral reef asteroid Acanthaster planci (L.). J Exp Mar Biol Ecol 65:

Lucas JS (1984) Growth, maturation and effects of diet in Acanthaster planci (L.) (Asteroidea) and hybrids reared in the laboratory. J Exp Mar Biol Ecol 79:

Luckhurst BE, Luckhurst K (1978) Analysis of the Influence of Substrate Variables on Coral Reef Fish Communities. Mar Biol 49:317–323

Lundquist CJ, Botsford LW (2004) Model projections of the fishery implications of the Allee effect in broadcast spawners. Ecological Applications 14:

MacArthur RH, Pianka ER (1966) On Optimal Use of a Patchy Environment. Am Nat 100:

MacNeil M, Chong-Seng K, Pratchett D, Thompson C, Messmer V, Pratchett M (2017) Age and growth of an outbreaking Acanthaster cf. solaris population within the Great Barrier Reef. Diversity (Basel) 9:18

MacNeil MA, Mellin C, Pratchett MS, Hoey J, Anthony KRN, Cheal AJ, Miller I, Sweatman H, Cowan ZL, Taylor S, Moon S, Fonnesbeck CJ (2016) Joint estimation of crown of thorns (Acanthaster planci) densities on the Great Barrier Reef. PeerJ 4:

Madin JS, Connolly SR (2006) Ecological consequences of major hydrodynamic disturbances on coral reefs. Nature 444:477–480

Marsh JA (1970) Primary Productivity of Reef-Building Calcareous Red Algae. Source: Ecology 51:

Matthews SA, Shoemaker K, Pratchett MS, Mellin C (2020) COTSMod: A spatially explicit metacommunity model of outbreaks of crown-of-thorns starfish and coral recovery. pp 259–290

Matthews SA, Williamson DH, Beeden R, Emslie MJ, Abom RTM, Beard D, Bonin M, Bray P, Campili AR, Ceccarelli DM, Fernandes L, Fletcher CS, Godoy D, Hemingson CR, Jonker MJ, Lang BJ, Morris S, Mosquera E, Phillips GL, Sinclair-Taylor TH, Taylor S, Tracey D, Wilmes JC, Quincey R (2024) Protecting Great Barrier Reef resilience through effective management of crown-of-thorns starfish outbreaks. PLoS One 19:e0298073

Maya PHM, Smit KP, Burt AJ, Frias-Torres S (2016) Large-scale coral reef restoration could assist natural recovery in Seychelles, Indian Ocean. Nat Conserv 16:1–17

McWilliam M, Pratchett MS, Hoogenboom MO, Hughes TP (2020) Deficits in functional trait diversity following recovery on coral reefs. Proceedings of the Royal Society B: Biological Sciences 287:

Meiling S, Muller EM, Smith TB, Brandt ME (2020) 3D Photogrammetry Reveals Dynamics of Stony Coral Tissue Loss Disease (SCTLD) Lesion Progression Across a Thermal Stress Event. Front Mar Sci 7:

Mellin C, Thompson A, Jonker MJ, Emslie MJ (2019) Cross-shelf variation in coral community response to disturbance on the Great Barrier Reef. Diversity (Basel) 11:

Mendonca V, Al Jabri M, Al Ajmi I, Al Muharrami M, Al Areimi M, Al Aghbari H (2010) Persistent and expanding population outbreaks of the corallivorous starfish Acanthaster planci in the northwestern Indian Ocean: Are they really a consequence of unsustainable starfish predator removal through overfishing in coral reefs, or a response to a changing environment? Zool Stud 49:108–123

Mercier A, Hamel JF (2009) Endogenous and exogenous control of gametogenesis and spawning in echinoderms. Adv Mar Biol 55:

Meyer JL, Schultz ET (1985) Tissue condition and growth rate of corals associated with schooling fish. Limnol Oceanogr 30:157–166

Miller I (2000) Historical patterns and current trends in the broadscale distribution of crown-of-thorns starfish in the northern and central sections of the Great Barrier Reef. 2:

Miller I, Jonker M, Coleman G (2009) Crown-of-thorns starfish and coral surveys using the manta tow and SCUBA search techniques.

Miller I, Sweatman H, Cheal A, Emslie M, Johns K, Jonker M, Osborne K (2015) Origins and implications of a primary crown-of-thorns starfish outbreak in the southern great barrier reef. J Mar Biol 2015:

Millican HR, Byrne M, Keesing J, Foo SA (2024) Feeding biology of crown-of-thorns seastars across sites differing in Acropora availability. Mar Environ Res 200:106655

Million WC, Ruggeri M, O'Donnell S, Bartels E, Conn T, Krediet CJ, Kenkel CD (2022) Evidence for adaptive morphological plasticity in the Caribbean coral, Acropora cervicornis. Proc Natl Acad Sci U S A 119:

Mills SC (2012) Density-dependent prophylaxis in the coral-eating crown-of-thorns sea star, Acanthaster planci. Coral Reefs 31:

Moberg F, Folke C (1999) Ecological goods and services of coral reef ecosystems. Ecological Economics 29:

Moore RJ (1990) Persistent and Transient Populations of the Crown-of-Thorns Starfish, Acanthaster Planci.

Moran PJ (1986) The Acanthaster phenomenon. Oceanography and Marine Biology 24:379–480

Moran PJ, De'ath G (1992a) Estimates of the abundance of the crown-of-thorns starfish Acanthaster planci in outbreaking and non-outbreaking populations on reefs within the Great Barrier Reef. Mar Biol 113:

Moran PJ, De'ath G (1992b) Estimates of the abundance of the crown-of-thorns starfish Acanthaster planci in outbreaking and non-outbreaking populations on reefs within the Great Barrier Reef. Mar Biol 113:

Moran PJ, Death G, Baker VJ, Bass DK, Christie CA, Miller IR, Miller-Smith BA, Thompson AA (1992) Pattern of outbreaks of crown-of-thorns starfish (Acanthaster planci l.) along the great barrier reef since 1966. Mar Freshw Res 43:

Mudge L, Bruno JF (2023) Disturbance intensification is altering the trait composition of Caribbean reefs, locking them into a low functioning state. Sci Rep 13:

Nakamura M, Okaji K, Higa Y, Yamakawa E, Mitarai S (2014) Spatial and temporal population dynamics of the crown-of-thorns starfish, Acanthaster planci, over a 24-year period along the central west coast of Okinawa Island, Japan. Mar Biol 161:2521–2530

Naumann MS, Niggl W, Laforsch C, Glaser C, Wild C (2009) Coral surface area quantification-evaluation of established techniques by comparison with computer tomography. Coral Reefs 28:109–117

Newman SP, Meesters EH, Dryden CS, Williams SM, Sanchez C, Mumby PJ, Polunin NVC (2015) Reef flattening effects on total richness and species responses in the Caribbean. Journal of Animal Ecology 84:1678–1689

Nishihira M, Yamazato K (1974) Human interference with the coral ref community an Acanthaster infestation at Okinawa. 577–590

Odum HT, Odum EP (1955) Trophic Structure and Productivity of a Windward Coral Reef Community on Eniwetok Atoll. 25:

Olson RR (1987) In situ culturing as a test of the larval starvation hypothesis for the crown-of-thoms starfish, Acanthaster planci. Limnol Oceanogr 32:

Ormond R, Bradbury R, Bainbridge S, Fabricius K, Keesing J, Devantier L, Medlay P, Steven A (1990) Test of a model of regulation of crown-of-thorn starfish by fish predators.

Ormond RFG, Campbell AC, Head SH, Moore RJ, Rainbow PR, Saunders AP (1973) Formation and breakdown of aggregations of the Crown-of-Thorns Starfish, Acanthaster planci (L.). Nature 246:

Ormond RFG, Hanscomb NJ, Beach DH (1976) Food selection and learning in the crown-of-thorns starfish, Acanthaster planci (L) . Mar Behav Physiol 4:

Osborne K, Dolman AM, Burgess SC, Johns KA (2011a) Disturbance and the dynamics of coral cover on the Great Barrier Reef (1995-2009). PLoS One 6:

Osborne K, Dolman AM, Burgess SC, Johns KA (2011b) Disturbance and the Dynamics of Coral Cover on the Great Barrier Reef (1995–2009). PLoS One 6:e17516

Oudejans RCHM, van der Sluis I, van der Plas AJ (1979) Changes in the biochemical composition of the pyloric caeca of female seastars,Asterias rubens, during their annual reproductive cycle. Mar Biol 53:231–238

Parker GA, Ramm SA, Lehtonen J, Henshaw JM (2018) The evolution of gonad expenditure and gonadosomatic index (GSI) in male and female broadcast-spawning invertebrates. Biological Reviews 93:693–753

Pastor-de-Ward CT, Rubilar T, Díaz-de-Vivar ME, Gonzalez-Pisani X, Zarate E, Kroeck M, Morsan E (2007) Reproductive biology of Cosmasterias lurida (Echinodermata: Asteroidea) an anthropogenically influenced substratum from Golfo Nuevo, Northern Patagonia (Argentina). Mar Biol 151:205–217

Pearson RG, Endean RG (1969) A preliminary study of the coral predator Acanthaster planci (L.) (Asteroidea) on the Great Barrier Reef. Fisheries Notes, Queensland Department of Harbours and Marine 3:

Perry CT, Alvarez-Filip L (2019) Changing geo-ecological functions of coral reefs in the Anthropocene. Funct Ecol 33:976–988

Perry CT, Edinger EN, Kench PS, Murphy GN, Smithers SG, Steneck RS, Mumby PJ (2012) Estimating rates of biologically driven coral reef framework production and erosion: A new census-based carbonate budget methodology and applications to the reefs of Bonaire. Coral Reefs 31:853–868

Peter Doll (2024) Predation rates on Crown-of-Thorns Starfish relative to fisheries management zones.

Plagányi É, Ellis N, Blamey L, Morello E, Norman-Lopez A, Robinson W, Sporcic M, Sweatman H (2014) Ecosystem modelling provides clues to understanding ecological tipping points. Mar Ecol Prog Ser 512:99–113

Plagányi ÉE, Babcock RC, Rogers J, Bonin M, Morello EB (2020) Ecological analyses to inform management targets for the culling of crown-of-thorns starfish to prevent coral decline. Coral Reefs 39:1483–1499

van der Plas AJ, Voogt PA (1982) The biochemical composition of the pyloric caeca and its relation to DNA levels in the female starfishAsterias rubens during the reproductive cycle. J Comp Physiol 148:49–55

Porter JW (1972) Predation by Acanthaster and Its Effect on Coral Species Diversity. Am Nat 106:

Potts DC (1981) Crown of thorns starfish - man-induced pest or natural phenomenon? Ecology of Pests

Pratchett Morgan, Uthicke Sven, Open Access Publishing in European Networks. (2017a) Biology, Ecology and Management of Crown-of-Thorns Starfish. MDPI AG - Multidisciplinary Digital Publishing Institute,

Pratchett MS (2001) Influence of coral symbionts on feeding preferences of crown-of-thorns starfish Acanthaster planci in the western pacific. Mar Ecol Prog Ser 214:

Pratchett MS (2005) Dynamics of an outbreak population of Acanthaster planci at Lizard Island, northern Great Barrier Reef (1995-1999). Coral Reefs 24:453–462

Pratchett MS (2007) Feeding Preferences of Acanthaster planci (Echinodermata: Asteroidea) under Controlled Conditions of Food Availability 1.

Pratchett MS (2010) Changes in coral assemblages during an outbreak of Acanthaster planci at Lizard Island, northern Great Barrier Reef (1995-1999). Coral Reefs 29:717–725

Pratchett MS, Caballes CF, Cvitanovic C, Raymundo ML, Babcock RC, Bonin MC, Bozec YM, Burn D, Byrne M, Castro-Sanguino C, Chen CCM, Condie SA, Cowan ZL, Deaker DJ, Desbiens A, Devantier LM, Doherty PJ, Doll PC, Doyle JR, Dworjanyn SA, Fabricius KE, Haywood MDE, Hock K, Hoggett AK, Høj L, Keesing JK, Kenchington RA, Lang BJ, Ling SD, Matthews SA, McCallum HI, Mellin C, Mos B, Motti CA, Mumby PJ, Stump RJW, Uthicke S, Vail L, Wolfe K, Wilson SK (2021a) Knowledge gaps in the biology, ecology, and management of the Pacific crown-of-thorns sea star Acanthaster sp. on Australia's Great Barrier Reef. Biological Bulletin 241:

Pratchett MS, Caballes CF, Messmer V, Fletcher CS, Westcott DA (2020) Movement patterns of Pacific crown-of-thorns starfish (Acanthaster cf. solaris) linked to habitat structure and prey availability. Report to the National Environmental Science Program.

Pratchett MS, Caballes CF, Rivera-Posada JA, Sweatman HPA (2014) Limits to understanding and managing outbreaks of crown- of- thorns starfish (Acanthaster spp.). Oceanography and Marine Biology. CRC Press, pp 133–200

Pratchett MS, Caballes CF, Wilmes JC, Matthews S, Mellin C, Sweatman HPA, Nadler LE, Brodie J, Thompson CA, Hoey J, Bos AR, Byrne M, Messmer V, Fortunato SAV, Chen CCM, Buck ACE, Babcock RC, Uthicke S (2017b) Thirty years of research on crown-of-thorns starfish (1986-2016): Scientific advances and emerging opportunities. Diversity (Basel) 9:

Pratchett MS, Caballes CF, Wilmes JC, Matthews S, Mellin C, Sweatman HPA, Nadler LE, Brodie J, Thompson CA, Hoey J, Bos AR, Byrne M, Messmer V, Fortunato SAV, Chen CCM, Buck ACE, Babcock RC, Uthicke S (2017c) Thirty years of research on crown-of-thorns starfish (1986-2016): Scientific advances and emerging opportunities. Diversity (Basel) 9:

Pratchett MS, Cumming GS (2019) Managing cross-scale dynamics in marine conservation: Pest irruptions and lessons from culling of crown-of-thorns starfish (Acanthaster spp.). Biol Conserv 238:

Pratchett MS, Heron SF, Mellin C, Cumming GS (2021b) Recurrent Mass-Bleaching and the Potential for Ecosystem Collapse on Australia's Great Barrier Reef. In: Canadell J.G., Jackson R.B. (eds) Ecosystem Collapse and Climate Change. Springer, pp 265–289

Pratchett MS, McCowan D, Maynard JA, Heron SF (2013) Changes in Bleaching Susceptibility among Corals Subject to Ocean Warming and Recurrent Bleaching in Moorea, French Polynesia. PLoS One 8:

Pratchett MS, Nadler LE, Burn D, Lang BJ, Messmer V, Caballes CF (2021c) Reproductive investment and fecundity of Pacific crown-of-thorns starfish (Acanthaster cf. solaris) on the Great Barrier Reef. Mar Biol 168:

Pratchett MS, Schenk TJ, Baine M, Syms C, Baird AH (2009) Selective coral mortality associated with outbreaks of Acanthaster planci L. in Bootless Bay, Papua New Guinea. Mar Environ Res 67:230–236

R Core Team (2021) R: A Language and Environment for Statistical Computing. R Foundation for Statistical Computing

Raymond J, Himmelman J, Guderley H (2004) Sex differences in biochemical composition, energy content and allocation to reproductive effort in the brooding sea star Leptasterias polaris. Mar Ecol Prog Ser 283:179–190

Reguero BG, Storlazzi CD, Gibbs AE, Shope JB, Cole AD, Cumming KA, Beck MW (2021) The value of US coral reefs for flood risk reduction. Nat Sustain 4:688–698

Reichelt RE, Bradbury RH, Moran PJ (1990a) Distribution of Acanthaster planci outbreaks on the Great Barrier Reef between 1966 and 1989. Coral Reefs 9:97–103

Reichelt RE, Bradbury RH, Moran PJ (1990b) The crown-of-thorns starfish, Acanthaster planci, on the Great Barrier Reef. 13:

Remmers T, Grech A, Roelfsema C, Gordon S, Lechene M, Ferrari R (2024) Close-range underwater photogrammetry for coral reef ecology: a systematic literature review. Coral Reefs 43:35–52

Roche RC, Pratchett MS, Carr P, Turner JR, Wagner D, Head C, Sheppard CRC (2015) Localized outbreaks of Acanthaster planci at an isolated and unpopulated reef atoll in the Chagos Archipelago. Mar Biol 162:1695–1704

Rogers JGD, Pláganyi ÉE, Babcock RC (2017) Aggregation, Allee effects and critical thresholds for the management of the crown-of-Thorns starfish Acanthaster planci. Mar Ecol Prog Ser 578:99–114

Rossi P, Castagnetti C, Capra A, Brooks AJ, Mancini F (2020) Detecting change in coral reef 3D structure using underwater photogrammetry: critical issues and performance metrics. Applied Geomatics 12:3–17

Saponari L, Montano S, Seveso D, Galli P (2015) The occurrence of an Acanthaster planci outbreak in Ari Atoll, Maldives. Marine Biodiversity 45:599–600

Scandol JP, James MK (1992) Hydrodynamics and Larval dispersal: a Population Model of Acanthaster planci on the Great Barrier Reef. Aust J Mar Freshwater Res 43:583–96

Scheibling RE (1981) The Annual Reproductive Cycle of Oreaster reticulatus (L.) (Echinodermata:Asteroidea) and Interpopulation Differences in Reproductive Capacity. mar Biol Ecol 54:

Seveso D, Stahl JH, Landes A (2024) An outbreak of Acanthaster spp. in the Gulf of Oman (United Arab Emirates). Marine Biodiversity 54:62

Souter DW (2007) The ecology of individual specimens Acanthaster planci in low density populations.

Stimson J, Kinzie RA (1991) The temporal pattern and rate of release of zooxanthellae from the reef coral Pocillopora damicornis (Linnaeus) under nitrogen-enrichment and control conditions. Mar Biol, Ecol 153:63

Stump Richard (1996) An investigation to describe the population dynamics of Acanthaster planci (L.) around Lizard Island, Cairns Section, Great Barrier Reef Marine Park. CRC Reef Research Centre,

Stump RJ (1994) Age determination and life-history characteristics of Acanthaster planci(L.)(Echinodermata:Asteroida). James Cook University

Sully S, Burkepile DE, Donovan MK, Hodgson G, van Woesik R (2019) A global analysis of coral bleaching over the past two decades. Nat Commun 10:1264

Sweatman H (2008) No-take reserves protect coral reefs from predatory starfish. Current Biology 18:598–599

Sweatman H, Cappo M (2018) Do no-take zones reduce the likelihood of outbreaks of the Crown-of-thorns starfish?

Sweatman HP (1996) Commercial fishes as predators of adult Acanthaster planci.

Sweatman HPA, Bass DK, Cheal AJ, Coleman G, Miller ER, Ninio R, Osborne K, Oxley WG, Ryan DAJ, Thompson AA, Tomkins P (1998) Long-term monitoring of the Great Barrier Reef. Status Report Number 3.

Tkachenko KS, Hoang DT (2022) Concurrent effect of crown-of-thorns starfish outbreak and thermal anomaly of 2020 on coral reef communities of the Spratly Islands (South China Sea). Marine Ecology 43:

Tokeshi M, Daud JRP (2011) Assessing feeding electivity in Acanthaster planci: A null model analysis. Coral Reefs 30:227–235

Torres-Pulliza D, Dornelas MA, Pizarro O, Bewley M, Blowes SA, Boutros N, Brambilla V, Chase TJ, Frank G, Friedman A, Hoogenboom MO, Williams S, Zawada KJA, Madin JS (2020) A geometric basis for surface habitat complexity and biodiversity. Nat Ecol Evol 4:1495–1501

Trapon ML, Pratchett MS, Penin L (2011) Comparative effects of different disturbances in coral reef habitats in Moorea, French Polynesia. J Mar Biol 2011:1–11

Urbina-Barreto I, Chiroleu F, Pinel R, Fréchon L, Mahamadaly V, Elise S, Kulbicki M, Quod JP, Dutrieux E, Garnier R, Henrich Bruggemann J, Penin L, Adjeroud M (2021a) Quantifying the shelter capacity of coral reefs using photogrammetric 3D modeling: From colonies to reefscapes. Ecol Indic 121:

Urbina-Barreto I, Garnier R, Elise S, Pinel R, Dumas P, Mahamadaly V, Facon M, Bureau S, Peignon C, Quod JP, Dutrieux E, Penin L, Adjeroud M (2021b) Which Method for Which Purpose? A

Comparison of Line Intercept Transect and Underwater Photogrammetry Methods for Coral Reef Surveys. Front Mar Sci 8:

Uthicke S, Doyle JR, Gomez Cabrera M, Patel F, McLatchie MJ, Doll PC, Chandler JF, Pratchett MS (2024a) eDNA monitoring detects new outbreak wave of corallivorous seastar (Acanthaster cf. solaris) at Lizard Island, Great Barrier Reef. Coral Reefs 43:857–866

Uthicke S, Fisher EE, Patel F, Diaz-Guijarro B, Doyle JR, Messmer V, Pratchett MS (2019) Spawning time of Acanthaster cf. solaris on the Great Barrier Reef inferred using qPCR quantification of embryos and larvae: do they know it's Christmas? Mar Biol 166:133

Uthicke S, Lamare M, Doyle JR (2018) eDNA detection of corallivorous seastar (Acanthaster cf. solaris) outbreaks on the Great Barrier Reef using digital droplet PCR. Coral Reefs 37:

Uthicke S, Pratchett MS, Bronstein O, Alvarado JJ, Wörheide G (2024b) The crown-of-thorns seastar species complex: knowledge on the biology and ecology of five corallivorous Acanthaster species. Mar Biol 171:32

Uthicke S, Schaffelke B, Byrne M (2009) A boom-bust phylum? Ecological and evolutionary consequences of density variations in echinoderms. Ecol Monogr 79:3–24

Vanhatalo J, Hosack GR, Sweatman H (2017) Spatiotemporal modelling of crown-of-thorns starfish outbreaks on the Great Barrier Reef to inform control strategies. Journal of Applied Ecology 54:188–197

Veal CJ, Holmes G, Nunez M, Hoegh-Guldberg O, Osborn J (2010) A comparative study of methods for surface area and three dimensional shape measurement of coral skeletons. Limnol Oceanogr Methods 8:241–253

Vine PJ (1973) Crown of thorns (Acanthaster planci) plagues: The Natural Causes Theory. Atoll Res Bull 166:

Virgen-Urcelay A, Donner SD (2023) Increase in the extent of mass coral bleaching over the past half-century, based on an updated global database. PLoS One 18:

Wallner WE (1987) Factors affecting insect population dynamics: differences between outbreak and non-outbreak species. Annual review of entomology Vol 32

Weber JN, Woodhead PMJ (1970) Ecological studies of the coral predator Acanthaster planci in the south pacific. Mar Biol 6:

Westcott DA, Fletcher CS, Gladish DW, Macdonald S, Condie S (2021) Integrated Pest Management Crown-of-Thorns Starfish Control Program on the Great Barrier Reef: Current Performance and Future Potential Technical Report.

Westcott DA, Fletcher CS, Kroon FJ, Babcock RC, Plagányi EE, Pratchett MS, Bonin MC (2020) Relative efficacy of three approaches to mitigate Crown-of-Thorns Starfish outbreaks on Australia's Great Barrier Reef. Sci Rep 10:

Wickham H (2016) ggplot2: Elegant Graphics for Data Analysis. Springer-Verlag , New York

Williams GJ, Graham NAJ, Jouffray J, Norström A V., Nyström M, Gove JM, Heenan A, Wedding LM (2019) Coral reef ecology in the Anthropocene. Funct Ecol 33:1014–1022

Wilmes JC, Caballes CF, Cowan ZL, Hoey AS, Lang BJ, Messmer V, Pratchett MS (2018) Contributions of pre- versus post-settlement processes to fluctuating abundance of crown-of-thorns starfishes (Acanthaster spp.). Mar Pollut Bull 135:332–345

Wilmes JC, Hoey AS, Pratchett MS (2020) Contrasting size and fate of juvenile crown-of-thorns starfish linked to ontogenetic diet shifts. Proceedings of the Royal Society B: Biological Sciences 287:

Wilson BR (1972) Western Australian coral reefs, with preliminary notes on a study at Kendrew Island, Dampier Archipelago. 47–58

Wolfe K, Graba-Landry A, Dworjanyn SA, Byrne M (2017) Superstars: Assessing nutrient thresholds for enhanced larval success of Acanthaster planci, a review of the evidence. Mar Pollut Bull 116:

Wooldridge SA (2009) Water quality and coral bleaching thresholds: Formalising the linkage for the inshore reefs of the Great Barrier Reef, Australia. Mar Pollut Bull 58:

Wooldridge SA, Brodie JE (2015) Environmental triggers for primary outbreaks of crown-of-thorns starfish on the Great Barrier Reef, Australia. Mar Pollut Bull 101:805–815

Wright JT, Dworjanyn SA, Rogers CN, Steinberg PD, Williamson JE, Poore AGB (2005) Density-dependent sea urchin grazing: differential removal of species, changes in community composition and alternative community states. Mar Ecol Prog Ser 298:

Yamaguchi M (1973) Early life histories of coral reef asteroids, with special reference to Acanthaster planci (L.). Biology and Geology of Coral Reefs.

Yamaguchi M (1974) Growth of Juvenile Acanthaster planci (L.) in the Laboratory. Pac Sci 28:

Yasuda N, Ogasawara K, Kajiwara K, Ueno M, Oki K, Taniguchi H, Kakuma S, Okaji K, Nadaoka K (2010) Latitudinal differentiation in the reproduction patterns of the crown-of-thorns starfish Acanthaster planci through the Ryukyu Island Archipelago. Plankton Benthos Res 5:

Zann L, Brodie J, Berryman C, Naqasima M (1987) Recruitment, ecology, growth and behavior of juvenile Acanthaster planci (L.) (Echinodermata: Asteroidea). Bull Mar Sci 41:

Zann L, Brodie J, Vuki V (1990) Coral Reels History and dynamics of the crown-of-thorns starfish Acanthaster planci (L.) in the Suva area, Fiji. Coral Reefs 9:

Zawada KJA, Madin JS, Baird AH, Bridge TCL, Dornelas M (2019) Morphological traits can track coral reef responses to the Anthropocene. Funct Ecol 33:962–975

Appendix 1 - Supplementary information for Chapter 1

Table S1: *Demographic, biological and behavioural traits of crown of thorns starfish (Acanthaster cf. solaris), during different key phases of an outbreak cycle*

	Non-outbreaking population *(pre-outbreak, high food availability)*	**Outbreaking population** *(peak densities, assumed to be food-limited)*	**Post-outbreaking population** *(aftermath, low food availability)*
Densities	• Adult densities vary between <1/ha (Nakamura et al., 2014; Chesher 1969) to <100/ha (Pearson & Endean, 1969) • Juvenile densities – 0 – 0.16/m^{-2} (Zann et al., 1990) or <1.25/250m^{-2} (Engelhardt et al., 2000) • Limited data on larval densities	• Adult densities vary between 15 CoTS/ha - 7,000 /ha) (Moran and De'ath, 1992; Dumas et al, 2020) • Juvenile densities - 0.6 – 20.6/ m^{-2} (Zann et al., 1990) or 1.25- 3.3/250m^{-2} (Engelhardt et al., 2000) • Limited data on larval densities	• Adult densities recorded 0 - 0.15 CoTS/250m^2 (Engelhardt et al., 2000) • Juvenile densities – 0.3 - 1.9/250m^{-2} (Engelhardt et al., 2000) • Limited data on larval densities
Body size	• Maximum body sizes recorded up to 75cm (Stump, 1996). Mean size of populations >40cm (Pratchett, 2005). • Size structure of population is variable due to multiple cohorts (Pratchett, 2005; Engelhardt et al., 2001).	• Maximum body sizes recorded as markedly smaller (Kettle, 1990; Lawrence and Lane, 1982) – median size of outbreaking population = 349mm (Macneil et al., 2017), modal size = 300-350 (Pratchett, 2005) • Size structure of population may be unimodal due to mass recruitment event (Pratchett et al., 2014) - <150mm variation in sizes (Birkeland & Lucas, 1980)	• Smaller maximum sizes due to low proportions of adult CoTS (Pratchett, 2005; Engelhardt et al., 2000) • Majority of population in size class 0-15cm (Engelhardt et al., 2000)
Growth rates	• Predictable and determinant growth rates, following von Bertalanffy growth pattern. (Branham et al., 1971; Wilson and Marsh 1974; and Zann et al., 1990) • Growth limited only by morphometry and physiological demands (Souter, 2007; Kenchington, 1977)	• Growth constrained by unfavourable diet/food limitation (Yamaguchi, 1974; Lucas, 1984). • Gonad development prioritised over somatic growth, which can result in slower growth rates (Birkeland and Lucas, 1990; Caballes and Pratchett, 2014).	• Juvenile CoTS may exhibit growth stasis when coral prey is depleted 'juveniles in waiting' hypothesis (Deaker et al., 2020)

	• Algae feeding growth rates are slow: (1.5-2.6mm/month) (Yamaguchi, 1974; Zann et al., 1987; Wilmes et al., 2016) • Coral feeding growth rates are (16.7-25mm/month) (Yamaguchi, 1974; Zann et al., 1987)	• Growth rates – 0.54 intrinsic rate of increase (Macneil, 2017)	
Mortality	• Long-lived individuals > 7-13 years (Zann et al., 1990; Chesher, 1969) • Holling type III functional response – mortality governed by predation and senility (Pratchett et al., 2017; Moore 1990) • Limited data on mortality of adults in non-outbreaking populations • Limited data on mortality of settling larvae/recruits (Zann et al., 1987; Caballes et al., 2022)	• Shorter lifespans 1-5 years (Moran, 1986; Zann et al., 1990) • Holling type II functional response - mortality governed by prey limitation • Rapid pronounced declines in entire population often observed, but data on this is limited (Pratchett et al., 2017; Zann et al., 1990). • Limited data on mortality of settling larvae/recruits (Zann et al., 1987; Caballes et al., 2022)	• Limited data on mortality of post-outbreak populations including larvae/recruits, juveniles and adults
Individual Fecundity / reproduction condition	• Extremely high fecundity of both males and females (>100 million eggs and >53 billion sperm for large individuals) (Babcock et al., 2016; Pratchett et al., 2021). • Females produce large oocytes with strong gamete competence and energy reserves for larvae (Caballes, 2016)	• Lower fecundity expected according to size-based fecundity models (Babcock et al., 2016) i.e. <2 million eggs for 35mm starfish (Pratchett et al., 2021) • Food limitation proven to reduce gonad size, fecundity, quality of oocytes and larvae energy reserves (Caballes, 2016; Kettle, 1990), but this has not been tested in the field • Sexual maturity may be reached at smaller sizes i.e 150mm (Yamaguchi, 1974).	• Limited data on reproductive condition of post-outbreak adult CoTS
Aggregation (reproduction)	• Modelling studies show low density CoTS must slightly aggregate to relieve Allee	• Modelling studies show weak or moderate aggregation is optimal for	• Limited data on aggregation behaviour

	effect (Rogers et al., 2017) but there is limited data on aggregation prior to spawning from the field.	high density populations during spawning, to limit effect of polyspermy (Rogers et al., 2017). This has been observed in the field by Babcock et al. (1994).	and spawning of post-outbreak populations
Spawning behaviour	• Spawn synchronously to achieve higher likelihood of fertilisation	• Spawn synchronously to achieve higher likelihood of fertilisation (Beach et al., 1975)	• No data on spawning behaviour in post-outbreak populations
Recruitment	• High mortality at early life stages due to predation on larvae by coral polyps and predation of juveniles (Cowan, 2020; Caballes et al., 2022) • Larvae preferentially settle near conspecifics for suitable habitat (Chesher, 1969; Ormond et al., 1973)	• Settling larvae attracted to feeding aggregations. Lower predation by corals polyps due to cleared settlement substrate by feeding CoTS (Ormond et al., 1973). • 'Hidden army' juveniles may wait in the rubble until coral cover is restored (Deaker et al., 2020)	• 'Hidden army' juveniles may wait in the rubble until coral cover is restored (Deaker et al., 2020)
Sex ratios	• Limited conclusive data. Some evidence for equal sex ratios (Pearson & Endean, 1969) and some for male skewed populations (Caballes, 2017)	• Limited conclusive data. Some evidence for equal sex ratios (Babcock & Mundy, 1992; Pearson & Endean, 1969; Nishiri & Yamazato, 1974) and sone evidence for male-skewed sex ratios towards end of outbreak (Pratchett et al., 2010; Caballes et al 2017; Stump, 1994).	• Limited data on this but some evidence for male skewed ratios in the aftermath of an outbreak (Stump, 1994; Pratchett et al., 2010; Caballes et al., 2016)
Feeding electivity	• Strong preference for Acroporidae and Pocilloporidae corals as adults (Pearson & Endean, 1969; Brauer et al., 1970; De'ath & Moran, 1998) • Preferences linked to efficient feeding, nutritional quality and learnt response to most abundant prey (Moran, 1986) • Some geographical variation in preferred prey where Acroporids are absent (Pratchett, 2001)	• Strong preference for Acroporidae and Pocilloporidae corals does not change but wider diets are consumed when preferred corals are not available (selectivity changes, not preferences) (Keesing, 1990; Keesing, 2019) • Evidence of non-scleractinian prey consumption (Glynn, 1987; Keesing, 1990)	• Juveniles maintain a CCA diet rather than shifting to feed on coral (Deaker et al., 2020)

		• Optimal foraging theory explains plastic feeding behaviour (Macarthur & Pianka, 1969) • CoTS may emigrate to search for preferred prey, or save energy and consume non-preferred prey (Ling et al., 2020)	
Feeding rates	• Feeding rates vary from 116 $cm^2.day^{-1}$ (Pearson & Endean 1969) to 478$cm^2.day^{-1}$ (Keesing & Lucas 1992), limited data on outbreaking vs non-outbreaking however faster feeding rates recorded for larger individuals. • Feed slowly and infrequently due to high nutritional quality of prey items (Pratchett et al., 2014), however large CoTS feed regularly due to higher metabolic demands (Keesing, 1990).	• Feeding rates vary from 116 $cm^2.day^{-1}$ (Pearson & Endean 1969) to 478$cm^2.day^{-1}$ (Keesing & Lucas 1992), limited data on outbreaking vs non-outbreaking however faster feeding rates recorded for larger individuals. • Intraspecific competition for food (Keesing, 1990) and low nutritional value of non-preferred corals, may cause more frequent feeding in these populations.	• Limited data on feeding rates or time spent feeding in post-outbreak populations
Diel behaviour	• Smaller individuals generally cryptic during the day (Keesing, 1995; Chesher, 1969; Cheney, 1974), and move to feed during the night • Very large individuals >40 may not hide (Keesing, 1990).	• Daytime feeding common (Chesher, 1969; Cheney, 1974). Movement and feeding during both day and night unless very small (<20cm) (Ling et al., 2020).	• Limited data on diel behaviour of post-outbreak populations
Movement	• Generally localised movement in response to high percent live cover (Keesing & Lucas, 1992; Souter, 2007). Exhibit 'homing' behaviour with small daily displacement <1m (Ling et al., 2020) and tracked routes to preferred refuge spots.	• 'Roaming' prey-searching mode of movement, moving up to 20m per day (Ling et al., 2020), directional movement towards corals, without returning to refuge.	• Limited data on movement behaviour of post-outbreak populations
Feeding aggregations	• When preferred prey is abundant, limited movement from refuge (homing behaviour)	• Feeding aggregations likely as CoTS roam, searching for areas of higher coral cover (Vine,	• Limited data on the formation of feeding aggregations by post-outbreak populations

	meaning low likelihood of feeding aggregations (Ling et al., 2020). • Feeding aggregations may form with low density cots if availability of preferred prey is limited.	1973; Dana & Newman, 1973; Ling et al., 2020). • Use chemoattractant cues of conspecifics feeding on corals (Caballes, 2009)	• Populations with limited food availability may form aggregations on any restricted areas of coral left (Haywood et al., 2019; Dana et al., 1972; Weber & Woodhead 1970; Keesing et al., 2019)

Appendix 2 - Supplementary information for Chapter 4

Appendix 2a: 3D Photogrammetry Processes

Table S1: *Summary of processing parameters used in Agisoft Metashape (v1.7.6) software for model reconstruction of coral colonies*

Photogrammetry process	Parameters
Image acquisition	4k (30fps) videos were taken with GoPro Hero 11 Black cameras. Two sets of Agisoft Metashape coded targets were used: 12bit, inverted, 20% of full size, target centres 60 mm apart
Image processing and quality control*	Videos were imported into Agisoft Metashape and every fourth frame was selected and saved as .jpeg. Python script* disabled any images with image quality below 0.3 image threshold. Image sets ranged from 150-1400 images depending on coral complexity and size.
Target detection*	Tolerance 50 %, Type Circular 12 bit, ≥10 projections per target
Photo alignment*	Accuracy high, ≥ 90 % images aligned and visual check, Tie point limit 4,000, Python script was run to align photos.
Scaling*	Scale bars 0.06m cm separation, Error (pix) below 5, Total error < 0.02 and visual checked before 2nd python script
Depth maps**	High quality and mild filtering
Mesh**	Mesh build from depth maps
Texture**	Mapping mode: generic, Blending mode: mosaic, Texture size 8192
Colony cropping	Colonies were cropped manually using lasso tool for removing extraneous mesh material.
Model orientation	Model orientation was updated to show aerial view via 'transform object>update transform'
Metric derivation	Surface area of coral colony was derived from analyses tools, maximum diameter was manually derived with the measurement tool.
Average time per model	98 minutes

*1st Python script

**2nd Batch script

Appendix 2b: Model output and credible intervals

Listed below are model output tables for the 15 coral morphotaxa modelled during this study. The tables provide predicted surface area values (Projected 2D surface area and Total 3D surface area) for an arbitrary range of field values over the coral's size range, along with a credible range of values based on the observed data and the Bayesian model. Practitioners can use these tables to understand the range of uncertainty around the model estimates for given coral sizes/morphotaxa where smaller HPD widths represent higher confidence in model estimates.

Estimated marginal means (Emmeans) are presented for model estimates and Bayesian credible intervals (Highest Posterior Density Intervals, HPD) provide a range of values for these estimates where 95% of the posterior probability density is contained. Arbitrary field measurements of colony maximum diameter (D) were generated over taxa-specific size ranges using R studio 'seq' function.

i) *Acropora* - Other:

Model equation for Projected 2D surface area (PSA): $PSA = 0.448D^{2.046}$

Model equation for Total 3D surface area (TSA): $TSA = 0.837D^{2.459}$

Table S2: Predicted values ('emmeans') of Projected 2D surface area (PSA) and Total 3D surface area (TSA) for 20 example field measurements of colony maximum diameter (D) for '*Acropora* – Other'. Also shown are Bayesian credible intervals (Highest Posterior Density Intervals, HPD) to represent the uncertainty associated with emmeans values. HPDs capture the range of parameter values with the highest posterior distribution.

Field measurement of colony maximum diameter (D) (cm)	**Projected 2D surface area (PSA)**			**Total 3D surface area (TSA)**		
	Emmean (cm²)	**Lower HPD**	**upper HPD**	**Emmean (cm²)**	**Lower HPD**	**upper HPD**
5	**12**	9	15	**44**	27	75
6	**17**	14	21	**65**	40	101
7	**23**	19	27	**96**	61	142
8	**32**	27	37	**141**	96	203
9	**44**	37	51	**207**	148	290
11	**61**	53	69	**305**	227	415
13	**84**	74	94	**449**	345	603
15	**116**	103	129	**661**	520	867
18	**160**	144	178	**975**	768	1,246
21	**220**	198	245	**1,438**	1,145	1,841
24	**304**	270	338	**2,120**	1,644	2,672
28	**420**	370	473	**3,124**	2,357	4,000
33	**580**	512	669	**4,602**	3,340	6,034
39	**801**	694	934	**6,800**	4,936	9,572
45	**1,106**	939	1,305	**10,030**	6,789	14,206
53	**1,528**	1,270	1,831	**14,723**	9,648	21,735
62	**2,109**	1,721	2,579	**21,732**	13,576	33,141
73	**2,914**	2,327	3,632	**32,073**	19,336	51,455
85	**4,021**	3,158	5,118	**47,141**	27,776	80,856
100	**5,549**	4,254	7,170	**69,429**	39,401	125,946

ii) *Acropora* - Staghorn:

Model equation for Projected 2D surface area (PSA): $PSA = 0.186D^{1.981}$

Model equation for Total 3D surface area (TSA): $TSA = 0.838D^{2.024}$

Table S3: Predicted values ('emmeans') of Projected 2D surface area (PSA) and Total 3D surface area (TSA) for 20 example field measurements of colony maximum diameter (D) for '*Acropora* – staghorn'. Also shown are Bayesian credible intervals (Highest Posterior Density Intervals, HPD) to represent the uncertainty associated with emmeans values. HPDs capture the range of parameter values with the highest posterior distribution.

Field measurement of colony maximum diameter (D) (cm)	**Projected 2D surface area (PSA)**			**Total 3D surface area (TSA)**		
	Emmean (cm^2)	**Lower HPD**	**upper HPD**	**Emmean (cm^2)**	**Lower HPD**	**upper HPD**
5	**4**	1	23	**22**	4	133
6	**7**	2	31	**34**	6	170
8	**11**	3	41	**52**	11	237
10	**16**	5	56	**81**	19	317
12	**25**	9	80	**125**	35	433
15	**38**	15	107	**193**	62	592
18	**58**	25	147	**297**	109	807
23	**89**	44	207	**459**	195	1,126
28	**137**	72	271	**711**	339	1,534
35	**209**	121	369	**1,102**	601	2,149
43	**320**	205	507	**1,712**	990	2,873
54	**492**	342	714	**2,646**	1,769	4,273
66	**751**	546	1,053	**4,091**	2,874	6,072
82	**1,142**	846	1,597	**6,348**	4,525	9,357
102	**1,748**	1,230	2,489	**9,822**	6,692	15,020
127	**2,684**	1,811	4,213	**15,209**	9,430	24,790
157	**4,149**	2,445	6,797	**23,475**	13,218	43,056
195	**6,337**	3,506	11,941	**36,489**	17,210	71,434
242	**9,722**	4,747	20,209	**56,171**	23,419	122,504
300	**14,886**	6,441	34,561	**86,912**	33,699	225,622

iii) *Acropora* - Table:

Model equation for Projected 2D surface area (PSA): $PSA = 0.346D^{2.111}$

Model equation for Total 3D surface area (TSA): $TSA = 2.615D^{1.947}$

Table S4: Predicted values ('emmeans') of Projected 2D surface area (PSA) and Total 3D surface area (TSA) for 20 example field measurements of colony maximum diameter (D) for '*Acropora* – Table'. Also shown are Bayesian credible intervals (Highest Posterior Density Intervals, HPD) to represent the uncertainty associated with emmeans values. HPDs capture the range of parameter values with the highest posterior distribution.

Field measurement of colony maximum diameter (D) (cm)	**Projected 2D surface area (PSA)**			**Total 3D surface area (TSA)**		
	Emmean (cm^2)	**Lower HPD**	**upper HPD**	**Emmean (cm^2)**	**Lower HPD**	**upper HPD**
5	**10**	7	16	**60**	29	126
6	**15**	11	23	**88**	44	170
7	**23**	17	34	**129**	68	235
9	**35**	25	48	**188**	104	322
11	**53**	39	71	**274**	163	451
13	**80**	60	102	**399**	255	632
16	**120**	95	151	**581**	397	889
19	**182**	149	224	**846**	590	1,183
24	**274**	227	325	**1,235**	912	1,660
29	**412**	352	478	**1,801**	1,404	2,339
35	**621**	543	710	**2,634**	2,140	3,346
42	**935**	832	1,065	**3,845**	3,147	4,738
51	**1,409**	1,242	1,585	**5,598**	4,498	6,832
62	**2,126**	1,862	2,418	**8,173**	6,493	10,258
76	**3,201**	2,756	3,736	**11,942**	8,836	15,026
92	**4,828**	3,994	5,677	**17,418**	12,574	23,393
112	**7,278**	5,847	8,769	**25,453**	17,510	35,808
136	**10,975**	8,675	13,811	**37,258**	24,703	56,279
165	**16,537**	12,540	21,326	**54,407**	34,167	85,827
200	**24,891**	18,452	33,528	**79,316**	47,105	132,223

iv) *Astreopora*:

Model equation for Projected 2D surface area (PSA): $PSA = 0.252D^{2.293}$

Model equation for Total 3D surface area (TSA): $TSA = 0.425D^{2.434}$

Table S5: Predicted values ('emmeans') of Projected 2D surface area (PSA) and Total 3D surface area (TSA) for 20 example field measurements of colony maximum diameter (D) for '*Astreopora*'. Also shown are Bayesian credible intervals (Highest Posterior Density Intervals, HPD) to represent the uncertainty associated with emmeans values. HPDs capture the range of parameter values with the highest posterior distribution.

Field measurement of colony maximum diameter (D) (cm)	**Projected 2D surface area (PSA)**			**Total 3D surface area (TSA)**		
	Emmean (cm^2)	**Lower HPD**	**upper HPD**	**Emmean (cm^2)**	**Lower HPD**	**upper HPD**
5	**10**	6	17	**21**	7	72
5.5	**13**	8	22	**27**	10	85
6	**17**	10	26	**35**	15	99
7	**21**	14	32	**46**	22	120
8	**27**	19	39	**61**	30	135
9	**35**	25	47	**79**	44	167
10	**45**	34	58	**103**	61	190
11	**58**	46	73	**135**	88	234
12	**74**	61	92	**177**	117	279
13	**96**	79	116	**231**	152	343
15	**123**	99	147	**302**	196	451
17	**158**	125	193	**395**	253	618
19	**203**	157	258	**515**	319	882
21	**261**	196	349	**671**	352	1,131
23	**335**	240	464	**875**	431	1,667
26	**430**	290	621	**1,145**	504	2,387
29	**553**	366	864	**1,496**	597	3,443
32	**711**	442	1,152	**1,952**	722	5,106
36	**914**	538	1,551	**2,552**	834	7,374
40	**1,175**	642	2,051	**3,333**	929	10,372

v) *Fungia*:

Model equation for Projected 2D surface area (PSA): $PSA = 0.790D^{1.910}$

Model equation for Total 3D surface area (TSA): $TSA = 0.587D^{2.440}$

Table S6: Predicted values ('emmeans') of Projected 2D surface area (PSA) and Total 3D surface area (TSA) for 20 example field measurements of colony maximum diameter (D) for '*Fungia*'. Also shown are Bayesian credible intervals (Highest Posterior Density Intervals, HPD) to represent the uncertainty associated with emmeans values. HPDs capture the range of parameter values with the highest posterior distribution.

Field measurement of colony maximum diameter (D) (cm)	**Projected 2D surface area (PSA)**			**Total 3D surface area (TSA)**		
	Emmean (cm^2)	**Lower HPD**	**upper HPD**	**Emmean (cm^2)**	**Lower HPD**	**upper HPD**
5.0	**24**	20	30	**30**	16	67
6.4	**27**	23	33	**36**	19	70
6.8	**31**	26	36	**43**	25	81
7.3	**35**	30	41	**51**	31	92
7.7	**39**	34	45	**61**	38	106
8.2	**44**	39	51	**73**	49	124
8.8	**50**	44	56	**87**	59	142
9.3	**56**	51	64	**104**	76	167
10.0	**64**	57	71	**125**	92	191
10.6	**72**	65	81	**149**	107	210
11.3	**81**	73	91	**178**	128	246
12.0	**91**	82	103	**213**	153	295
12.8	**103**	91	115	**253**	185	366
13.7	**116**	103	131	**303**	210	426
14.6	**131**	115	150	**361**	244	522
15.5	**148**	129	171	**432**	293	668
16.5	**167**	143	193	**517**	332	825
17.6	**189**	161	221	**618**	367	1,000
18.8	**213**	178	253	**737**	431	1,276
20.0	**240**	202	295	**883**	456	1,517

vi) *Goniastrea*:

Model equation for Projected 2D surface area (PSA): $PSA = 0.727D^{1.882}$

Model equation for Total 3D surface area (TSA): $TSA = 0.919D^{2.273}$

Table S7: Predicted values ('emmeans') of Projected 2D surface area (PSA) and Total 3D surface area (TSA) for 20 example field measurements of colony maximum diameter (D) for '*Goniastrea'*. Also shown are Bayesian credible intervals (Highest Posterior Density Intervals, HPD) to represent the uncertainty associated with emmeans values. HPDs capture the range of parameter values with the highest posterior distribution.

Field measurement of colony maximum diameter (D) (cm)	**Projected 2D surface area (PSA)**			**Total 3D surface area (TSA)**		
	Emmean (cm^2)	**Lower HPD**	**upper HPD**	**Emmean (cm^2)**	**Lower HPD**	**upper HPD**
5.0	**15**	9	29	**36**	13	115
5.6	**19**	12	34	**47**	17	128
6.4	**24**	15	40	**62**	25	150
7.2	**30**	20	47	**81**	37	181
8.1	**38**	26	56	**107**	54	219
9.2	**47**	36	69	**141**	82	282
10.3	**60**	45	81	**186**	108	322
11.7	**75**	58	97	**245**	153	404
13.2	**94**	75	121	**323**	204	491
14.9	**118**	94	151	**425**	289	685
16.8	**148**	118	194	**562**	364	924
19.0	**187**	141	246	**740**	453	1,271
21.4	**234**	169	318	**976**	537	1,727
24.2	**293**	203	421	**1,286**	646	2,433
27.3	**369**	243	559	**1,689**	777	3,493
30.8	**465**	283	727	**2,225**	923	5,057
34.8	**584**	339	971	**2,920**	1,121	7,456
39.2	**732**	405	1,301	**3,858**	1,290	10,668
44.3	**921**	487	1,762	**5,082**	1,441	14,940
50.0	**1,156**	572	2,341	**6,690**	1,691	21,978

vii) *Lobophyllia*:

Model equation for Projected 2D surface area (PSA): $PSA = 0.539D^{2.008}$

Model equation for Total 3D surface area (TSA): $TSA = 0.698D^{2.190}$

Table S8: Predicted values ('emmeans') of Projected 2D surface area (PSA) and Total 3D surface area (TSA) for 20 example field measurements of colony maximum diameter (D) for '*Lobophyllia'*. Also shown are Bayesian credible intervals (Highest Posterior Density Intervals, HPD) to represent the uncertainty associated with emmeans values. HPDs capture the range of parameter values with the highest posterior distribution.

Field measurement of colony maximum diameter (D) (cm)	**Projected 2D surface area (PSA)**			**Total 3D surface area (TSA)**		
	Emmean (cm^2)	**Lower HPD**	**upper HPD**	**Emmean (cm^2)**	**Lower HPD**	**upper HPD**
5.0	**14**	8	23	**24**	12	50
5.9	**19**	12	31	**33**	17	63
6.9	**26**	17	40	**47**	26	83
8.0	**36**	24	53	**67**	39	112
9.4	**49**	35	70	**94**	61	155
11.0	**67**	51	94	**133**	87	199
12.9	**92**	70	121	**187**	133	275
15.1	**126**	97	158	**264**	190	368
17.7	**173**	140	216	**373**	273	499
20.7	**236**	191	290	**527**	397	704
24.2	**325**	265	404	**742**	560	992
28.3	**446**	354	554	**1,047**	785	1,425
33.2	**613**	484	787	**1,482**	1,069	2,018
38.8	**841**	635	1,093	**2,094**	1,463	2,994
45.5	**1,153**	858	1,580	**2,949**	1,948	4,375
53.2	**1,585**	1,145	2,263	**4,178**	2,712	6,715
62.3	**2,171**	1,511	3,223	**5,902**	3,604	9,868
73.0	**2,976**	1,904	4,414	**8,338**	4,703	14,640
85.4	**4,083**	2,555	6,404	**11,797**	6,322	22,128
100.0	**5,586**	3,335	9,105	**16,651**	8,260	32,576

viii) *Montipora* - encrusting:

Model equation for Projected 2D surface area (PSA): $PSA = 0.667D^{1.848}$

Model equation for Total 3D surface area (TSA): $TSA = 1.229D^{1.875}$

Table S9: Predicted values ('emmeans') of Projected 2D surface area (PSA) and Total 3D surface area (TSA) for 20 example field measurements of colony maximum diameter (D) for '*Montipora*'. Also shown are Bayesian credible intervals (Highest Posterior Density Intervals, HPD) to represent the uncertainty associated with emmeans values. HPDs capture the range of parameter values with the highest posterior distribution.

Field measurement of colony maximum diameter (D) (cm)	**Projected 2D surface area (PSA)**			**Total 3D surface area (TSA)**		
	Emmean (cm^2)	**Lower HPD**	**upper HPD**	**Emmean (cm^2)**	**Lower HPD**	**upper HPD**
5	**13**	8	24	**25**	11	53
6	**18**	11	31	**35**	17	70
7	**25**	16	41	**49**	27	95
9	**35**	24	54	**68**	41	122
10	**49**	34	71	**96**	58	152
12	**68**	50	95	**133**	88	204
15	**95**	72	125	**186**	130	267
18	**132**	103	166	**260**	187	358
21	**184**	149	231	**364**	273	492
25	**256**	211	322	**508**	384	670
30	**357**	282	439	**711**	529	954
36	**496**	384	630	**992**	728	1,414
43	**690**	511	897	**1,392**	947	2,017
51	**960**	705	1,345	**1,954**	1,253	3,006
61	**1,337**	910	1,921	**2,733**	1,642	4,480
73	**1,862**	1,213	2,825	**3,813**	2,157	6,805
88	**2,592**	1,606	4,178	**5,328**	2,766	9,969
105	**3,609**	2,145	6,241	**7,459**	3,586	14,872
125	**5,015**	2,866	9,335	**10,444**	4,701	22,520
150	**7,006**	3,651	13,337	**14,534**	6,040	33,659

ix) *Pocillopora*:

Model equation for Projected 2D surface area (PSA): $PSA = 0.324D^{2.133}$

Model equation for Total 3D surface area (TSA): $TSA = 0.709D^{2.50}$

Table S10: Predicted values ('emmeans') of Projected 2D surface area (PSA) and Total 3D surface area (TSA) for 20 example field measurements of colony maximum diameter (D) for '*Pocillopora*'. Also shown are Bayesian credible intervals (Highest Posterior Density Intervals, HPD) to represent the uncertainty associated with emmeans values. HPDs capture the range of parameter values with the highest posterior distribution.

Field measurement of colony maximum diameter (D) (cm)	**Projected 2D surface area (PSA)**			**Total 3D surface area (TSA)**		
	Emmean (cm^2)	**Lower HPD**	**upper HPD**	**Emmean (cm^2)**	**Lower HPD**	**upper HPD**
5	**10**	6	18	**40**	24	71
6	**14**	8	23	**56**	34	93
7	**18**	12	29	**80**	50	127
8	**25**	16	37	**113**	75	177
9	**33**	23	48	**160**	108	234
10	**45**	31	62	**225**	157	324
12	**60**	44	83	**318**	230	456
13	**81**	59	110	**451**	317	602
15	**108**	81	150	**637**	478	886
17	**145**	107	199	**900**	665	1,227
20	**195**	146	277	**1,277**	928	1,741
23	**263**	192	376	**1,804**	1,322	2,559
26	**354**	249	513	**2,554**	1,777	3,602
30	**475**	329	713	**3,618**	2,378	5,114
35	**639**	436	1,018	**5,125**	3,274	7,452
40	**858**	554	1,399	**7,234**	4,491	11,089
46	**1,154**	716	1,952	**10,207**	6,114	16,474
53	**1,552**	913	2,726	**14,440**	8,351	24,498
61	**2,084**	1,194	3,909	**20,437**	11,370	36,534
70	**2,809**	1,471	5,328	**28,915**	15,387	54,414

x) *Porites* - massive:

Model equation for Projected 2D surface area (PSA): $PSA = 0.763D^{1.956}$

Model equation for Total 3D surface area (TSA): $TSA = 4.58D^{1.836}$

Table S11: Predicted values ('emmeans') of Projected 2D surface area (PSA) and Total 3D surface area (TSA) for 20 example field measurements of colony maximum diameter (D) for '*Porites* - massive'. Also shown are Bayesian credible intervals (Highest Posterior Density Intervals, HPD) to represent the uncertainty associated with emmeans values. HPDs capture the range of parameter values with the highest posterior distribution.

Field measurement of colony maximum diameter (D) (cm)	**Projected 2D surface area (PSA)**			**Total 3D surface area (TSA)**		
	Emmean (cm^2)	**Lower HPD**	**upper HPD**	**Emmean (cm^2)**	**Lower HPD**	**upper HPD**
5	**18**	6	54	**88**	11	724
6	**25**	10	70	**120**	19	832
7	**35**	15	89	**164**	30	958
8	**48**	23	113	**224**	49	1,141
10	**67**	34	144	**304**	82	1,358
12	**93**	51	185	**413**	127	1,542
14	**129**	73	229	**558**	174	1,529
16	**177**	111	297	**763**	277	1,824
19	**247**	162	378	**1,037**	449	2,243
23	**343**	238	495	**1,412**	744	2,944
27	**476**	332	649	**1,928**	1,038	3,538
31	**662**	490	920	**2,602**	1,504	4,841
37	**918**	654	1,272	**3,544**	2,004	6,933
44	**1,275**	899	1,900	**4,788**	2,498	9,825
52	**1,769**	1,130	2,692	**6,495**	3,039	14,881
61	**2,460**	1,428	3,924	**8,831**	3,787	23,796
73	**3,408**	1,892	6,108	**11,939**	4,310	35,871
86	**4,742**	2,449	9,260	**16,175**	4,951	55,286
102	**6,597**	3,113	13,907	**21,898**	5,306	81,909
120	**9,165**	4,167	22,196	**29,697**	6,969	149,032

xi) *Seriatopora:*

Model equation for Projected 2D surface area (PSA): $PSA = 0.359D^{2.093}$

Model equation for Total 3D surface area (TSA): $TSA = 0.831D^{2.451}$

Table S12: Predicted values ('emmeans') of Projected 2D surface area (PSA) and Total 3D surface area (TSA) for 20 example field measurements of colony maximum diameter (D) for '*Seriatopora'*. Also shown are Bayesian credible intervals (Highest Posterior Density Intervals, HPD) to represent the uncertainty associated with emmeans values. HPDs capture the range of parameter values with the highest posterior distribution.

Field measurement of colony maximum diameter (D) (cm)	**Projected 2D surface area (PSA)**			**Total 3D surface area (TSA)**		
	Emmean (cm^2)	**Lower HPD**	**upper HPD**	**Emmean (cm^2)**	**Lower HPD**	**upper HPD**
5	**10**	6	17	**43**	19	93
6	**14**	9	22	**61**	31	129
7	**19**	13	29	**88**	47	171
8	**26**	18	39	**126**	70	224
9	**35**	25	50	**180**	103	298
10	**48**	35	65	**256**	166	428
12	**65**	49	86	**367**	244	592
14	**88**	68	114	**524**	360	812
16	**120**	93	152	**751**	529	1,098
19	**163**	129	208	**1,073**	773	1,563
22	**221**	169	277	**1,531**	1,055	2,144
25	**299**	230	387	**2,191**	1,502	3,205
29	**406**	307	541	**3,135**	2,103	4,808
33	**552**	401	745	**4,482**	2,926	7,245
39	**749**	533	1,056	**6,433**	3,966	10,920
45	**1,015**	700	1,485	**9,172**	5,104	15,752
52	**1,378**	916	2,087	**13,118**	6,960	24,326
60	**1,871**	1,205	2,964	**18,766**	9,565	38,401
69	**2,537**	1,537	4,093	**26,780**	12,574	58,129
80	**3,451**	2,031	5,892	**38,408**	16,371	86,910

xii) *Stylophora*:

Model equation for Projected 2D surface area (PSA): $PSA = 0.420D^{2.46}$

Model equation for Total 3D surface area (TSA): $TSA = 0.878D^{2.413}$

Table S13: Predicted values ('emmeans') of Projected 2D surface area (PSA) and Total 3D surface area (TSA) for 20 example field measurements of colony maximum diameter (D) for '*Stylophora*'. Also shown are Bayesian credible intervals (Highest Posterior Density Intervals, HPD) to represent the uncertainty associated with emmeans values. HPDs capture the range of parameter values with the highest posterior distribution.

Field measurement of colony maximum diameter (D) (cm)	**Projected 2D surface area (PSA)**			**Total 3D surface area (TSA)**		
	Emmean (cm^2)	**Lower HPD**	**upper HPD**	**Emmean (cm^2)**	**Lower HPD**	**upper HPD**
5	**11**	7	17	**43**	26	68
5.5	**15**	10	21	**58**	36	89
6	**19**	13	27	**80**	54	124
7	**25**	18	36	**109**	74	161
8	**33**	24	45	**150**	106	221
10	**43**	32	58	**206**	148	298
11	**56**	41	75	**283**	204	406
12	**74**	54	98	**386**	272	537
14	**96**	71	131	**529**	384	765
16	**125**	91	172	**726**	503	1,030
18	**164**	118	233	**996**	678	1,438
21	**214**	153	317	**1,366**	923	2,032
24	**280**	192	422	**1,871**	1,203	2,816
27	**365**	239	562	**2,570**	1,661	4,177
31	**477**	307	774	**3,517**	2,036	5,568
36	**625**	390	1,057	**4,828**	2,651	7,835
41	**818**	479	1,396	**6,618**	3,675	11,847
46	**1,071**	598	1,886	**9,079**	4,937	17,344
53	**1,399**	790	2,704	**12,506**	6,121	23,535
60	**1,825**	986	3,662	**17,126**	8,124	34,490

xiii) <u>Other - branching:</u>

Model equation for Projected 2D surface area (PSA): $\boldsymbol{PSA = 0.107D^{2.346}}$

Model equation for Total 3D surface area (TSA): $\boldsymbol{TSA = 0.651D^{2.212}}$

Table S14: Predicted values ('emmeans') of Projected 2D surface area (PSA) and Total 3D surface area (TSA) for 20 example field measurements of colony maximum diameter (D) for 'Other - branching'. Also shown are Bayesian credible intervals (Highest Posterior Density Intervals, HPD) to represent the uncertainty associated with emmeans values. HPDs capture the range of parameter values with the highest posterior distribution.

Field measurement of colony maximum diameter (D) (cm)	**Projected 2D surface area (PSA)**			**Total 3D surface area (TSA)**		
	Emmean (cm^2)	**Lower HPD**	**upper HPD**	**Emmean (cm^2)**	**Lower HPD**	**upper HPD**
10	**24**	6	95	**105**	37	356
11	**31**	9	120	**134**	50	421
12	**40**	13	137	**171**	71	518
14	**52**	18	159	**218**	99	631
15	**67**	24	185	**278**	139	766
17	**87**	36	237	**354**	182	855
19	**112**	49	275	**449**	239	982
22	**145**	67	316	**573**	314	1,148
24	**187**	94	379	**728**	422	1,357
27	**243**	129	455	**929**	566	1,642
30	**314**	181	562	**1,182**	769	1,996
33	**405**	239	675	**1,508**	1,025	2,433
37	**526**	325	869	**1,925**	1,342	2,939
41	**680**	427	1,113	**2,455**	1,678	3,541
46	**879**	548	1,438	**3,124**	2,231	4,616
52	**1,136**	712	1,901	**3,978**	2,750	5,821
58	**1,470**	846	2,408	**5,071**	3,363	7,429
64	**1,908**	1,050	3,245	**6,450**	4,040	9,795
72	**2,466**	1,228	4,417	**8,249**	4,878	13,087
80	**3,193**	1,472	6,153	**10,491**	5,840	17,694

xiv) <u>Other - encrusting:</u>

Model equation for Projected 2D surface area (PSA): $PSA = 0.639D^{1.876}$

Model equation for Total 3D surface area (TSA): $TSA = 0.802D^{2.024}$

Table S15: Predicted values ('emmeans') of Projected 2D surface area (PSA) and Total 3D surface area (TSA) for 20 example field measurements of colony maximum diameter (D) for 'Other - encrusting'. Also shown are Bayesian credible intervals (Highest Posterior Density Intervals, HPD) to represent the uncertainty associated with emmeans values. HPDs capture the range of parameter values with the highest posterior distribution.

Field measurement of colony maximum diameter (D) (cm)	**Projected 2D surface area (PSA)**			**Total 3D surface area (TSA)**		
	Emmean (cm^2)	**Lower HPD**	**upper HPD**	**Emmean (cm^2)**	**Lower HPD**	**upper HPD**
5	**13**	9	19	**21**	12	36
6	**17**	12	24	**28**	17	46
7	**22**	16	30	**36**	23	58
8	**29**	21	38	**48**	32	73
9	**37**	28	48	**64**	44	93
10	**48**	38	61	**85**	62	119
12	**63**	51	77	**112**	83	150
13	**81**	66	96	**149**	114	195
15	**105**	87	123	**196**	152	250
17	**137**	116	161	**260**	204	331
20	**178**	150	211	**345**	269	438
23	**231**	191	273	**455**	346	576
26	**299**	244	358	**603**	454	793
30	**388**	315	481	**796**	594	1,106
35	**504**	391	628	**1,054**	733	1,470
40	**654**	505	857	**1,397**	922	2,002
46	**847**	639	1,157	**1,845**	1,162	2,768
53	**1,097**	809	1,560	**2,445**	1,486	3,899
61	**1,421**	1,027	2,114	**3,235**	1,909	5,537
70	**1,844**	1,216	2,684	**4,293**	2,409	7,749

xv) <u>Other - massive:</u>

Model equation for Projected 2D surface area (PSA): $PSA = 0.611D^{2.00}$

Model equation for Total 3D surface area (TSA): $TSA = 0.573D^{2.414}$

Table S16: Predicted values ('emmeans') of Projected 2D surface area (PSA) and Total 3D surface area (TSA) for 20 example field measurements of colony maximum diameter (D) for 'Other - massive'. Also shown are Bayesian credible intervals (Highest Posterior Density Intervals, HPD) to represent the uncertainty associated with emmeans values. HPDs capture the range of parameter values with the highest posterior distribution.

Field measurement of colony maximum diameter (D) (cm)	**Projected 2D surface area (PSA)**			**Total 3D surface area (TSA)**		
	Emmean (cm^2)	**Lower HPD**	**upper HPD**	**Emmean (cm^2)**	**Lower HPD**	**upper HPD**
5	**15**	10	23	**28**	14	62
6	**20**	13	29	**38**	20	82
6	**26**	18	38	**53**	29	106
7	**33**	24	47	**72**	42	136
8	**43**	33	59	**99**	59	171
10	**56**	44	75	**135**	85	220
11	**73**	57	92	**186**	122	284
12	**95**	77	119	**255**	168	360
14	**123**	101	150	**349**	241	484
16	**160**	132	191	**480**	349	662
18	**208**	172	246	**655**	488	902
21	**269**	223	320	**897**	662	1,238
24	**349**	289	424	**1,235**	876	1,698
27	**454**	373	567	**1,704**	1,167	2,405
31	**589**	471	754	**2,330**	1,570	3,541
36	**765**	589	999	**3,199**	2,011	4,987
41	**993**	735	1,334	**4,385**	2,570	7,065
46	**1,290**	931	1,806	**6,025**	3,371	10,489
53	**1,681**	1,200	2,518	**8,244**	4,367	15,412
60	**2,189**	1,513	3,414	**11,328**	5,585	22,339

Appendix 2c: Bayesian model equation parameters

Table S17: *Non-linear parameter constants α + β along with lower and upper Highest Density Intervals (HDIs, 95%) standard deviation (SD), length, sample size and Bayesian r-squared values for modelled relationship between coral diameter* ***and projected (2D) planar area*** *for fifteen coral morphotaxa*

	α – scaling factor / intercept				**β – exponent/slope**						
Morphotaxon	***Median Estimate***	*Lower HDI (95%)*	*Upper HDI (95%)*	*SD*	***Median Estimate***	*Lower HDI (95%)*	*Upper HDI (95%)*	*SD*	***R²***	**length**	***n***
Acropora - other	**0.448**	0.289	0.706	1.256	**2.046**	1.905	2.197	0.075	0.99	2502	13
Acropora - table	**0.346**	0.168	0.713	1.440	**2.111**	1.928	2.295	0.094	0.98	2502	13
Acropora - staghorn	**0.186**	0.117	2.009	3.634	**1.981**	1.424	2.588	0.295	0.84	2502	14
Astreopora	**0.252**	0.067	0.998	1.995	**2.293**	1.764	2.779	0.260	0.94	2502	9
Fungia	**0.790**	0.415	1.441	1.384	**1.910**	1.657	2.171	0.134	0.99	2502	6
Goniastrea	**0.727**	0.203	3.467	2.033	**1.882**	1.339	2.297	0.155	0.89	2502	11
Lobophyllia	**0.539**	0.222	1.495	1.620	**2.008**	1.702	2.323	0.152	0.97	2502	10
Montipora - encrusting	**0.667**	0.219	2.019	1.727	**1.848**	1.517	2.195	0.171	0.95	2502	11
Porites - massive	**0.763**	0.121	6.052	2.76	**1.956**	1.408	2.525	0.291	0.91	2502	9
Pocillopora	**0.324**	0.108	0.943	1.752	**2.133**	1.766	2.528	0.194	0.94	2502	13
Seriatopora	**0.358**	0.139	1.009	1.660	**2.093**	1.767	2.423	0.167	0.97	2502	9
Stylophora	**0.4202**	0.175	1.068	1.576	**2.046**	1.6834	2.384	0.176	0.96	2502	10
Other - massive	**0.611**	0.249	1.472	1.604	**2.000**	1.700	2.302	0.159	0.96	2502	12
Other - encrusting	**0.639**	0.281	1.390	1.489	**1.876**	1.598	2.138	0.134	0.96	2502	13
Other - branching	**0.107**	0.005	5.125	5.764	**2.346**	1.368	3.168	0.460	0.94	2502	6

Table S18: *Non-linear parameter constants α + β along with lower and upper Highest Density Intervals (HDIs, 95%), standard deviation (SD), length, sample size and Bayesian r-squared values, for modelled relationship between coral diameter and* ***total (3D) surface area*** *for fifteen coral morphotaxa*

	α – scaling factor / intercept				**β – exponent/slope**						
Morphotaxon	***Median Estimate***	*Lower HDI (95%)*	*Upper HDI (95%)*	*SD*	***Median Estimate***	*Lower HDI (95%)*	*Upper HDI (95%)*	*SD*	R^2	**length**	***n***
Acropora - other	**0.837**	0.312	2.237	1.674	**2.459**	2.104	2.772	0.169	0.95	2502	13
Acropora - table	**2.670**	0.809	10.283	1.889	**1.940**	1.606	2.254	0.163	0.95	2502	13
Acropora - staghorn	**0.838**	0.055	16.25	4.268	**2.024**	1.411	2.708	0.330	0.81	2502	14
Astreopora	**0.417**	0.019	7.637	4.501	**2.445**	1.249	3.503	0.563	0.81	2502	9
Fungia	**0.612**	0.095	4.703	2.864	**2.425**	1.582	3.207	0.425	0.96	2502	6
Goniastrea	**0.919**	0.071	14.287	3.686	**2.273**	1.181	3.155	0.482	0.77	2502	11
Lobophyllia	**0.668**	0.185	2.253	1.879	**2.203**	1.791	2.564	0.198	0.96	2502	10
Montipora - encrusting	**1.227**	0.259	5.400	7.824	**1.873**	1.362	2.290	0.228	0.91	2502	11
Porites - massive	**4.584**	0.096	157.9	6.291	**1.836**	0.792	2.921	0.523	0.75	2502	9
Pocillopora	**0.710**	0.227	2.121	1.752	**2.504**	2.144	2.906	0.191	0.95	2502	13
Seriatopora	**0.832**	0.163	4.250	2.214	**2.450**	1.922	3.006	0.263	0.95	2502	9
Stylophora	**0.877**	0.319	2.507	1.699	**2.410**	2.039	2.845	0.202	0.96	2502	10
Other - massive	**0.560**	0.119	2.827	2.191	**2.423**	1.917	2.963	0.260	0.91	2502	12
Other - encrusting	**0.813**	0.266	2.46	1.747	**2.012**	1.633	2.398	0.188	0.93	2502	13
Other - branching	**0.648**	0.054	11.144	3.946	**2.208**	1.546	2.929	0.360	0.96	2502	6

Appendix 2d: Representative images of coral morphotaxa

Displayed below are example images of colonies from each morphotaxa group, screenshotted from Metashape Agisoft after model construction.

Table S19: *Example colonies of Acropora – other*

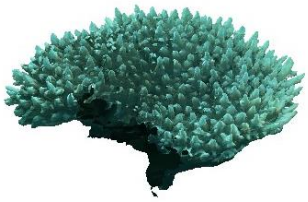
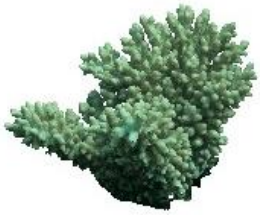
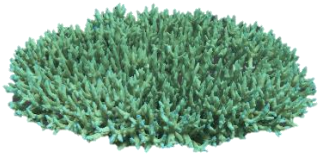
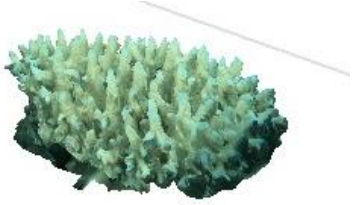
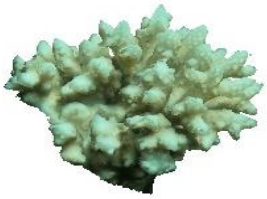
W75 	**W34** 	**W67** 
W50 	**W12** 	**W44** 

Table S20: Example colonies of Acropora - staghorn

W58 	**W38** 	**W63** 
W75 	**W61** 	**W39** 

Table S21: Example colonies of <u>Acropora - table</u>

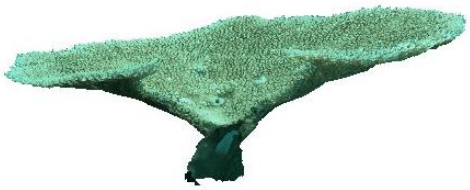
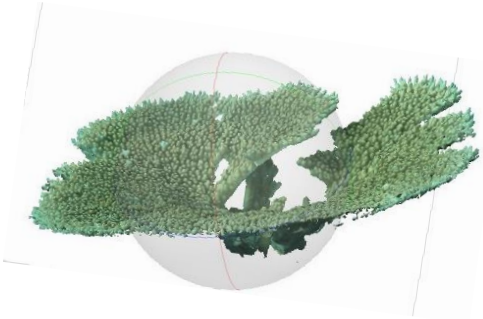
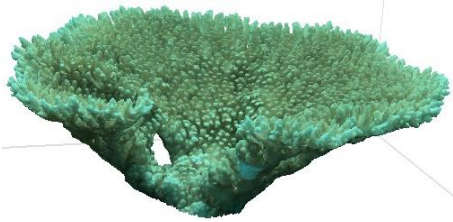
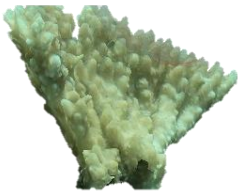
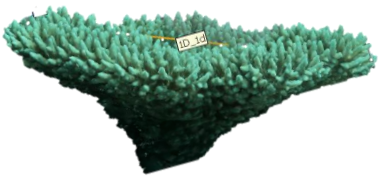
A53 	**W64** 	**CS68** 
W03 	**W10** 	**A49** 

Table S22: Example colonies of <u>Astreopora</u>

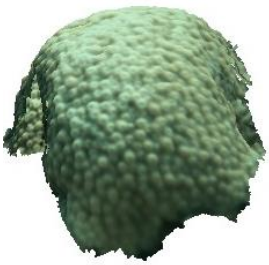
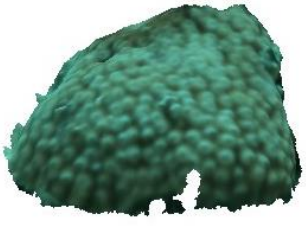
A63 	**W14** 	**W46** 
W11 	**J21** 	**A64** 

***Table S23: Example colonies of* Fungia**

A16a 	**A20** 	**W18** 
W19 	**W23** 	**W25** 

***Table S25: Example colonies of* Goniastrea**

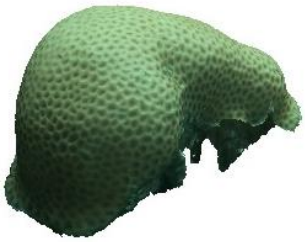
J33 	**W65** 	**W47** 
A61a 	 **W57**	**A27** 

***Table S24: Example colonies of* Lobophyllia**

W59 	**A11** 	**A21** 
W40 	**J03** 	**A02** 

***Table S26: Example colonies of* Montipora - encrusting**

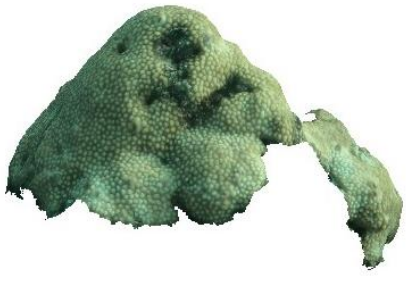
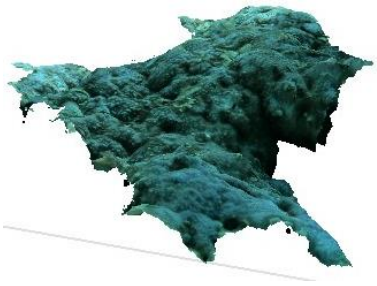
W66x 	**A37** 	**W24** 
W45 	**W82x** 	**W73** 

***Table S27: Example colonies of* Pocillopora**

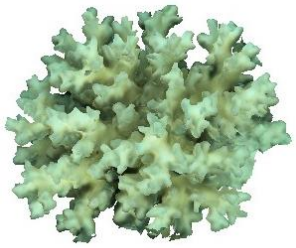
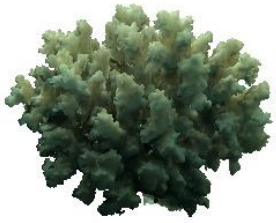
A06 	**A01** 	**A44** 
A46 	 **08**	**A05** 

Table S29: Example colonies of* Porites *– massive

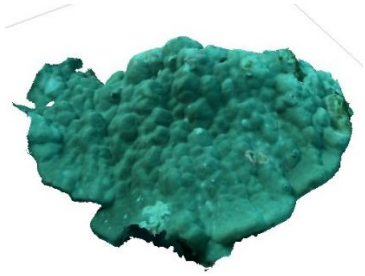
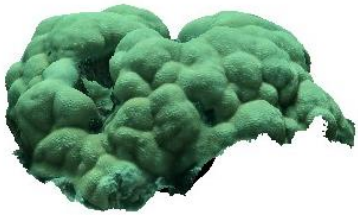
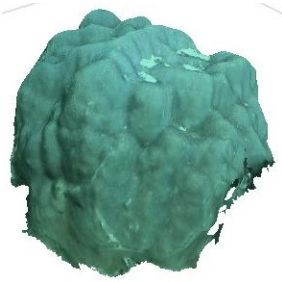
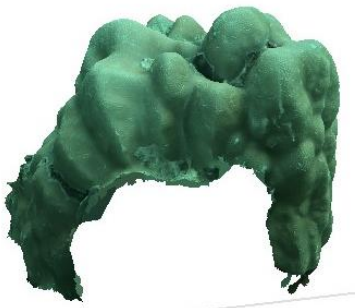
J33 	**W71x** 	**A44** 
W77 	 **0**	**W21** 

***Table S28: Example colonies of* Seriatopora**

A12 	**A14** 	**A29** 
A45 	**W22** 	**J14** 

***Table S30: Example colonies of* Stylophora**

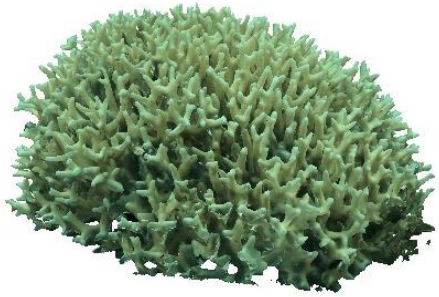
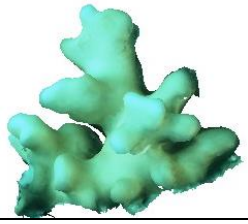
A30 	**A36** 	**W29** 
A45 	**D04** 	**A52** 

***Table S31: Example colonies of* Other - encrusting**

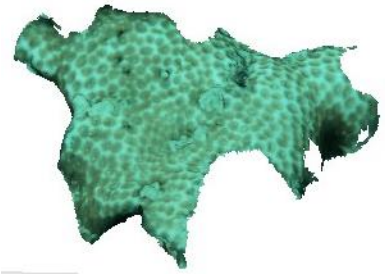
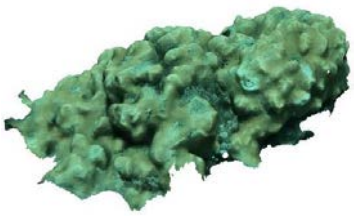
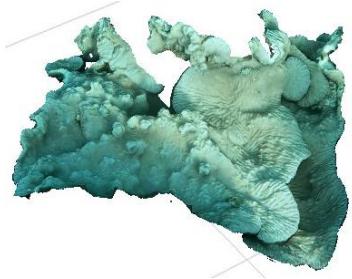
J07 	**A47** 	**W60x** 
B7 	**W52** 	**A19** 

Table S32: Example colonies of* Other - *massive

A23 	**A25** 
A29 	**W15** 

Appendix 3 - Supplementary information for Chapter 5

Appendix 3a. Colony-level feeding rates

i. Variable selection

Table S1: a) *Boosted regression tree presenting relative importance of different variables* ***b)*** *visual representation of BRT*

Variable	Relative influence
COT_size	45.75200
Density_inclScars	18.92453
*Acropora*_cover	15.75434
Total_coral_cover	12.18306
Region	6.465177
Season	0.920859

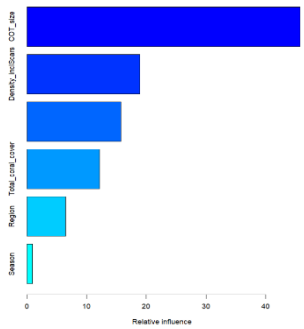


Table S2: *Model formulas and associated degrees of freedom (df) and AIC criterion. Selected model is highlighted in bold*

Model formulas	**df**	**AIC**
glmm_model_cat1 <- glmmTMB(log(daily_feeding_rate_colonies) ~ Size_category + Coral_cover_category + (1|Site)	9	1064.91
glmm_model_cat2 <- glmmTMB(log(daily_feeding_rate_colonies) ~ Size_category + Density_category + (1|Site)	8	944.39
glmm_model_cat3 <- glmmTMB(log(daily_feeding_rate_colonies) ~ Size_category + Coral_cover_category + Density_category + (1|Site)	**11**	**934.72**
glmm_model_cat4 <- glmmTMB(log(daily_feeding_rate_colonies) ~ Size_category + Acropora_category + Density_category + (1|Site)	11	933.00
glmm_model_cat5 <- glmmTMB(log(daily_feeding_rate_colonies) ~ Size_category + Acropora_category + Season + (1|Site)	10	1059.67
glmm_model_cat6 <- glmmTMB(log(daily_feeding_rate_colonies) ~ Size_category + Coral_cover_category + Season + (1|Site)	10	1060.90
glmm_NULL <- glmmTMB(log(daily_feeding_rate_colonies) ~ 1	2	1243.12

ii) GLMM Model output

Model formula: *glmm_model_cat3 <- glmmTMB(log(daily_feeding_rate_colonies) ~ Size_category + Coral_cover_category + Density_category + (1|Site)*

Response variable: log(daily_feeding_rate_planar_area)
Fixed effects: Size category, Coral cover category, Density category
Random effect: Site (n = 76)
Family: Gaussian (identity link)

Table S3: *Generalized Linear Mixed Model (GLMM) Results for Daily Feeding Rate (Colonies)*

Predictor	**Estimate**	**Std. Error**	**z-value**	**p-value**
Intercept	-1.227	0.207	-5.940	<0.001 ***
Size category (reference: 0-15 cm)				
15–25 cm	0.323	0.186	1.733	0.083 .
25–40 cm	0.621	0.166	3.740	<0.001 ***
>40 cm	0.959	0.167	5.740	<0.001 ***
Coral cover category (reference: 0-15%)				
15–30%	0.057	0.136	0.418	0.676
30–50%	0.031	0.129	0.243	0.808
>50%	-0.028	0.144	-0.193	0.847
Density category (reference: non-outbreaking <15/ha)				
Outbreaking (15–30/ha)	0.061	0.085	0.719	0.472
Severe outbreak (>30/ha)	0.038	0.084	0.457	0.648

Model Fit Statistics:

AIC: 963.0
BIC: 1008.6
Log-likelihood: -470.5
Residual deviance: 941.0
Number of observations: 469
Number of groups (Site): 76

R-squared marginal: 0.133
R-squared conditional: 0.161

iii) Predicted values

Table S4: *Estimated marginal means model predictions for **a)** body size class (colonies.d^{-1}) and **b)** coral cover class*

Body size class	Predicted	Conf. low	Conf. high
15-25cm	0.38	0.29	0.50
25-40cm	0.53	0.43	0.64
>40cm	0.75	0.62	0.90

Coral cover class	Predicted	Conf. low	Conf. high
0-15%	0.75	0.59	0.94
15-30%	0.81	0.68	0.97
30-50%	0.79	0.68	0.92
>50%	0.75	0.62	0.90

iv) Pairwise contrasts

Table S5: *Post-hoc tables of pairwise contrasts colonies for **a)** body size category and **b)** coral cover category **c)** population density*

a) Body size category

contrast	*ratio*	*SE*	*df*	*lower.CL*	*upper.CL*	*null*	*t.ratio*	*p.value*
(25-40cm) / (15-25cm)	1.35	0.151	467	1.007	1.801	1	0.042	**0.0419***
>40cm / (15-25cm)	1.89	0.221	467	1.397	2.554	1	5.434	**<0.0001***
>40cm / (25-40cm)	1.40	0.093	467	1.181	1.664	1		**<0.0001***

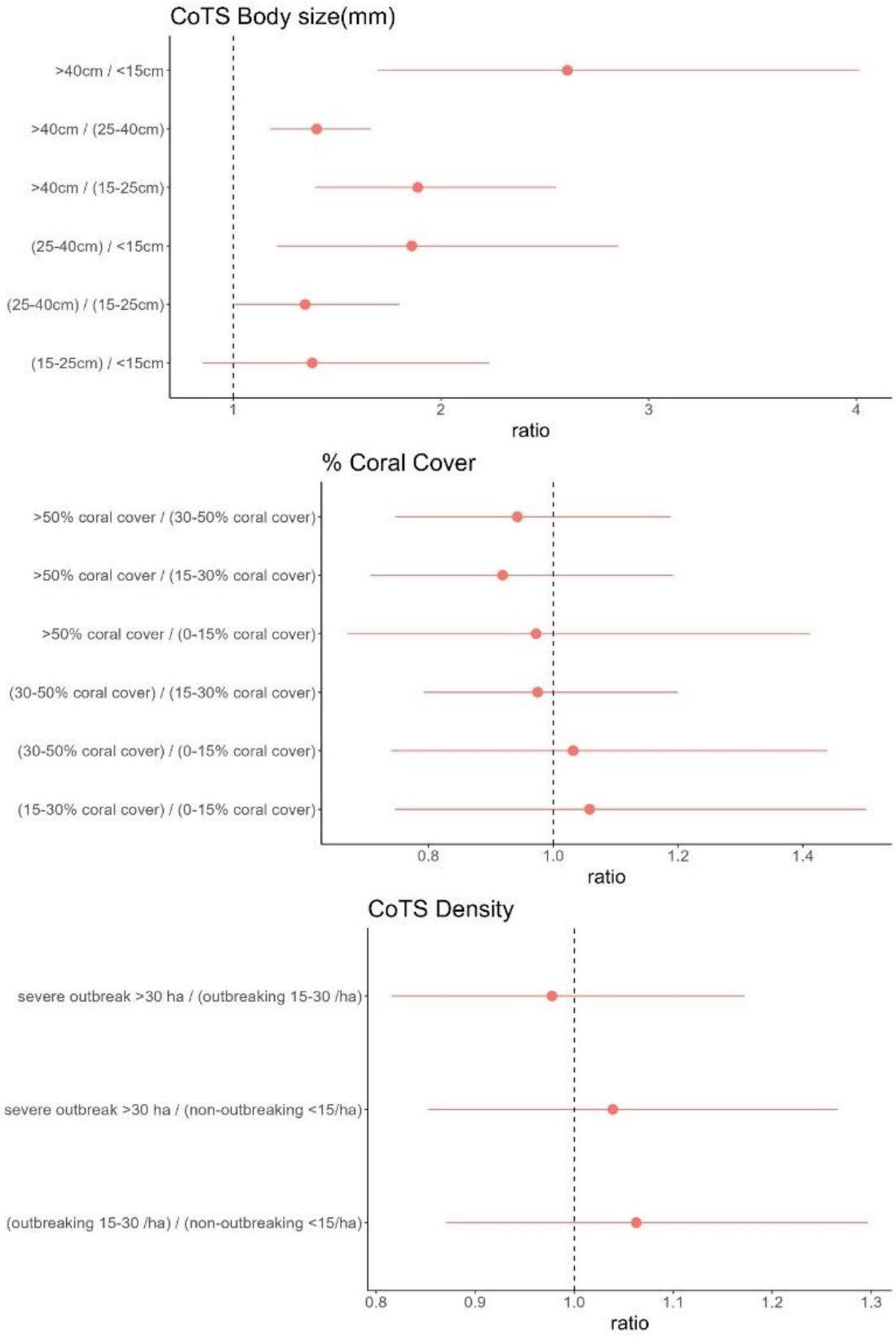
b) Coral cover

contrast	*ratio*	*SE*	*df*	*lower.CL*	*upper.CL*	*null*	*t.ratio*	*p.value*
(15-30% coral cover) / (0-15% coral cover)	1.06	0.14	467	0.74	1.50	1	0.42	0.97
(30-50% coral cover) / (0-15% coral cover)	1.03	0.13	467	0.74	1.43	1	0.24	0.99
(30-50% coral cover) / (15-30% coral cover)	0.97	0.07	467	0.79	1.20	1	-0.31	0.99
>50% coral cover / (0-15% coral cover)	0.97	0.14	467	0.67	1.41	1	-0.19	0.99
>50% coral cover / (15-30% coral cover)	0.91	0.09	467	0.71	1.19	1	-0.84	0.84
>50% coral cover / (30-50% coral cover)	0.94	0.08	467	0.75	1.19	1	-0.66	0.91

c) Population density

contrast	*ratio*	*SE*	*df*	*lower.CL*	*upper.CL*	*null*	*t.ratio*	*p.value*
(outbreaking 15 -30 /ha) / (non-outbreaking <15/ha)	1.06	0.09	467	0.87	1.30	1	0.719	0.75
(severe outbreak >30 ha) / (non-outbreaking <15/ha)	1.04	0.09	467	0.85	1.27	1	0.457	0.89
(severe outbreak >30 ha) / (outbreaking 15 -30 /ha)	0.98	0.08	467	0.82	1.17	1	-0.292	0.95

Figure S1: *Tukey's Caterpillar plot*



Appendix 3b. Planar area feeding rates

i. Variable selection

Table S6: a) *Boosted regression tree presenting relative importance of different variables* ***b)*** *visual representation of BRT*

Variable	Relative influence
COT_size	**58.6223**
Density_inclScars	16.7298
Acropora_cover	12.9689
Total_coral_cover	7.22723
Region	4.05501
Season	0.39666

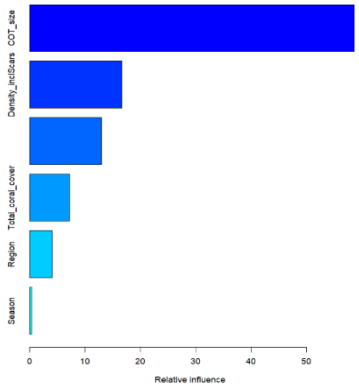


Table S7: *Model formulas and associated degrees of freedom (df) and AIC criterion. Selected model is highlighted in bold*

Model variables	**df**	**AIC**
glmm_model_cat1 <- glmmTMB(log(daily_feeding_rate_planar_area) ~ Size_category + Coral_cover_category + (1|Site)	9	1423.283
glmm_model_cat2 <- glmmTMB(log(daily_feeding_rate_planar_area) ~ Size_category + Density_category + (1|Site)	8	1292.218
glmm_model_cat3 <- glmmTMB(log(daily_feeding_rate_planar_area) ~ Size_category + Coral_cover_category + Density_category + (1|Site)	**11**	**1264.538**
glmm_model_cat4 <- glmmTMB(log(daily_feeding_rate_planar_area) ~ Size_category + Acropora_category + Density_category + (1|Site)	11	1268.754
glmm_model_cat5 <- glmmTMB(log(daily_feeding_rate_planar_area) ~ Size_category + Acropora_category + Season + (1|Site)	10	1427.745
glmm_model_cat6 <- glmmTMB(log(daily_feeding_rate_planar_area) ~ Size_category + Coral_cover_category + Season + (1|Site)	10	1424.023
glmm_NULL <- glmmTMB(log(daily_feeding_rate_planar_area) ~ 1	2	1747.790

ii) GLMM Model Output

Model formula: *glmm_planar <- glmmTMB(log(daily_feeding_rate_planar_area) ~* ***Size_category*** *+* ***Coral_cover_category*** *+* ***Density_category*** *+ (1\|****Site****)*

Response variable: log(daily_feeding_rate_planar_area)
Fixed effects: Size category, Coral cover category, Density category

Random effect: Site (n = 76)
Family: Gaussian (identity link)

Table S8: *Generalized Linear Mixed Model (GLMM) Results for Daily Feeding Rate (Planar Area)*

Predictor	Estimate	Std. Error	z-value	p-value
Intercept	2.069	0.312	6.627	<0.001 ***
Size category (reference: 0-15 cm)				
15–25 cm	1.035	0.272	3.801	<0.001 ***
25–40 cm	1.928	0.248	7.761	<0.001 ***
>40 cm	2.663	0.251	10.597	<0.001 ***
Coral cover category (reference: 0-15%)				
15–30%	0.176	0.204	0.861	0.389
30–50%	0.184	0.197	0.933	0.351
>50%	0.613	0.225	2.724	0.006 **
Density category (reference: non-outbreaking <15/ha)				
Outbreaking (15–30/ha)	0.039	0.129	0.300	0.764
Severe outbreak (>30/ha)	0.229	0.133	1.723	0.085

Model Fit Statistics:

AIC: 1284.5
BIC: 1330.1
Log-likelihood: -631.3
Residual deviance: 1262.5
Number of observations: 466
Number of groups (Site): 76

R-squared marginal: 0.358
R-squared conditional: 0.438

ii) Predicted values

Table S9: *Estimated marginal means model predictions for **a)** body size category, planar area.d^{-1} (with coral cover held constant), **b)** coral cover category*

Body Size class	Predicted	Conf. low	Conf. high
15-25cm	36.73	25.14	53.67
25-40cm	101.59	76.97	134.09
>40cm	221.99	169.95	289.97

Coral cover class	Predicted	Conf. low	Conf. high
0-15%	114.00	82.58	157.38
15-30%	140.49	110.37	178.83
30-50%	136.64	111.26	167.81
>50%	221.99	169.95	289.97

iii) Pairwise contrasts

Table S10: *Post-hoc tables of pairwise contrasts (planar area) for **a)** body size category and **b)** coral cover category, **c)** population density*

a) Body size category

contrast	*ratio*	*SE*	*df*	*lower.CL*	*upper.CL*	*null*	*t.ratio*	*p.value*
(25-40cm) / (15-25cm)	**2.44**	**0.41**	**446**	**1.59**	**3.72**	**1**	**5.44**	**<0.0001***
>40cm / (15-25cm)	**5.09**	**0.90**	**446**	**3.25**	**7.96**	**1**	**9.39**	**<0.0001***
>40cm / (25-40cm)	**2.08**	**0.20**	**446**	**1.62**	**2.68**	**1**	**7.56**	**<0.0001***

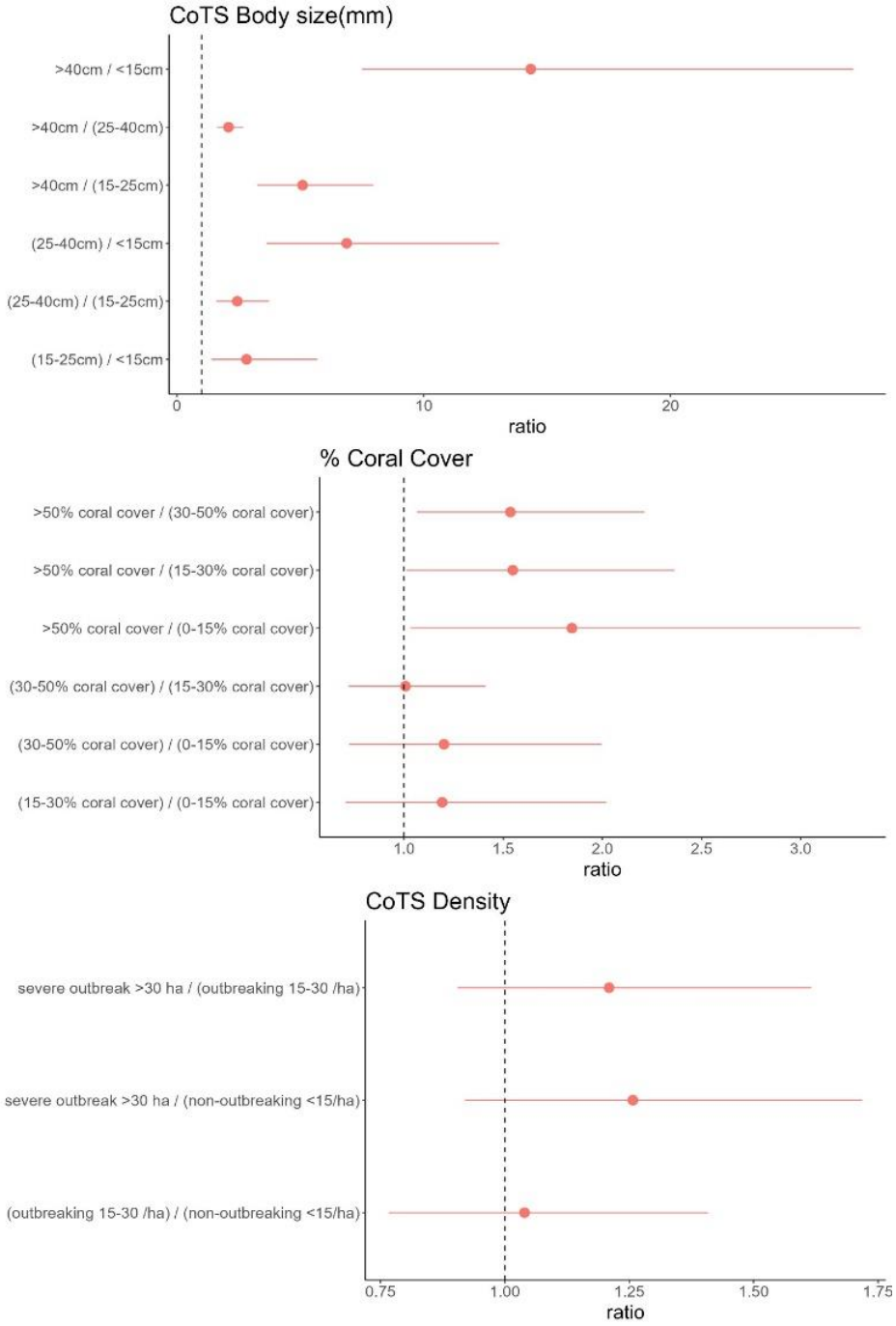
b) Coral cover category

contrast	*ratio*	*SE*	*df*	*lower.CL*	*upper.CL*	*null*	*t.ratio*	*p.value*
(15-30% coral cover) / (0-15% coral cover)	1.19	0.24	446	0.70	2.02	1	0.86	0.82
(30-50% coral cover) / (0-15% coral cover)	1.20	0.24	446	0.72	1.99	1	0.93	0.79
(30-50% coral cover) / (15-30% coral cover)	1.01	0.13	446	0.72	1.41	1	0.06	0.99
>50% coral cover / (0-15% coral cover)	**1.84**	**0.41**	**446**	**1.03**	**3.30**	**1**	**2.72**	**0.034***
>50% coral cover / (15-30% coral cover)	**1.55**	**0.25**	**446**	**1.01**	**2.36**	**1**	**2.66**	**0.040***
>50% coral cover / (30-50% coral cover)	**1.54**	**0.22**	**446**	**1.07**	**2.21**	**1**	**3.03**	**0.013***

c) Population density

contrast	*ratio*	*SE*	*df*	*lower.CL*	*upper.CL*	*null*	*t.ratio*	*p.value*
(outbreaking 15 -30 /ha) / (non-outbreaking <15/ha)	1.04	0.13	464	0.77	1.41	1	0.30	0.95
(severe outbreak >30 ha) / (non-outbreaking <15/ha)	1.26	0.17	464	0.92	1.72	1	1.72	0.19
(severe outbreak >30 ha) / (outbreaking 15 -30 /ha)	1.21	0.15	464	0.91	1.61	1	1.54	0.27

Figure S2: *Tukey's Caterpillar plots of pairwise comparisons*



Appendix 3c. 3D surface area feeding rates

i) Variable selection

Table S11: a) *Boosted regression tree presenting relative importance of different variables* ***b)*** *visual representation of BRT*

Variable	Relative influence
COT_size	46.853684
Density_inclScars	19.113482
Acropora_cover	13.716435
Total_coral_cover	12.254750
Region	6.650194
Season	1.411454

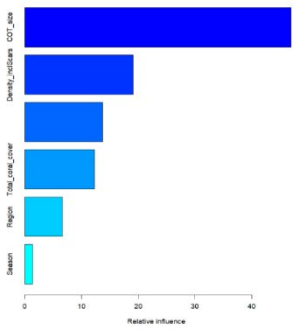


Table S12: *Model formulas and associated degrees of freedom (df) and AIC criterion. Selected model is highlighted in bold*

Model variables	**df**	**AIC**
glmm_model_cat1 <- glmmTMB(log(daily_feeding_rate_surface_area) ~ Size_category + Coral_cover_category + (1|Site)	9	1483.733
glmm_model_cat2 <- glmmTMB(log(daily_feeding_rate_surface_area) ~ Size_category + Density_category + (1|Site)	8	1343.961
glmm_model_cat3 <- glmmTMB(log(daily_feeding_rate_surface_area) ~ Size_category + Coral_cover_category + Density_category + (1|Site)	**11**	**1317.774**
glmm_model_cat4 <- glmmTMB(log(daily_feeding_rate_surface_area) ~ Size_category + Acropora_category + Density_category + (1|Site)	10	1319.988
glmm_model_cat5 <- glmmTMB(log(daily_feeding_rate_surface_area) ~ Size_category + Acropora_category + Season + (1|Site)	9	1485.686
glmm_model_cat6 <- glmmTMB(log(daily_feeding_rate_surface_area) ~ Size_category + Coral_cover_category + Season + (1|Site)	10	1484.724
glmm_NULL <- glmmTMB(log(daily_feeding_rate_surface_area) ~ 1	2	1806.912

ii) GLMM Model Output

Model formula: *glmm_planar <- glmmTMB(log(daily_feeding_rate_surface_area) ~* ***Size_category*** *+* ***Coral_cover_category*** *+* ***Density_category*** *+ (1\|**Site**)*

Response variable: log(daily_feeding_rate_surface_area)
Fixed effects: Size category, Coral cover category, Density category
Random effect: Site (n = 76)
Family: Gaussian (identity link)

Table S13: *Generalized Linear Mixed Model (GLMM) Results for Daily Feeding Rate (3D surface Area)*

Predictor	Estimate	Std. Error	z-value	p-value
Intercept	3.600	0.335	10.763	<0.001 ***
Size category (reference: 0-15 cm)				
15–25 cm	1.063	0.289	3.683	<0.001 ***
25–40 cm	1.932	0.265	7.306	<0.001 ***
>40 cm	2.719	0.268	10.153	<0.001 ***
Coral cover category (reference: 0-15%)				
15–30%	0.282	0.219	1.284	0.199
30–50%	0.264	0.212	1.244	0.214
>50%	0.678	0.245	2.772	0.006 **
Density category (reference: non-outbreaking <15/ha)				
Outbreaking (15–30/ha)	0.058	0.138	0.423	0.673
Severe outbreak (>30/ha)	0.281	0.143	1.965	0.049 *

Model Fit Statistics:

AIC: 1336.5
BIC: 1382.1
Log-likelihood: -657.2
Residual deviance: 1314.5
Number of observations: 466
Number of groups (Site): 76

R-squared marginal: 0.340
R-squared conditional: 0.435

iii) Predicted values

Table S14: *Estimated marginal means model predictions for **a)** body size category, 3D surface area.d^{-1} (with coral cover held constant), **b)** coral cover category*

Size class	Predicted	Conf. low	Conf. high
15-25cm	191.40	128.42	285.27
25-40cm	523.92	391.23	701.61
>40cm	1214.92	917.20	1609.28

Coral cover class	Predicted	Conf. low	Conf. high
0-15%	536.98	382.45	753.95
15-30%	769.07	596.60	991.39
30-50%	729.30	596.60	991.39
>50%	1214.92	917.20	1609.28

iv) Pairwise contrasts

Table S15: *Post-hoc tables of pairwise contrasts (planar area) for **a)** body size category and **b)** coral cover category, **c)** population density*

a) Body size category

contrast	*ratio*	*SE*	*df*	*lower.CL*	*upper.CL*	*null*	*t.ratio*	*p.value*
(25-40cm) / (15-25cm)	**2.39**	**0.41**	**464**	**1.53**	**3.73**	**1**	**5.01**	**<0.001***
>40cm / (15-25cm)	**5.24**	**0.96**	**464**	**3.26**	**8.41**	**1**	**9.02**	**<0.001***
>40cm / (25-40cm)	**2.19**	**0.22**	**464**	**1.68**	**2.87**	**1**	**7.64**	**<0.001***

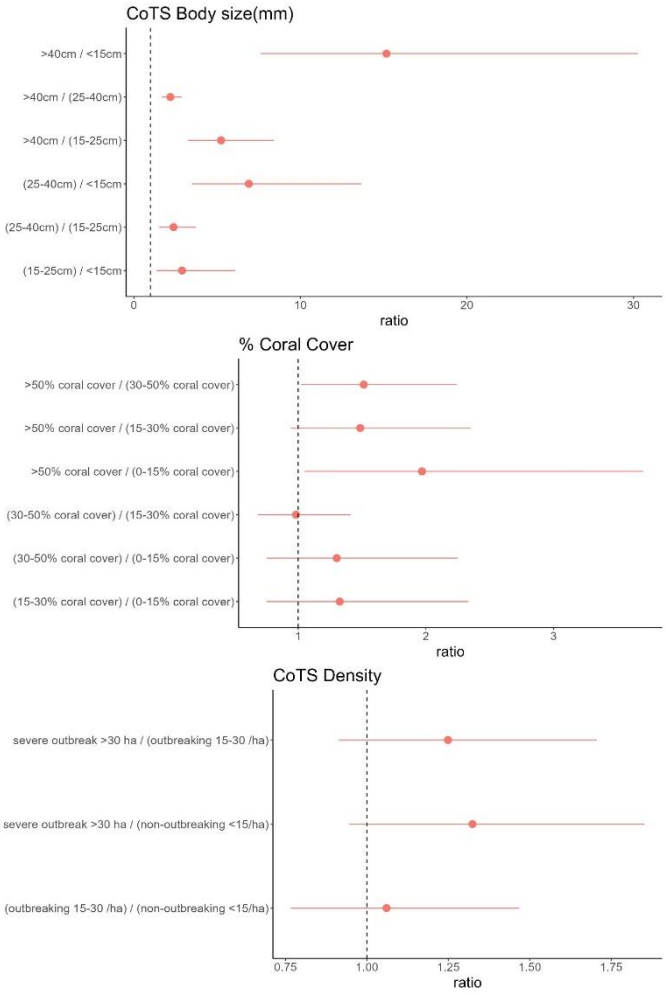
b) Coral cover category

contrast	*ratio*	*SE*	*df*	*lower.CL*	*upper.CL*	*null*	*t.ratio*	*p.value*
(15-30% coral cover) / (0-15% coral cover)	1.33	0.29	464	0.75	2.33	1	1.28	0.57
(30-50% coral cover) / (0-15% coral cover)	1.30	0.28	464	0.75	2.24	1	1.24	0.60
(30-50% coral cover) / (15-30% coral cover)	0.99	0.14	464	0.68	1.41	1	-0.13	1.00
>50% coral cover / (0-15% coral cover)	**1.96**	**0.48**	**464**	**1.05**	**3.70**	**1**	**2.72**	**0.03***
>50% coral cover / (15-30% coral cover)	1.48	0.26	464	0.94	2.35	1	2.23	0.11
>50% coral cover / (30-50% coral cover)	**1.51**	**0.23**	**464**	**1.02**	**2.24**	**1**	**2.71**	**0.03***

d) Population density

contrast	*ratio*	*SE*	*df*	*lower.CL*	*upper.CL*	*null*	*t.ratio*	*p.value*
(outbreaking 15 -30 /ha) / (non-outbreaking <15/ha)	1.06	0.15	464	0.77	1.47	1	0.42	0.91
(severe outbreak >30 ha) / (non-outbreaking <15/ha)	1.32	0.19	464	0.95	1.85	1	1.97	0.12
(severe outbreak >30 ha) / (outbreaking 15 -30 /ha)	1.24	0.17	464	0.91	1.70	1	1.68	0.22

Figure S3: *Tukey's caterpillar plot*



Appendix 4 - Supplementary information for Chapter 6

Table S1: *Bayesian generalized mixed-effect model formulas. Formulas model various predictors against i) PCI, ii) Lipid content, iii) GSI, iv) oocyte area*

	Model formula	Fitting Bayesian model
PCI response (with *Acropora*)	PCI.form <- bf(PCI ~ scale(Density_avg) + scale(Lipid.content) + scale(log(Acro.cover)) + (1|Day_of_survey) + (1|Region), family=gaussian())	PCI.form.brm <- brm(PCI.form, data=new_feeding_dataset, prior=priors_PCI, sample_prior = 'only', iter=7000, warmup=1500, chains=3, cores = 3, thin=5, refresh=0, backend= "cmdstanr")
PCI response (with Total coral cover)	PCItcc.form <- bf(PCI ~ scale(Density_avg) + scale(Lipid.content) + scale(log(Total.coral.cover)) + (1|Day_of_survey) + (1|Region), family=gaussian())	PCItcc.form.brm <- brm(PCItcc.form, data=new_feeding_dataset, prior=priors_PCI, sample_prior = 'only', iter=7000, warmup=1500, chains=3, cores = 3, thin=5, refresh=0, backend= "cmdstanr")
Lipid content response (with *Acropora*)	Lipid.form <- bf(Lipid.content ~ scale(Density_avg) + scale(log(Acro.cover)) + (1|Day_of_survey) + (1|Region), family=gaussian())	Lipid.form.brm <- brm(Lipid.form, data=new_feeding_dataset, prior=priors_lipid, sample_prior = 'only', iter=7000, warmup=1500, chains=3, cores = 3, thin=5, refresh=0, backend= "cmdstanr")
Lipid content response (with Total coral cover)	Lipidtcc.form <- bf(Lipid.content ~ scale(Density_avg) + scale(log(Total.coral.cover)) + (1|Day_of_survey) + (1|Region), family=gaussian())	Lipidtcc.form.brm <- brm(Lipidtcc.form, data=new_feeding_dataset, prior=priors_lipid, sample_prior = 'only', iter=7000, warmup=1500, chains=3, cores = 3, thin=5, refresh=0, backend= "cmdstanr")
GSI response (with *Acropora*)	GSI.form <- bf(GSI ~ scale(Density_avg) + scale(Lipid.content) + scale(log(Acro.cover)) + (1|Day_of_survey) + (1|Region), family=gaussian())	GSI.form.brm <- brm(GSI.form, data=new_feeding_dataset, prior=priors_GSI, sample_prior = 'only', iter=7000, warmup=1500, chains=3, cores = 3, thin=5, refresh=0, backend= "cmdstanr")
GSI response (with Total coral cover)	GSItcc.form <- bf(GSI ~ scale(Density_avg) + scale(Lipid.content) + scale(log(Total.coral.cover)) + (1|Day_of_survey) + (1|Region),	GSItcc.form.brm <- brm(GSItcc.form, data=new_feeding_dataset, prior=priors_GSI, sample_prior = 'only', iter=7000,

	family=gaussian())	warmup=1500, chains=3, cores = 3, thin=5, refresh=0, backend= "cmdstanr")
Oocyte area response (with *Acropora*)	oocyte.form <- bf(oocyte.area ~ scale(Density_avg) + scale(log(Acro.cover)) + (1|Day_of_survey) + (1|Region), family=gaussian())	oocyte.form.brm <- brm(oocyte.form, data=new_feeding_dataset, prior=priors_oocyte, sample_prior = 'only', iter=7000, warmup=1500, chains=3, cores = 3, thin=5, refresh=0, backend= "cmdstanr")
Oocyte area response (with Total coral cover)	oocyte.formTCC <- bf(oocyte.area ~ scale(Density_avg) + scale(log(Total.coral.cover)) + (1|Day_of_survey) + (1|Region), family=gaussian())	oocyteTCC.form.brm <- brm(oocyte.formTCC, data=new_feeding_dataset, prior=priors_oocyte, sample_prior = 'only', iter=7000, warmup=1500, chains=3, cores = 3, thin=5, refresh=0, backend= "cmdstanr")

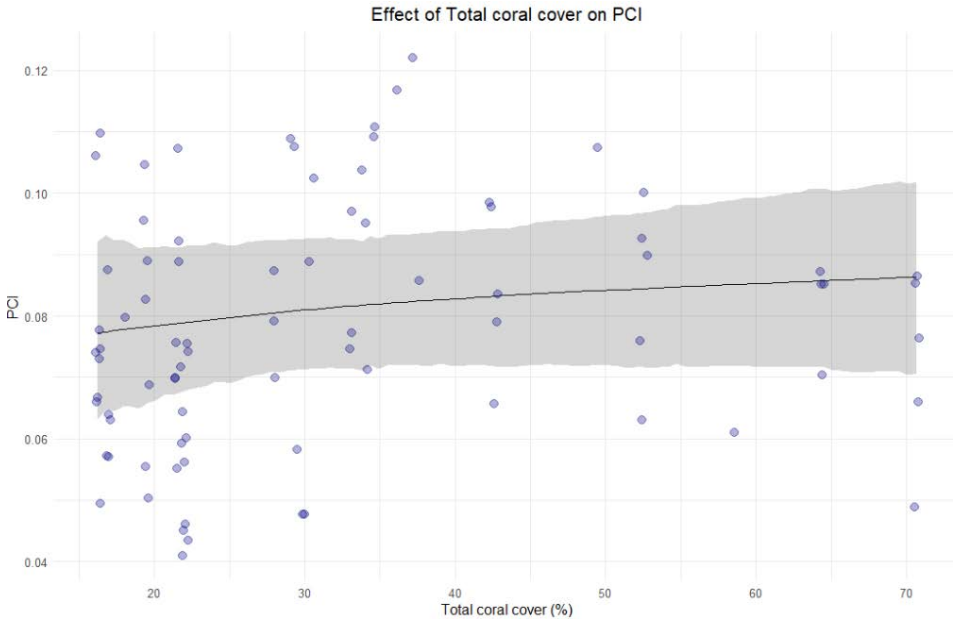


Figure S1: *Relationship between Total coral cover and Pyloric Caeca Index (PCI; pyloric caeca wet weight to body wet weight ratio). Black line represents the posterior median estimates of PCI as modelled using a Bayesian Generalized Linear Mixed Model (BGLMM). The grey ribbon represents 95% Highest Posterior Density (HPD) interval as credible intervals. Observed values of PCI are displayed as points*

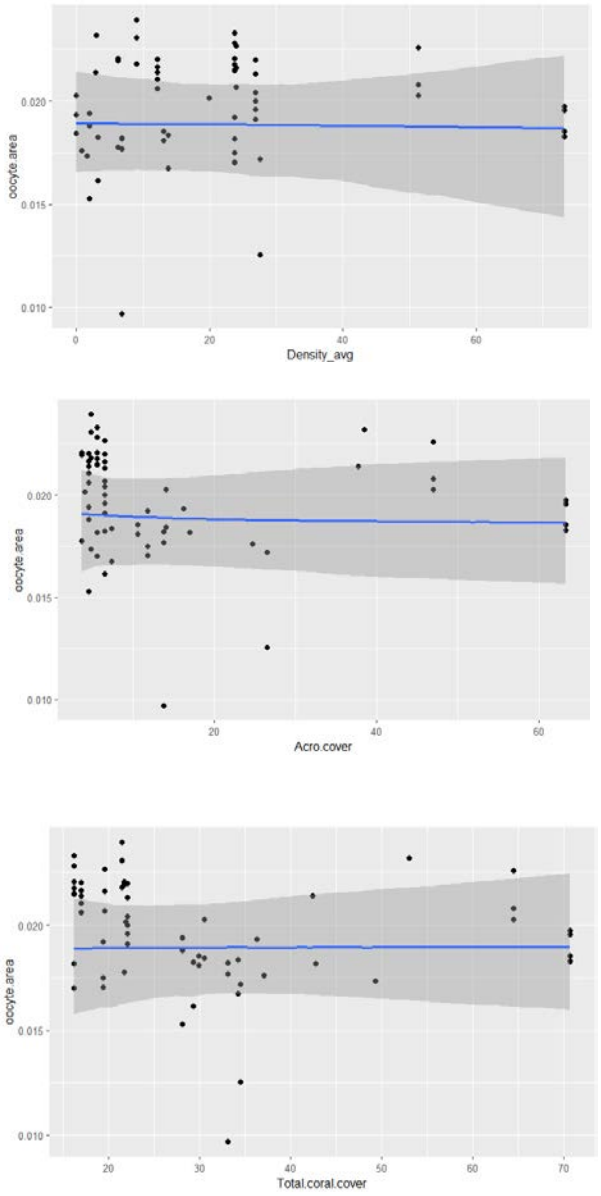


Figure S2: *Relationship between* ***a)*** *Population density,* ***b)*** *Acropora cover (%) and* ***c)*** *Total coral cover on mean oocyte area. Black lines represent the posterior median estimates of oocyte area as modelled using a Bayesian Generalized Linear Mixed Model (BGLMM). The grey ribbon represents 95% Highest Posterior Density (HPD) interval as credible intervals. Observed values of mean oocyte area for individual starfish are displayed as points*

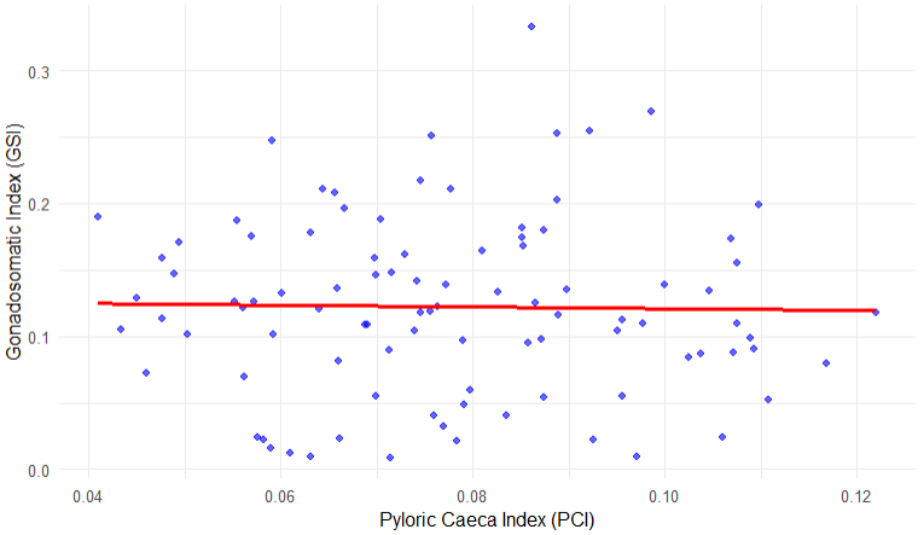


Figure S3: *Relationship between Pyloric Caeca Index (PCI) and Gonadosomatic Index (GSI. Blue points represent values for a single starfish, red line depicts trendline*